Journal of Nanotechnology

Applications of Nanomaterials in Biology and Medicine

Guest Editors: Lifeng Dong, Michael M. Craig, Dongwoo Khang, and Chunying Chen

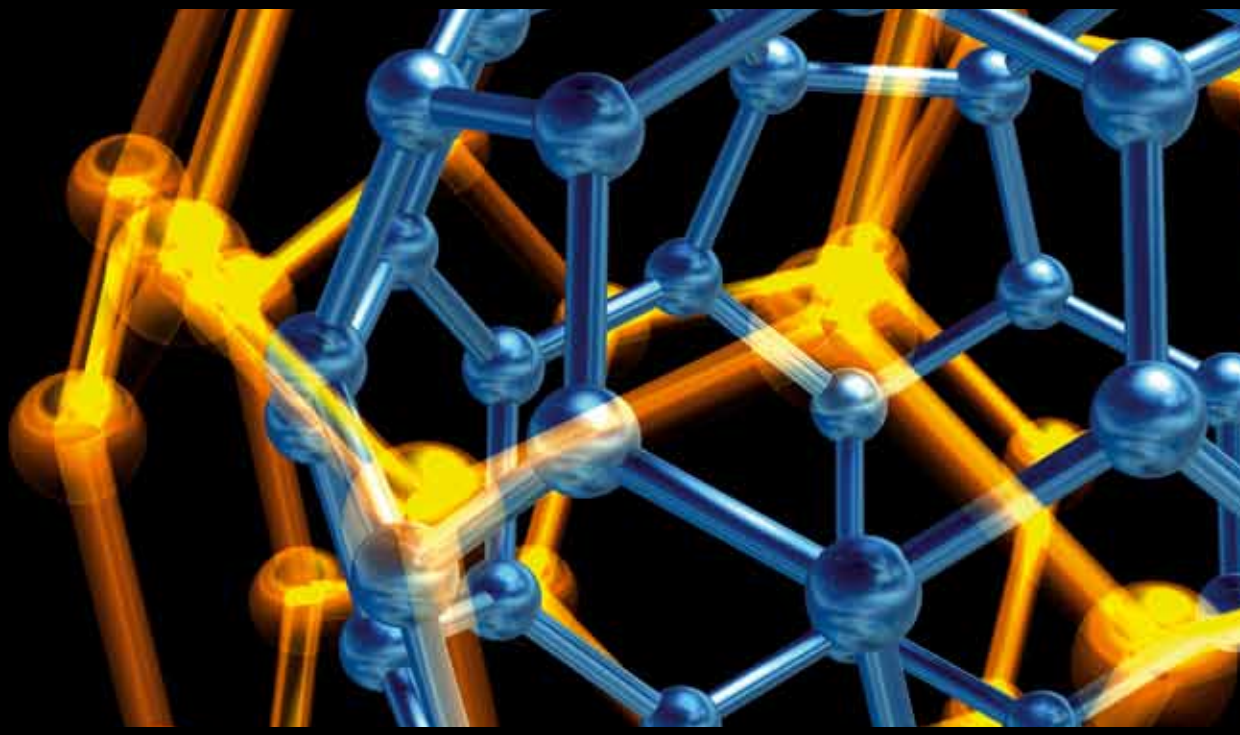

Applications of Nanomaterials in Biology and Medicine

Journal of Nanotechnology

Applications of Nanomaterials in Biology and Medicine

Guest Editors: Lifeng Dong, Michael M. Craig, Dongwoo Khang, and Chunying Chen

Editorial Board

Contents

Hindawi Publishing Corporation
Journal of Nanotechnology
Volume 2012, Article ID 816184, 2 pages
doi:10.1155/2012/816184

Editorial

Applications of Nanomaterials in Biology and Medicine

Lifeng Dong,[1,2] Michael M. Craig,[3] Dongwoo Khang,[4] and Chunying Chen[5]

[1] *College of Materials Science and Engineering, Qingdao University of Science and Technology, Qingdao 266042, China*
[2] *Department of Physics, Astronomy, and Materials Science, Missouri State University, Springfield, MO 65897, USA*
[3] *Department of Biomedical Sciences, Missouri State University, Springfield, MO 65897, USA*
[4] *School of Nano and Advanced Materials Engineering, Gyeongsang National University, Gyeongnam 660-701, Republic of Korea*
[5] *National Center for Nanoscience and Technology, Beijing 100190, China*

Correspondence should be addressed to Lifeng Dong, lifengdong@missouristate.edu

Received 17 May 2012; Accepted 17 May 2012

Due to nanoscale effects and increased surface area, nanomaterials have been investigated as promising tools for the advancement of diagnostic biosensors, drug and gene delivery, and biomedical imaging. In comparison to their larger counterparts, nanomaterials have unique physicochemical and biological properties. Many properties of nanomaterials, such as size, shape, chemical composition, surface structure and charge, aggregation and agglomeration, and solubility, can greatly influence their interactions with biomolecules and cells. For example, nanoparticles with size-tunable light emission have been employed to produce exceptional images of tumor sites; single-walled carbon nanotubes, having diameters comparable to the width of DNA molecules, have demonstrated an impressive potential as high-efficiency delivery transporters for biomolecules into cells. Therefore, the main emphasis of this special issue focuses on the development of some nanomaterials and their applications in biology and medicine.

This special issue contains three review articles and six research articles. Among the review articles, T. Kaur et al. examine and discuss bacteriophage nanomedicine applications and the immunomodulator effects of bacteriophage exposure and treatment modalities in paper titled "*Immunocompatibility of bacteriophages as nanomedicines*." K. J. Flores et al. highlight the literature relating to gene-based vaccines, especially DNA vaccines, and explore the combination of RNA and nanomaterials (e.g., gold nanoparticles, nanoliposomes, and dendrimers) for prevention and treatment of disease in paper titled "*Tipping the proteome with gene-based vaccines: weighing in on the role of nanomaterials*." Z. Zhang and C. Huang summarize recent developments in the field of intra-articular drug delivery systems using micro/nanocarriers, such as polymeric micro/nanoparticles, liposomes, and hydrogels, in paper titled "*Micro- and nanocarrier mediated intra-articular drug delivery systems for the treatment of osteoarthritis*."

Among the six research articles, four articles are related to the study of carbon nanotubes. M. Mananghaya et al. use density functional theory to investigate the solubility and reactivity of single-walled carbon nanotubes (SWCNTs) in paper titled "*Theoretical investigation on the solubilization in water of functionalized single-wall carbon nanotubes*." H. Haniu et al. report effects of graphitization temperature and diameter of multiwalled carbon nanotubes on their biological responses, such as cell viability, total reactive oxygen, and/or nitrogen species productions, and cytokine secretion in paper titled "*Manufacturing strategy for multiwalled carbon nanotubes as a biocompatible and innovative material*." J. Harvey et al. show that SWCNTs facilitate DNA delivery into microvascular endothelial cells, even their nuclei, thus suggesting that carbon nanotubes have therapeutic potential as drug and gene vehicles in paper titled "*Uptake of single-walled carbon nanotubes conjugated with DNA by microvascular endothelial cells*." L. Dong et al. demonstrate SWCNTs' antibacterial properties against *Salmonella enterica* and *Escherichia coli*, indicating that carbon nanotubes could become an effective alternative to antibiotics in dealing with drug-resistant and multidrug-resistant bacterial strains in paper titled "*Antimicrobial activity of single-walled carbon nanotubes suspended in different surfactants*." S. Anuchapreeda et al. develop a new formulation of a curcumin lipid nanoemulsion of 47–55 nm

for cancer chemotherapy in paper titled "*Preparation of lipid nanoemulsions incorporating curcumin for cancer therapy.*" R. K. DeLong et al. comparatively characterize nucleic acid conjugates with protamine and gold nanoparticles in the nano range of concentrations by UV/Vis spectrum, dynamic laser light scattering, fluorimetry, and gel electrophoresis in paper titled "*Biomolecular triconjugates formed between gold, protamine, and nucleic acid: comparative characterization on the nanoscale*."

Lastly, the editors would like to acknowledge and thank all authors for their contributions to this special issue and the reviewers for their time and dedication.

Lifeng Dong
Michael M. Craig
Dongwoo Khang
Chunying Chen

Hindawi Publishing Corporation
Journal of Nanotechnology
Volume 2012, Article ID 247427, 13 pages
doi:10.1155/2012/247427

Review Article

Immunocompatibility of Bacteriophages as Nanomedicines

Tranum Kaur, Nafiseh Nafissi, Olla Wasfi, Katlyn Sheldon, Shawn Wettig, and Roderick Slavcev

School of Pharmacy, University of Waterloo, Health Sciences Campus, 10 Victoria Street South, Kitchener, ON, Canada N2L 3C4

Correspondence should be addressed to Roderick Slavcev, slavcev@uwaterloo.ca

Received 23 July 2011; Revised 15 January 2012; Accepted 24 January 2012

Academic Editor: Chunying Chen

Bacteriophage-based medical research provides the opportunity to develop targeted nanomedicines with heightened efficiency and safety profiles. Filamentous phages also can and have been formulated as targeted drug-delivery nanomedicines, and phage may also serve as promising alternatives/complements to antibiotics. Over the past decade the use of phage for both the prophylaxis and the treatment of bacterial infection, has gained special significance in view of a dramatic rise in the prevalence of antibiotic resistance bacterial strains. Two potential medical applications of phages are the treatment of bacterial infections and their use as immunizing agents in diagnosis and monitoring patients with immunodeficiencies. Recently, phages have been employed as gene-delivery vectors (phage nanomedicine), for nearly half a century as tools in genetic research, for about two decades as tools for the discovery of specific target-binding proteins and peptides, and for almost a decade as tools for vaccine development. As phage applications to human therapeutic development grow at an exponential rate, it will become essential to evaluate host immune responses to initial and repetitive challenges by therapeutic phage in order to develop phage therapies that offer suitable utility. This paper examines and discusses phage nanomedicine applications and the immunomodulatory effects of bacteriophage exposure and treatment modalities.

1. Introduction

Discovered independently by Frederick Twort and Félix d'Hérelle, respectively, in 1915 and 1917, bacteriophages are bacterial viruses that exist in two different life cycles and may or may not lyse their bacterial hosts as lytic and temperate bacteriophages, respectively [1–3]. While the ability of phage to attack bacteria has been known since their discovery, our knowledge about phage interactions with mammalian cells is very limited. Bacteriophages have been used clinically to treat human bacterial infections for about 80 years in the countries of the former Soviet Union and Eastern Europe [4]. Although historically their clinical use as antibacterials preceded that of antibiotics, both clinically and commercially, due to the advent of the "age of antibiotics" in the 1940s, phages were quickly declined as a therapeutic option. Despite their obvious efficacy in curing antibiotic-resistant infections, there are important caveats to their safe and efficient clinical application, and in consideration of these phage therapy is still at best considered an "experimental" treatment option.

The recent global increase in the emergence of multidrug-resistant (MDR) clinical strains of bacteria has led us to the precarious situation of entering a "post-antibiotic era" of untreatable infections and epidemics [5, 6]. The systematic overuse of antibiotics by the medical and agricultural professions during the last century has precipitated a powerfully selective environment for MDR strains, resistant to even the most potent antibiotics available [6]. To further aggravate the situation, antibiotic research appears to have reached a dead end with even newer "last chance" modified molecules like linezolid and vancomycin now facing growing episodes of resistance and eventual inefficacy [7, 8]. Moreover, only three new classes of antibiotics (lipopeptides, oxazolidinones, and streptogramins) have entered the medicine market in the last four decades all of which are indicated for the treatment of gram-positive (G^+) bacterial infections [9].

Matsuzaki et al. [10] summarized the advantages of phage therapy over antibiotic therapy as follows: (i) it is effective against multidrug-resistant pathogenic bacteria; (ii) substitution of the normal microbial flora does not

occur because the phage kills only the targeted pathogenic bacteria; (iii) it can respond quickly to the appearance of phage-resistant bacterial mutants because the frequency of phage mutation is significantly higher than that of bacteria; (iv) developing costs for a phage treatment are cheaper than that of new antibiotics; (v) side-effects of phage therapy are very rare compared to the antibiotic therapy [10, 11]. However, while phages as specific and self-replicating/limiting antibacterials offer several advantages over antibiotics, their usage in mammals requires careful consideration and understanding of the host-mediated obstacles that challenge appropriate safety and efficacy as synergistic antibiotic cotherapeutics or replacements. Global fears now abound that the medical world may be thrust into conditions resembling the pre-antibiotic era and that procedures such as chemotherapy, wound control during surgery, and transplant immunosuppression are at risk yet again. These fears have rekindled the interest in the development of phage therapeutics to ensure long-term, efficient, safe, and harmless treatment options [12]. Phages have also been demonstrated to modulate immune system function. A primary example of this phenomenon includes the inhibition of both bacteria- and LPS-induced respiratory burst by human blood phagocytes [13]. It has also been suggested that phage may normalize cytokine production by blood cells isolated from patients [14], although this study was largely uncontrolled and further confirmation of this therapeutic bystander effect is warranted. Nonetheless, the increasing clinical and technological use of bacteriophages requires that all aspects of phage-mammal interactions be explored.

2. Applications

2.1. Phage Display. Tumor-targeting peptide display on phage surface is a direct and fast screening approach with promising results for targeting drugs into tumor cells [15]. Identification of ligand-receptor interaction in order to find the appropriate receptor on target cell facilitated by phage display technology play a crucial role in disease diagnosis, profiling, imaging, and therapy.

Advanced disease cell targeting relies on phage display technologies, in which polypeptides with desired binding profiles can be "serially selected, in a process called biopanning" [17]. Here, the heterologous peptide/protein coding gene is translationally fused to the bacteriophage capsid protein gene, where the resultant phages not only carry the gene encoding the displayed protein/peptide but are also capable of replication to amplify the construct (Figure 1). While phage display was traditionally employed to screen cDNA libraries, the application has more recently been applied to surmount some therapeutic gene delivery obstacles. This is achieved through the identification of highly specific and selective ligands that can deliver nanocarriers to the site of disease [16]. The combination of phage-display technology with nanocarrier-based drug-delivery systems is a novel approach toward creating more effective and safe therapies [15]. This approach is perhaps most suitably applied toward cancer therapy, in which the tumor-specific phage expressing peptides specific to a broad array of tumors are screened from billion phages by their specific affinity with uniquely expressed tumor receptors [18, 19]. Various studies demonstrate the successful application of isolated peptides for specific targeting and delivery of pharmaceutical nanocarriers, such as liposomes, to tumors. Wang et al. applied this protocol to prepare doxorubicin-loaded PEGylated liposomes modified with phage-panned proteins specific towards MCF-7 breast cancer cells and demonstrated that this strategy provides strong specific binding with target cells and increased cytotoxicity *in vitro* [15]. They proposed that the design and construction of novel nanomedicines targeted to a variety of cellular receptors is facilitated through self-assembly of selected phage proteins and "stealth" liposomes.

Recently, Bedi et al., demonstrated phage-targeted siRNA nanopharmaceuticals through their encapsulation into liposomes targeted to the breast tumor cells with preselected intact phage proteins [20]. "The presence of pVIII coat protein fused to a MCF-7 cell-targeting peptide "DMPGTVLP" in the liposomes was confirmed by Western blotting. This approach offers the potential for development of new anticancer siRNA-based targeted nanomedicines." On similar lines, Nicol et al. were able to devise a strategy for targeting the cardiac vasculature through the use of *in vivo* phage display to identify target peptides that are selective to the heart in two rat strains [21]. They hypothesized that, by cloning these peptides into the fiber protein of adenovirus, a potential targeted delivery system could be created. Interestingly, several peptides that are derived from phage-displayed peptide library screening have been applied as new therapeutics in clinical trials, further validating phage-display targeted nanomedicine as a viable strategy that warrants further investigation and exploitation.

2.2. Phage Vaccine Technology. Kurzepa et al. first demonstrated that the injection of phage T7 into a mammalian host resulted in elevated interferon levels [22]. The potential application of bacteriophages as immunization tool was proposed since it was observed that the immune response was stimulated by the phage genome and not coat proteins. Interestingly, the isolated T7 genome did not show an interferon response suggesting that the phage coat protein ensures safe delivery of the genome in a form required to confer an immune response. As such, phage particles have been applied in DNA vaccine technology as a safe container for DNA delivery. The vaccine gene and its expression cassette are cloned into phage genome, and purified phage lysate can be directly injected into the host as a means of immunization [23]. Modified phage particles package their nucleic acid carrying the vaccine expressing sequence in their protein coat, likely protecting it from sources of degradation, before and after administration. Different small and large animal models have been vaccinated by phage DNA vaccines, and the results demonstrated a significantly higher and long-lasting antibody response compared to naked DNA vaccine or even purified recombinant protein [23–25]. Furthermore, as an exogenous antigen, the phage particle efficiently targets antigen-presenting cells (APCs), thereby stimulating a

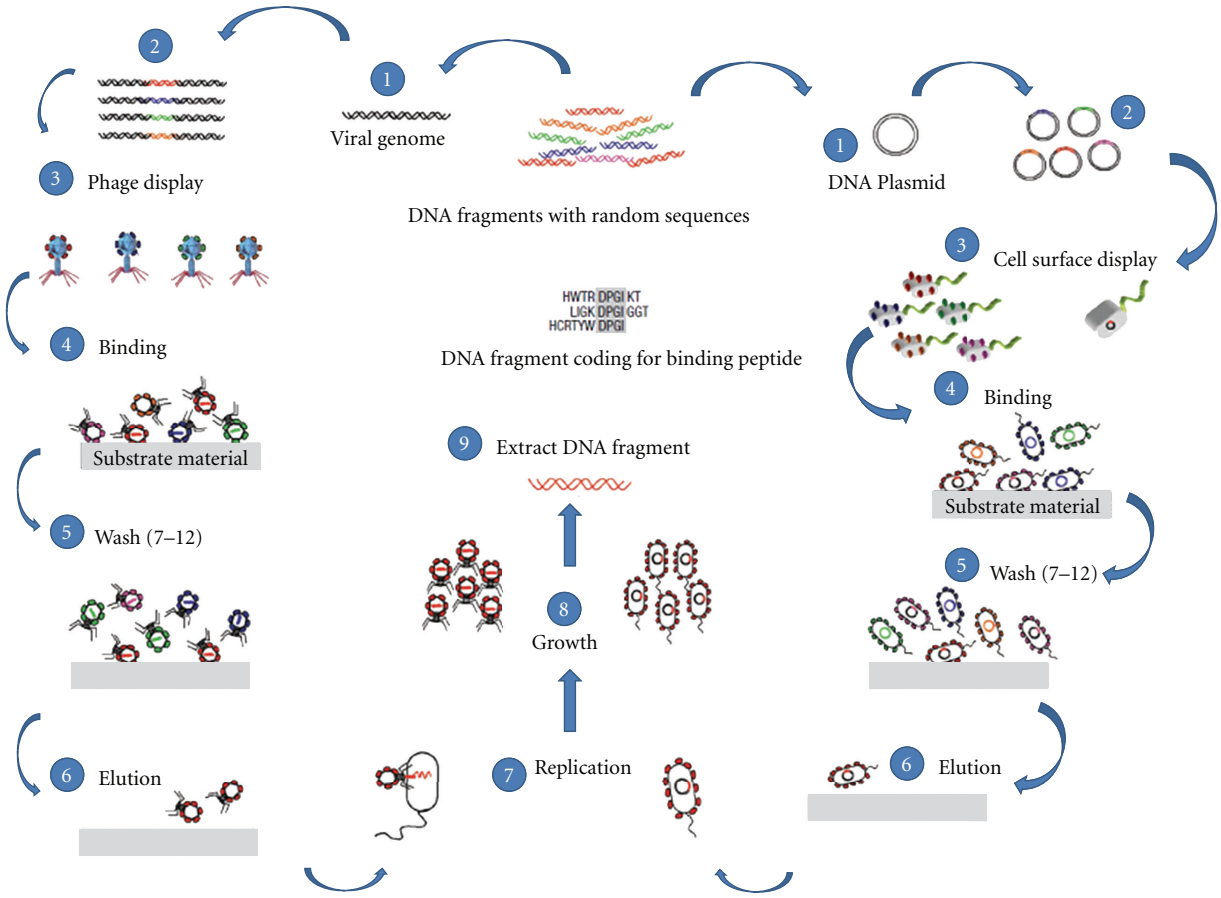

Figure 1: Phage display and cell surface display. Principles of the protocols used for selecting polypeptide sequences that have binding affinity to given inorganic substrates (Source: Nat Mater. 2003, 2(9):577-85.) [16].

superior specific humoral immune response to the vaccine [4], compared to standard "naked" DNA vaccine approaches.

Phage display as a new tool for developing modern vaccines demonstrates a unique application of bacteriophages in vaccine design and is influenced by the immunomodulatory effects of phage exposure (summarized in Table 1). The premise of phage-display vaccination exploits the capability of certain phages to display a specific antigenic peptide or protein on their surface via a translational fusion with capsid protein(s) [30]. Alternatively, phages displaying peptide libraries can be screened with a specific antiserum to isolate novel protective antigens or mimotopes—peptides that mimic the secondary structure and antigenic properties of a protective carbohydrate, protein, or lipid, despite possessing a different primary structure. Two different strategies have been defined for phage display: (1) translational fusion of antigen coding sequence to coat protein gene and (2) Artificial conjugation of antigen to the coat protein; both of which are robust and allow for a wide array of antigens to be displayed. In addition, since phage particles are themselves immunogenic, the antigen displayed on the phage is already combined with a natural adjuvant, which eliminate the necessity of alternative adjuvant protein purification and further conjugation with the vaccine [31]. This fact dramatically reduces the cost for generating new vaccines while enhancing efficiency. In addition, since phages are unable to replicate and in eukaryotic cells in the absence of a suitable prokaryotic host, these therapeutics behave as inert particulate antigens [23]. In recent years, work has shown that whole phage particles can be applied to deliver vaccine expression cassette cloned into their genome or express antigens on their surface. The combination of the above two promising technologies may result in "hybrid phages" to create inexpensive, easily manipulated, and rapid production cocktail vaccines [4].

2.3. Phage-Phagocyte Interactions in Antitumor Therapies. Bacteriophages and their demonstrated ability to influence mammalian immune systems have also been exploited to develop novel microbial strategies versus cancer development. Bloch first suggested that phage may possess anticancer activity and was able to demonstrate preferential accumulation of phages in cancer tissue and subsequent inhibition of tumor growth [32]. This was also confirmed by Kantoch and Mordarski in 1958 [33] and in studies done subsequently by Dabrowska et al. in 2004, 2005, and 2007 [26, 34–36]. The models of the studies were the wild-type bacteriophage T4 and its substrain HAP1 (with enhanced affinity for melanoma cells), a pentameric protein occurring

Table 1: Immunomodulatory effects of bacteriophage exposure.

Phage interactions	Immunomodulatory effects	Reference
Phage-phagocyte interactions in antitumor therapies	Phages expressing Fab fragment specific for tumor accumulated in the tumor tissue and induced humoral and cellular immune responses, leading to solid tumor regression in mice.	[22]
	T4 phages interacting with B3 integrins modulated the function of human T cells and platelets. Bone marrow dendritic cells did not confer similar results, but a significant delay in tumor growth was observed.	[26, 27]
Antiphage immune response	As foreign exogenous antigens, phages induce strong antiphage humoral responses resulting in rapid and efficient neutralization and clearance upon subsequent exposure. Phages circulating in the blood were inactivated by macrophages of the RES in synergy with antiphage antibodies—an outcome that would quickly diminish the efficacy of phage therapy upon subsequent exposures. Repeated use of a phage as a therapeutic, in addition to the interactions with the innate immune system, would result in the stimulation of memory cells, clone amplification, and subsequent antibody production. Phage mutagenesis followed by repeated administration of phage therapy and selection for long-circulating phage is an elegant method that permitted investigators to select and isolate mutant phage that persevere from the blood of a mouse.	[22, 28, 29]
Bacteriophages and Reactive Oxygen Species Production	Phage-mediated inhibition of ROS production by phagocytes is an important phenomenon contributing to the beneficial effects of phage therapy in patients with sepsis, a clinical setting where excessive production of ROS appears to play an important role, and agents interfering with ROS have been advocated for treatment.	[22]

on the phage heads. Phages significantly inhibited lung metastasis of B16 melanoma cells (T4 by 47% and HAP1 by 80%). The potential ability of $\beta 3$ integrins on the surfaces of some (including cancer) cells to bind the KGD (Lys-Gly-Asp) motif of phage protein 24 was proposed. Further, it seems that by occupying the $\alpha v\beta 3$ integrin receptor, phages could deprive neoplastic cells from growth signals provided by extracellular matrix proteins. In addition, studies confirmed that blocking $\beta 3$ integrins by ligand analogs inhibits the binding of phages to cancer cells, which seems to confirm the hypothesis. Binding to mammalian cells by phage may also be achieved via nonintegrin receptors. For example, it has been suggested that CD26 is closely involved in HIV cell entry [37]. Importantly, the slower growth was only observed if purified phage preparations were applied. Raw phage lysates, containing numerous bacterial debris, for example, a high LPS concentration, induced a large acceleration of tumor development [26]. Moreover, oral application of a bacteriophage preparation is safer and at least as effective as i.p. [35]. After their studies on binding to cancer cells *in vitro* and attenuating tumour growth and metastases *in vivo*, Dabrowska et al. described a nonsense mutation in the hoc gene that differentiates bacteriophage HAP1 and its parental strain T4. In this study, the antimetastatic activity of the T2 phage, which does not express protein Hoc, with those of T4 and HAP1 was compared in the B16 melanoma lung colonies and found that HAP1 and T2 decreased metastases with equal effect, more strongly than did T4 [36]. The increased antitumor activity of HAP1 may be related to the fact that this phage has a damaged Hoc protein, a protein which symmetrically protrudes from the capsid. Removal of this steric barrier and the free exposition of KGD ligand may be the reason for the stronger inhibition of metastasis. Later, Eriksson et al. described the inhibition of tumor growth by tumor-specific phages, which induced the infiltration of polymorphonuclear leukocytes (PMNs) and the secretion of IL-12 (p70) and interferon γ. Hence, bacteriophages are able to induce expression of cytokines which could alter the immunosuppressive tumor microenvironment and potentiate neutrophil-mediated tumor destruction [38]. Phage specificity to the tumor confers a more localized immune response at the target cell. This is extremely important to maximize the safety of anticancer treatments considering the devastating side effects of other options like chemotherapy on nontumor tissues in patients undergoing cancer therapy. Regardless of the mechanisms of action, the involvement of phages in oncology seems very promising.

2.4. Bacteriophages and Reactive Oxygen Species Production. Aerobic organisms require oxygen for the oxidation of nutrients and energy generation, where in this process different waste and byproducts are inevitably produced. Although oxygen is essential for all aerobic organisms, its reactive metabolites are highly toxic to all organisms. *Reactive oxygen species* (ROS) interact with a variety of cellular components, including proteins, lipids, and nucleic acids. ROS are believed to be responsible for the initiation as well as the progression of cancer. The microenvironment of cancer cells shows high level of oxidative stress, which promotes cell proliferation and stimulates tumor progression [39]. In addition, ROS are employed by neutrophils and mononuclear phagocytes to

neutralize endocytosed antigenic material. However, intensified production of ROS molecules may devastate the body's endogenous antioxidant defense mechanisms, and lead to oxidative stress, which are involved in causing many different disorders mainly result in serious tissue damage [40], or induce immune cells apoptosis depending on the severity of oxidative damage. Therefore, ROS-suppressive effects may be beneficial in controlling many different adverse effects. Some studies support the possible interactions between phages and mammalian cells by providing evidence of inhibition of ROS formation by bacteriophages. In fact, antibiotic therapy of Gram-negative bacteria leads to excessive release of bacterial lipopolysaccharide (LPS), and LPS may in turn activate neutrophils to produce ROS. It was demonstrated that bacteriophages are capable of reducing the production of ROS by phagocytes in the presence of bacteria. The mechanism of action appears quite complex as phages alone do not impart this phenotype, but rather involves not only phage-phagocyte interaction but also phage-LPS interaction and bacterial lysis [41]. Some phages recognize and bind LPS that serves as their natural bacterial receptor [42]. Phage-mediated inhibition of ROS production by phagocytes may be a very important phenomenon contributing to the beneficial effects of phage therapy in patients with sepsis [43], a clinical setting where excessive production of ROS appears to play an important role and agents interfering with ROS have been advocated for treatment [44].

2.5. Phage Lysins as Antimicrobials. Bacteriophages have been used in East Europe and the Former Soviet Union to treat bacterial infections even after the advent and global use of antibiotics, which saw this alternative treatment option fading in western countries. However, over the past two decades with the global spread of antibiotic-resistant infections, research interests in the West have once again turned to alternative treatment modalities. While a plethora of evidence exists confirming the effectiveness of the application of intact phage particles to treat specific bacterial infections, recent advances in molecular biology now also allowed for the development of novel phage-derived enzymes, such as lysins [45]. Bacteria-phage coevolution has yielded phage endolysins encoded by ds DNA phage that specifically lyse their host bacterial cell by hydrolysing one of the four major bonds in the peptidoglycan layer that forms the bacterial cell wall. The majority of studies to date demonstrate that these are modular enzymes with lytic domains that preserve their parental specificities when fused. Endolysins are composed of at least two distinctly separate functional domains: a C-terminal cell-wall binding domain, which directs the enzyme to its target, and an N-terminal catalytic domain that is comprised of one or more of the following types of peptidoglycan hydrolases: endopeptidases, muramidases (lysozyme), N-acetylmuramoyl- L-alanine amidases, and glucosamidases [46]. Phage endolysins are particularly effective against gram-positive bacterial pathogens with an exposed cell wall, whereby the purified endolysin can lyse the cell from without. Purified endolysins are now extensively used not only in the food industry primarily to combat against *Listeria monocytogenes* contamination [47] but also in medical setting, primarily against streptococcal and *staphylococcal species*. Pal amidase encoded by pneumococcal bacteriophage Dp-1 [48], PlyC from the streptococcal, and Cpl-1 encoded by the pneumococcal phage Cp-1 have been shown to be effective antimicrobial agents against *Streptococcus pneumoniae* [49]. Furthermore, phage EFAP-1-derived EFAL-1 endolysin has been shown to rapidly and potently lyse antibiotics-resistant enterococcal strains to control "disease-causing *Enterococcus* spp." [49]. One particular endolysin of interest in our research group is staphylococcal phage-K-derived endolysin, LysK which can be considered as perspective antimicrobial agent against *Staphylococcus aureus (S. aureus)*. LysK is a monomeric 495 amino acid protein, was first isolated in 2005, and it has been shown to be active against a broad spectrum of staphylococci including those of the most medical importance such as methicillin-resistant *S. aureus* (MRSA) and vancomycin-resistant *S. aureus* (VRSA) [50]. More recent studies of this lysin are focused primarily on its enzymatic properties [51]. This is of great importance in determining the optimal conditions of use as well as for future storage.

Recently, it has been shown that a newly developed chimeric endolysin called ClyS once purified is active against MRSA, vancomycin intermediate (VISA), and methicillin-sensitive (MSSA) strains of *S. aureus in vitro*. In addition, this lysin also proved to have synergistic interactions with both vancomycin and oxacillin *in vitro* and have synergistic protection of septic death *in vivo* against MRSA [52]. The i*n vivo* mouse studies were also promising where a nasal decolonization model demonstrated a 2-log reduction in viability of MRSA cells one hour following a single treatment with ClyS and one IP dose of ClyS also protected against death by MRSA in a mouse septicemia model [53]. Very similar results were reported on novel phage-derived enzyme "cysteine-histidine amino peptidase" with excellent anti-staphylococcal properties [54]. From these results additional treatment options have been suggested which combine antibiotic and phage therapy to fight against multi-drug resistant bacterial infections. However, most of the research and development of phage lysine technologies has been performed in a small scale, resulting in very few commercially available products to date. In fact, the true value of phage-derived antimicrobial agents will be unambiguously realized once these products enter into broad clinical application and commercial availability [45].

3. Immune Responses

It can be expected that humans have been exposed to several species of phage which begins shortly after birth, particularly those specific for human natural flora. The ongoing microbiome project has revealed that bacteria in our gut, skin, and other body cavities outnumber our human cells by a factor of at least 100 [55, 56]. The bacterial symbionts are likely to maintain their presence despite the dynamics of the intestine and the host immune system through their interaction with the mucus gel layer overlying the intestinal epithelium as well as a process for obtaining host tolerance [57]. Like eukaryotic

viruses, phages are nucleoproteinaceous in composition, comprised of a nucleic acid genome and encased within a protein coat and in some cases lipids within their capsids or even capsid envelopes. These proteins and DNA are recognized by mammalian hosts as foreign antigens, and as such phages stimulate an immune response that subjects them to neutralization and clearance by the host immune system [58]. The use of phage in the construction of elegant new therapeutics such as targeted gene delivery vehicles, anticancer agents, scFv carriers, and other clinical applications also requires the consideration of phage immunogenicity and circulation longevity in developing efficacious biologics [55–57]. In addition, there is a limited understanding and lack of data focusing on phage pharmacokinetics (PK) and pharmacodynamics [59], although some important effort has been lent toward modeling phage absorption, distribution, metabolism, and excretion (ADME) profiles [60]. Table 2 describes the advantages and disadvantages of using phage as nanomedicine in various fields. Many questions around the capabilities of phage to get into the circulatory system of higher organisms still remain as this determines the potential phage activity in nanomedicine and antibacterial treatment and will be addressed here [61]. This paper will focus mainly on host-mediated responses to phage therapy, discussing current knowledge of immunomodulatory effects of bacteriophage exposure and treatment modalities.

3.1. Antiphage Innate Immunity. The issue of bacteriophage interactions with the mammalian immune system and its components is still not precisely defined. Phages entering eukaryotic hosts are highly immunogenic foreign antigens that can interact with the innate immune system to induce specific humoral as well as cellular immune responses [65]. Evidence increasingly suggests that phages influence mammalian immune responses, including the attenuation of specific and nonspecific immune reactions, and maintenance of local immune tolerance to gut microorganism-derived antigens. Phage preparations administered orally may down regulate the antigen-processing abilities of intestinal dendritic cells, whereas phages administered intravenously are rapidly phagocytosed by liver cells [66]. Soluble CD14 and LPS-binding protein are major serum factors with the ability to bind pathogens and initiate innate immune responses. Although innate immunity cannot be entirely separated from its adaptive counterpart, for the purpose of clarity, we will also discuss antiphage immunity according to the mechanism(s) of neutralization and clearance.

3.1.1. Phage-Specific Innate Cellular Immune Responses

Pathogen-Associated Molecular Patterns (PAMPs). Host cells express pattern recognition receptors (PRRs) that sense pathogen-associated molecular patterns (PAMPs). PAMPs can also be recognized by a series of soluble pattern-recognition receptors in the blood that function as opsonins and can initiate the complement pathways. Most body defense cells have pattern-recognition receptors for these common PAMPS, and so there is an immediate response against the invading microorganism/phage. The best-characterized pattern-recognition receptors are Toll-like receptors (TLRs) [67–69], so named due to their homology to the Toll receptors, first discovered in *Drosophila*. TLR-2 was originally described to recognize LPS, a major constituent of the outer membrane of Gram-negative (G^-) bacteria, whereas later studies have identified TLR-4 as the central transmembrane component of the LPS receptor [70, 71]. TLR9 was first shown to recognize deoxycytidylate-phosphate-deoxyguanylate (CpG) regions in bacterial DNA and is now known to be important in defending against different viral and parasitic pathogens [72]. Abundant portions of unmethylated CpG dinucleotides (CpG motifs) that are found in prokaryotic (primarily bacterial) genomes as well as synthetic oligonucleotides [72, 73] containing CpG motifs have in recent years been shown to activate the innate immune system and can elicit a Th1-dominated response, resulting in release of a wide range of cytokines (IFN-γ, IL-2, IL-6, IL-18, and TNF-α) [74–76]. This discovery has opened door for research into the use of CpG motifs for the use as a powerful adjuvant for DNA vaccines and/or immunomodulatory agents not only to direct an adaptive long-lived immune response against pathogenic agents, but also to prevent unwanted Th2 humoral immune responses [76]. Moreover, CpG DNA also has the unique property of being able to connect the innate and adaptive immune responses through its ability to activate antigen-presenting cells (APCs). Macrophages, dendritic cells, and epithelial cells have a set of transmembrane receptors that recognize different types of PAMPs, which in turn lead to the expression of various cytokine genes (IL-12 which stimulates the production of Th1 cells, IL-23, which stimulates the production of Th17 cells, and IL-6) [68].

It is also known that the time of clearance (degradation/elimination) of bacteriophages in mammalian organisms depends on their surface protein properties [77]. Assuming that phage structural surface proteins are responsible for their recognition as foreign antigens and rapid clearance by the reticuloendothelial system (RES), attenuation of immunogenicity should thus be possible via alterations to these surface antigens. Employing this logic, Merril et al. devised an elegant strategy to decrease phage immunogenicity and increase the persistence of phages P22 and λ within mice [78]. This since patented system consists of growing phages on a mutator *E. coli* strain then serially passaging them through mice 10 times, each time selecting for residual phage that persist for several hours. This technique led to their isolation of λ capsid mutants that persisted for more than 18 hours [78]. Mutation(s) conferring RES evasion and prolonged persistence within the mouse were mapped to the λ *E* gene, a mono-hexameric major capsid protein. The success of this technique not only opens the door to the application of phage as longer-lasting, circulating biologics; but more fundamentally also strongly suggests that evasion of the RES through a single point mutation must mitigate clearance through a specific immunity mechanism; likely the prevention of opsonization and/or highly efficient antibody-mediated endocytosis. However, this technique has not been tested to retain function in

Table 2: Advantages and disadvantages of phages as nanomedicines.

Phage nanomedicine platform	Advantages	Disadvantages	Reference
Filamentous phages as drug-delivery platform	Targeted drug-conjugated filamentous phage nanoparticles are unique antibody-drug conjugates and they have been shown to inhibit target cells *in vitro* with a potentiation factor of 1000-fold over the corresponding free drug in one study.	The pharmacokinetics, the biodistribution, and the immunogenicity of conjugated phages are still under study. Repeated administration of phage results in amplified immune response and rapid neutralization and clearance of the phage.	[62]
Phage as antibacterial nanomedicines	Phages are effective against multidrug-resistant pathogenic bacteria; phage specificity prevents damage to original microflora; phages respond quickly to the appearance of resistant bacterial mutants; phages offer low scale-up costs; phages side effects are very rare compared to the antibiotic therapy. Due to the different mechanism of bactericidal action phage provide the opportunity for combined approaches with antibiotics improving antibacterial potency in some cases by up to 2×10^4-fold higher than antibiotic alone.	Bacterial cells may similarly build resistance against phage infection. Other barriers to infection include restriction or exclusion systems that block propagation. Phage may horizontally transfer toxicity between hosts via generalized or specialized transduction. Some of these barriers may be overcome by using a cocktail strategy, phage incapable of transduction, or genetic modification.	[27, 63]
Phages display of peptide as a targeted nanomedicine	Phages not only provide the basis to pan for potential peptides that bind a specific receptor but also can serve as a targeting nanomedicine platform to shuttle drugs and/or genes, or to specific cells, or modulate the activity of these receptors.	Potential for phage to confer immunogenicity against self antigens that are presented on surface of phage if similar to that found in the mammalian host.	[64]
	Landscape phage-based approach has decreased drawbacks compared to the chemical modified nanocarriers with cancer-selective peptides.	Localized targeting of tumour cells may not be sufficient for some phage-based antitumour strategies.	[15]

human subjects. Consistent with this, Molenaar et al. have shown that the specificity and delivery efficiency of the filamentous M13 phage into parenchymal and Kupffer cells of the liver with the incorporation of targeting ligands [29]. In their study they investigated the pharmacokinetics and processing of native and receptor-targeted phage in mice. S-radiolabeled M13 was chemically modified by conjugation of either galactose (lacM13) or succinic acid groups (sucM13) to the coat protein of the phage to stimulate uptake by galactose recognizing hepatic receptors and scavenger receptors, respectively. Receptor-mediated endocytosis of modified phage reduced the plasma half-life of native M13 ($t(1/2) = 4.5$ h) to 18 min for lactosylated and 1.5 min for succinylated bacteriophage. Internalization of sucM13 was complete within 30 min after injection and resulted in up to 5000-fold reduction of bioactive phage within 90 min.

Phagocytes/Macrophages. The ability of bacteriophages to reduce ROS production by polymorphonuclear leukocytes (PMNs) in the presence of bacteria or their endotoxins has been recently confirmed [43]. It has been shown that a purified T4 phage preparation with low-endotoxin content could significantly diminish the luminol-dependent chemiluminescence of peripheral blood polymorphonuclear leukocytes stimulated by lipopolysaccharide [43, 70]. It was suggested that phage-mediated inhibition of LPS- or bacteria-stimulated ROS production by PMNs may be attributed not only to phage-PMNs interactions but also to phage-LPS interactions and bacterial lysis [43]. Although the mechanism of phage inactivation by PMNs is not clearly understood, the involvement of hypochloric acid, a highly reactive metabolite generated during PMN stimulation, is likely involved. Hypocholoric acid likely imparts damage to the nucleic acids and capsid proteins alike, resulting in viral neutralization [31]. Decades earlier, Inchley [79] reported that T4 was almost completely cleared from mice by PMNs within 30 minutes of injection, and similar results of phage clearance have also demonstrated for T2, φX174, λ, and P22 [78, 80, 81]. While the RES is capable of rapid phage clearance, particularly in the thymus and the liver, significant titers of infective phage have also been rescued from the mouse spleen several days following inoculation, irrespective of the route of immunization [77, 79]. The relatively poor phagocytic activity of splenic macrophages may serve to preserve phage, allowing efficient viral sampling by B cells. The macrophage is critical component of innate immunity and front-line response against tissue invasion. Once activated, macrophages produce an assortment of microbicidal effectors and immunoregulatory cytokines that act to eliminate the invasion agent and influence the course of ensuing cognate immune response. The RES is comprised of pinocytic reticular and endothelial cells, and phagocytic monocytes and macrophages, and while pinocytosis may play a negligible role in RES clearance of phage, phagocytic cells account for rapid and significant removal of administered phage. Kupffer cells (specialized liver mononuclear

phagocytes) were shown to be the primary cells responsible for this activity in mice [79]. Bacteriophages applied intravenously (i.v.) to mice accumulated mainly in the liver at a rate 12 times greater than that seen in the spleen, but phage titers decreased much faster than those in other organs. Splenic macrophages also clear bacteriophages, but the action of these cells on phage clearance and degradation has been shown to be four times lower than that of the Kupffer cells [79]. Nelstrop et al. demonstrated that "immune" macrophages, obtained by laparotomy after prior immunization of rabbit by the investigated phage T1, inactivated bacteriophages faster than "nonimmune" ones. Furthermore, they showed that macrophages are capable of cellular immunity with no involvement of humoral factors, whereby clearance of phages was observed with no simultaneous detection of produced antibodies [82]. In naive, germ-free mice that had never been previously exposed to bacteria or bacteriophages (as such possessing no antibodies that could confound results), bacteriophages were shown to be rapidly cleared by the spleen, liver, and other filtering organs of the RES [6, 83].

Dendritic Cells. Apart from the above-mentioned key players of innate cellular immunity, dendritic cells (DCs) play a key role in the initiation of the immune response, mainly by priming T-cell- and antibody-mediated adaptive immunity [84]. The immunological activity of dendritic cells has been investigated for many years, and although *in vivo* experiments have demonstrated the phagocytic activity of these cells, verification of these observations *in vitro* has been difficultly proven. The endocytosis of latex microspheres by dendritic cells was probably the first convincing proof of the phagocytic abilities of these cells observed outside a living organism, and, unlike artificial particles, phagocytosis of bacteriophage T4 by dendritic cells appears to be far stronger [85]. Electron microscope images showed an agglomeration of viral particles around dendritic cells. Moreover, the phages seemed to be trapped in phagolysosomes and devoid of their outer coat during phagocytosis [85]. It has been demonstrated that DCs could affect host immune priming after both oral and i.v. phage administration. These cells prime T cells, for example, for IFN-gamma production, and they are applied as an adjuvant in antitumor therapies. DCs were shown to increase their antitumor action when stimulated by purified T4 phage preparations. In addition, it was demonstrated that *in vitro* interaction between T4 phages and bone-marrow-derived dendritic cells (BM-DCs) followed by tumor antigen activation modifies the immune response in tumor-bearing mice and leads to a significant delay in MC38 mouse colon carcinoma growth [65]. It is suggested that pretreatment of DCs with phages can be considered as beneficial and a novel strategy in antitumor immunotherapy.

3.1.2. Phage-Mediated Innate Humoral Immune Responses. Through the use of a T7-phage peptide display library, Sokoloff et al. found a correlation between the peptides displayed and survival of the phage in rat circulatory system. They noted that, in rat blood, peptides with carboxy-terminal lysine or arginine residues protected the phage against complement-mediated inactivation by binding C-reactive protein [86]. In contrast, phages resistant to inactivation in human serum were instead found to display C-terminal tyrosine residues. Unlike in rats, C-reactive protein is not elevated in humans [87], and the protective protein was suspected to be α2-macroglobulin. Kim et al. were the first to claim in their published research article that PEGylation can increase survival of infective phage by delaying immune responses and indicating that this approach can increase the efficacy of bacteriophage therapy. Their results show that PEGylation of phages can reduce cellular immune response such as antigen-specific T-cell proliferation, decreasing release of associated cytokines. In their work on both naïve and immunized mice, PEGylated Felix-O1 phage (i) decreased induction of Th1-associated cytokines such as IFN-γ and other cytokines such as IL-6, (ii) lowered splenocyte proliferation, which would be expected to support longer survival of modified phage particles, and did not affect phage stability [88]. Compared with the survival increases seen with the PEGylated phages, the increases in antigen-specific IgG production upon the second challenge with native phage were only marginal. In addition, no significant difference in survival of PEGylated or native Felix-O1 in immunized mice was found. It is suggested that more modification on the available PEGylation chemistry may improve the blood circulation in pre-immunized animals [89].

3.2. Antiphage Adaptive Immunity. A large portion of what we know to be adaptive immunity concerns the activation of complex pathways, more specifically those that are activated by the innate system and are memory dependent. In most cases T and B cells of the adaptive branch of immunity ultimately clear pathogens from the body and provide long-lived memory cells to prevent further activation or damage [90]. The activation of the complement cascade by cell surface recognition proteins or by secreted antibody results in the release complement cleavage products that interact with a wide range of cell surface receptors found on myeloid, lymphoid, and stromal cells. This intricate interaction among complement activation products and cell surface receptors provides a basis for the regulation of both B- and T-cell responses [91]. Three potential ways that the complement system can be activated prior to an acquired response by nonclonal means are the alternative pathway which recognizes surfaces lacking certain carbohydrates that are common to eukaryotic organisms, the classical pathway, which can be triggered by low-affinity "polyspecific" or cross-reactive IgM antibodies binding to repetitive epitopes that bacterial and viral surfaces characteristically present, and a pathway that is initiated by mannan-binding lectin [92]. A central protein of the complement system that provides a link between innate and adaptive immunity is C3, which is critical to immune defense. The above three pathways of complement activation converge at the activation of C3 yielding a diverse set of biological responses [93]. As foreign exogenous antigens, the administration of phage will generally induce a strong antiphage humoral response. Phage endocytosis by specialized antigen-presenting cells (APCs), whereby

immunogenic epitopes are presented to antigen-specific T-helper cells, will result in the formation of memory cells following primary immunization. This confers rapid and efficient neutralization and clearance of the antigen upon subsequent exposure. Bacteriophages circulating in the blood are inactivated by macrophages of the RES in synergy with antiphage antibodies—an outcome that would quickly diminish the efficacy of bacteriophage therapy upon subsequent exposures [28]. Repeated use of a phage as a therapeutic, in addition to the interactions with the innate immune system, would stimulate memory cells and result in the production of antibodies. Such activation of the adaptive immune system relies on somatic mutations and clonal expansion of T and B cells, which can take at least three to five days. Immunization with bacteriophage phiX174 has been used extensively to diagnose and monitor primary and secondary immunodeficiencies [62, 94]. Patients with a variety of conditions, including T-cell or T/B-cell interaction dysfunctions such as adenosine deaminase deficiency [95], X-linked immunodeficiency with hyper IgM and CD40 ligand deficiency [96], major histocompatibility complex class II deficiency [97], and HIV disease itself [98, 99] have been evaluated with this method. Patient immune responses to bacteriophage phiX174 immunization with T-cell or T/B-cell interaction deficiencies are characterized by abated or absent antibody titers after repeated immunizations as well as limited immunoglobulin isotype switching from IgM to IgG. In normal individuals injected with the highly immunogenic phage phiX174, the phage is normally cleared within three days and a primary immunoglobulin M response can be observed that peaks two weeks after the initial injection or immunization [100]. If another injection is made six weeks later, the IgM and IgG antibody titers increase and peak within one week of the second injection; subsequent phage injections result in further increases in the IgG titers. However, no detectable antibody response to phage, even after repeated injections was seen in patients with severe combined immune deficiency (SCID), which is characterized by the absence of both B and T cell functions. These patients also had prolonged phage circulation period [83]. Further, bacteriophage phiX174 immunization has been used to measure CD4 T cell function *in vivo* in human immunodeficiency virus (HIV)-infected patients across all disease stages and phiX174 immunization seems to be a useful tool for measuring immune function *in vivo* [101]. In this study, function was evaluated by measuring the ability of T cells to provide help to B cells in antibody production, amplification, and isotype switching. *In vivo* humoral responses to phage phiX174 have been used for more than 30 years in clinical immunology as a measure of T helper cell-dependent antibody production [73, 101, 102].

Interestingly, phage immunological responses may vary, in particular with respect to prior infection with host strains of bacteria. In patients with acute staphylococcal infection, antiphage antibody titer was reported to arise very strongly. The titers were particularly elevated during infections: a fourfold rise was observed within 6–14 days of acute staphylococcal infections, whereas a fall in the titer correlated with treatment and was usually slow and followed the clinical regression of the infection [103, 104]. Synnott et al. explored the possibility of oral administration of a recombinant T2 bacteriophage oral vaccine against *Salmonella typhimurium* in mice, where they fused segments of the *Salmonella* flagellin proteins FliC and FljB to the N terminal of the T2 SOC (small outer capsid protein) [105]. Over a 14-day period BALB/c mice were orally administered twice daily, either purified recombinant protein or fused T2 protein, then monitored for anti-FliCm or anti-FlijBm IgA production. No significant response was seen until day 33, with concentrations peaking 47 days after the initial administration and subsiding after 61 days. While they noted that 465 times less protein was displayed by the phage as compared to the recombinant protein dose, the degree of immune response was similar. This finding suggests that phage display increases the immunogenicity of the displayed protein, and in fact the phage particle could act as an adjuvant in clinical trials [105]. However, the mechanism by which a peptide displayed on a phage particle produces a greater immune response than a greater quantity of the same peptide in free form requires further investigation. In addition, there was a large variation between individual mice in a given group, with some showing no response at all. Mice administered with recombinant protein in particular showed a large disparity between three mice with no reaction, one with a moderate reaction, and one that had a huge reaction in this recent study and therefore requires verification from further studies.

3.3. Factors Affecting Phage Immune Responses. The nature of an immune response versus the formation of phage antigens is influenced by number of factors: (1) the physicochemical properties of the phage including the size and number of different surface epitopes, (2) the route of immunization; some routes tend to impart active immunity, while others confer tolerance, (3) the dose of phage administered; low doses of antigen have been shown to stimulate cell-mediated Th1 cytokine profiles while higher doses stimulate the Th2 pathway, (4) patient history of exposure; primary antibody response to phage in naive individuals would be much less efficient in clearing phage antigens than secondary exposure in primed individuals due to B-cell maturation, isotype switching, and affinity maturation; and (5) antibody and cytokine profile of—different isotypes impart different functions.

Given the intimate relation bacterial strains and their phage have with human, the large number of unstudied phage strains that are associated with the human microbiome and, in light of the recent studies, the available concerning phage interactions with animals and humans are still very limited and need further investigations for their advancing use as nanomedicine and as phage therapy.

4. Conclusion

Phage has come a long way since first being applied as antibacterials and is being revisited as with a serious eye in light of the upsurge of multi-drug-resistant clinical strains.

These versatile and malleable entities are further being engineered into new exciting phage-based therapeutics such as targeted gene-delivery vehicles and as anticancer agents. However, their usage in mammals requires careful consideration and understanding of the host-specific immune response when being applied as synergistic antibiotic cotherapeutics or replacements. Phage can and do interact with mammalian innate immunity to elicit specific humoral and cellular immune responses. Although efficient clearance of phage may be primarily mediated by the RES of innate immunity, adaptive responses to phage immunizations cannot be underestimated. Depending upon the phage display and structural surface proteins, attenuation of immunogenicity/tolerance and rapid clearance by the RES could potentially be modified via alterations to the highly immunogenic surface antigens. Repeated use of a phage as a therapeutic, in addition to the interactions with the innate immune system, stimulates memory cells and results in the production of antibodies. However, phage immunological responses may vary, in particular with respect to prior infection with host strains of bacteria, plus different phage strains may mediate different effects on the immune system. The immune response is mostly dose and time dependent; thus experimental conditions in phage therapy trials must be carefully monitored for variations in time, dose, and route of administration as well as presence of adjuvants and other immunogenic agents that all impact tolerance. Given the intimate relationship of phage with human's right from the birth, for phage therapy to develop into a viable clinical alternative, it will require far more rigorous and controlled investigation into host-specific immune responses.

Abbreviations

APCs: Antigen-presenting cells
CTL: Cytotoxic T lymphocytic
DCs: Dendritic cells
CpG: Deoxycytidylate-phosphate-deoxyguanylate
IFN-γ: Interferon gamma
ILs: Interleukins
Igs: Immunoglobulins
I.m.: Intramuscular
I.p.: Intraperitoneal
I.v.: Intravenous
LPS: Lipopolysaccharide
MDR: Multidrug resistant
NF-κB: Nuclear transcription factor
ODNs: Oligodinucleotides
PAMPs: Pathogen-associated molecular patterns
Pfu: Plaque forming unit
PK: Pharmacokinetics
PD: Pharmacodynamics
PMNs: Polymorphonuclear leukocytes
ROS: Reactive oxygen species
RES: Reticuloendothelial system
SCID: Severe combined immune deficiency
S.c.: Subcutaneous
TLRs: Toll-like receptors
TNF: Tumor necrosis factor.

Authors' Contribution

T. Kaur and N. Nafissi contributed equally to this work.

Conflict of Interests

The authors declare that there is no conflict of interests.

References

[1] F. W. Twort, "Further investigations on the nature of ultramicroscopic viruses and their cultivation," *The Journal of Hygiene (London)*, vol. 36, pp. 204–235, 1936.
[2] F. d'Herelle, "Technique de la recherche du microbe filtrant bactériophage (Bacteriophagum intestinale)," *Comptes Rendus des Seances de la Societe de Biologie Paris*, vol. 81, pp. 1060–1062, 1918.
[3] F. d'Herelle, "Sur un microbe invisible antagoniste des bacilles dysentériques," *Comptes Rendus de l'Académie des Sciences Paris*, vol. 165, pp. 373–375, 1917.
[4] J. R. Clark and J. B. March, "Bacteriophages and biotechnology: vaccines, gene therapy and antibacterials," *Trends in Biotechnology*, vol. 24, no. 5, pp. 212–218, 2006.
[5] J. Alisky, K. Iczkowski, A. Rapoport, and N. Troitsky, "Bacteriophages show promise as antimicrobial agents," *Journal of Infection*, vol. 36, no. 1, pp. 5–15, 1998.
[6] R. M. Carlton, "Phage therapy: past history and future prospects," *Archivum Immunologiae et Therapiae Experimentalis*, vol. 47, no. 5, pp. 267–274, 1999.
[7] T. L. Smith, M. L. Pearson, K. R. Wilcox et al., "Emergence of vancomycin resistance in *Staphylococcus aureus*. Glycopeptide-Intermediate *Staphylococcus aureus* Working Group," *The New England Journal of Medicine*, vol. 340, pp. 493–501, 1999.
[8] Y. Taj, F. E. Abdullah, and S. U. Kazmi, "Current pattern of antibiotic resistance in *Staphylococcus aureus* clinical isolates and the emergence of vancomycin resistance," *Journal of the College of Physicians and Surgeons Pakistan*, vol. 20, no. 11, pp. 728–732, 2010.
[9] A. Parisien, B. Allain, J. Zhang, R. Mandeville, and C. Q. Lan, "Novel alternatives to antibiotics: bacteriophages, bacterial cell wall hydrolases, and antimicrobial peptides," *Journal of Applied Microbiology*, vol. 104, no. 1, pp. 1–13, 2008.
[10] S. Matsuzaki, M. Rashel, J. Uchiyama et al., "Bacteriophage therapy: a revitalized therapy against bacterial infectious diseases," *Journal of Infection and Chemotherapy*, vol. 11, no. 5, pp. 211–219, 2005.
[11] S. Matsuzaki, M. Yasuda, H. Nishikawa et al., "Experimental protection of mice against lethal *Staphylococcus aureus* infection by novel bacteriophage ϕMR11," *Journal of Infectious Diseases*, vol. 187, no. 4, pp. 613–624, 2003.
[12] K. Szczaurska-Nowak, K. Dabrowska, M. Celka et al., "Antitumor effect of combined treatment of mice with cytostatic agents and bacteriophage T4," *Anticancer Research*, vol. 29, no. 6, pp. 2361–2370, 2009.
[13] B. R. Levin and J. J. Bull, "Population and evolutionary dynamics of phage therapy," *Nature Reviews Microbiology*, vol. 2, no. 2, pp. 166–173, 2004.
[14] B. Weber-Dabrowska, M. Zimecki, and M. Mulczyk, "Effective phage therapy is associated with normalization of cytokine production by blood cell cultures," *Archivum Immunologiae et Therapiae Experimentalis*, vol. 48, no. 1, pp. 31–37, 2000.

[15] T. Wang, G. G. Dsouza, D. Bedi et al., "Enhanced binding and killing of target tumor cells by drug-loaded liposomes modified with tumor-specific phage fusion coat protein," *Nanomedicine*, vol. 5, no. 4, pp. 563–574, 2010.

[16] M. Sarikaya, C. Tamerler, A. K. Y. Jen, K. Schulten, and F. Baneyx, "Molecular biomimetics: nanotechnology through biology," *Nature Materials*, vol. 2, no. 9, pp. 577–585, 2003.

[17] A. Sergeeva, M. G. Kolonin, J. J. Molldrem, R. Pasqualini, and W. Arap, "Display technologies: application for the discovery of drug and gene delivery agents," *Advanced Drug Delivery Reviews*, vol. 58, no. 15, pp. 1622–1654, 2006.

[18] T. Mori, "Cancer-specific ligands identified from screening of peptide-display libraries," *Current Pharmaceutical Design*, vol. 10, no. 19, pp. 2335–2343, 2004.

[19] L. R. H. Krumpe and T. Mori, "The use of phage-displayed peptide libraries to develop tumor-targeting drugs," *International Journal of Peptide Research and Therapeutics*, vol. 12, no. 1, pp. 79–91, 2006.

[20] D. Bedi, T. Musacchio, O. A. Fagbohun et al., "Delivery of siRNA into breast cancer cells via phage fusion protein-targeted liposomes," *Nanomedicine*, vol. 7, no. 3, pp. 315–323, 2011.

[21] C. G. Nicol, L. Denby, O. Lopez-Franco et al., "Use of in vivo phage display to engineer novel adenoviruses for targeted delivery to the cardiac vasculature," *FEBS Letters*, vol. 583, no. 12, pp. 2100–2107, 2009.

[22] A. Kurzepa, K. Dabrowska, G. Skaradziński, and A. Górski, "Bacteriophage interactions with phagocytes and their potential significance in experimental therapy," *Clinical and Experimental Medicine*, vol. 9, no. 2, pp. 93–100, 2009.

[23] J. R. Clark and J. B. March, "Bacterial viruses as human vaccines?" *Expert Review of Vaccines*, vol. 3, no. 4, pp. 463–476, 2004.

[24] J. R. Clark and J. B. March, "Bacteriophage-mediated nucleic acid immunisation," *FEMS Immunology and Medical Microbiology*, vol. 40, no. 1, pp. 21–26, 2004.

[25] J. B. March, J. R. Clark, and C. D. Jepson, "Genetic immunisation against hepatitis B using whole bacteriophage λ particles," *Vaccine*, vol. 22, no. 13-14, pp. 1666–1671, 2004.

[26] K. Dabrowska, A. Opolski, J. Wietrzyk et al., "Anticancer activity of bacteriophage T4 and its mutant HAP1 in mouse experimental tumour models," *Anticancer Research*, vol. 24, no. 6, pp. 3991–3995, 2004.

[27] E. Pajtasz-Piasecka, J. Rossowska, D. Duś, B. Weber-Dabrowska, A. Zabłocka, and A. Górski, "Bacteriophages support anti-tumor response initiated by DC-based vaccine against murine transplantable colon carcinoma," *Immunology Letters*, vol. 116, no. 1, pp. 24–32, 2008.

[28] W. Fortuna, R. Międzybrodzki, B. Weber-Dabrowska, and A. Górski, "Bacteriophage therapy in children: facts and prospects," *Medical Science Monitor*, vol. 14, no. 8, pp. RA126–RA132, 2008.

[29] T. J. M. Molenaar, I. Michon, S. A. M. de Haas, T. J. C. Van Berkel, J. Kuiper, and E. A. L. Biessen, "Uptake and processing of modified bacteriophage M13 in mice: implications for phage display," *Virology*, vol. 293, no. 1, pp. 182–191, 2002.

[30] S. S. de Almeida, A. A. C. Magalhães, S. C. Soares et al., "The phage display technique: advantages and recent patents," *Recent Patents on DNA and Gene Sequences*, vol. 5, no. 2, pp. 136–148, 2011.

[31] A. Kurzepa, K. Dabrowska, G. Skaradziński, and A. Górski, "Bacteriophage interactions with phagocytes and their potential significance in experimental therapy," *Clinical and Experimental Medicine*, vol. 9, no. 2, pp. 93–100, 2009.

[32] H. Bloch, "Experimental investigation on the relationships between bacteriophages and malignant tumors," *Archives of Virology*, vol. 1, pp. 481–496, 1940.

[33] M. Kantoch and M. Mordarski, "Binding of bacterial viruses by tumor cells in vitro," *Postępy Higieny i Medycyny Doświadczalnej*, vol. 12, no. 2, pp. 191–192, 1958.

[34] K. Dabrowska, A. Opolski, J. Wietrzyk et al., "Antitumor activity of bacteriophages in murine experimental cancer models caused possibly by inhibition of $\beta 3$ integrin signaling pathway," *Acta Virologica*, vol. 48, no. 4, pp. 241–248, 2004.

[35] K. Dabrowska, A. Opolski, J. Wietrzyk et al., "Activity of bacteriophages in murine tumor models depends on the route of phage administration," *Oncology Research*, vol. 15, no. 4, pp. 183–187, 2005.

[36] K. Dabrowska, M. Zembala, J. Boratynski et al., "Hoc protein regulates the biological effects of T4 phage in mammals," *Archives of Microbiology*, vol. 187, no. 6, pp. 489–498, 2007.

[37] T. Ohtsuki, H. Tsuda, and C. Morimoto, "Good or evil: CD26 and HIV infection," *Journal of Dermatological Science*, vol. 22, no. 3, pp. 152–160, 2000.

[38] F. Eriksson, P. Tsagozis, K. Lundberg et al., "Tumor-specific bacteriophages induce tumor destruction through activation of tumor-associated macrophages," *Journal of Immunology*, vol. 182, no. 5, pp. 3105–3111, 2009.

[39] M. Nishikawa, "Reactive oxygen species in tumor metastasis," *Cancer Letters*, vol. 266, no. 1, pp. 53–59, 2008.

[40] M. Nishikawa, M. Hashida, and Y. Takakura, "Catalase delivery for inhibiting ROS-mediated tissue injury and tumor metastasis," *Advanced Drug Delivery Reviews*, vol. 61, no. 4, pp. 319–326, 2009.

[41] A. Przerwa, M. Zimecki, K. Świtała-Jeleń et al., "Effects of bacteriophages on free radical production and phagocytic functions," *Medical Microbiology and Immunology*, vol. 195, no. 3, pp. 143–150, 2006.

[42] R. Miedzybrodzki, K. Switala-Jelen, W. Fortuna et al., "Bacteriophage preparation inhibition of reactive oxygen species generation by endotoxin-stimulated polymorphonuclear leukocytes," *Virus Research*, vol. 131, no. 2, pp. 233–242, 2008.

[43] B. Weber-Dabrowska, M. Mulczyk, and A. Gorski, "Bacteriophages as an efficient therapy for antibiotic-resistant septicemia in man," *Transplantation Proceedings*, vol. 35, no. 4, pp. 1385–1386, 2003.

[44] V. M. Victor, M. Rocha, J. V. Esplugues, and M. De la Fuente, "Role of free radicals in sepsis: antioxidant therapy," *Current Pharmaceutical Design*, vol. 11, no. 24, pp. 3141–3158, 2005.

[45] J. J. Gill, T. Hollyer, and P. M. Sabour, "Bacteriophages and phage-derived products as antibacterial therapeutics," *Expert Opinion on Therapeutic Patents*, vol. 17, no. 11, pp. 1341–1350, 2007.

[46] S. C. Becker, J. Foster-Frey, A. J. Stodola, D. Anacker, and D. M. Donovan, "Differentially conserved staphylococcal SH3b_5 cell wall binding domains confer increased staphylolytic and streptolytic activity to a streptococcal prophage endolysin domain," *Gene*, vol. 443, no. 1-2, pp. 32–41, 2009.

[47] M. J. Loessner, A. Schneider, and S. Scherer, "Modified Listeria bacteriophage lysin genes (ply) allow efficient overexpression and one-step purification of biochemically active fusion proteins," *Applied and Environmental Microbiology*, vol. 62, no. 8, pp. 3057–3060, 1996.

[48] J. Varea, B. Monterroso, J. L. Sáiz et al., "Structural and thermodynamic characterization of Pal, a phage natural chimeric lysin active against pneumococci," *The Journal of Biological Chemistry*, vol. 279, no. 42, pp. 43697–43707, 2004.

[49] D. Nelson, R. Schuch, P. Chahales, S. Zhu, and V. A. Fischetti, "PlyC: a multimeric bacteriophage lysin," *Proceedings of the National Academy of Sciences of the United States of America*, vol. 103, no. 28, pp. 10765–10770, 2006.

[50] S. O'Flaherty, R. P. Ross, W. Meaney, G. F. Fitzgerald, M. F. Elbreki, and A. Coffey, "Potential of the Polyvalent anti-Staphylococcus bacteriophage K for control of antibiotic-resistant staphylococci from hospitals," *Applied and Environmental Microbiology*, vol. 71, no. 4, pp. 1836–1842, 2005.

[51] L. Y. Filatova, S. C. Becker, D. M. Donovan, A. K. Gladilin, and N. L. Klyachko, "LysK, the enzyme lysing *Staphylococcus aureus* cells: specific kinetic features and approaches towards stabilization," *Biochimie*, vol. 92, no. 5, pp. 507–513, 2010.

[52] A. Daniel, C. Euler, M. Collin, P. Chahales, K. J. Gorelick, and V. A. Fischetti, "Synergism between a novel chimeric lysin and oxacillin protects against infection by methicillin-resistant *Staphylococcus aureus*," *Antimicrobial Agents and Chemotherapy*, vol. 54, no. 4, pp. 1603–1612, 2010.

[53] M. Pastagia, C. Euler, P. Chahales, J. Fuentes-Duculan, J. G. Krueger, and V. A. Fischetti, "A novel chimeric lysin shows superiority to mupirocin for skin decolonization of methicillin-resistant and -sensitive *Staphylococcus aureus* strains," *Antimicrobial Agents and Chemotherapy*, vol. 55, no. 2, pp. 738–744, 2011.

[54] M. Fenton, R. P. Ross, O. Mcauliffe, J. O'Mahony, and A. Coffey, "Characterization of the staphylococcal bacteriophage lysin CHAP K," *Journal of Applied Microbiology*, vol. 111, no. 4, pp. 1025–1035, 2011.

[55] A. Letarov and E. Kulikov, "The bacteriophages in human- and animal body-associated microbial communities," *Journal of Applied Microbiology*, vol. 107, no. 1, pp. 1–13, 2009.

[56] S. R. Gill, M. Pop, R. T. DeBoy et al., "Metagenomic analysis of the human distal gut microbiome," *Science*, vol. 312, no. 5778, pp. 1355–1359, 2006.

[57] J. L. Sonnenburg, L. T. Angenent, and J. I. Gordon, "Getting a grip on things: how do communities of bacterial symbionts become established in our intestine?" *Nature Immunology*, vol. 5, no. 6, pp. 569–573, 2004.

[58] A. S. Srivastava, T. Kaido, and E. Carrier, "Immunological factors that affect the in vivo fate of T7 phage in the mouse," *Journal of Virological Methods*, vol. 115, no. 1, pp. 99–104, 2004.

[59] B. L. Shacklett and P. A. Anton, "HIV infection and gut mucosal immune function: updates on pathogenesis with implications for management and intervention," *Current Infectious Disease Reports*, vol. 12, no. 1, pp. 19–27, 2010.

[60] R. J. H. Payne and V. A. A. Jansen, "Pharmacokinetic principles of bacteriophage therapy," *Clinical Pharmacokinetics*, vol. 42, no. 4, pp. 315–325, 2003.

[61] K. Dabrowska, K. Switała-Jelen, A. Opolski, B. Weber-Dabrowska, and A. Gorski, "A review: bacteriophage penetration in vertebrates," *Journal of Applied Microbiology*, vol. 98, no. 1, pp. 7–13, 2005.

[62] H. D. Ochs, S. D. Davis, and R. J. Wedgwood, "Immunologic responses to bacteriophage phi-X 174 in immunodeficiency diseases," *Journal of Clinical Investigation*, vol. 50, no. 12, pp. 2559–2568, 1971.

[63] I. Yacoby, H. Bar, and I. Benhar, "Targeted drug-carrying bacteriophages as antibacterial nanomedicines," *Antimicrobial Agents and Chemotherapy*, vol. 51, no. 6, pp. 2156–2163, 2007.

[64] S. M. Moghimi, A. C. Hunter, and J. C. Murray, "Nanomedicine: current status and future prospects," *FASEB Journal*, vol. 19, no. 3, pp. 311–330, 2005.

[65] E. Pajtasz-Piasecka, J. Rossowska, D. Duś, B. Weber-Dabrowska, A. Zabłocka, and A. Górski, "Bacteriophages support anti-tumor response initiated by DC-based vaccine against murine transplantable colon carcinoma," *Immunology Letters*, vol. 116, no. 1, pp. 24–32, 2008.

[66] A. Górski, E. Wazna, B. W. Dabrowska, K. Dabrowska, K. Świtała-Jeleń, and R. Międzybrodzki, "Bacteriophage translocation," *FEMS Immunology and Medical Microbiology*, vol. 46, no. 3, pp. 313–319, 2006.

[67] H. An, C. Qian, and X. Cao, "Regulation of Toll-like receptor signaling in the innate immunity," *Science China Life Sciences*, vol. 53, no. 1, pp. 34–43, 2010.

[68] L. Diacovich and J. P. Gorvel, "Bacterial manipulation of innate immunity to promote infection," *Nature Reviews Microbiology*, vol. 8, no. 2, pp. 117–128, 2010.

[69] R. Ostuni, I. Zanoni, and F. Granucci, "Deciphering the complexity of Toll-like receptor signaling," *Cellular and Molecular Life Sciences*, vol. 67, no. 24, pp. 4109–4134, 2011.

[70] K. Hoshino, O. Takeuchi, T. Kawai et al., "Cutting edge: toll-like receptor 4 (TLR4)-deficient mice are hyporesponsive to lipopolysaccharide evidence for TLR4 as the Lps gene product," *Journal of Immunology*, vol. 162, no. 7, pp. 3749–3752, 1999.

[71] R. B. Yang, M. R. Mark, A. Gray et al., "Toll-like receptor-2 mediates lipopolysaccharide-induced cellular signalling," *Nature*, vol. 395, no. 6699, pp. 284–288, 1998.

[72] S. Bauer, C. J. Kirschning, H. Häcker et al., "Human TLR9 confers responsiveness to bacterial DNA via species-specific CpG motif recognition," *Proceedings of the National Academy of Sciences of the United States of America*, vol. 98, no. 16, pp. 9237–9242, 2001.

[73] A. Rubinstein, Y. Mizrachi, L. Bernstein et al., "Progressive specific immune attrition after primary, secondary and tertiary immunizations with bacteriophage ϕX174 in asymptomatic HIV-1 infected patients," *AIDS*, vol. 14, no. 4, pp. F55–F62, 2000.

[74] K. L. Elkins, T. R. Rhinehart-Jones, S. Stibitz, J. S. Conover, and D. M. Klinman, "Bacterial DNA containing CpG motifs stimulates lymphocyte-dependent protection of mice against lethal infection with intracellular bacteria," *Journal of Immunology*, vol. 162, no. 4, pp. 2291–2298, 1999.

[75] K. Heeg and S. Zimmermann, "CpG DNA as a Th1 trigger," *International Archives of Allergy and Immunology*, vol. 121, no. 2, pp. 87–97, 2000.

[76] A. M. Krieg, "The role of CpG motifs in innate immunity," *Current Opinion in Immunology*, vol. 12, no. 1, pp. 35–43, 2000.

[77] M. R. Geier, M. E. Trigg, and C. R. Merril, "Fate of bacteriophage lambda in non immune germ free mice," *Nature*, vol. 246, no. 5430, pp. 221–223, 1973.

[78] C. R. Merril, B. Biswas, R. Carlton et al., "Long-circulating bacteriophage as antibacterial agents," *Proceedings of the National Academy of Sciences of the United States of America*, vol. 93, no. 8, pp. 3188–3192, 1996.

[79] C. J. Inchley, "The actvity of mouse Kupffer cells following intravenous injection of T4 bacteriophage," *Clinical and Experimental Immunology*, vol. 5, no. 1, pp. 173–187, 1969.

[80] C. J. Inchley and J. G. Howard, "The immunogenicity of phagocytosed T4 bacteriophage: cell replacement studies with splenectomized and irradiated mice," *Clinical and Experimental Immunology*, vol. 5, no. 1, pp. 189–198, 1969.

[81] J. W. Uhr and G. Weissman, "Intracellular distribution and degradation of bacteriophage in mammalian tissues," *The Journal of Immunology*, vol. 94, pp. 544–550, 1965.

[82] A. E. Nelstrop, G. Taylor, and P. Collard, "Studies on phagocytosis. II. In vitro phagocytosis by macrophages," *Immunology*, vol. 14, no. 3, pp. 339–346, 1968.

[83] C. R. Merril, D. Scholl, and S. L. Adhya, "The prospect for bacteriophage therapy in Western medicine," *Nature Reviews Drug Discovery*, vol. 2, no. 6, pp. 489–497, 2003.

[84] A. M. Cuesta, E. Suarez, M. Larsen et al., "Enhancement of DNA vaccine potency through linkage of antigen to filamentous bacteriophage coat protein III domain I," *Immunology*, vol. 117, no. 4, pp. 502–506, 2006.

[85] R. Barfoot, S. Denham, L. A. Gyure et al., "Some properties of dendritic macrophages from peripheral lymph," *Immunology*, vol. 68, no. 2, pp. 233–239, 1989.

[86] A. V. Sokoloff, I. Bock, G. Zhang, M. G. Sebestyén, and J. A. Wolff, "The interactions of peptides with the innate immune system studied with use of T7 phage peptide display," *Molecular Therapy*, vol. 2, no. 2, pp. 131–139, 2000.

[87] R. Miedzybrodzki, W. Fortuna, B. Weber-Dabrowska, and A. Gorski, "A retrospective analysis of changes in inflammatory markers in patients treated with bacterial viruses," *Clinical and Experimental Medicine*, vol. 9, no. 4, pp. 303–312, 2009.

[88] K. P. Kim, J. D. Cha, E. H. Jang et al., "PEGylation of bacteriophages increases blood circulation time and reduces T-helper type 1 immune response," *Microbial Biotechnology*, vol. 1, no. 3, pp. 247–257, 2008.

[89] M. A. Croyle, N. Chirmule, Y. Zhang, and J. M. Wilson, "PEGylation of E1-deleted adenovirus vectors allows significant gene expression on readministration to liver," *Human Gene Therapy*, vol. 13, no. 15, pp. 1887–1900, 2002.

[90] J. Zhang, X. Xiao, W. Liu, G. Demirci, and X. C. Li, "Inhibitory receptors of the immune system: functions and therapeutic implications," *Cellular and Molecular Immunology*, vol. 6, no. 6, pp. 407–414, 2009.

[91] M. C. Carroll, "The complement system in regulation of adaptive immunity," *Nature Immunology*, vol. 5, no. 10, pp. 981–986, 2004.

[92] D. T. Fearon, "The complement system and adaptive immunity," *Seminars in Immunology*, vol. 10, no. 5, pp. 355–361, 1998.

[93] B. J. C. Janssen and P. Gros, "Structural insights into the central complement component C3," *Molecular Immunology*, vol. 44, no. 1–3, pp. 3–10, 2007.

[94] R. J. Wedgwood, H. D. Ochs, and S. D. Davis, "The recognition and classification of immunodeficiency diseases with bacteriophage phiX 174," *Birth Defects*, vol. 11, no. 1, pp. 331–338, 1975.

[95] H. D. Ochs, R. H. Buckley, R. H. Kobayashi et al., "Antibody responses to bacteriophage ϕX174 in patients with adenosine deaminase deficiency," *Blood*, vol. 80, no. 5, pp. 1163–1171, 1992.

[96] K. Seyama, S. Nonoyama, I. Gangsaas et al., "Mutations of the CD40 ligand gene and its effect on CD40 ligand expression in patients with X-linked hyper IgM syndrome," *Blood*, vol. 92, no. 7, pp. 2421–2434, 1998.

[97] S. Nonoyama, A. Etzioni, H. Toru et al., "Diminished expression of CD40 ligand may contribute to the defective humoral immunity in patients with MHC class II deficiency," *European Journal of Immunology*, vol. 28, no. 2, pp. 589–598, 1998.

[98] L. J. Bernstein, H. D. Ochs, R. J. Wedgwood, and A. Rubinstein, "Defective humoral immunity in pediatric acquired immune deficiency syndrome," *Journal of Pediatrics*, vol. 107, no. 3, pp. 352–357, 1985.

[99] H. D. Ochs, A. K. Junker, A. C. Collier, F. S. Virant, H. H. Handsfield, and R. J. Wedgwood, "Abnormal antibody responses in patients with persistent generalized lymphadenopathy," *Journal of Clinical Immunology*, vol. 8, no. 1, pp. 57–63, 1988.

[100] I. R. Cohen and L. C. Norins, "Antibiodies of the IgG, IgM, and IgA classes in newborn and adult sera reactive with gram-negative bacteria," *Journal of Clinical Investigation*, vol. 47, no. 5, pp. 1053–1062, 1968.

[101] I. Fogelman, V. Davey, H. D. Ochs et al., "Evaluation of CD4+ T cell function in vivo in HIV-infected patients as measured by bacteriophage phiX174 immunization," *Journal of Infectious Diseases*, vol. 182, no. 2, pp. 435–441, 2000.

[102] W. T. Shearer, D. J. Lugg, H. M. Rosenblatt et al., "Antibody responses to bacteriophage ϕX-174 in human subjects exposed to the Antarctic winter-over model of spaceflight," *Journal of Allergy and Clinical Immunology*, vol. 107, no. 1, pp. 160–164, 2001.

[103] S. A. Hedstrom and C. Kamme, "Antibodies against staphylococcal bacteriophages in human sera. II. Assay of antibodies in exacerbation and regression of chronic staphylococcal osteomyelitis," *Acta Pathologica et Microbiologica Scandinavica—Section B*, vol. 81, no. 6, pp. 749–752, 1973.

[104] C. Kamme, "Antibodies against staphylococcal bacteriophages in human sera. I. Assay of antibodies in healthy individuals and in patients with staphylococcal infections," *Acta Pathologica et Microbiologica Scandinavica—Section B*, vol. 81, no. 6, pp. 741–748, 1973.

[105] A. Synnott, K. Ohshima, Y. Nakai, and Y. Tanji, "IgA response of BALB/c mice to orally administered *Salmonella typhimurium* flagellin-displaying T2 bacteriophages," *Biotechnology Progress*, vol. 25, no. 2, pp. 552–558, 2009.

Hindawi Publishing Corporation
Journal of Nanotechnology
Volume 2012, Article ID 843170, 9 pages
doi:10.1155/2012/843170

Review Article

Tipping the Proteome with Gene-Based Vaccines: Weighing in on the Role of Nanomaterials

Kristin J. Flores,[1] Michael Craig,[1] Adam Wanekaya,[2] Lifeng Dong,[3] Kartik Ghosh,[3] Joshua J. Smith,[1] and Robert K. DeLong[1]

[1] *Department Biomedical Sciences, Missouri State University, Cell and Molecular Biology Program, Professional Building, Springfield, MO 65897, USA*
[2] *Department Chemistry, Missouri State University, Temple Hall, Springfield, MO 65897, USA*
[3] *Department Physics, Astronomy & Materials Science, Missouri State University, Kemper Hall, Springfield, MO 65897, USA*

Correspondence should be addressed to Kristin J. Flores, kristin377@live.missouristate.edu

Received 16 June 2011; Accepted 9 November 2011

Academic Editor: Chunying Chen

Since the first generation of DNA vaccines was introduced in 1988, remarkable improvements have been made to improve their efficacy and immunogenicity. Although human clinical trials have shown that delivery of DNA vaccines is well tolerated and safe, the potency of these vaccines in humans is somewhat less than optimal. The development of a gene-based vaccine that was effective enough to be approved for clinical use in humans would be one of, if not the most important, advance in vaccines to date. This paper highlights the literature relating to gene-based vaccines, specifically DNA vaccines, and suggests possible approaches to boost their performance. In addition, we explore the idea that combining RNA and nanomaterials may hold the key to successful gene-based vaccines for prevention and treatment of disease.

1. Introduction

Gene-based vaccines have been extensively studied in recent years in the hope of unlocking their potential as preventative or therapeutic tools against infectious diseases, cancer, autoimmune diseases, and other conditions resulting from molecular defects. An ideal vaccine is safe, highly immunogenic, nonintegrating, easy to manipulate, stable, and inexpensive to produce. In addition to these characteristics, a therapeutic vaccine must not be compromised by any preexisting immunity of the patient against the vaccine delivery vehicle [1–5].

Gene-based vaccines approach this ideal and demonstrate several advantages over conventional vaccines. However, gene-based vaccines, specifically DNA vaccines, have produced disappointing results in human clinical trials, suggesting that there is something missing from this puzzle. The gene-based approach requires a performance boost before these vaccines will be suitable for the clinic. One approach may be to explore the benefits of using RNA vaccines rather than DNA vaccines. This approach raises the issue of stability and delivery, which in turn suggests potential roles for nanomaterials as vital components in gene-based vaccines.

Nanomaterials harness the power to act as stabilizing delivery vehicles for gene-based vaccines. With their small size and large surface area, nanomaterials have the ability to deliver a high payload of DNA or RNA [6], thus increasing the efficacy of gene-based vaccines. Among the most common nanomaterials studied for vaccine delivery are metallic and magnetic nanoparticles, nanoliposomes, and dendrimers [7]. This paper touches on the recent developments in gene-based vaccines and their advantages in terms of inducing both a cellular and humoral response. The idea that RNA, along with nanomaterials, could play a critical role in the development of the ideal gene-based vaccine is also discussed, as well as the nanomaterials' potential advantage in terms of binding, stabilization, and delivery.

2. Overview of Current Approaches in Vaccines

Conventional vaccines are composed of recombinant proteins, live-attenuated viruses, purified bacterial or virus components, or conjugates of proteins with polysaccharide carriers [3]. These vaccines have a long track record and have been widely used to eradicate numerous infectious diseases, such as smallpox, poliomyelitis, and diphtheria [8]. However, conventional vaccines suffer from numerous problems. For example, recombinant protein vaccines are extremely costly to produce, often tedious to purify, and do not effectively induce $CD8^+$ T cells [3, 4]. Conventional vaccines that employ recombinant viruses have their own risks, including reversion, inadvertent spread of infection, insertional mutagenesis, and the induction of autoimmunity [3–5]. In addition to these risks, there are numerous diseases for which conventional vaccines are not effective; alternatively, gene-based vaccines demonstrate tremendous promise in several of these areas, including cancer [7, 9], tuberculosis [10, 11], HIV [12], and malaria [13, 14].

3. DNA Vaccines

3.1. Delivery. The concept behind DNA vaccines was developed by Wolff et al. using reporter genes to show that the types of cells that are transfected are dependent on the route and method of delivery [15]. DNA vaccines can be delivered to cells by several different routes, including, but not limited to, intramuscular, intraepidermal, intravenous, intranasal, oral, and subcutaneous delivery [1, 4, 16, 17]. Delivery methods are numerous and include injection, tattooing, particle-mediated biolistic bombardment, electroporation, laser, and ultrasound. Intramuscular injection is the most common method, which leads predominantly to transfection of myocytes [4, 15, 17, 18].

In the search for a delivery method that induces a stronger immune response, much attention has been given to particle-mediated biolistic bombardment via the gene gun. For this method, recombinant plasmid DNA, containing the gene coding for a specific antigen, is affixed to an inert particle, such as a gold microparticle, and forced into the target cells by high-pressure gun. Delivery by the gene gun has been employed in the direct transfection of epidermal keratinocytes, Langerhans cells, and dendritic cells [19, 20]. Studies performed by Mendez et al. demonstrated that the DNA vaccine dosage required to induce full protection in mice challenged with *Leishmania major* was five times smaller using the gene gun than subcutaneous or intramuscular injection [21]. Interestingly, another study reported that approximately 100-fold less DNA is required for an equivalent immune response than that achieved with needle injection in mice [22]. Both these studies clearly indicate that the efficacy of DNA vaccines is improved when delivered by particle-mediated biolistic techniques rather than by intramuscular injection.

3.2. Mechanism of Action. Although the exact mechanisms and pathways are still under investigation, DNA vaccines are believed to be relatively simple tools for transfection, leading to antigen production with the ultimate goal of an immune response. The plasmid DNA that encodes the desired antigen is under the control of a mammalian promoter and can be produced seamlessly in bacteria [23]. The optimized, desired gene sequence is delivered by one of several methods, and the plasmid is transported to the nucleus where it uses the host's transcriptional and translational machinery to produce the desired protein product. Proteases cleave the protein into peptides, which can be presented subsequently by the MHC class I molecules to induce the $CD8^+$ T lymphocytes [3, 4, 24, 25]. The dendritic cells endocytose then express the antigen via MHC class I and MHC class II molecules, thereby inducing both the $CD4^+$ and $CD8^+$ T lymphocyte populations [19, 20]. The major advantage of this vaccination approach is endogenous expression of the encoded antigen, resulting in either direct processing of the protein in an antigen presenting cell or in cross-presentation, as illustrated in Figure 1 [19–29].

3.3. Potential Issues. The general consensus in the current literature is that DNA vaccines are considered safe because they are not living and do not replicate. Yet there are a few concerns that have been raised, such as the induction of autoimmunity against the patient's DNA [23, 30], as well as undirected integration, which may lead to insertional mutagenesis by inducing oncogenes or silencing tumor suppressor genes [16, 31]. During plasmid production, antibiotic resistance genes are used as a selection tool, and this use has raised concern that antibiotic resistance could be transferred to the patient's enteric bacteria [16, 32]. To eliminate this concern entirely, there are other selection methods that are available, including auxotrophy complementation [33], repressor titration [34], and protein-based antidote/poison selection strategies [35]. Despite these concerns, DNA vaccines have an impeccable safety record in preclinical work and clinical trials [16, 23]. It is because of this record that these potential safety concerns, although closely monitored, have become secondary to the attempts to enhance the efficacy and immunogenicity of DNA vaccines.

3.4. Enhancing DNA Vaccines. There are many possible approaches to enhancing the efficacy and immunogenicity. As previously mentioned, the route and method of delivery can have a profound effect on the outcome of vaccination. Codon optimization, promoter sequences, introns, enhancers, polyadenylation signals, and unmethylated cytosine-guanine dinucleotide (CpG) repeats can be modified within the plasmid to yield maximum expression of the protein product [32, 36–41]. Another popular option is using formulation adjuvants. The most common of these include proteins, conjugates of small molecules, liposomes, and micro- and nanoparticles [3, 6, 7]. The answer to the problem of enhancing the efficacy and immunogenicity of DNA vaccines likely resides in a novel combined approach. The goal is to enhance the benefits by an effective delivery system combined with various adjuvants. Nanomaterials, which can act as both the delivery vehicle and stabilizing

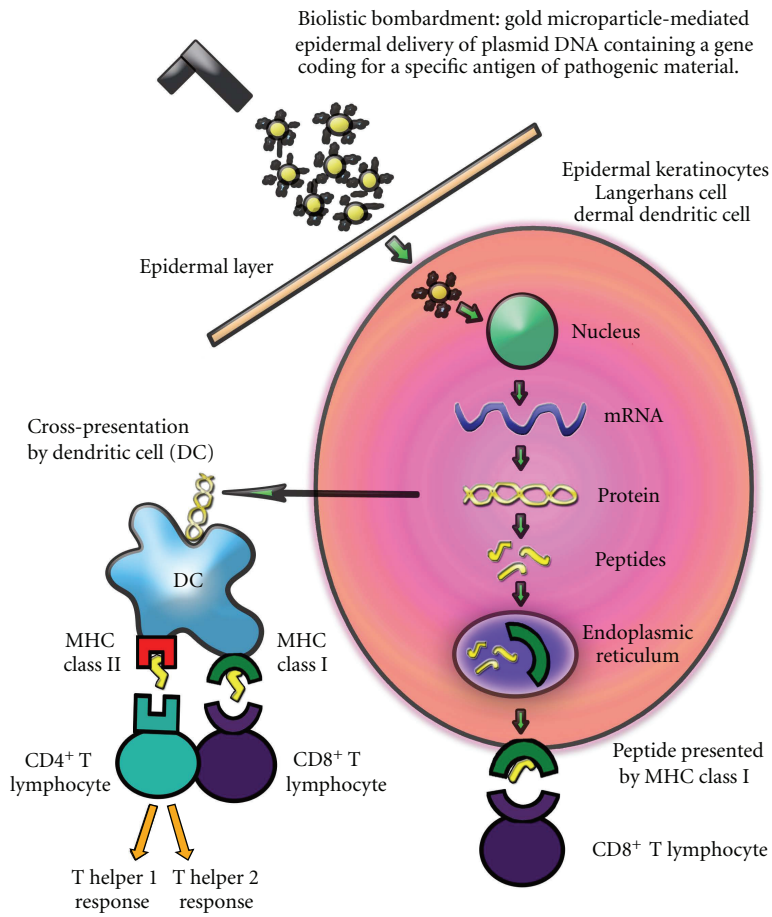

Figure 1: Basic mechanism of action for DNA vaccines delivered by particle-mediated biolistic bombardment and the resulting immune response. Using DNA attached to the gold particles provides increased stability and higher payload, and the dosage requirement is significantly lower than that for intramuscular injection.

adjuvant [7, 42], are likely to play a crucial role and will be discussed later.

4. RNA Vaccines

4.1. Simplified Mechanism of Action. One major advantage of RNA vaccines is that the RNA acts in the cytoplasm and is translated directly to proteins, therefore bypassing nuclear localization and transcription necessary for DNA vaccines [3, 4]. Just as in DNA vaccines, RNA vaccines activate both the cellular and humoral pathways of the immune response [42–52]. Other advantages of RNA are that it is easily degraded and is rapidly cleared from the tissue, resulting in greater control of the outcome [47]. This situation is in contrast to DNA vaccines that carry the risk of insertional mutagenesis, thus altering the host cell gene expression in an undesirable and uncontrollable fashion.

A substantial amount of research exists regarding the use of RNA in diverse forms, including messenger RNA, short interfering RNA, and splice-site switching oligomers [42–52], some of which are discussed later in this paper. There has also been a surge in the interest in double-stranded RNA, especially polyinosinic:polycytidilic acid, also known as poly I:C. Poly I:C is a promising adjuvant for vaccines, especially cancer, since it is a potent immunostimulant and powerful activator of the toll-like receptor-3 (TLR3) and melanoma differentiation-associated protein-5 (MDA5) [42, 53].

4.2. Stability in Storage and Delivery. Another widespread concern is that RNA is too unstable for storage and delivery to be an effective player in gene therapy. Although RNA is unstable, new evidence shows that it may be better suited for vaccines than researchers had originally thought [43, 44]. Just as the difficulties pertaining to RNA stability during storage are being solved, solutions to problems associated with stability during delivery are being addressed. Although a few studies have demonstrated that even unprotected RNA may be able to induce cytotoxic T lymphocyte responses in patients [5, 51–55], there are ongoing efforts to stabilize RNA molecules in order to make delivery more efficient and enhance the effect.

RNA vaccines avoid many of the potential problems with DNA vaccines, and they require a less complicated pathway to exert their effect. RNA vaccines may very well

be essential to the success of future vaccine strategies for fighting infectious diseases, cancer, and other conditions caused by molecular defects. However, just as with DNA vaccines, there are some difficulties that need to be overcome before RNA vaccines can be optimized into the ideal gene-based vaccine. Stability and delivery are the main targets for optimization, and nanomaterials offer promising candidates for these targets.

5. Nanomaterials: The Missing Piece to the Puzzle

The term nanomaterials encompasses a broad and fascinating range of molecules and compounds. However, for the purposes of this paper, the focus will be on select nanomaterials with the ability to enhance the delivery and effect of gene-based vaccines, especially RNA vaccines. Due to their unique physicochemical properties, nanomaterials are promising platforms for gene-based vaccines. They offer many biomedical advantages, including increased stability, efficient delivery, desirable biodistribution, and specific cell targeting, just to name a few [53]. The uptake of nanomaterials by cells, specifically cells of the immune system, is influenced by numerous factors [53, 56–60]. Different nanomaterials and their distinct characteristics, such as size, morphology, and surface chemistry, play a role in the specific internalization pathway, the effect of the nanomaterial on the cell, and its biodistribution [56–59].

There are numerous approaches and advantages for nanomaterial-mediated delivery of nucleic acids. Compared to viral delivery systems for gene-based vaccines, nanomaterial-mediated delivery systems offer a higher payload and greater stabilization potential. Often when nanomaterials are complexed with biomolecules, the result is an improvement in stability, biocompatibility, and retention of other desirable characteristics for both the nanoparticle and the biomolecule [42, 55]. These improvements are important for delivery into the body where exposure to physiological fluids, nucleases, and other biological components create endless obstacles for the nanomaterial:nucleic acid complex to reach its target.

5.1. Gold Nanoparticles. Like DNA vaccines, RNA can be affixed onto functionalized gold micro- or nanoparticles and delivered by particle-mediated biolistic bombardment [48, 56, 57]. The surface of the gold can be functionalized with specific tumor targeting agents, which are often a ligand for a specific receptor on the target cell surface not expressed on other cells. This targeting agent increases the transfection efficiency of the vaccine. Qui et al. used the functionalized gold particle-mediated gene gun to deliver three different mRNA molecules into several tissue types. Protein expression from RNA transcripts of the three reporter genes was detected after *in vitro* delivery in monolayer and suspension cell cultures, and in rat liver tissues, mouse liver, and epidermal tissues after *in vivo* delivery [48].

Experiments performed by Sandhu et al. indicate that gold nanoparticles were eight times more efficient at condensing and delivering nucleic acid compared to the commonly used polyethyleneimine polymer [57]. Protamine, an arginine-rich protein, can be used in conjunction with the RNA and gold nanoparticles. Protamine, which is necessary for DNA condensation in spermatogenesis, also enhances the stability of the RNA and protects it from degradation by RNases by condensing the RNA into a nanoparticle. In addition to its function as a stabilizer for RNA, protamine is known to be a cell-penetrating molecule and acts as a strong danger signal to the immune system, activating the immune response through a MyD-88-dependent pathway [46]. Delong et al. reported that combining the nucleic acid: protamine complex with gold nanoparticles forms a nanocomplex that can be analyzed by dynamic laser light scattering particle analysis (DLLS), gel shift mobility assays, and fluorescence [55]. In other work, the researchers reported that the RNA structure and vaccine bioactivity were retained even after exposure to physical, chemical, and thermal degradation. They demonstrated that the biological activity of the RNA was conserved by using a splice-site switching assay and delivering siRNA against a key cancer target, B-Raf [55]. A schematic of the nanocomplex formation for siRNA delivery is shown in Figure 2. It is important to note that condensing the RNA with protamine and attaching it to gold nanoparticles may be useful for numerous types of RNA, including siRNA, antisense RNA, and messenger RNA.

5.2. Nanoliposomes. Another common method of stabilization is to use liposomes, or nanoliposomes, as protective carriers of nucleic acids. Liposomes are cationic lipids that form stable complexes with negatively charged nucleic acids through electrostatic interactions [49]. The association of nucleic acids with lipids or polymers results in positively charged particles small enough for entry through the negatively charged plasma membrane by endocytosis, resulting in the formation of a double-bilayer vesicle. In the process of maturation of the endosome into a lysosome, the endosome may rupture, and the nucleic acid cargo could be released into the cytoplasm. Translocation to the nucleus might result in gene expression for DNA [49–51]. In addition to cellular entry by endocytosis, as illustrated in Figure 3, nanoliposomes may also fuse with the membrane and unload their cargo directly into the cytosol.

Changes in the surface charge on nanoliposomes can improve delivery and cellular uptake. Liposomes themselves can be immunostimulatory, a characteristic that could enhance the immunogenicity of the vaccine, or they can be coated with a polymer, such as derivatives of polyethylene glycol and others, to prevent recognition by the immune system [3, 7, 50, 51]. The data suggest that antigen-presenting cells are better able to sequester nanoliposomes than larger-sized liposomes. Cationic liposomes are much more potent in eliciting an immune response than anionic or neutral liposomes. The surface of the liposome can also be modified with various ligands to allow targeting to specific tissues or cells [49, 50].

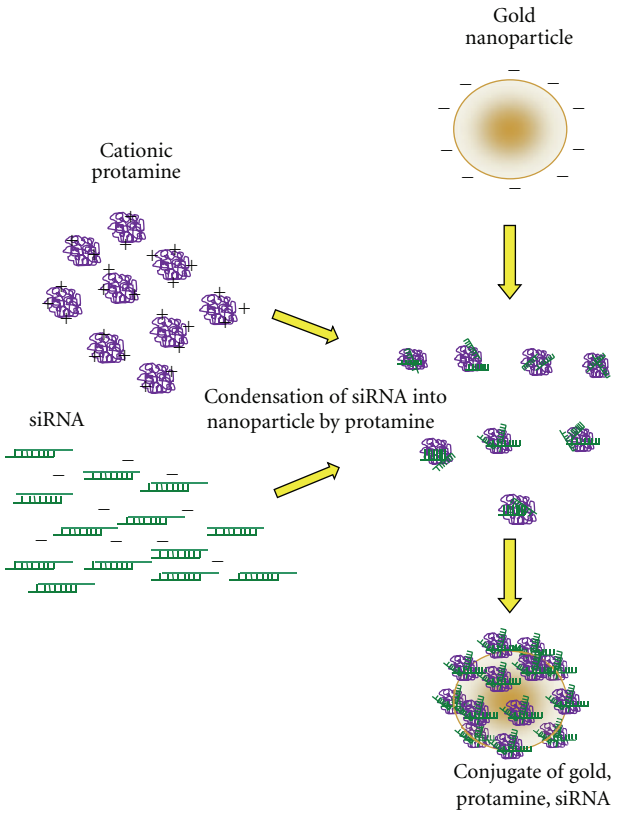

Figure 2: Graphical representation of the formation of complexes between gold nanoparticles, protamine, and siRNA. The cationic protamine condenses the RNA into nanoparticles, assisting its stabilization and protecting it from degradation. The protamine: RNA complexes then bind to the surface of the gold nanoparticle, which confers more stability and protection.

5.3. Dendrimers. Dendrimers are highly branched synthetic polymers with a high-density positive surface charge. Polyamidoamine (PAMAM) dendrimers are able to condense nucleic acids into a nanoparticle; such condensation has been shown to protect them from nuclease degradation [7, 55]. Dendrimers are also known to be cell-penetrating molecules. There are different generations of PAMAM dendrimers, and this parameter, along with the size-to-charge ratio, is important in the formation of stable nanoparticles [61]. An increase in the PAMAM dendrimer generation has been correlated to an increase in the delivery efficiency, yet it is well-known that the higher generation dendrimers are also cytotoxic [59–65]. The nucleic acid binding characteristics must be carefully balanced with the cytotoxicity, often executed by functionalization of the dendrimer branches. An example of this functionalization is amine acetylation of PAMAM dendrimers. This acetylation decreases the interaction of siRNA with the dendrimers, thereby facilitating the unpackaging of siRNA in target cells. The increased release of the siRNA cargo from the dendrimer in the cell leads to an increase in transfection efficiency [61, 64].

Different generations of PAMAM dendrimers have been complexed to other nanoparticles to stabilize and deliver DNA and RNA [61]. Pan et al. complexed magnetic nanopartcles to PAMAM dendrimers and antisense *survivin* oligonucleotides. Human cells from breast and liver tumors were incubated with these nanocomplexes and subsequently, the samples were subjected to analysis by 3-(4,5-dimethylthiazol-2-yl)-2,5-diphenyltetrazolium bromide (MTT), quantitative RT-PCR, Western blot, and transmission electron microscopy. The results demonstrated that within 15 minutes, the nanocomplexes had entered the tumor cells and significant downregulation of the targeted *survivin* gene and its protein product were observed. The authors reported in addition that cell proliferation was inhibited in a dose-dependent and time-dependent manner [61].

5.4. Nanomaterials and Nanotoxicity. Nanomaterials can have very different physicochemical properties compared with bulk materials of the same chemical composition. Some of these properties (small size, large surface area, etc.) that make nanomaterials desirable for biomedical use also generate potential risks for cytotoxicity. Results from numerous experiments with various nanomaterials suggest that size, surface area, morphology, surface chemistry, and chemical composition are the major determinants of nanomaterial uptake and cytotoxicity [54, 56–65, 67, 68]. Just like many other nanosciences, the study of nanotoxicity has become an area of intense focus; however, researchers are still trying to develop an improved understanding of the pathways and mechanisms involved.

Experiments performed by Kroll et al. [62] demonstrated the influence of physicochemical properties on cytotoxicity by using different groups of engineered nanoparticles with the same chemical composition. For example, some of the samples used were prepared using identical particle preparations, but one sample was dispersed at a different pH. Other samples varied in their surface area, particle size, or surface chemistry. The researchers used three *in vitro* assays on ten different cell lines to monitor different stages of cytotoxicity: oxidative stress, cellular metabolic activity, and cell death. The outcome of this study, although too extensive to elaborate here, confirms that *in vitro* toxicity cannot be linked to a single, specific physicochemical property of the nanomaterial. Kroll et al. suggest that the response is due to the combined effects of the size, morphology, surface chemistry, and chemical composition of the nanomaterial, yet the effects are also cell-type dependent, and the results vary depending on the endpoint used to measure toxicity.

Because dendrimers have enormous potential as delivery vehicles for therapeutic nucleic acids, it is important to harness that potential while still balancing the cytotoxic effects. There are numerous approaches to reducing the cytotoxicity while maintaining optimal function, including binding hydrophilic polymers to the outermost branches of the dendrimers, creating half-generation dendrimers, and modifying some of the cationic amine groups to neutralize them [59–65].

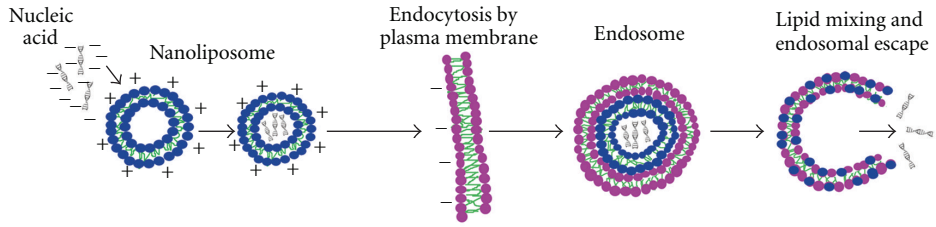

Figure 3: Nanoliposome-mediated endocytosis of therapeutic nucleic acids. After escape from the endosome, if the nucleic acid cargo is DNA, then nuclear translocation will occur, permitting the DNA to be transcribed and subsequently translated. If the nucleic acid cargo is RNA, it is translated in the cytoplasm.

Table 1: Summary of current data and future direction for gene-based vaccines.

	DNA Vaccines [1–42, 66]	RNA Vaccines [5, 42–55]	Future Direction: RNA and Nanomaterials [6, 53, 55–65, 67–77]
Design	Relatively easy, inexpensive, and quick to construct. Easy to manipulate. Does not require cold chain.	Relatively easy, inexpensive, and quick to construct. Can be produced in large amounts *in vitro* from DNA template.	Functionalized nanomaterials can be conjugated to further stabilize RNA and to increase penetration.
Delivery	IM injection is most common, but often requires prime/boost. Biolistic bombardment with DNA-coated gold microparticles is currently most efficient. Needle-free delivery via Bioinjector.	Currently, there is no standard delivery method; IM injection is most common. Liposome carriers can also be used.	Gene gun delivery of RNA conjugated with dendrimers and various nanoparticles as stabilizing delivery vehicles.
Stability	Generally stable at room temperature. Long shelf life.	Unstable for storage unless oxidation, hydrolysis, and contact with nucleases are prevented. Quickly degraded in physiological fluid, although studies show unprotected RNA can induce immune response.	Complexing the RNA with multiple nanomaterials can have a compounding effect to increase stability for storage and delivery.
Safety	Considered relatively safe, though there is theoretical risk of insertional mutagenesis after integration, induction of autoimmunity, and transfer of antibiotic resistance.	Rapidly cleared from tissue and does not need to enter nucleus; therefore, there is no risk of insertional mutagenesis after integration, induction of autoimmunity, or transfer of antibiotic resistance.	Continue researching the effect of shape, size, and surface chemistry on biocompatibility and cellular interactions of various nanomaterials.
Immunogenicity	Activate both cellular and humoral pathways. Poor result in human clinical trials. Must be transported to the nucleus in order to exert biological effect.	Activate both cellular and humoral pathways. No need to cross nuclear membrane to exert its biological effect. No need to be replicated or transcribed.	Complex RNA to nanomaterials that recognize and target specific cells. Continue research on nanomaterials that penetrate the cell membrane with adverse cellular effects.

Gold nanoparticles are generally considered safe and biocompatible [68–72]. Studies performed by Chithrani et al. indicate that 50 nm spheres of citric acid ligand-stabilized gold nanoparticles are endocytosed by HeLa cells more rapidly than 14 nm and 74 nm spheres [68]. Goodman et al. studied cationic and anionic gold nanoparticles and determined that the cationic particles exhibit moderate toxicity, while anionic gold particles were nontoxic [69]. The researchers suggested that the mechanism for toxicity was related to the initial electrostatic binding of the cationic particles to the negatively charged cell membrane, while the anionic particles were repelled from the cell surface, thereby reducing the toxicity. In experiments studying the effect of the morphology of gold nanoparticles on uptake and toxicity, again executed by Chithrani et al., it was determined that nanorods and nanospheres are both taken up by HeLa cells, although nanorods were taken up at a much slower rate [70]. Other nanomaterials, such as iron oxide [73, 74], zinc oxide [75–77], silicon dioxide [78, 79], quantum dots [80], and many more are under investigation for their potential as biocompatible gene-delivery vehicles.

6. Summary

In summary, the search for an ideal vaccine has led to gene-based approaches because they have numerous advantages over conventional vaccines. The fundamental advantage of gene-based vaccines is that they induce both the cellular and humoral pathways of the immune system, a capability

that conventional vaccines have been unable to achieve. The problems with the performance of DNA vaccines have given rise to the idea of using various forms of RNA in place of DNA. Although RNA offers definite advantages over DNA for use in vaccines, this approach generates new questions relating to RNA stability for storage and delivery. Many of the concerns about RNA stability have been addressed, and using nanomaterials as stabilizing delivery vehicles could be essential to the solution of these issues. Table 1 summarizes the current advantages and challenges not only of DNA and RNA vaccines, but also of RNA vaccines enhanced with nanomaterials, which we see as the future of gene-based vaccines.

7. Conclusion

On the horizon, nanomaterials may tip the balance and finally be able to deliver on the promise of gene vaccines and achieve a beneficial change in the proteome. RNA vaccines, which can be robustly translated into protein antigens that can more effectively elicit an immunotherapeutic Th1 and Th2 response, represent a powerful and promising solution for cancer and infectious diseases that have eluded cures so far. Critical to this solution will be identifying nanomaterials that permit RNA entry into cells, bypassing the cell membrane while at the same time protecting the RNA from many nucleases that can destroy it. This route could potentially enable a more prolonged and sustained expression of the encoded proteins, and hence, weighing in more heavily on the overall proteomic pattern on the key cells of the immune system. With further work, it may be possible to construct RNA nanoconjugates having these key capabilities built into them.

At present, there is a massive effort to identify nanomaterials that, while providing the above advantages, elicit the desired alterations in the cellular proteome, but which do not have untoward, off-target, or other undesirable effects. The proteome is complex and our understanding of how it can be modulated selectively is evolving. The effects of these bionanoconjugates on the binding, stabilization, and delivery of DNA and RNA vaccines, in addition to how these novel bionanomaterials "tip the proteome" is perhaps one of the critical scientific questions of the 21st century.

Acknowledgments

The authors would like to thank our collaborators, particularly Dr. Richard Garrad and Dr. Christopher Field, for their generous support, encouragement, and helpful discussions. R. K. Dlong, K. Ghosh, M. Craig, and A.Wanekaya are supported by an AREA/R15 Grant from the National Cancer Institute entitled, "Anti-Cancer RNA Nanoconjugates" (1 R15 CA139390-01).

References

[1] J. J. Donnelly, J. B. Ulmer, and M. A. Liu, "Minireview: DNA vaccines," *Life Sciences*, vol. 60, no. 3, pp. 163–172, 1996.

[2] J. J. Donnelly, A. Friedman, D. Martinez et al., "Preclinical efficacy of a prototype DNA vaccine: enhanced protection against antigenic drift in influenza virus," *Nature Medicine*, vol. 1, no. 6, pp. 583–587, 1995.

[3] M. Vajdy, I. Srivastava, J. Polo, J. Donnelly, D. O'Hagan, and M. Singh, "Mucosal adjuvants and delivery systems for protein-, DNA- and RNA-based vaccines," *Immunology and Cell Biology*, vol. 82, no. 6, pp. 617–627, 2004.

[4] W. W. Leitner, H. Ying, and N. P. Restifo, "DNA and RNA-based vaccines: principles, progress and prospects," *Vaccine*, vol. 18, no. 9-10, pp. 765–777, 1999.

[5] K. L. Jones, D. Drane, and E. J. Gowans, "Long-term storage of DNA-free RNA for use in vaccine studies," *BioTechniques*, vol. 43, no. 5, pp. 675–681, 2007.

[6] R. K. DeLong, R. Knowle, and A. Werner, "R4 peptide-pDNA nanoparticle coated HepB vaccine microparticles: sedimentation, partitioning, and spray freeze dry bioprocesses," *Journal of Nanoscience and Nanotechnology*, vol. 6, no. 9-10, pp. 2783–2789, 2006.

[7] A. Bolhassani, S. Safaiyan, and S. Rafati, "Improvement of different vaccine delivery systems for cancer therapy," *Molecular Cancer*, p. 3, 2011.

[8] T. D. Nandedkar, "Nanovaccines: recent developments in vaccination," *Journal of biosciences*, vol. 34, no. 6, pp. 995–1003, 2009.

[9] C. P. Mao and T. C. Wu, "Inhibitory RNA molecules in immunotherapy for cancer," *Methods in Molecular Biology*, vol. 623, pp. 325–339, 2010.

[10] T. Xue, E. Stavropoulos, M. Yang et al., "RNA encoding the MPT83 antigen induces protective immune responses against Mycobacterium tuberculosis infection," *Infection and Immunity*, vol. 72, no. 11, pp. 6324–6329, 2004.

[11] M. Ingolotti, O. Kawalekar, D. J. Shedlock, K. Muthumani, and D. B. Weiner, "DNA vaccines for targeting bacterial infections," *Expert Review of Vaccines*, vol. 9, no. 7, pp. 747–763, 2010.

[12] X. Ma, D. Wang, Y. Wu et al., "AIDS treatment with novel anti-HIV compounds improved by nanotechnology," *AAPS Journal*, vol. 12, no. 3, pp. 272–278, 2010.

[13] S. Scheiblhofer, R. Weiss, and J. Thalhamer, "Genetic vaccination approaches against malaria based on the circumsporozoite protein," *Wiener Klinische Wochenschrift*, vol. 118, no. 3, pp. 9–17, 2006.

[14] R. Wang, D. L. Doolan, T. P. Le et al., "Induction of antigen-specific cytotoxic T lymphocytes in humans by a malaria DNA vaccine," *Science*, vol. 282, no. 5388, pp. 476–480, 1998.

[15] J. A. Wolff, R. W. Malone, P. Williams et al., "Direct gene transfer into mouse muscle in vivo," *Science*, vol. 247, no. 4949 I, pp. 1465–1468, 1990.

[16] M. A. Kutzler and D. B. Weiner, "DNA vaccines: ready for prime time?" *Nature Reviews Genetics*, vol. 9, no. 10, pp. 776–788, 2008.

[17] S. Manam, B. J. Ledwith, A. B. Barnum et al., "Plasmid DNA vaccines: tissue distribution and effects of DNA sequence, adjuvants and delivery method on integration into host DNA," *Intervirology*, vol. 43, no. 4-6, pp. 273–281, 2000.

[18] T. M. Fu, J. B. Ulmer, M. J. Caulfield et al., "Priming of cytotoxic T lymphocytes by DNA vaccines: requirement for professional antigen presenting cells and evidence for antigen transfer from myocytes," *Molecular Medicine*, vol. 3, no. 6, pp. 362–371, 1997.

[19] J. J. Donnelly, M. A. Liu, and J. B. Ulmer, "Antigen presentation and DNA vaccines," *American Journal of Respiratory and Critical Care Medicine*, vol. 162, no. 4, pp. S190–S193, 2000.

[20] A. Porgador, K. R. Irvine, A. Iwasaki, B. H. Barber, N. P. Restifo, and R. N. Germain, "Predominant role for directly transfected dendritic cells in antigen presentation to CD8+ T cells after gene gun immunization," *Journal of Experimental Medicine*, vol. 188, no. 6, pp. 1075–1082, 1998.

[21] S. Méndez, Y. Belkaid, R. A. Seder, and D. Sacks, "Optimization of DNA vaccination against cutaneous leishmaniasis," *Vaccine*, vol. 20, no. 31-32, pp. 3702–3708, 2002.

[22] N. A. Doria-Rose and N. L. Haigwood, "DNA vaccine strategies: candidates for immune modulation and immunization regimens," *Methods*, vol. 31, no. 3, pp. 207–216, 2003.

[23] M. A. Liu and J. B. Ulmer, "Human Clinical Trials of Plasmid DNA Vaccines," *Advances in Genetics*, vol. 55, pp. 25–40, 2005.

[24] M. Howarth and T. Elliott, "The processing of antigens delivered as DNA vaccines," *Immunological Reviews*, vol. 199, pp. 27–39, 2004.

[25] K. L. Rock and L. Shen, "Cross-presentation: underlying mechanisms and role in immune surveillance," *Immunological Reviews*, vol. 207, pp. 166–183, 2005.

[26] C. A. Janeway, P. Travers, M. Walport, and M. Slomchik, "The immune system in health & disease," in *Immunobiology: The Immune System in Health and Disease*, pp. 613–662, 6th edition, 2005.

[27] R. Wang, D. L. Doolan, T. P. Le et al., "Induction of antigen-specific cytotoxic T lymphocytes in humans by a malaria DNA vaccine," *Science*, vol. 282, no. 5388, pp. 476–480, 1998.

[28] N. P. Restifo, H. Ying, L. Hwang, and W. W. Leitner, "The promise of nucleic acid vaccines," *Gene Therapy*, vol. 7, no. 2, pp. 89–92, 2000.

[29] M. J. Roy, M. S. Wu, L. J. Barr et al., "Induction of antigen-specific CD8+ T cells, T helper cells, and protective levels of antibody in humans by particle-mediated administration of a hepatitis B virus DNA vaccine," *Vaccine*, vol. 19, no. 7-8, pp. 764–778, 2000.

[30] D. M. Klinman, F. Takeshita, S. Kamstrup et al., "DNA vaccines: capacity to induce auto-immunity and tolerance," *Developments in Biologicals*, vol. 104, pp. 45–51, 2000.

[31] R. L. Sheets, J. Stein, T. S. Manetz et al., "Biodistribution of DNA plasmid vaccines against HIV-1, Ebola, Severe Acute Respiratory Syndrome, or West Nile virus is similar, without integration, despite differing plasmid backbones or gene inserts," *Toxicological Sciences*, vol. 91, no. 2, pp. 610–619, 2006.

[32] J. A. Williams, A. E. Carnes, and C. P. Hodgson, "Plasmid DNA vaccine vector design: impact on efficacy, safety and upstream production," *Biotechnology Advances*, vol. 27, no. 4, pp. 353–370, 2009.

[33] F. Soubrier, B. Cameron, B. Manse et al., "pCOR: a new design of plasmid vectors for nonviral gene therapy," *Gene Therapy*, vol. 6, no. 8, pp. 1482–1488, 1999.

[34] J. Mairhofer and R. Grabherr, "Rational vector design for efficient non-viral gene delivery: challenges facing the use of plasmid DNA," *Molecular Biotechnology*, vol. 39, no. 2, pp. 97–104, 2008.

[35] C. Y. Szpirer and M. C. Milinkovitch, "Separate-component-stabilization system for protein and DNA production without the use of antibiotics," *BioTechniques*, vol. 38, no. 5, pp. 775–781, 2005.

[36] A. Yadava and C. F. Ockenhouse, "Effect of codon optimization on expression levels of a functionally folded malaria vaccine candidate in prokaryotic and eukaryotic expression systems," *Infection and Immunity*, vol. 71, no. 9, pp. 4961–4969, 2003.

[37] L. Frelin, G. Ahlén, M. Alheim et al., "Codon optimization and mRNA amplification effectively enhances the immunogenecity of the hepatitis C virus nonstructural 3/4A gene," *Gene Therapy*, vol. 11, no. 6, pp. 522–533, 2004.

[38] J. Zur Megede, M. C. Chen, B. Doe et al., "Increased expression and immunogenicity of sequence-modified human immunodeficiency virus type 1 gag gene," *Journal of Virology*, vol. 74, no. 6, pp. 2628–2635, 2000.

[39] L. Ramakrishna, K. K. Anand, K. M. Mohankumar, and U. Ranga, "Codon optimization of the Tat antigen of human immunodeficiency virus type 1 generates strong immune responses in mice following genetic immunization," *Journal of Virology*, vol. 78, no. 17, pp. 9174–9189, 2004.

[40] W. Böhm, A. Kuhröber, T. Paier, T. Mertens, J. Reimann, and R. Schirmbeck, "DNA vector constructs that prime hepatitis B surface antigen-specific cytotoxic T lymphocyte and antibody responses in mice after intramuscular injection," *Journal of Immunological Methods*, vol. 193, no. 1, pp. 29–40, 1996.

[41] D. M. Klinman, "CpG DNA as a vaccine adjuvant," *Expert Review of Vaccines*, vol. 2, no. 2, pp. 305–315, 2003.

[42] R. K. DeLong, C. M. Reynolds, Y. Malcolm, A. Schaeffer, T. Severs, and A. Wanekaya, "Functionalized gold nanoparticles for the binding, stabilization, and delivery of therapeutic DNA, RNA, and other biological macromolecules," *Nanotechnology, Science and Applications*, vol. 3, no. 1, pp. 53–63, 2010.

[43] G. Tavernier, O. Andries, J. Demeester, N. N. Sanders, S. C. De Smedt, and J. Rejman, "mRNA as gene therapeutic: how to control protein expression," *Journal of Controlled Release*, 2010.

[44] S. Pascolo, "Messenger RNA-based vaccines," *Expert Opinion on Biological Therapy*, vol. 4, no. 8, pp. 1285–1294, 2004.

[45] J. P. Carralot, B. Weide, O. Schoor et al., "Production and characterization of amplified tumor-derived cRNA libraries to be used as vaccines against metastatic melanomas," *Genetic Vaccines and Therapy*, vol. 3, article 6, 2005.

[46] B. Scheel, R. Teufel, J. Probst et al., "Toll-like receptor-dependent activation of several human blood cell types by protamine-condensed mRNA," *European Journal of Immunology*, vol. 35, no. 5, pp. 1557–1566, 2005.

[47] B. Scheel, S. Aulwurm, J. Probst et al., "Therapeutic anti-tumor immunity triggered by injections of immunostimulating single-stranded RNA," *European Journal of Immunology*, vol. 36, no. 10, pp. 2807–2816, 2006.

[48] P. Qiu, P. Ziegelhoffer, J. Sun, and N. S. Yang, "Gene gun delivery of mRNA in situ results in efficient transgene expression and genetic immunization," *Gene Therapy*, vol. 3, no. 3, pp. 262–268, 1996.

[49] S. Espuelas, A. Roth, C. Thumann, B. Frisch, and F. Schuber, "Effect of synthetic lipopeptides formulated in liposomes on the maturation of human dendritic cells," *Molecular Immunology*, vol. 42, no. 6, pp. 721–729, 2005.

[50] K. S. Korsholm, E. M. Agger, C. Foged et al., "The adjuvant mechanism of cationic dimethyldioctadecylammonium liposomes," *Immunology*, vol. 121, no. 2, pp. 216–226, 2007.

[51] B. Schell, S. Braedel, J. Probst et al., "Immunostimulating capacities of stabilized RNA molecules," *European Journal of Immunology*, vol. 34, no. 2, pp. 537–547, 2004.

[52] J.-P. Carralot, J. Probst, I. Hoerr et al., "Polarization of immunity induced by direct injection of naked sequence-stabilized mRNA vaccines," *Cellular and Molecular Life Sciences*, vol. 61, no. 18, pp. 2418–2424, 2004.

[53] B. S. Zolnik, A. Gonzalez-Fernandez, N. Sadrieh, and M. A. Dobrovolskaia, "Minireview: nanoparticles and the immune system," *Endocrinology*, vol. 151, no. 2, pp. 458–465, 2010.

[54] S. McCartney, W. Vermi, S. Gilfillan et al., "Distinct and complementary functions of MDA5 and TLR3 in poly(I:C)-mediated activation of mouse NK cells," *Journal of Experimental Medicine*, vol. 206, no. 13, pp. 2967–2976, 2009.

[55] R. K. DeLong, U. Akhtar, M. Sallee et al., "Characterization and performance of nucleic acid nanoparticles combined with protamine and gold," *Biomaterials*, vol. 30, no. 32, pp. 6451–6459, 2009.

[56] A. M. Alkilany and C. J. Murphy, "Toxicity and cellular uptake of gold nanoparticles: what we have learned so far?" *Journal of Nanoparticle Research*, vol. 12, no. 7, pp. 2313–2333, 2010.

[57] K. K. Sandhu, C. M. McIntosh, J. M. Simard, S. W. Smith, and V. M. Rotello, "Gold nanoparticle-mediated transfection of mammalian cells," *Bioconjugate Chemistry*, vol. 13, no. 1, pp. 3–6, 2002.

[58] K. L. Aillon, Y. Xie, N. El-Gendy, C. J. Berkland, and M. L. Forrest, "Effects of nanomaterial physicochemical properties on in vivo toxicity," *Advanced Drug Delivery Reviews*, vol. 61, no. 6, pp. 457–466, 2009.

[59] R. K. DeLong, L. Cillessen, C. Reynolds et al., "Biomolecular triconjugates formed between gold, protamine, and nucleic acid: comparative characterization on the nanoscale," *Journal of Nanotechnology*, vol. 2012, Article ID 954601, 9 pages, 2012.

[60] M. A. Dobrovolskaia, P. Aggarwal, J. B. Hall, and S. E. McNeil, "Preclinical studies to understand nanoparticle interaction with the immune system and its potential effects on nanoparticle biodistribution," *Molecular Pharmaceutics*, vol. 5, no. 4, pp. 487–495, 2008.

[61] B. Pan, D. Cui, Y. Sheng et al., "Dendrimer-modified magnetic nanoparticles enhance efficiency of gene delivery system," *Cancer Research*, vol. 67, no. 17, pp. 8156–8163, 2007.

[62] A. Kroll, C. Dierker, C. Rommel et al., "Cytotoxicity screening of 23 engineered nanomaterials using a test matrix of ten cell lines and three different assays," *Particle and Fibre Toxicology*, vol. 8, no. 9, 2011.

[63] S. Shah, Y. Liu, W. Hu, and J. Gao, "Modeling particle shape-dependent dynamics in nanomedicine," *Journal of Nanoscience and Nanotechnology*, vol. 11, no. 2, pp. 919–928, 2011.

[64] C. L. Waite, S. M. Sparks, K. E. Uhrich, and C. M. Roth, "Acetylation of PAMAM dendrimers for cellular delivery of siRNA," *BMC Biotechnology*, vol. 9, no. 38, 2009.

[65] S. K. Sohaebuddin, P. T. Thevenot, D. Baker, J. W. Eaton, and L. Tang, "Nanomaterial cytotoxicity is composition, size, and cell type dependent," *Particle and Fibre Toxicology*, vol. 7, no. 22, 2010.

[66] R. J. Mumper and Z. Cui, "Genetic immunization by jet injection of targeted pDNA-coated nanoparticles," *Methods*, vol. 31, no. 3, pp. 255–262, 2003.

[67] L. Yan, Zhao F., S. li, Z. Hu, and Y. Zhao, "Low-toxic and safe anomaterials by surface-chemical design, carbon nanotubes, fullerenes, metallofullerenes, and graphemes," *Nanoscale*, vol. 3, pp. 362–382, 2011.

[68] B. D. Chithrani, A. A. Ghazani, and W. C. W. Chan, "Determining the size and shape dependence of gold nanoparticle uptake into mammalian cells," *Nano Letters*, vol. 6, no. 4, pp. 662–668, 2006.

[69] C. M. Goodman, C. D. McCusker, T. Yilmaz, and V. M. Rotello, "Toxicity of gold nanoparticles functionalized with cationic and anionic side chains," *Bioconjugate Chemistry*, vol. 15, no. 4, pp. 897–900, 2004.

[70] B. D. Chithrani and W. C. W. Chan, "Elucidating the mechanism of cellular uptake and removal of protein-coated gold nanoparticles of different sizes and shapes," *Nano Letters*, vol. 7, no. 6, pp. 1542–1550, 2007.

[71] Y. Pan, S. Neuss, A. Leifert et al., "Size-dependent cytotoxicity of gold nanoparticles," *Small*, vol. 3, no. 11, pp. 1941–1949, 2007.

[72] W. H. de Jong, W. I. Hagens, P. Krystek, M. C. Burger, A. J. A. M. Sips, and R. E. Geertsma, "Particle size-dependent organ distribution of gold nanoparticles after intravenous administration," *Biomaterials*, vol. 29, no. 12, pp. 1912–1919, 2008.

[73] B. Gaihre, M. S. Khil, and H. Y. Kim, "In vitro anticancer activity of doxorubicin-loaded gelatin-coated magnetic iron oxide nanoparticles," *Journal of Microencapsulation*, vol. 28, no. 4, pp. 286–293, 2011.

[74] A. Hanini, A. Schmitt, K. Kacem, F. Chau, S. Ammar, and J. Gavard, "Evaluation of iron oxide nanoparticle biocompatibility," *International Journal of Nanomedicine*, vol. 6, pp. 787–794, 2011.

[75] V. Sharma, D. Anderson, and A. Dhawan, "Zinc oxide nanoparticles induce oxidative stress and genotoxicity in human liver cells (HepG2)," *Journal of Biomedical Nanotechnology*, vol. 7, no. 1, pp. 98–99, 2011.

[76] B. C. Heng, X. Zhao, E. C. Tan et al., "Evaluation of the cytotoxic and inflammatory potential of differentially shaped zinc oxide nanoparticles," *Archives of Toxicology*, vol. 85, no. 12, pp. 1517–1528, 2011.

[77] R. Roy, A. Tripathi, M. Das, and P. D. Dwivedi, "Cytotoxicity and uptake of zinc oxide nanoparticles leading to enhanced inflammatory cytokines levels in murine macrophages: comparison with bulk zinc oxide," *Journal of Biomedical Nanotechnology*, vol. 7, no. 1, pp. 110–111, 2011.

[78] Z. Xu, L. Chou, and J. Sun, "Effects of SiO_2 nanoparticles on HFL-I activating ROS-mediated apoptosis via p53 pathway," *Journal of Applied Toxicology*. In press.

[79] J. C.K. Lai, G. Ananthakrishnan, S. Jandhyam et al., "Treatment of human astrocytoma U87 cells with silicon dioxide nanoparticles lowers their survival and alters their expression of mitochondrial and cell signaling proteins," *International Journal of Nanomedicine*, vol. 5, no. 1, pp. 715–723, 2010.

[80] T. S. Hauck, R. E. Anderson, H. C. Fischer, S. Newbigging, and W. C. W. Chan, "In vivo quantum-dot toxicity assessment," *Small*, vol. 6, no. 1, pp. 138–144, 2010.

Hindawi Publishing Corporation
Journal of Nanotechnology
Volume 2012, Article ID 270383, 11 pages
doi:10.1155/2012/270383

Research Article

Preparation of Lipid Nanoemulsions Incorporating Curcumin for Cancer Therapy

Songyot Anuchapreeda,[1,2] Yoshinobu Fukumori,[2] Siriporn Okonogi,[3] and Hideki Ichikawa[2]

[1] *Division of Clinical Microscopy, Department of Medical Technology, Faculty of Associated Medical Sciences, Chiang Mai University, Chiang Mai 50200, Thailand*
[2] *Faculty of Pharmaceutical Sciences and Cooperative Research Center of Life Sciences, Kobe Gakuin University, Minatojima 1-1-3, Chuo-ku, Kobe 650-8586, Japan*
[3] *Department of Pharmaceutical Sciences, Faculty of Pharmacy, Chiang Mai University, Chiang Mai 50200, Thailand*

Correspondence should be addressed to Hideki Ichikawa, ichikawa@pharm.kobegakuin.ac.jp

Received 17 June 2011; Revised 31 August 2011; Accepted 6 September 2011

Academic Editor: Michael M. Craig

The aim of this study was to develop a new formulation of a curcumin lipid nanoemulsion having the smallest particle size, the highest loading, and a good physical stability for cancer chemotherapy. Curcumin lipid nanoemulsions were prepared by a modified thin-film hydration method followed by sonication. Soybean oil, hydrogenated L-α-phosphatidylcholine from egg yolk, and cosurfactants were used to formulate the emulsions. The resultant nanoemulsions showed mean particle diameter of 47–55 nm, could incorporate 23–28 mg curcumin per 30 mL, and were stable in particle size for 60 days at 4°C. The cytotoxicity studies of curucumin solution and curcumin-loaded nanoemulsion using B16F10 and leukemic cell lines showed IC_{50} values ranging from 3.5 to 30.1 and 22.2 to 53.7 μM, respectively. These results demonstrated the successful incorporation of curcumin into lipid nanoemulsion particles with small particle size, high loading capacity, good physical stability, and preserved cytotoxicity.

1. Introduction

Curcumin (diferuloylmethane), a phenolic compound believed to be the main pharmacological agent in turmeric, possesses antioxidant activity *in vitro* [1, 2] and is used in lipid peroxidation tests [3]. Curcumin is effective for preventing and ameliorating gastric lesions. It also possesses anti-inflammatory [4], antibacterial [5, 6], antifungal and antiyeast [7], antihypocholesterolemic [8], anticancer [9–12], antimutagen [13], antiparasitic [14], antitumor-promoting [15], antiproliferative [16], MDR modulator effects [17], and so on.

The chemical structure of curcumin isolated from turmeric powder is shown in Figure 1. Commercial-grade curcumin (such as from Sigma-Aldrich), when isolated from the powdered dry rhizome of *Curcuma longa* Linn, contains approximately 77% curcumin, 17% demethoxycurcumin, and 3% bisdemethoxycurcumin. Curcumin pigments can absorb the visible light at a wavelength between 420–425 nm.

The safety of *Curcuma longa* Linn and its derivatives has been studied in various animal models [18]. It has been shown that turmeric is not toxic to animals even at high doses. A single feeding of a 30% turmeric diet to rats did not produce any toxic effects. In a 24-h acute toxicity study, mice were fed turmeric extracts at a daily dosage of 0.5, 1.0, or 3.0 g/kg. No increase in the mortality rate was observed when compared to the respective controls. A 90-day feeding of turmeric extracts resulted in no significant weight gain [18].

The cytotoxicity of curcumin was examined using the MTT assay in cancer cell lines; Hep-2 (human larynx), PC-9, PC-14 (human lung cancers), Hep-1 (mouse hepatoma), F-25 (mutate H-ras transfected NIH mouse fibroblast), and leukemic cell lines. The authors found that curcumin is a potent antiproliferative agent for the tested cancer cell lines [19, 20]. A recent report indicates that pure curcumin concentration for oncogene target inhibition and inhibitory effect on cancer cell proliferation is ~15–20 μM [21].

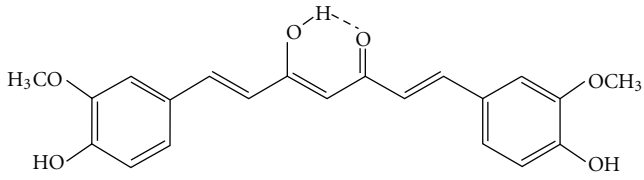

Figure 1: Chemical structure of curcumin.

In order to deliver curcumin to targeted organs, its hydrophobic property needs to be modified. A wide variety of drug carriers has been studied as a mean of improving the therapeutic efficacy of drugs. The small size of carriers is very important for the biodistribution in the body. The capillaries are so small that red blood cells can only travel through them in single file. The capillaries measure approximately 5–10 μm in diameter. Particles larger than this size cannot be circulated in the body and become entrapped in the capillary bed. Thus, the particle diameter should be generally smaller than micrometers for the particles to be circulated in the blood vessels. In addition, reduction in the particle diameter to less than 100 nm is thought to decrease their removal by the reticuloendothelial system and increase their extravasation from the smallest capillaries [22, 23]. Thus, nanotechnology is one of the effective methods to be used for the delivery of curcumin.

Many studies have been published on the production of nanoparticles to incorporate curcumin. Bisht et al. [24] proposed the polymeric nanoparticle formulation encapsulating curcumin as "nanocurcumin" for human cancer therapy. The nanocurcumin was confirmed to have a narrow particle size distribution with an average size of 50 nm. Furthermore, nanocurcumin could induce cellular apoptosis, inhibit nuclear factor kappa B (NFκB), and downregulate the steady state levels of multiple proinflammatory cytokines (interleukin-(IL-) 6, IL-8, and tumor necrosis factor alpha (TNFα)) in pancreatic cancer cells [24]. In a recent report, curcumin was also prepared in the form of liposomes (nanodelivery vehicles primarily composed of phospholipids) coated with antibodies specific to a prostate membrane-specific antigen. The coated-liposomes were approximately 100–150 nm. The liposomal curcumin showed antiproliferative activity on human prostate cancer cell lines (LNCaP and C42B) in a tetrazolium dye-based (MTT) assay [25]. Furthermore, curcumin was encapsulated in the form of alginate-chitosan-pluronic composite nanoparticles for its delivery to cancer cells. The particles were spherical in shape with an average size of 100 ± 20 nm. The half-maximal inhibitory concentration for encapsulated curcumin was 14.34 μM [26].

Lipid emulsions have also been used as a promising drug delivery device to target tissues [27, 28]. Many studies have shown the validity of a lipid emulsion as parenteral drug delivery device [29–31]. Emulsions are heterogeneous mixtures of 2 or more immiscible liquids with an emulsifier used to stabilize the dispersed droplets. They have certain advantages such as good biocompatibility, biodegradability, physical stability, and ease of large-scale production. In addition, they can incorporate hydrophobic and amphipathic drugs because of their structural characteristics. Since curcumin has a hydrophobic nature, it can be the payload of a lipid emulsion. Thus, a lipid emulsion can be a promising device for the delivery of curcumin.

The aim of this study was to prepare curcumin in the form of a lipid emulsion with reduced particle size and increased curcumin loading. The preparation of the formulation was modified from the standard formulation of gadolinium-containing nanoemulsions described in our previous reports [32, 33]. The effects of the type of oil and cosurfactant on particle diameter were studied. Moreover, the curcumin lipid emulsion was also evaluated on incorporation efficiency, physical stability after production, and cytotoxicity in cancer cell lines.

2. Materials and Methods

2.1. Chemicals. Hydrogenated L-α-phosphatidylcholine from egg yolk (HEPC), soybean oil, polysorbate 80 (polyoxyethylene (20) sorbitanmonooleate, Tween 80), and chloroform were purchased from NacalaiTesque Inc., Kyoto, Japan. In HEPC, the phospholipid content was more than 99% and the phosphatidylcholine content was approximately 70%. Lecithin from soybean was purchased from WAKO Pure Chemical Industries, Osaka, Japan. Curcumin from *Curcuma Longa* Linn (Turmeric) was purchased from Sigma-Aldrich, St. Louis, MO, USA. Polyoxyethylene hydrogenated castor oil 60 (Cremophor-HR60, HCO-60) was supplied by BASF, Ludwigshafen, Germany. Dimethyl sulfoxide (DMSO), 3-(4,5-dimethylthiazolyl-2)-2, 5-diphenyl tetrazolium bromide (MTT) were purchased from Sigma-Aldrich (St. Louis, MO, USA). RPMI-1640 and penicillin-streptomycin were purchased from GIBCO Invitrogen (Grand Island, NY, USA). Fetal bovine serum (FBS) was obtained from Biochrom AG (Berlin, Germany). Ethanol was purchased from Fluka Chemicals (Buchs, Switzerland).

2.2. Preparation of Curcumin-Containing Lipid Nanoemulsion. Curcumin-containing lipid nanoemulsions were prepared by a modified thin-film hydration method at room temperature (24°C) as previously reported [32, 33]. Briefly, the emulsions consisted of soybean oil or lecithin (phosphatidylcholine), water, curcumin, HEPC, and an appropriate co-surfactant. The oil and HEPC were dissolved in 2 mL of chloroform. Curcumin was dissolved in 4 mL of chloroform. Co-surfactant (HCO-60 or Tween 80) was dissolved in 2 mL of chloroform (HCO-60) or distilled water (Tween 80). The mixture of the 3 solutions was dried by rotary evaporation and subjected to subsequent vacuum desiccation for 3–5 h to generate the dried thin film. The dried thin film was hydrated with 30 mL of distilled water warmed at 55–60°C in a bath-type sonicator (BRANSON-Yamato 2510, BRANSONIC, Emerson-Japan, Kanagawa, Japan), followed by vigorous mixing and sonicating for 5 min to create coarse lipid emulsions. The fine lipid emulsions were prepared by 30–60 min sonication under N_2 atmosphere with a bath-type sonicator, which was thermostated at 55–60°C. The sonication was performed as follows: 3 min sonication and

subsequent 2 min cooling, which were repeated for 30–60 min. Excess curcumin was removed by centrifugation at 3000 rpm for 15 min. The supernatant was collected as curcumin lipid nanoemulsion sample. Three different batches of lipid nanoemulsions were prepared with each formulation. The prepared curcumin lipid nanoemulsions were evaluated regarding particle size, curcumin concentration, and percent incorporation efficiency (% IE) described below.

2.3. Particle Size Measurement. The particle diameter of the nanoemulsions was measured by a dynamic light scattering method using Zetasizer 3000HS_A (Malvern Instrument, UK) at room temperature. Particle size data were expressed as the mean of the Z-average of 3 independent batches of the nanoemulsions.

2.4. Determination of Curcumin Concentration and Incorporation Efficiency. Curcumin in lipid nanoemulsions was quantified using a simple colorimetric assay at 450 nm as described previously [25]. Briefly, a standard curve was generated from known concentrations of curcumin in HBSE-Triton X-100 (10 mM HEPES, 140 mM NaCl, 4 mM EDTA, and 1% Triton X-100). After centrifugation, 4 mL of HBSE-Triton X-100 was added to 25 μL of the curcumin lipid nanoemulsion to determine the curcumin concentration in the nanoemulsion. The absorbance was measured on a spectrophotometer (UV-150-02, SHIMADZU Corporation, Japan). The amount of curcumin in the lipid nanoemulsion was calculated from the final concentration of curcumin after preparation. The curcumin incorporation efficiency (% IE) in the lipid nanoemulsion was calculated by the following equation:

$$\%\ \text{IE} = \frac{(\text{Measured amount of curcumin in lipid nanoemulsion})}{(\text{Total amount of curcumin applied in preparing lipid nanoemulsion})} \times 100. \quad (1)$$

2.5. Solubility of Curcumin. To determine the solubility of curcumin, 3 different solutions, including soybean oil, 1.25% (w/v) Tween 80 in distilled water, and 1.25% Tween 80 with 0.83% HEPC in distilled water were tested in this study. For determining the solubility of curcumin in soybean oil, 3.5 mg of curcumin was added to a test tube containing 1 mL of soybean oil. The mixture solutions were vortexed, allowed to cool, and kept at 24°C overnight. Thereafter, they were centrifuged at 3000 rpm for 15 min at 24°C. Undissolved curcumin, which was observed at the bottom of the test tube, was eliminated by centrifugation. Then, the amount of curcumin in soybean oil was determined by spectrophotometry at an absorbance of 450 nm.

For determining the solubility of curcumin in the Tween 80 aqueous solutions without (Tween 80 solution) or with HEPC (Tween 80-HEPC solution), 1.0 mg of curcumin was added to a test tube containing 1 mL of the aqueous solutions, followed by vortexing. The solutions were warmed and vortexed every 5 min in a water bath (60°C) for 1 h. After being allowed to cool and stand at 24°C overnight, they were centrifuged at 3000 rpm for 15 min at 24°C. The concentrations of curcumin in the supernatant of both Tween 80 and Tween 80-HEPC solutions were measured spectrophotometrically.

2.6. Cells and Cell Culture Conditions. B16F10 (mouse melanoma cell line) was cultured in DMEM containing 10% fetal calf serum, 100 units/mL penicillin, and 100 μg/mL streptomycin. Four types of leukemic cell lines, including HL60 (promyelocytic leukemia), K562 (chronic myelocytic leukemia), Molt4 (lymphoblastic leukemia), and U937 (monocytic leukemia), were cultured in RPMI-1640 medium containing 10% fetal calf serum, 1 mM L-glutamine, 100 units/mL penicillin, and 100 μg/mL streptomycin. These cell lines were maintained in a humidified incubator with an atmosphere of 95% air and 5% CO_2 at 37°C. When the cells reached confluency, they were harvested and plated for consequent passages or for nanoemulsion curcumin treatments.

2.7. MTT Assay. Cell viability was determined by the MTT test method. MTT (5 mg/mL) was dissolved in PBS. B16F10 and leukemic cells were cultured in 96-well plates (1.0×10^4 and 3.0×10^3 cells/well, resp.) containing 100 μL medium prior to treatment with curcumin and curcumin-loaded nanoemulsion at 37°C for 24 h. Subsequently, 100 μL fresh medium containing various concentrations (4.23, 8.47, 16.97, 33.93, and 67.86 μM) of curcumin or the corresponding curcumin-loaded nanoemulsion were added to each well, and incubated for another 48 h. Diluted curcumin solutions were freshly prepared in DMSO prior to each experiment. The final concentration of DMSO in culture medium was 0.2% (v/v). Diluted curcumin-loaded nanoemulsion was prepared in completed RPMI-1640 medium. The curcumin concentrations from curcumin-loaded nanoemulsion were determined by the colorimetric assay as previously described [24] using the HBSE buffer containing Triton X-100. The amount of curcumin in nanoemulsion was determined by comparing to the standard curcumin curve. Then, curcumin concentrations were calculated and diluted for the equal concentrations with equimolar of conventional curcumin to test cytotoxicity by MTT assay. The nanoemulsion without curcumin was used as vehicle control. The metabolic activity of each well was determined by MTT assay and compared to those of untreated cells. After removal of 100 μL medium, MTT dye solution was added (15 μL/100 μL medium) and the plates were incubated at 37°C for 4 h in a humidified 5% CO_2 atmosphere. After that, 200 μL of DMSO were added to each well, and mixed thoroughly to dissolve the dye crystals. The absorbance was measured using an ELISA

Table 1: Formulations of curcumin-loaded lipid nanoemulsion.

Component	Formulation							
	1	2	3	4	5	6	7	8
Soybean oil (mL)	1	1	—	—	1	1	1	1
Lecithin (mL)	—	—	1	1	—	—	—	—
HCO-60 (mg)	—	375	—	375	—	—	—	—
Tween 80 (mg)	375	—	375	—	375	375	375	375
HEPC (mg)	250	250	250	250	250	250	250	250
Curcumin (mg)	15	15	15	15	30	60	120	240
Distilled water (mL)	30	30	30	30	30	30	30	30

plate reader (Biotek EL 311) at 570 nm with a reference wavelength of 630 nm. High optical density readings corresponded to a high intensity of dye color, that is, to a high number of viable cells able to metabolize MTT salts. The fractional absorbance was calculated by the following formula:

$$\%\ \text{Cell survival} = \frac{\text{Mean absorbance in test wells}}{\text{Mean absorbance in control wells}} \times 100. \quad (2)$$

The average cell survival obtained from triplicate determinations at each concentration was plotted as a dose response curve. The experiment was carried out in 3 batches of nanoemulsion preparations in 3 time-independent experiments. The 50% inhibition concentration (IC_{50}) of the active substances was determined as the lowest concentration which reduced cell growth by 50% in treated compared to untreated culture or vehicle control culture (0.4% DMSO in culture medium). The IC_{50}s were mean ± standard error (SE) and compared for their activities.

2.8. In Vitro Release Kinetics of Curcumin-Loaded Nanoemulsion. Curcumin-loaded nanoemulsion at the concentration of 7 mg in 25% human serum in PBS was put into dialysis bag with pore size of 50°A (5 nm). The dialysis bag was kept in dark bottle containing 25% human serum in PBS with total volume of 150 mL. The condition was controlled under constant stirring in water bath set as 37°C. Sample (1 mL) was collected at certain time intervals of 2, 4, 6, 12, 24, 36, 48, 60, and 72 h. The fresh medium was added after withdrawal. The curcumin concentration in the sample was determined by colorimetric assay measured at 450 nm as compared to standard curcumin as described previously [25].

2.9. Statistical Analysis. Statistical analysis was performed using the SPSS software (version 10.0). All experiments were repeated at least 3 times. The data were expressed as the mean (standard deviation and standard error; SD and SE). Statistical differences between the means were tested by one-way ANOVA. Probability values $P < 0.01$ and $P < 0.05$ were considered as significant.

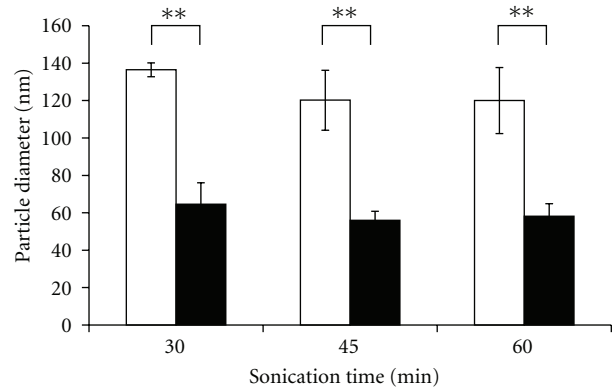

Figure 2: Effect of co-surfactants and sonication time on the particle diameter of curcumin-loaded lipid nanoemulsions. Closed bar: Tween 80, formulation 1. Open bar: HCO-60, formulation 2. Data are represented as the mean ± standard deviation of 3 independent experiments ($n = 3$). **Significantly different from the HCO-60 formulation ($P < 0.01$) by one-way ANOVA.

3. Results

3.1. Formulations and Operational Factors. The formulations and preparation conditions were optimized by changing the co-surfactant type, sonication time, and oil type. First of all, in order to evaluate the effect of co-surfactant and sonication time on the mean particle diameter of lipid nanoemulsions, a series of nanoemulsions was prepared with increasing sonication times in the presence of Tween 80 (formulation 1) or HCO-60 (formulation 2; Table 1). Herein, 15 mg of curcumin was used as the initial loading dose. In this experiment, soybean oil was used as oil component for curcumin lipid nanoemulsions.

The nanoemulsions prepared by using Tween 80 as a co-surfactant revealed the significant decrease in size as compared to HCO-60 ($P < 0.01$; Figure 2). The sonication time did not result in a difference in particle diameter among the nanoemulsions prepared with different sonication times (30, 45, or 60 min) in both HCO-60 and Tween 80 formulations. The mean particle diameters of lipid nanoemulsions with HCO-60 prepared with a sonication time of 30, 45, and 60 min were 136.5, 120.2, and 120.0 nm, respectively,

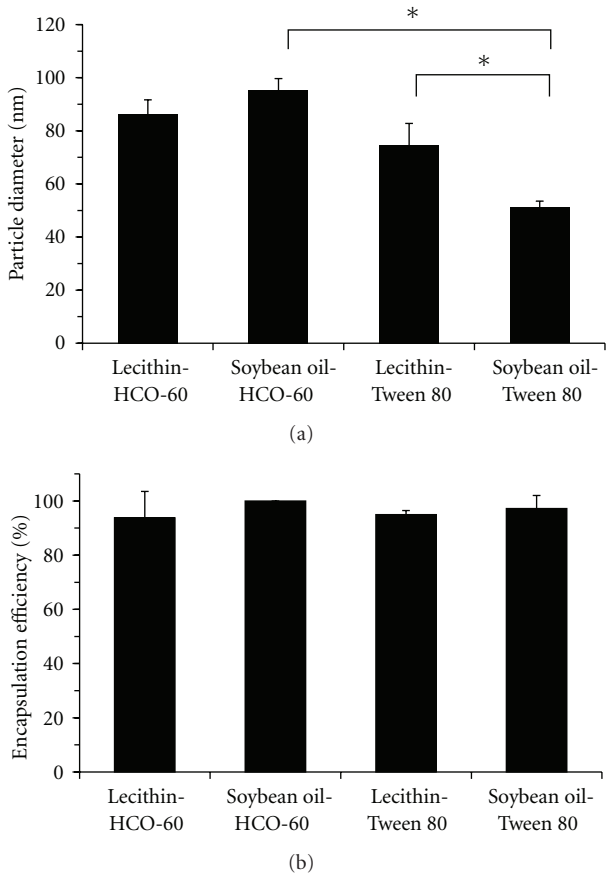

Figure 3: Effect of lipid type on the particle diameter (a) and percent incorporation efficiency (% IE) (b) of curcumin lipid nanoemulsions. Formulation: 1, 2, 3, and 4 in Table 1. Data are represented as the mean ± standard deviation of 3 independent experiments ($n = 3$). *Significantly different ($P < 0.05$) by one-way ANOVA.

while those with Tween 80 were 64.6, 56.0, and 58.2 nm, respectively. The prolongation of the sonication time from 30 min to 45 min resulted only in a slight decrease in the mean particle diameter in HCO-60 and Tween 80 (11.8 and 13.9%, resp.). The polydispersity indices ranged from 0.24 to 0.32. Thus, 30 min of sonication was chosen for the following experiments.

3.2. Effect of Oil Type on Particle Size of Emulsion. The 4 formulations of curcumin-loaded lipid nanoemulsions in this experiment are shown in Table 1 (formulations 1–4). Curcumin nanoemulsions using soybean oil showed smaller particle sizes than those using lecithin (Figure 3(a)). The mean particle diameters of the nanoemulsions composed of soybean oil with Tween 80 and those of lecithin with Tween 80 were 51.0 and 74.6 nm, respectively. The nanoemulsions composed of soybean oil with Tween 80 were significantly smaller in particle diameter (by 31.6%; $P < 0.05$) than those composed of lecithin with Tween 80. The mean particle diameter of soybean oil nanoemulsions with Tween 80 was significantly smaller (by 46.5%; $P < 0.05$) than those with

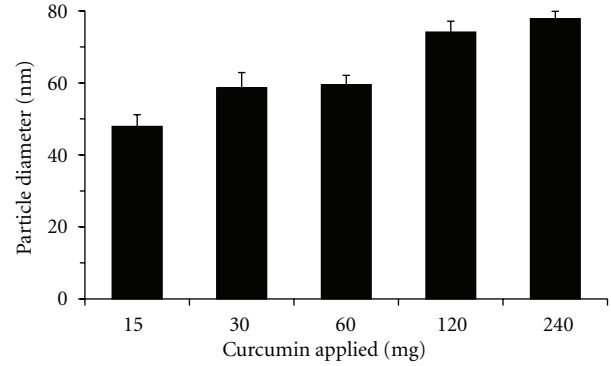

Figure 4: Effect of the amount of curcumin on the particle diameter of the emulsion. Formulation: 1, 5 to 8 in Table 1.

HCO-60. While the nanoemulsions composed of lecithin and soybean oil with HCO-60 did not show any significant difference in particle diameter in the statistical analysis, the polydispersity indices ranged from 0.22 to 0.37.

Figure 3(b) shows the % IE values of curcumin in the 4 lipid nanoemulsions prepared with formulations 1 to 4. The % IE in these 4 formulations was in the range of 93.8%–100%. The incorporated amount of curcumin in the nanoemulsions was in the range of 14.1–15.0 mg in total. Macroscopic observation clearly showed that free curcumin was poorly soluble in distilled water; in contrast, the prepared curcumin lipid nanoemulsions were absolutely transparent, with the hue derived from the natural color of curcumin. Furthermore, the curcumin lipid nanoemulsions with lecithin showed more transparency than those with soybean oil.

3.3. Enrichment of Curcumin in Nanoemulsions. The 5 formulations of curcumin-enriched lipid nanoemulsion are also listed in Table 1 (formulations 1, 5–8). The effects of the weight ratio of curcumin to HEPC on the mean particle diameters and particle size distributions of the emulsions are shown in Figures 4 and 5, respectively. Here, Tween 80 was used as a co-surfactant. As the amount of curcumin applied increased from 15 mg (formulation 1) to 30 mg (formulation 5), 60 mg (formulation 6), 120 mg (formulation 7), and 240 mg (formulation 8), the particle diameter of the nanoemulsion increased from 47.9 to 58.6, 59.5, 74.1, and 77.8 nm, respectively (Figure 4). When the nanoemulsions were centrifuged for separation of excess curcumin after sonication, pellets of excess curcumin could be observed when more than 30 mg of curcumin were added, in a manner depending on the amount applied. The particle size distributions had a single peak each, with the polydispersity indices ranging from 0.22 to 0.51 (Figure 5).

When all lipid nanoemulsions were examined for % IE after centrifugation, we found that % IE decreased depending on the amount of curcumin applied (Figure 6). However, the % IEs at 15 and 30 mg were not significantly different. Moreover, the color of the curcumin lipid nanoemulsion exhibited no difference when more than 30 mg of curcumin-was applied, suggesting a similar concentration of curcumin.

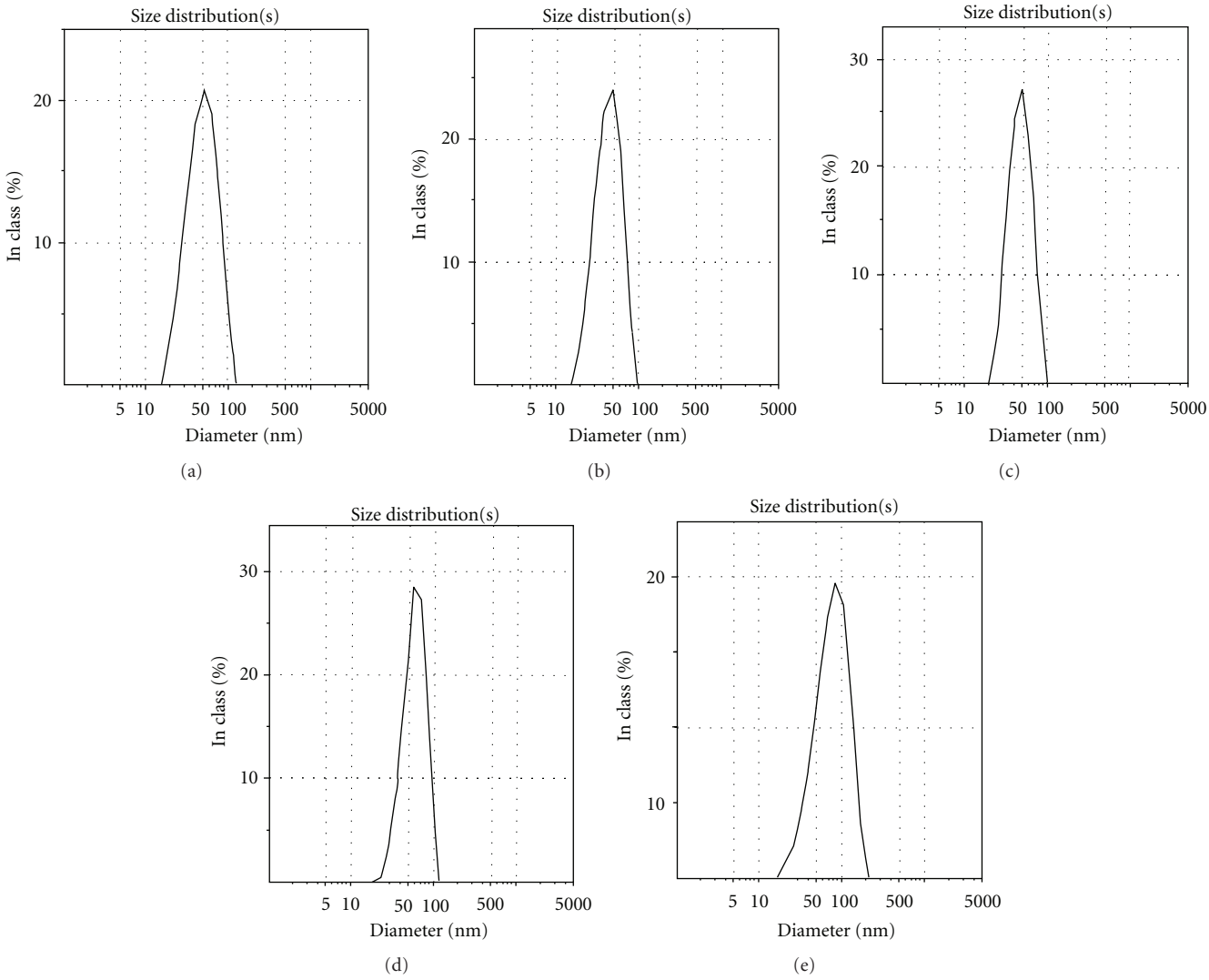

Figure 5: Particle size distributions of curcumin-loaded lipid nanoemulsions in formulations 1(a), 5(b) to 8(e).

3.4. Physical Stability Study. The time course-dependent change in the mean particle diameter of the lipid nanoemulsions prepared with 15, 30, and 60 mg of curcumin during storage at 4°C for 60 days is presented in Figure 7. The mean particle diameters at day 60 were 54.9, 58.2, and 56.8 nm, corresponding to 15, 30, and 60 mg of curcumin applied. No significant changes due to dispersion instability were observed.

3.5. Effect of Curcumin-Loaded Nanoemulsionon Cytotoxicity. By using curcumin-loaded nanoemulsion prepared with formulation 5 (Table 1), the cytotoxic effects of the nanoemulsion at various concentrations (0–67.86 μM or 0–25 μg/mL) on B16F10, K562, Molt4, U937, and HL-60 cell lines for 48 h by MTT assay were investigated. The results are shown in Figure 8. Cucumin-loaded nanoemulsion is capable of inhibiting cell growth of all cell lines. The IC_{50} values (mean ± SE) of cucumin-loaded nanoemulsion treatment were 22.2 ± 0.6, 53.7 ± 0.23, 30.3 ± 4.4, 35.8 ± 1.7, and 23.5 ± 1.1, respectively, whereas the curcumin treatment were 3.5 ± 0.5, 38.7 ± 2.0, 14.4 ± 2.3, 30.1 ± 0.9, and 15.7 ± 1.6 μM, respectively (Table 2). The IC_{50} value of curcumin-loaded nanoemulsion is significantly different when compared to curcumin treatment in B16F10 cells ($P < 0.05$). However, four leukemic cell lines did not show different inhibitory effect between curcumin-loaded nanoemulsion and curcumin treatments. The nanoemulsion control did not show any different cytotoxic effect on all cancer cells (IC_{50} values > 67.86 μM).

3.6. In Vitro Release Kinetics of Curcumin-Loaded Nanoemulsion. The release kinetics of curcumin-loaded nanoemulsion prepared with formulation 5 (Table 1) demonstrated approximately a 25% release of curcumin from the nanoemulsion at 72 h, when dispersed in 25% human serum containing-phosphate buffer saline at pH 7.4 (Figure 9). However, the release kinetics in phosphate buffer saline was 1.4% at 72 h.

Table 2: IC_{50} values (μM) of curcumin and curcumin-loaded nanoemulsion on B16F10, K562, Molt4, U937, and HL-60 cell lines.

Treatment	IC_{50} (μM)				
	B16F10	K562	Molt4	U937	HL-60
Curcumin	3.5 ± 0.5	38.7 ± 2.0	14.4 ± 2.3	30.1 ± 0.9	15.7 ± 1.6
Curcumin-loaded nanoemulsion	22.2 ± 0.6*	53.7 ± 0.23	30.3 ± 4.4	35.8 ± 1.7	23.5 ± 1.1
Nanoemulsion control	>67.9	>67.9	>67.9	>67.9	>67.9

Each value denotes the mean ± SE of three independent experiments ($n = 3$).
*Significantly different from the curcumin ($P < 0.05$).

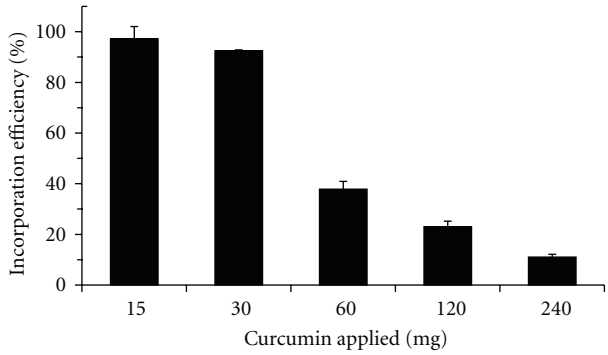

Figure 6: Effect of the amount of curcumin applied on the percent incorporation efficiency (% IE) in formulations 1, 5 to 8. Data are the mean ± standard deviation of 3 independent experiments ($n = 3$).

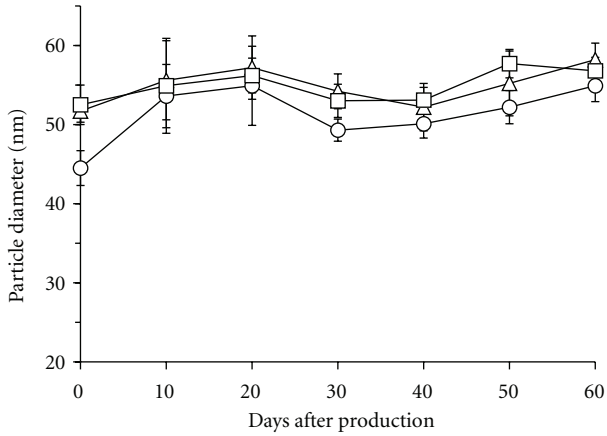

Figure 7: Physical stability of curcumin lipid emulsion in formulations 1, 5, and 6 during storage at 4°C for 60 days. Curcumin applied (mg): circle, 15; triangle, 30; square, 60. Data are represented as the mean ± standard deviation of 3 independent experiments ($n = 3$).

4. Discussion

The criteria for designing curcumin-containing lipid nanoemulsions for cancer therapy were as follows: the particle diameter of the emulsion had to be smaller than 100 nm (50–90 nm); the curcumin content had to be as high as possible; the surface of the emulsions had to be modified with hydrophilic moieties to allow prolonged circulation in the blood.

Curcumin is a lipophilic molecule and exists in its enol-tautomer form (Figure 1). It exhibits limited solubility in water, slight solubility in methanol, and good solubility in DMSO and chloroform [34]. To overcome its limited water solubility, a number of new approaches have been investigated to deliver curcumin effectively by using lipid-based nanoparticulate carriers such as liposome encapsulation [35, 36]. The formulation of the curcumin lipid nanoemulsion in this study was modified from the one used for the preparation of gadolinium-containing emulsions in the previous studies [32, 33]. The main components of those emulsions were soybean oil, water, Gd-diethylenetriaminepentaacetic acid-distearylamine (Gd-DTPA-SA, a highly lipophilic compound), and HEPC. HCO-60 was used as an effective co-surfactant, which could reduce the particle size and also enrich gadolinium in the nanoemulsion. Moreover, Tween 80 was also one of the effective co-surfactants to reduce the particle diameter to 52.7 nm in gadolinium-containing nanoemulsions, whereas it increased the particle diameter with increasing amounts of Gd-DTPA-SA in the nanoemulsion. Thus, this experiment was designed to study the effect of both HCO-60 and Tween 80 on particle size reduction and physical stability to identify the appropriate co-surfactant for curcumin lipid nanoemulsions.

A good emulsion was obtained in the preliminary experiments with HEPC. Hence, HEPC was selected as an emulsifier for curcumin-containing lipid nanoemulsions (Table 1). Then, the formulation and preparation conditions were optimized by changing the co-surfactant type, sonication time, and oil type. In order to evaluate the effect of co-surfactant and sonication time on the mean particle diameter of the lipid nanoemulsions, a series of samples were prepared with HCO-60 or Tween 80 as co-surfactant and soybean oil as oil component by increasing the sonication time at 15 mg of the initial curcumin loading (formulations 1 to 4, Table 1). The nanoemulsions were prepared at an HEPC-to-co-surfactant weight ratio of 1 : 1.5. Thus, the outer monolayer of the oil core in the lipid nanoemulsions would be composed of a HEPC-to-HCO-60 molar ratio of 7.6 : 2.4 or an HEPC-to-Tween 80 molar ratio of 5.4 : 4.6, assuming that all surfactant molecules were arranged on the interface of the oil core and water.

The sonication was effective to reduce the particle size of the nanoemulsions. In case of the Gd-DTPA-SA emulsion study, the particle diameter was gradually reduced by prolonging the sonication time [32, 33], leading to a decrease in

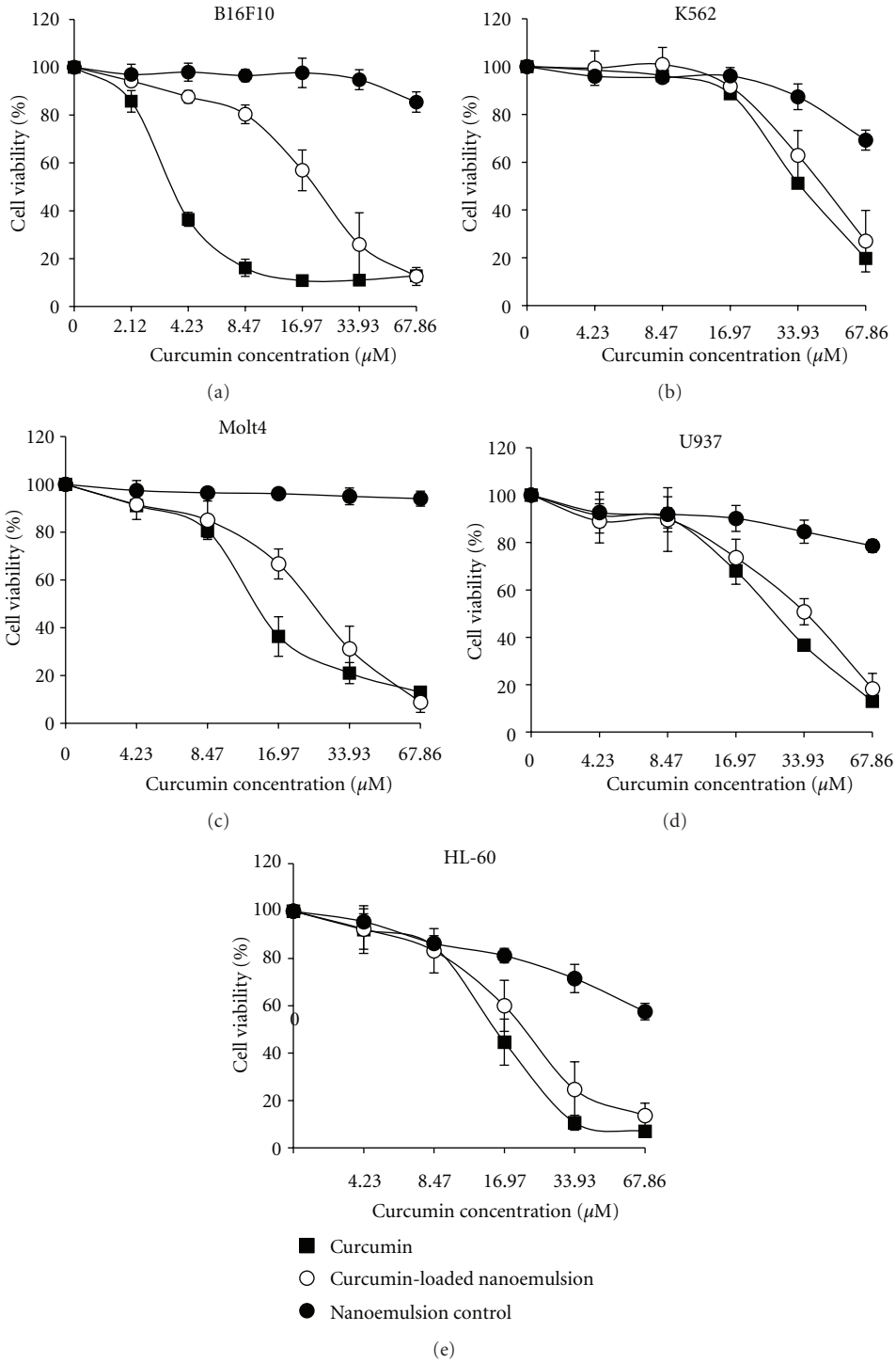

Figure 8: Cytotoxicity of curcumin and curcumin-loaded nanoemulsionon B16F10, K562, Molt4, U937, and HL-60 cell lines. ■: curcumin treatment, ○: curcumin-loaded nanoemulsion, ●: nanoemulsion control. Data are the mean ± standard error (SE) of three independent experiments ($n = 3$).

the diameter from 306 to 239 nm within 2 h. In the present study, 30 min sonication could rapidly decrease the particle diameter of the lipid nanoemulsions (Figure 2).

In this study, Tween 80 and HCO-60 were selected because they were effective co-surfactants in terms of particle size reduction in Gd-DTPA-SA-containing nanoemulsions [32, 33]. The present results showed that emulsion particles using Tween 80 were much smaller than those using HCO-60 (Figure 2). Thus, Tween 80 was selected to be the co-surfactant in our further studies. Nevertheless, both Tween

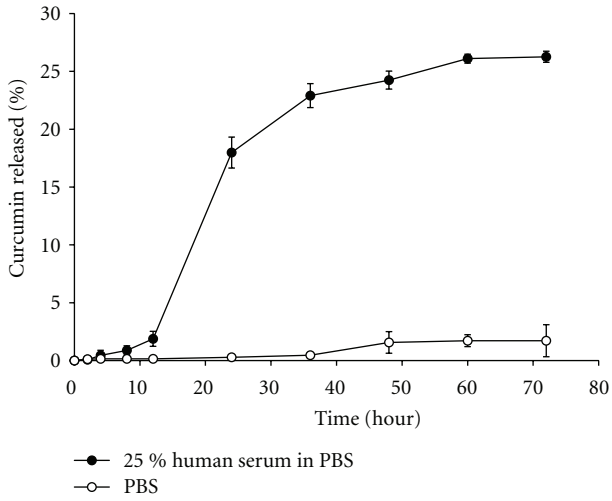

Figure 9: *In vitro* release kinetics of curcumin-loaded nanoemulsion. ●: 25% Human serum in PBS, ○: PBS.

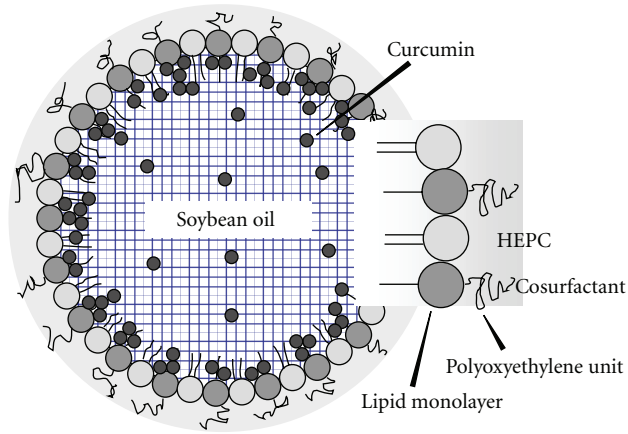

Figure 10: Schematic drawing of the particle structure of the curcumin-loaded lipid nanoemulsion.

80 and HCO-60 have been commonly used as stabilizers in commercially available lipid emulsion preparations for a long period of time [37, 38]. Thus, they can possibly be used as co-surfactants in curcumin nanoemulsions because they provided the curcumin emulsions with a particle diameter small enough for long-term circulation in the blood and also to extravasate through blood capillaries in tumors.

Soybean oil and lecithin obtained from soybean were examined as oil components. Both oil types have been widely used as a model system for lipid emulsion studies and are generally used for commercially available fat emulsions. In general, the formula of intralipid was made of 10–30% w/w soybean oil and 1.2% w/w lecithin. Lecithin also comes from soybean oil products. The amount of phospholipids in soybean oil and lecithin is 1.48–3.08% and 28.9–44.1%, respectively [39]. However, the viscosities of soybean oil and lecithin are 69 mPa·s and 10000 mPa·s, respectively, at 24°C. In this study, the curcumin nanoemulsion with soybean oil showed smaller particle diameters than that with lecithin (Figure 3(a)). This difference in the particle diameter can be attributed to the lower viscosity of soybean oil: it can allow breakup of the oil droplets readily by the sonic wave generated from the ultrasonication treatment and thus possibly allow to form the smaller-sized nanoemulsion [32].

The % IE of the curcumin lipid nanoemulsion was markedly decreased by the increasing total amount of curcumin applied (Figure 6), thereby implying that there were excess amounts of free curcumin after the emulsifying process. This result indicated that the lipid nanoemulsions were limited in their capacity to incorporate curcumin. Compared to the loading amount of curcumin in liposomes in the previous report [25], our formulation exhibited an 8-fold higher loading amount of curcumin.

According to solubility test based on formulation 5 (Table 1), the value of solubility of curcumin in 30 mL of Tween 80-HEPC (0.375 g and 0.250 g in 30 mL distilled water) aqueous solution was 20.5 ± 1.4 mg while that in 1 mL of soybean oil was confirmed to be 2.4 mg. Thus, it would be reasonable to consider that curcumin could be well solubilized in part of surfactant-phospholipid layer of the nanoemulsion rather than in soybean oil core particles. As shown in Figure 6, the amounts of curcumin incorporated in the emulsions prepared with formulations 5 to 8 were calculated as 27.7, 22.7, 27.6, and 26.4 mg for 30, 60, 120, and 240 mg of curcumin applied, respectively. These values agreed well with the value estimated from the solubility data (22.9 mg in total), suggesting that approximately 90% of curcumin incorporated in the emulsion might exist in the surface phospholipid-surfactant monolayer of the oil core particles. This might allow us to draw a possible structural scheme of the lipid nanoemulsion incorporating curcumin (Figure 10).

The anticancer properties of curcumin-loaded nanoemulsion, using mouse melanoma and leukemic cell lines as an experimental model system, and directly comparing its activities to curcumin were investigated. As demonstrated in Table 2, the curcumin-loaded nanoemulsion showed cytotoxicities to all cancer cells. The IC_{50} values were ranged from 22.2 to 53.7 μM. However, curcumin-loaded nanoemulsion exhibited higher cytotoxic effects in B16F10 than those of leukemic cells and showed the significant difference when compared to curcumin treatment. This might be the reason of the difference in cell phenotype that B16F10 is fibroblast cell and obtained from mouse. The B16F10 cell itself was more sensitive to curcumin than leukemic cell lines with the IC_{50} value of 3.5 μM. There were no significant difference of curcumin-loaded nanoemulsion and curcumin in four leukemic cell lines. Nevertheless, curcumin-loaded nanoemulsion showed lower cytotoxic effects on mouse melanoma and slightly lower on human leukemic cells possibly due to the limited availability of curcumin by slow and uncompleted release of curcumin from the nanoemulsion particles within 24 to 72 h. The result is in parallel to the cytotoxicity of polymeric nanoparticle-encapsulated curcumin (nanocurcumin) in pancreatic XPA-1 cell line with the IC_{50} value of ~20 μM [24]. Inhibitory effect of liposomal curcumin (5–10 μM) for 24–48 h on

human prostate cancer cell lines (LNCaP and C42B) resulted in at least 70–80% inhibition of cellular proliferation without affecting cell viability [25]. In comparison to nanoemulsion control, it was much less cytotoxic on cancer cells. There was a report that showed that the surfactants themselves can influence MTT assay [40]. However, concentration of Tween 80 in nanoemulsion of this experiment did not affect cell cytotoxicity as shown in Figure 8. Taken together, the activity of curcumin after incorporation into nanoemulsion seems to be determined by the curcumin release kinetics and the stability in activity on cancer cells.

5. Conclusions

This study showed the successful production of a curcumin lipid nanoemulsion with small particle size at a high yield. The curcumin lipid nanoemulsion was prepared by the thin-layer hydration method in a bath-type sonicator. The use of Tween 80 in the lipid nanoemulsion formulation instead of HCO-60 used previously resulted in a small particle size. The particle diameter of the lipid emulsion was decreased to 47–56 nm with small polydispersity. When increasing amounts of curcumin were added, the amount of curcumin incorporated in the emulsion was saturated. Approximately 90% of curcumin in the nanoemulsion was estimated to be in the surface layer of the oil core particles. Through the present study, an appropriate formulation for producing curcumin lipid nanoemulsions was found to be 1 mL soybean oil, 30 mg of cucumin, 250 mg of HEPC, 375 mg of Tween 80, and 30 mL of water. This formulation resulted in a curcumin-loaded lipid nanoemulsion stable in size for 60 days at 4°C. The results from the cytotoxicity test provide a strong evidence for curcumin-loaded nanoemulsion as effective nanodelivery vehicles that present the bioavaialbility of curcumin. Moreover, we demonstrated the noncytotoxicity of the nanoemulsion formulation *in vitro*, underscoring the potential of this nanoparticle as a carrier for hydrophobic drugs.

Acknowledgments

A part of this work was supported by the Matsumae International Foundation (MIF), Japan, the Thailand Government Budget, and National Research Council of Thailand (NRC).

References

[1] M. L. Kuo, T. S. Huang, and J. K. Lin, "Curcumin, an antioxidant and anti-tumor promoter, induces apoptosis in human leukemia cells," *Biochimica et Biophysica Acta*, vol. 1317, no. 2, pp. 95–100, 1996.

[2] R. Selvam, L. Subramanian, R. Gayathri, and N. Angayarkanni, "The anti-oxidant activity of turmeric (*Curcuma longa*)," *Journal of Ethnopharmacology*, vol. 47, no. 2, pp. 59–67, 1995.

[3] Sreejayan and M. N. A. Rao, "Curcuminoids as potent inhibitors of lipid peroxidation," *Journal of Pharmacy and Pharmacology*, vol. 46, no. 12, pp. 1013–1016, 1994.

[4] H. P. Ammon, N. H. Safayhi, T. Mack, and J. Sabieraj, "Mechanism of antiinflammatory actions of curcumine and boswellic acids," *Journal of Ethnopharmacology*, vol. 38, no. 2-3, pp. 113–119, 1993.

[5] A. Banerjee and S. S. Nigam, "Antimicrobial efficacy of the essential oil of *Curcuma longa*," *Indian Journal of Medical Research*, vol. 68, no. 5, pp. 864–866, 1978.

[6] S. T. N. Bhavani and M. V. Sreenivasa, "Effect of turmeric (*Curcuma longa*) fractions on the growth of some intestinal & pathogenic bacteria in vitro," *Indian Journal of Experimental Biology*, vol. 17, no. 12, pp. 1363–1366, 1979.

[7] T. Sawada, J. Yamahara, S. Shimazu, and T. Ohta, "Evaluation of crude drugs by bioassay. III. Comparison with local variation of contents and the fungistatic action of essential oil from the root of *Curcuma longa*," *Shoyakugaku Zasshi*, vol. 25, no. 1, pp. 11–16, 1971.

[8] D. S. Rao, N. C. Sekhara, M. N. Satyanarayana, and M. Srinivasan, "Effect of curcumin on serum and liver cholesterol levels in the rat," *Journal of Nutrition*, vol. 100, no. 11, pp. 1307–1315, 1970.

[9] P. Limtrakul, S. Anuchapreeda, S. Lipigorngoson, and F. W. Dunn, "Inhibition of carcinogen induced c-Ha-ras and c-fos proto-oncogenes expression by dietary curcumin," *BMC Cancer*, vol. 1, no. 1, article 1, pp. 1–7, 2001.

[10] S. Anuchapreeda, P. Limtrakul, P. Thanarattanakorn, S. Sittipreechacharn, and P. Chanarat, "Inhibitory effect of curcumin on WT1 gene expression in patient leukemic cells," *Archives of Pharmacal Research*, vol. 29, no. 1, pp. 80–87, 2006.

[11] S. Anuchapreeda, P. Thanarattanakorn, S. Sittipreechacharn, P. Chanarat, and P. Limtrakul, "Curcumin inhibits WT1 gene expression in human leukemic K562 cells," *Acta Pharmacologica Sinica*, vol. 27, no. 3, pp. 360–366, 2006.

[12] S. Anuchapreeda, S. Tima, C. Duangrat, and P. Limtrakul, "Effect of pure curcumin, demethoxycurcumin, and bisdemethoxycurcumin on WT1 gene expression in leukemic cell lines," *Cancer Chemotherapy and Pharmacology*, vol. 62, no. 4, pp. 585–594, 2008.

[13] K. Polasa, T. C. Raghuram, T. Prasanna Krishna, and K. Krishnaswamy, "Effect of turmeric on urinary mutagens in smokers," *Mutagenesis*, vol. 7, no. 2, pp. 107–109, 1992.

[14] R. G. Roy, N. M. Madesayaa, and R. B. Ghosh, "Study on inhalation therapy by an indigenous compound on *P. vivax* and *P. falciparum* infections: a preliminary communication," *Indian Journal of Medical Research*, vol. 64, no. 10, pp. 1451–1455, 1976.

[15] M. A. Azuine and S. V. Bhide, "Chemopreventive effect of turmeric against stomach and skin tumors induced by chemical carcinogens in Swiss mice," *Nutrition and Cancer*, vol. 17, no. 1, pp. 77–83, 1992.

[16] T. Dorai, Y. C. Cao, B. Dorai, R. Buttyan, and A. E. Katz, "Therapeutic potential of curcumin in human prostate cancer. III. Curcumin inhibits proliferation, induces apoptosis, and inhibits angiogenesis of LNCaP prostate cancer cells *in vivo*," *Prostate*, vol. 47, no. 4, pp. 293–303, 2001.

[17] S. Anuchapreeda, R. Muangmoonchai, and P. Limtrakul, "Effect of curcuminoids on *MDR1* gene promoter activity in human cervical carcinoma cells," *Chiang Mai Medical Bulletin*, vol. 41, no. 4, pp. 189–202, 2002.

[18] T. N. Bhavani Shankar, N. V. Shantha, and H. P. Ramesh, "Toxicity studies on turmeric (*Curcuma longa*): acute toxicity studies in rats, guinea pigs and monkeys," *Indian Journal of Experimental Biology*, vol. 18, no. 1, pp. 73–75, 1980.

[19] P. Limtrakul, W. Chearwae, and S. Anuchapreeda, "The effect of curcumin on the proliferation of cancer cell lines," *Chiang Mai Medical Bulletin*, vol. 38, no. 3-4, pp. 55–61, 1999.

[20] S. Anuchapreeda, W. Sadjapong, C. Duangrat, and P. Limtrakul, "The cytotoxic effect of curcumin, demethoxycurcumin and bisdemethoxycurcumin purified from Turmeric powder on leukemic cell lines," *Bulletin of Chiang Mai Associated Medical Sciences*, vol. 39, no. 1, pp. 60–71, 2006.

[21] S. Semsri, S. R. Krig, L. Kotelawala, C. A. Sweeney, and S. Anuchapreeda, "Inhibitory mechanism of pure curcumin on Wilms' tumor 1 (WT1) gene expression through the PKCα signaling pathway in leukemic K562 cells," *FEBS Letters*, vol. 585, no. 14, pp. 2235–2242, 2011.

[22] T. M. Allen, C. Hansen, and J. Rutledge, "Liposomes with prolonged circulation times: factors affecting uptake by reticuloendothelial and other tissues," *Biochimica et Biophysica Acta*, vol. 981, no. 1, pp. 27–35, 1989.

[23] Y. Kato, K. Watanabe, M. Nakakura, T. Hosokawa, E. Hayakawa, and K. Ito, "Blood clearance and tissue distribution of various formulations of α-tocopherol injection after intravenous administration," *Chemical and Pharmaceutical Bulletin*, vol. 41, no. 3, pp. 599–604, 1993.

[24] S. Bisht, G. Feldmann, S. Soni et al., "Polymeric nanoparticle-encapsulated curcumin ("nanocurcumin"): a novel strategy for human cancer therapy," *Journal of Nanobiotechnology*, vol. 5, article 3, pp. 1–18, 2007.

[25] R. L. Thangapazham, A. Puri, S. Tele, R. Blumenthal, and R. K. Maheshwari, "Evaluation of a nanotechnology-based carrier for delivery of curcumin in prostate cancer cells," *International Journal of Oncology*, vol. 32, no. 5, pp. 1119–1123, 2008.

[26] R. K. Das, N. Kasoju, and U. Bora, "Encapsulation of curcumin in alginate-chitosan-pluronic composite nanoparticles for delivery to cancer cells," *Nanomedicine*, vol. 6, no. 1, pp. e153–e160, 2010.

[27] J. J. Wheeler, K. F. Wong, S. M. Ansell, D. Masin, and M. B. Bally, "Polyethylene glycol modified phospholipids stabilize emulsions prepared from triacylglycerol," *Journal of Pharmaceutical Sciences*, vol. 83, no. 11, pp. 1558–1564, 1994.

[28] F. Liu and D. Liu, "Long-circulating emulsions (oil-in-water) as carriers for lipophilic drugs," *Pharmaceutical Research*, vol. 12, no. 7, pp. 1060–1064, 1995.

[29] A. Kurihara, Y. Shibayama, A. Mizota et al., "Lipid emulsions of palmitoylrhizoxin: effects of composition on lipolysis and biodistribution," *Biopharmaceutics and Drug Disposition*, vol. 17, no. 4, pp. 331–342, 1996.

[30] Y. Wang, G. M. Mesfin, C. A. Rodríguez et al., "Venous irritation, pharmacokinetics, and tissue distribution of tirilazad in rats following intravenous administration of a novel supersaturated submicron lipid emulsion," *Pharmaceutical Research*, vol. 16, no. 6, pp. 930–938, 1999.

[31] R. C. Marānhao, B. Garicochea, E. L. Silva et al., "Plasma kinetics and biodistribution of a lipid emulsion resembling low- density lipoprotein in patients with acute leukemia," *Cancer Research*, vol. 54, no. 17, pp. 4660–4666, 1994.

[32] M. Miyamoto, K. Hirano, H. Ichikawa, Y. Fukumori, Y. Akine, and K. Tokuuye, "Preparation of gadolinium-containing emulsions stabilized with phosphatidylcholine-surfactant mixtures for neutron-capture therapy," *Chemical and Pharmaceutical Bulletin*, vol. 47, no. 2, pp. 203–208, 1999.

[33] M. Miyamoto, K. Hirano, H. Ichikawa, Y. Fukumori, Y. Akine, and K. Tokuuye, "Biodistribution of gadolinium incorporated in lipid emulsions intraperitoneally administered for neutron-capture therapy with tumor-bearing hamsters," *Biological and Pharmaceutical Bulletin*, vol. 22, no. 12, pp. 1331–1340, 1999.

[34] F. Payton, P. Sandusky, and W. L. Alworth, "NMR study of the solution structure of curcumin," *Journal of Natural Products*, vol. 70, no. 2, pp. 143–146, 2007.

[35] L. Li, F. S. Braiteh, and R. Kurzrock, "Liposome-encapsulated curcumin: in vitro and in vivo effects on proliferation, apoptosis, signaling, and angiogenesis," *Cancer*, vol. 104, no. 6, pp. 1322–1331, 2005.

[36] K. Maiti, K. Mukherjee, A. Gantait, B. P. Saha, and P. K. Mukherjee, "Curcumin-phospholipid complex: preparation, therapeutic evaluation and pharmacokinetic study in rats," *International Journal of Pharmaceutics*, vol. 330, no. 1-2, pp. 155–163, 2007.

[37] C. F. Hung, T. L. Hwang, C. C. Chang, and J. Y. Fang, "Physicochemical characterization and gene transfection efficiency of lipid emulsions with various co-emulsifiers," *International Journal of Pharmaceutics*, vol. 289, no. 1-2, pp. 197–208, 2005.

[38] A. Chinsriwongkul, P. Opanasopit, T. Ngawhirunpat, N. Chareansriwilaiwat, W. Sila-On, and U. Ruktanonchai, "Physicochemical properties of lipid emulsions formulated with high-load all-trans-retinoic acid," *PDA Journal of Pharmaceutical Science and Technology*, vol. 61, no. 6, pp. 461–471, 2007.

[39] W. J. Hurstand and R. A. Martin Jr., "The analysis of phospholipids in soy lecithin by HPLC," *Journal of American Oil Chemists' Society*, vol. 61, no. 9, pp. 1462–1463, 1984.

[40] Y. Li, S. Le Maux, H. Xiao, and D. J. McClements, "Emulsion-based delivery systems for tributyrin, a potential colon cancer preventative agent," *Journal of Agricultural and Food Chemistry*, vol. 57, no. 19, pp. 9243–9249, 2009.

Hindawi Publishing Corporation
Journal of Nanotechnology
Volume 2012, Article ID 780815, 6 pages
doi:10.1155/2012/780815

Research Article

Theoretical Investigation on the Solubilization in Water of Functionalized Single-Wall Carbon Nanotubes

Michael Mananghaya,[1,2] Emmanuel Rodulfo,[1] Gil Nonato Santos,[1] and Al Rey Villagracia[1]

[1] *Physics Department, De La Salle University-Manila, Taft Avenue, Manila 1004, Philippines*
[2] *Physics Department, Mapúa Institute of Technology, Muralla Street, Intramuros, Manila 1002, Philippines*

Correspondence should be addressed to Michael Mananghaya, mike_mananghaya@yahoo.com

Received 14 July 2011; Revised 28 August 2011; Accepted 5 September 2011

Academic Editor: Lifeng Dong

An important technique to increase the solubility and reactivity of carbon nanotube is through functionalization. In this study, the effects of functionalization of some single-walled carbon nanotubes (SWCNTs) were investigated with the aid of density functional theory. The SWCNT model used in the study consists of a finite, (5, 0) zigzag nanotube segment containing 60 C atoms with hydrogen atoms added to the dangling bonds of the perimeter carbons. There are three water-dispersible SWCNTs used in this study that were functionalized with (a) formic acid, as a model of carboxylic acid, (b) isophthalic acid, as a model aromatic dicarboxylic acid, and (c) benzenesulfonic acid, as a model aromatic sulfonic acid. Binding energies of the organic radicals to the nanotubes are calculated, as well as the HOMO-LUMO gaps and dipole moments of both nanotubes and functionalized nanotubes. Binding was found out to be thermodynamically favorable. The functionalization increases the electrical dipole moments and results in an enhancement in the solubility of the nanotubes in water manifested through favorable changes in the free energies of solvation. This should lower the toxicity of nanotubes and improve their biocompatibility.

1. Introduction

Single-walled carbon nanotubes (SWCNTs) are allotropes of carbon and possess various novel properties that make them useful in the field of nanotechnology and pharmaceuticals. SWCNTs are tubular in shape, made of graphite, nanometers in diameter, and several millimeters in length and have a very broad range of electronic, thermal, and structural properties. These properties vary with the kind of nanotubes defined by its diameter, length, chirality or twist, and wall nature. Their unique surface area, stiffness, strength, and resilience have led to much excitement in the field of pharmacy. Nanostructured materials hold promise for a wide range of technological applications and are increasingly studied, not only for their possible applications in electronics, optics and mechanical materials, but also specifically having enormous potential in nanomedicine [1–11]. Because of this, it is imperative to examine the toxicity of these carbon-based nanostructures. Previous toxicological evaluations of single-walled carbon nanotubes have been conducted, both in cell culture and in vivo. One example, using an SWCNT surfactant stabilized system where the Fe content was significantly high, reported an elevated cytotoxic response [12]. Warheit et al. [13] observed an increase in inflammatory response in the lung cavities of rats. While these studies report potential negative implications of SWCNT, they did not use a SWCNT sample easily dispersed in water via covalently bound functional groups.

Carbon nanotubes (CNTs) are insoluble in water. For successful biomedical applications of nanotubes the solubility problem may be overcome in part by chemical functionalization of the CNT surface, resulting in an increased compatibility of the functionalized CNT with water [1]. Functionalization has led to improved compatibility with a variety of biological components. Functionalization has been obtained both through non-covalent-binding schemes [10] or covalent binding at the CNT surface [7–9].

Studies done previously, evaluated the differential cytotoxicity of water-suspendable fullerenes on human dermal fibroblasts (HDFs) in culture [14]. It was concluded that as

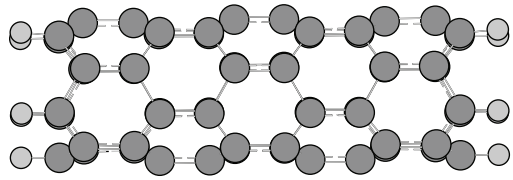

Figure 1: Optimized geometry of the finite (5, 0) zigzag SWCNT ($C_{60}H_{20}$). Gray color depicts carbon atoms and light gray is hydrogen.

the degree of functionalization on the surface of the fullerene cage increases, the cytotoxicity of the fullerene decreases significantly. The simple act of functionalizing the fullerene with either carboxyl or hydroxyl groups decreased the cytotoxic response over seven orders of magnitudes for HDF, human liver carcinoma cells, and neuronal human astrocyte cell lines. Different molecules have been employed to functionalize CNT into customized species that may simultaneously carry several nanostructures (multifunctionalization) to detect, allow imaging; and deliver therapeutical loads [15].

Essentially, the need to improve biodistribution, pharmacokinetics, and solubility, as well as the need to diminish the toxicity of the CNT [1] are fundamental problems addressed through computational simulation and modeling. The aim of this research is to perform density functional theory (DFT) calculations [16] to investigate how the nanotube properties change due to covalent functionalization of certain organic groups to side walls and tips of the nanotubes, improving its solubility in water. Functionalization enhances the biocompatibility, potentially diminishing toxicity and therefore paves the way to rational modifications and/or design of new nanostructured species for efficient targeting and drug delivery.

2. Methodology

To investigate the effects of functionalization of SWCNT in increasing their solubility we build a finite model (5, 0) zigzag nanotube segment containing 60 C atoms with hydrogen atoms added to the dangling bonds of the perimeter carbons and the resulting formula is $C_{60}H_{20}$, see Figure 1. This nanotube model system is similar to Jaffe's model [17]. The nanotubes are covalently functionalized with the following organic molecules: (a) formic acid, CO_2H_2, as a model of carboxylic acid, Figure 2 shows the functionalization at the sidewall and Figure 3 shows the functionalization at the tip of the SWCNT which is a typical product of the oxidation of carbon nanotubes [9, 10], (b) isophthalic acid, $C_6H_4(CO_2H)_2$, as a model aromatic dicarboxylic acid, see Figure 4, [18], and (c) benzenesulfonic acid, $C_6H_5SO_3H$, as a model aromatic sulfonic acid, see Figure 5 [18]. These molecules have been investigated for their capability of drug delivery and diagnostic applications.

All calculations were performed using DFT with a hybrid functional B3LYP [19–22] and a 3–21 G basis set [23]. Charge densities were analyzed by the Mulliken method [24]. For open-shell molecular radicals, the unrestricted

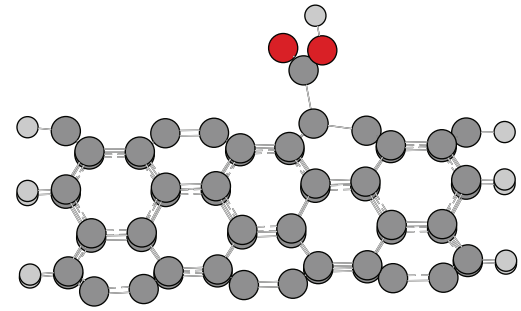

Figure 2: Optimized geometry of the finite (5, 0) zigzag SWCNT ($C_{60}H_{20}$) with the formic acid radical at the tube sidewall. Gray color depicts carbon atoms; light gray is hydrogen and red is oxygen.

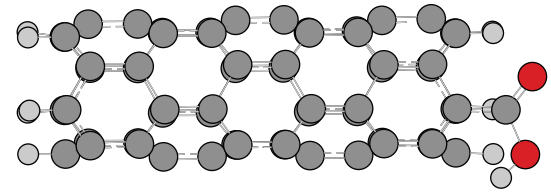

Figure 3: Optimized geometry of the finite (5, 0) zigzag SWCNT ($C_{60}H_{19}$) with the formic acid radical at the tube tip. Gray color depicts carbon atoms; light gray is hydrogen and red is oxygen.

formalism was used. The present level of calculation, DFT (UB3LYP)/3–21 G, is known to produce reasonable results [25] for bond lengths, bond angles, and bond energies for a wide range of molecules. The computations were carried out on a computer using the *ab initio* quantum chemistry package, Gaussian 09 (G09) [26], with the default convergence thresholds for DFT optimization calculations.

Electronic structure descriptors have been computed to analyze the geometrical and electronic changes that may lead to a better solubility of the functionalized nanotubes. Among them are the electronic HOMO-LUMO gap (H-L gap), the dipole moment (μ_{dip}), and the Gibbs free energy of solvation (ΔG_{solv}). The HOMO-LUMO gap, in the case of open electronic shell systems, is computed between the highest of the HOMOs and the lowest of the LUMOs, regardless of the spin type. For all systems with a doublet multiplicity (one unpaired electron), this always resulted in the HOMO (alpha)-LUMO (beta) gap.

The solubility of a given molecule in a solvent can be assessed by measuring its Gibbs free energy of solvation. A number of quantum mechanical continuum solvation models were developed for this purpose [27, 28]. We have chosen the polarizable continuum model (PCM) as implemented in G09. This originated from the Onsager continuum model [28] and was formulated by Tomasi et al. [27, 29–31], which takes into account the solute interactions with the solvent, modeled as a continuum dielectric medium in which a cavity is built to accommodate the solute molecule.

3. Results and Discussions

3.1. Structural Parameters. We have used the G09 code to optimize the geometries for the finite SWCNT. The resulting

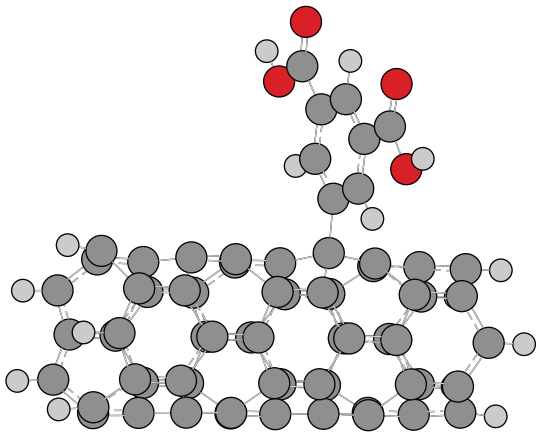

Figure 4: Optimized geometry of the finite (5, 0) zigzag SWCNT ($C_{60}H_{20}$) with the isophthalic acid radical at the tube sidewall. Gray color depicts carbon atoms; light gray is hydrogen and red is oxygen.

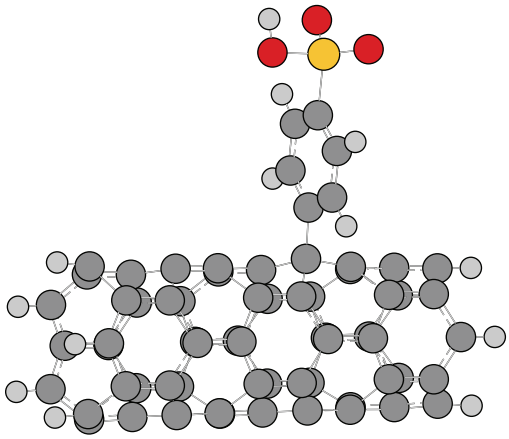

Figure 5: Optimized geometry of the finite (5, 0) zigzag SWCNT ($C_{60}H_{20}$) with the benzenesulfonic acid radical at the tube sidewall. Gray color depicts carbon atoms; light gray is hydrogen, yellow is sulfur and red is oxygen.

optimized structures are shown in Figure 1. The finite (5, 0) nanotube $C_{60}H_{20}$ has an optimized length of 11.32 Å and a diameter of 3.90 Å. Computed length agrees with a value of 11.36 Å obtained by Jaffe's model [17] and computed SWCNT diameter also compares well with the value 3.92 Å in their paper.

Presented in Figures 2 and 3 are the optimized structures for two possible ways of functionalizing the finite SWCNT with formic acid. Figure 2 shows the functionalization at the sidewall of the nanotube wherein we take the organic molecule already in its radical form, $^{\cdot}CO_2H$, attached by its C atom to the nanotube sidewall. In Figure 3 the functionalization at the tip of the SWCNT was carried out as another possibility because it is known that closed nanotube tips react with strong oxidizing agents, opening the tip and filling the dangling bonds with carboxylic acid molecules. The optimized structure for the functionalization of the SWCNT sidewall with the isophthalic acid radical $^{\cdot}C_6H_3(CO_2H)_2$. is given in Figure 4. We have also studied the functionalization of the SWCNT sidewall with the benzenesulfonic acid, $^{\cdot}C_6H_4SO_3H$; the optimized structure is shown in Figure 5. These molecules have been used in studies of covalent functionalization of SWCNT capability for drug delivery [15, 18].

3.2. Binding Energies. Binding energies of the radicals to the nanotube, E_b, are defined for the reaction

$$\text{ORG} + \text{SWCNT} \longrightarrow \text{ORG-SWCNT}, \quad (1)$$

where ORG is any of the studied organic radicals and ORG-SWCNT is the corresponding functionalized nanotube. Therefore

$$E_b = E(\text{ORG-SWCNT}) - E(\text{SWCNT}) - E(\text{ORG}). \quad (2)$$

The binding energy is negative if functionalization is thermodynamically favorable. To avoid considering the artificial rupture of C–H bonds involving functionalization at the tip, one H atom was previously removed and the nanotube structure was reoptimized before functionalization with the formic acid radical. The studied reactions are:

$$^{\cdot}CO_2H + C_{60}H_{20} \longrightarrow CO_2H\text{-SWCNT} \quad (\text{on sidewall}) \quad (3)$$

$$^{\cdot}C_6H_3(CO_2H)_2 + C_{60}H_{20} \longrightarrow C_6H_3(CO_2H)_2\text{-SWCNT} \quad (\text{on sidewall}) \quad (4)$$

$$^{\cdot}C_6H_4SO_3H + C_{60}H_{20} \longrightarrow C_6H_4SO_3H - \text{SWCNT} \quad (\text{on sidewall}) \quad (5)$$

$$^{\cdot}CO_2H + C_{60}H_{19} \longrightarrow CO_2H\text{-SWCNT} \quad (\text{on tip}) \quad (6)$$

Since the energies of the organic radicals are required in (2), their structures were also optimized. The functionalization reactions (3) to (6) are thermodynamically favorable, as can be seen in Table 1, and the resulting binding energies are between −2 eV to –4 eV.

3.3. Electronic Properties. Electronic properties computed for the functionalized SWCNT is displayed in Table 1 for the $C_{60}H_{20}$ nanotube and the functionalized SWCNT. These include the HOMO-LUMO gaps (H-L gap), the dipole moments (μ_{dip}); and the Gibbs free energy of solvation (ΔG_{solv}). The HOMO-LUMO gap of the infinite (5, 0) SWCNT is zero, because that nanotube is metallic. A negligible HOMO-LUMO gap develops in the finite nanotube model (0.05 eV), in agreement. The spatial distributions of the HOMO orbitals of the SWCNT and the tube with H atom missing from the tip, SWCNT radical, are shown in Figure 6. These orbitals display a similar delocalization over the whole tube, but the main difference is that the HOMO of the SWCNT radical has a noticeable lobe at the defect, suggesting a dangling bond at this site. Spatial

Table 1: Electronic properties for the $C_{60}H_{20}$ nanotube and the functionalized SWCNT formed in the reactions (3)–(6). The properties are HOMO-LUMO gap (H-L gap), magnitude of the dipole moment (μ_{dip}), and the Gibbs free energy of solvation (ΔG_{solv}).

System	E_b (eV)	H-L gap (eV)	μ_{dip} (debye)	ΔG_{solv} (eV)
SWCNT	—	0.05	0.34	−0.73
CO_2H-SWCNT (sidewall)	−2.00	0.38	3.60	−0.98
$C_6H_3(CO_2H)_2$-SWCNT (sidewall)	−2.73	0.41	3.96	−1.16
$C_6H_4SO_3H$-SWCNT (sidewall)	−3.59	0.38	3.80	−1.12
CO_2H-SWCNT radical (tip)	−3.88	0.41	9.79	−1.05

distributions of the LUMO orbitals for the same nanotubes are given in Figure 7. A prominent accumulation of the orbital distribution appears at the vacancy position of the missing H atom in the SWCNT radical. The localized lobes are responsible for the reactivity of the nanotube.

In Table 1 we can observe an important increase of the magnitude of the dipole moments of the functionalized nanotubes compared to the nanotube that is not functionalized. The $C_{60}H_{20}$ has a small dipole moment of 0.34 debye and the values of the dipole moments of the functionalized SWCNT are much larger. The substantial increase in the dipole moment is expected to modify the interaction of the functionalized nanotubes with a polar solvent such as water, potentially increasing their solubilities in the physiological medium.

3.4. Solubilization. Solubility can be assessed by measuring its Gibbs free energy of solvation. The Gibbs free energy of solvation, ΔG_{solv}, is computed as the difference between the optimized energies of the species in the solvent (PCM) and vacuum (gas phase),

$$\Delta G_{solv} = E_{PCM} - E_{gas}. \quad (7)$$

The PCM; as implemented in G09 which takes into account the solvent interactions with the solute within a cavity in a continuum dielectric medium approximation for the solvent; was used to calculate the optimized energies of the species in the solvent such as water. Solubility of a given molecule in water requires a negative value of ΔG_{solv}. All the calculated ΔG_{solv} of the functionalized nanotubes, given in Table 1, are negative. If we compare with the ΔG_{solv} obtained for the unfunctionalized nanotube, we see that solubility in water is larger for the functionalized nanotubes. This is in agreement with the experiment performed in vitro cytotoxicity screens on HDF by Sayes et al. [18] wherein the sidewall functionalized SWCNT with phenyl-SO_3H and phenyl-$(COOH)_2$ samples are found out to be substantially less cytotoxic than unfunctionalized SWCNT in water. On the other hand, the solvation Gibbs free energy for the SWCNT is –0.73 eV, which is predicted to be slightly soluble. It is a little surprising for the tube, but this is an artifact of the finite model with artificial C–H bonds at the tips. These slightly polarizable bonds induce an artificial minor solubility in the model SWCNT. However, in all cases, the solubility increases dramatically and substantially by using the technique of functionalization with the said organic radicals.

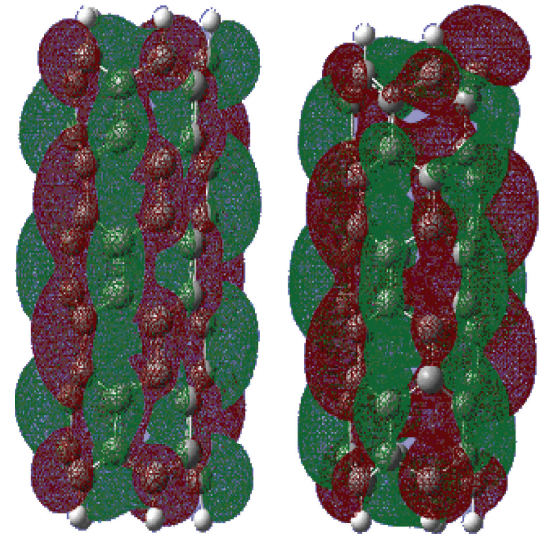

(a) (b)

Figure 6: Spatial distribution of the HOMO orbitals for (a) the $C_{60}H_{20}$ nanotube and (b) the nanotube radical with a missing H atom from the tip $C_{60}H_{19}$. The wave function isosurfaces of values +0.01 and −0.01 $(e/Å^3)^{1/2}$ are shown in red and green, respectively.

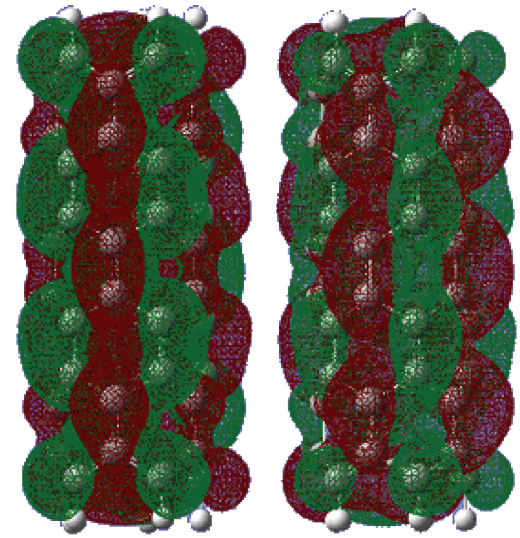

(a) (b)

Figure 7: Spatial distribution of the LUMO orbitals for (a) the $C_{60}H_{20}$ nanotube and (b) the nanotube radical with a missing H atom from the tip $C_{60}H_{19}$. The wave function isosurfaces of values +0.01 and −0.01 $(e/Å^3)^{1/2}$ are shown in red and green, respectively.

4. Conclusions

Density functional theory using mainly the G09 code was used to investigate the functionalization of SWCNT with open ends capped with H atoms with three different kinds of acids that help to improve their solubility in water and could make nanotubes more biocompatible. The nanotube has been functionalized with formic acid, isophthalic acid; and benzenesulfonic acid. Electronic exchange and correlation effects have been treated with the gradient-corrected B3LYP functional.

The functionalization with these organic molecules, either on the nanotube sidewall or tip sites where a hydrogen atom has been removed, is thermodynamically favorable. The enhanced dipole moment of the nanotubes due to functionalization is manifested in the improvement of their solubility in water as assessed by a calculation of the solvation free energies of the functionalized nanotubes employing the PCM polarizable continuum model. Functionalization enhances nanotubes biocompatibility, thus reducing the toxicity and the chance of tissue accumulation, for their future use in drug delivery.

Acknowledgments

This work was supported in part by the Department of Science and Technology, Philippine Council for Advanced Science and Technology Research and Development (DOST, PCASTRD), Philippine Council for Industry, Energy and Emerging Technology Research and Development (PCIEERD) and by the De La Salle University-Manila Faculty. The ideas in this paper would not have crystallized in the present form without the incisive remarks of Melanie Y. David.

References

[1] N. Sinha and J. T. W. Yeow, "Carbon nanotubes for biomedical applications," *IEEE Transactions on Nanobioscience*, vol. 4, no. 2, pp. 180–195, 2005.

[2] N. Sinha, J. Ma, and J. T. W. Yeow, "Carbon nanotube-based sensors," *Journal of Nanoscience and Nanotechnology*, vol. 6, no. 3, pp. 573–590, 2006.

[3] C. Klumpp, K. Kostarelos, M. Prato, and A. Bianco, "Functionalized carbon nanotubes as emerging nanovectors for the delivery of therapeutics," *Biochimica et Biophysica Acta*, vol. 1758, no. 3, pp. 404–412, 2006.

[4] A. Bianco, K. Kostarelos, and M. Prato, "Applications of carbon nanotubes in drug delivery," *Current Opinion in Chemical Biology*, vol. 9, no. 6, pp. 674–679, 2005.

[5] A. Bianco, "Carbon nanotubes for the delivery of therapeutic molecules," *Expert Opinion on Drug Delivery*, vol. 1, no. 1, pp. 57–65, 2004.

[6] P. Couvreur and C. Vauthier, "Nanotechnology: intelligent design to treat complex disease," *Pharmaceutical Research*, vol. 23, no. 7, pp. 1417–1450, 2006.

[7] R. Singh, D. Pantarotto, D. McCarthy et al., "Binding and condensation of plasmid DNA onto functionalized carbon nanotubes: toward the construction of nanotube-based gene delivery vectors," *Journal of the American Chemical Society*, vol. 127, no. 12, pp. 4388–4396, 2005.

[8] A. Bianco, K. Kostarelos, C. D. Partidos, and M. Prato, "Biomedical applications of functionalised carbon nanotubes," *Chemical Communications*, no. 5, pp. 571–577, 2005.

[9] M. Prato, K. Kostarelos, and A. Bianco, "Functionalized carbon nanotubes in drug design and discovery," *Accounts of Chemical Research*, vol. 41, no. 1, pp. 60–68, 2008.

[10] N. W. S. Kam and H. Dai, "Carbon nanotubes as intracellular protein transporters: generality and biological functionality," *Journal of the American Chemical Society*, vol. 127, no. 16, pp. 6021–6026, 2005.

[11] A. De La Zerda, C. Zavaleta, S. Keren et al., "Carbon nanotubes as photoacoustic molecular imaging agents in living mice," *Nature Nanotechnology*, vol. 3, no. 9, pp. 557–562, 2008.

[12] N. W. S. Kam, T. C. Jessop, P. A. Wender, and H. Dai, "Nanotube molecular transporters: internalization of carbon nanotube-protein conjugates into mammalian cells," *Journal of the American Chemical Society*, vol. 126, no. 22, pp. 6850–6851, 2004.

[13] D. B. Warheit, B. R. Laurence, K. L. Reed, D. H. Roach, G. A. M. Reynolds, and T. R. Webb, "Comparative pulmonary toxicity assessment of single-wall carbon nanotubes in rats," *Toxicological Sciences*, vol. 77, no. 1, pp. 117–125, 2004.

[14] C. M. Sayes, J. D. Fortner, W. Guo et al., "The differential cytotoxicity of water-soluble fullerenes," *Nano Letters*, vol. 4, no. 10, pp. 1881–1887, 2004.

[15] X. Yang, Z. Zhang, Z. Liu, Y. Ma, R. Yang, and Y. Chen, "Multi-functionalized single-walled carbon nanotubes as tumor cell targeting biological transporters ," *Journal of Nanoparticle Research*, vol. 10, no. 5, pp. 815–822, 2008.

[16] R. G. Parr and W. Yang, *Density Functional Theory of Atoms and Molecules*, Oxford University Press, Oxford, UK, 1989.

[17] R. L. Jaffe, "Quantum chemistry study of fullerene and carbon nanotube fluorination," *Journal of Physical Chemistry B*, vol. 107, no. 38, pp. 10378–10388, 2003.

[18] C. M. Sayes, F. Liang, J. L. Hudson et al., "Functionalization density dependence of single-walled carbon nanotubes cytotoxicity in vitro," *Toxicology Letters*, vol. 161, no. 2, pp. 135–142, 2006.

[19] A. D. Becke, "Density-functional exchange-energy approximation with correct asymptotic behavior," *Physical Review A*, vol. 38, no. 6, pp. 3098–3100, 1988.

[20] C. Lee, W. Yang, and R. G. Parr, "Development of the Colle-Salvetti correlation-energy formula into a functional of the electron density," *Physical Review B*, vol. 37, no. 2, pp. 785–789, 1988.

[21] S. H. Vosko, L. Wilk, and M. Nusair, "Accurate spin-dependent electron liquid correlation energies for local spin density calculations: a critical analysis," *Canadian Journal of Physics*, vol. 58, no. 8, pp. 1200–1211, 1980.

[22] A. D. Becke, "Density-functional thermochemistry. III. The role of exact exchange," *The Journal of Chemical Physics*, vol. 98, no. 7, pp. 5648–5652, 1993.

[23] J. S. Binkley, J. A. Pople, and W. J. Hehre, "Self-consistent molecular orbital methods. 21. Small split-valence basis sets for first-row elements," *Journal of the American Chemical Society*, vol. 102, no. 3, pp. 939–947, 1980.

[24] R. S. Mulliken, "Electronic population analysis on LCAO-MO molecular wave functions. I," *The Journal of Chemical Physics*, vol. 23, no. 10, pp. 1833–1840, 1955.

[25] F. D'Souza, M. E. Zandler, P. M. Smith et al., "A ferrocene-C60-dinitrobenzene triad: synthesis and computational, electrochemical, and photochemical studies," *Journal of Physical Chemistry A*, vol. 106, no. 4, pp. 649–656, 2002.

[26] M. J. Frisch, G. W. Trucks, H. B. Schlegel et al., *Gaussian 09, Revision A.1*, Gaussian, Inc., Pittsburgh, Pa, USA, 2009.

[27] J. Tomasi, B. Mennucci, and R. Cammi, "Quantum mechanical continuum solvation models," *Chemical Reviews*, vol. 105, no. 8, pp. 2999–3093, 2005.

[28] L. Onsager, "Electric moments of molecules in liquids," *Journal of the American Chemical Society*, vol. 58, no. 8, pp. 1486–1493, 1936.

[29] E. Cancès and B. Mennucci, "New applications of integral equations methods for solvation continuum models: ionic solutions and liquid crystals," *Journal of Mathematical Chemistry*, vol. 23, no. 3-4, pp. 309–326, 1998.

[30] E. Cancès, B. Mennucci, and J. Tomasi, "A new integral equation formalism for the polarizable continuum model: theoretical background and applications to Isotropic and anisotropic dielectrics," *Journal of Chemical Physics*, vol. 107, no. 8, pp. 3032–3041, 1997.

[31] B. Mennucci, E. Cancès, and J. Tomasi, "Evaluation of solvent effects in isotropic and anisotropic dielectrics and in ionic solutions with a unified integral equation method: theoretical bases, computational implementation, and numerical applications," *Journal of Physical Chemistry B*, vol. 101, no. 49, pp. 10506–10517, 1997.

Hindawi Publishing Corporation
Journal of Nanotechnology
Volume 2012, Article ID 937819, 6 pages
doi:10.1155/2012/937819

Research Article

Manufacturing Strategy for Multiwalled Carbon Nanotubes as a Biocompatible and Innovative Material

Hisao Haniu,[1] Naoto Saito,[2] Yoshikazu Matsuda,[3] Yuki Usui,[4] Kaoru Aoki,[5] Masayuki Shimizu,[5] Nobuhide Ogihara,[5] Kazuo Hara,[5] Seiji Takanashi,[5] Masanori Okamoto,[5] Koichi Nakamura,[5] Norio Ishigaki,[5] Tamotsu Tsukahara,[6] and Hiroyuki Kato[5]

[1] *Institute of Carbon Science and Technology, Shinshu University, 3-1-1 Asahi, Matsumoto, Nagano 390-8621, Japan*
[2] *Department of Applied Physical Therapy, Shinshu University School of Health Sciences, Nagano 390-8621, Japan*
[3] *Clinical Pharmacology Educational Center, Nihon Pharmaceutical University, Saitama 362-0806, Japan*
[4] *Research Center for Exotic Nanocarbons, Shinshu University, Nagano 390-8621, Japan*
[5] *Department of Orthopaedic Surgery, Shinshu University School of Medicine, Nagano 390-8621, Japan*
[6] *Department of Integrative Physiology and Bio-System Control, Shinshu University School of Medicine, Nagano 390-8621, Japan*

Correspondence should be addressed to Hisao Haniu, hhaniu@shinshu-u.ac.jp

Received 29 June 2011; Accepted 26 August 2011

Academic Editor: Lifeng Dong

We investigated the relationship between differences in multiwalled carbon nanotubes (MWCNTs) and the biological responses they elicit in order to develop biocompatible MWCNTs. We exposed human bronchial epithelial (BEAS-2B) cells to two sizes and six grades of MWCNTs and measured the resulting cell viability, total reactive oxygen and/or nitrogen species (tROS/RNS) production, and cytokine secretion. Although differences in cellular tROS production were associated with differences in grades of MWCNTs, the graphitization temperature of MWCNTs apparently did not influence tROS production. However, cell viability was affected by MWCNT graphitization temperature and diameter. Moreover, cytokine secretion was apparently affected by treatment temperature, but not MWCNT diameter. We concluded that the highest temperature resulted in the most biocompatibility because impurities and carbon defects were removed from the MWCNTs. However, other mechanisms are possible. Therefore, it is important to optimize each type of MWCNT by monitoring biological responses that type elicits during the manufacturing stage for applications involving biology and medicine.

1. Introduction

Due to their unique properties, MWCNTs have potential applications in a wide variety of industries including biomedical fields [1]. Many uses for MWCNTs have been proposed including biosensors, drug and vaccine delivery vehicles, and novel biomaterials [2]. However, before such biomaterials can be incorporated into new and existing biomedical devices, the biocompatibility of MWCNTs must be thoroughly investigated because Takagi et al. and Poland et al. reported that mice injected intraperitoneally with MWCNTs exhibited toxicological responses similar to those seen in mice exposed to asbestos [3, 4]. Although some investigators have investigated the safety of inhalation or intratracheal administration of MWCNTs *in vivo*, a clear conclusion cannot be drawn from the results of these experiments [5–9]. Similarly, results from *in vitro* studies do not provide a consistent picture of the safety of MWCNTs; some studies indicate that MWCNTs cause cytotoxicity and cytokine production [10–12], but others indicate that MWCNTs did not cause any significant biological responses [13, 14].

It is a crucial to determine whether MWCNTs cause inflammation when used as a biomaterial. Oxidant stress is thought to be a likely cause of some possible MWCNT-mediated biological responses. Therefore, oxidative stress, as a cause of inflammation, attracts attention, and the transition metal catalyst residues CNTs might be major

Table 1: Basic properties of MWCNTs.

MWCNT type	MWCNT-150						Testing method
abbreviation name	NT15	NT15+Fe	NT15-30	NT15-26	NT15-22	NT15-13	
Graphitization temperature (°C)	3000[b]	3000[b]	3000[c]	2600[c]	2200[c]	—	
Additional treatment	—	Fe_2O_3[d]	—	—	—	—	
Diameter (nm)	150						FE-SEM
Length (μm)	7–10						FE-SEM
Iron content (ppm)	34	730	<20	<20	60	13000	ICP-MS
R value (I_d/I)[a]	0.3	0.3	0.2	0.5	0.9	1.4	Raman spectroscopy (785 nm)
MWCNT type	MWCNT-80						Testing method
abbreviation name	NT08	NT08+Fe	NT08-30	NT08-26	NT08-22	NT08-13	
Graphitization temperature (°C)	3000[b]	3000[b]	3000[c]	2600[c]	2200[c]	—	
Additional treatment	—	Fe_2O_3[d]	—	—	—	—	
Diameter (nm)	80						FE-SEM
Length (μm)	7–10						FE-SEM
Iron content (ppm)	1700	2200	<20	<20	360	21000	ICP-MS
R value (I_d/I)[a]	n/a						Raman spectroscopy (785 nm)

[a] R refers to the intensity of D band over the intensity of G band.
[b] MWCNTs were heated at Showa denko.
[c] MWCNTs were heated in our laboratory.
[d] NT15 and NT08 were added Fe_2O_3 (1000 : 1), mixed, and sonicated in 0.02% triton-X100 solution. Then, they were filtered and dried at 120°C.
n/a = not available.

cause of oxidative stress [15, 16]. It is known that the impurities in MWCNTs before graphitization (We named the MWCNTs "As-grown.") can be removed by thermal treatment for graphitization, and MWCNTs produced for commercial uses are additionally heat treated. In fact, we reported that the heat-treated MWCNTs did not represent cell proliferation inhibition although As-grown MWCNTs indicated cytotoxicity on U937 human monoblastic leukemia cells [17]. However, U937 cells do not endocytose MWCNTs, and the results were different for a human bronchial epithelial cell line (BEAS-2B cells), which endocytoses heat-treated MWCNTs [18]. BEAS-2B cells are of bronchial epithelium cell origin and are susceptible to cytotoxicity.

In this study, we examined cytotoxicity, oxidative stress, and inflammation, as for index of biological responses, using two sizes of MWCNTs with varying iron concentration in BEAS-2B cells to clarify more important factor during the manufacturing stage to improve the biocompatibility.

2. Materials and Methods

2.1. Carbon Nanotubes. We used commercial MWCNT materials, vapor-grown carbon fiber (VGCF, Showa Denko, Tokyo, Japan) and vapor-grown carbon fiber-S (VGCF-S, Showa Denko, Tokyo, Japan), that were manufactured by a chemical vapor deposition method [19], and As-grown MWCNTs before the graphitization were also provided by Showa Denko. Information on each type of MWCNT, including the abbreviated name (e.g., NT15, NT08), additional treatments in our laboratory, and properties, is listed in Table 1. MWCNTs were sterilized in an autoclave at 121°C for 15 min. MWCNTs were vortexed for 1 min in PBS (−) containing 0.1% gelatin (Nacalai Tesque, Kyoto, Japan) and sonicated with a water-bath sonicator for 30 min. Dispersed

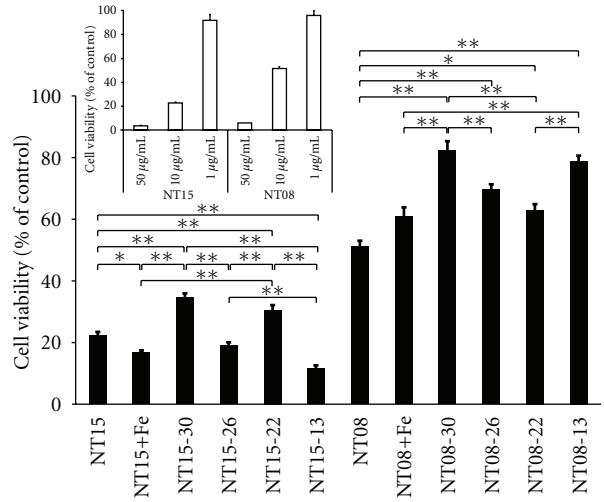

Figure 1: The viability of BEAS-2B cells treated with different MWCNTs. The cells were exposed to MWCNTs for 24 h. The small graph shows the dose effects of NT15 and NT08 on the cell viability. The large graph shows the cell viability associated with 10 μg/mL treatment of each MWCNT in the MWCNT-150 and MWCNT-80 series. (Mean ± SE, $n = 6$, $^*P < 0.05$, $^{**}P < 0.01$.)

MWCNTs suspended in the PBS-gelatin dispersant were added to cell culture medium at 1/100 volume in each of the following experiments.

2.2. Cell Culture. The human bronchial epithelial cell line, BEAS-2B, was purchased from the American Type Culture Collection (Manassas, Va, USA). BEAS-2B cells were cultured in Ham's nutrient mixture F-12 with 10% fetal bovine serum at 37°C in a 5% CO_2 humidified incubator and passaged

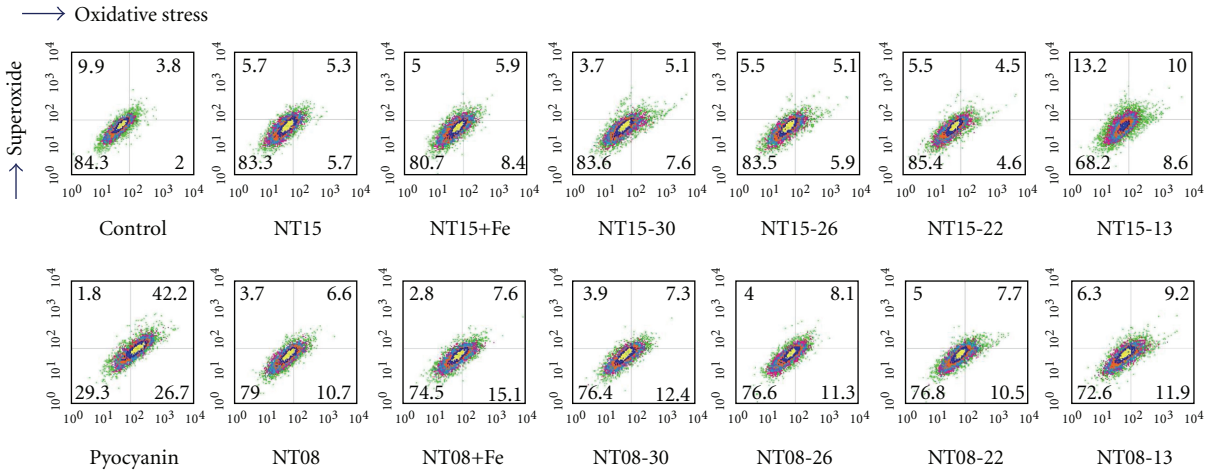

Figure 2: The tROS production in BEAS-2B cells treated with different MWCNTs. The cells were exposed to MWCNTs for 1 or 24 h, then stained with two color ROS detection reagents, and analyzed using FCM. Image shows the cell population of the fraction separated by oxidative stress and superoxide for 1 h (10,000 cells). The numbers in the image reflect the percentage of the cell population in each quadrant.

twice each week. For each study, the cells were seeded at a density of 5×10^5 cells/mL and adhered for 24 h.

2.3. Alamar Blue (AB) Assay. To assess the viability of cells exposed to different MWCNTs, we performed an Alamar blue assay (AlamarBlue cell viability reagent; Invitrogen, Carlsbad, Calif, USA), according to the manufacturer's instructions. Cells were plated in 96-well plates and incubated for 24 h at 37°C in the culture medium containing VGCF in dispersant or only dispersant control medium. Viable cells metabolized the dye, resulting in an increase of fluorescence following excitation/emission at 550/600 nm with a fluorescence multiplate reader (PowerScan 4, DS Pharma Biomedical, Osaka, Japan). Cytotoxic activity was calculated as follows: percent cytotoxicity = 100 × experimental value/control value. Test media were assayed six times for each treatment condition.

2.4. Total ROS/Superoxide Production. To determine total reactive oxygen and/or nitrogen species (tROS/RNS) production in the cells exposed to MWCNTs, we used a total ROS/superoxide detection kit (Enzo Life Sciences, Plymouth Meeting, Pa, USA). Cells were plated into 24-well plates and incubated for 24 h so cells could adhere to the substrate. Cells were then incubated for 1 or 24 h at 37°C in the presence or absence of MWCNTs. Pyocyanin (100 μM) was used as a reactive oxygen species (ROS) inducer. Following exposing to MWCNTs, the cells were treated with oxidative stress detection reagent (OSDR) and superoxide detection reagent (SDR) for 30 min. Cells were then washed once in 1 × wash buffer and harvested with trypsin-EDTA. Finally, the cells were suspended with 0.3 mL of 10% FBS in 1 × wash buffer and passed through nylon mesh. These cells were subjected to flow cytometry (FCM; FACSCalibur, Becton Dickinson, San Jose, Calif, USA) in the FL1 channel for OSDR signals and FL2 channel for SDR signals. The cells were separated into four fractions, and the fractions were named tROS (FL1 and FL2 positive), superoxide (FL1 negative and FL2 positive), peroxide (FL1 positive and FL2 negative), and negative (FL1 and FL2 negative).

2.5. Cytokine Measurement. Cytokines in the culture supernatant were measured by a BD cytometric bead array flex set assay (Human soluble protein master buffer kit & Human IL-6 and IL-8 flex sets; BD Biosciences, San Jose, Calif, USA), according to the manufacturer's protocol Briefly, BEAS-2B cells that had been cultured in 24-well plate for 24 h were exposed to 10 μg/mL of MWCNT in dispersant for 24 h, and the resulting supernatant was collected by centrifugation. Then cytokine capture beads (for IL-6 and IL-8) were mixed with supernatant samples or cytokine standards in FCM tubes. The mixtures were vortexed, and antibody for fluorescence detection was added to each tube. The samples were then incubated at room temperature for 2 h. Following incubation, beads were washed once by wash buffer and resuspended prior to reading with an FCM.

2.6. Statistical Analysis. Data are presented as mean ± SE. Statistical significant was determined by analysis of variance (ANOVA) followed by the Student's t-test to compare the controls with each sample, and the Tukey-Kramer method for comparisons between different types of MWCNTs. $P < 0.05$ was considered statistically significant.

3. Results

3.1. Cell Viability. Cell viability was measured using AB assay method. The viability value for each experimental sample was expressed as percentage of the control sample, which was designated as 100% viable (Figure 1). NT15 and NT08 which are commercial MWCNTs decreased the cell viability depending on the concentration. At a concentration of 10 μg/mL, all MWCNTs in the NT08 series were associated with a viability associated higher than that associated with MWCNTs in the NT15 series. Moreover, commercial MWCNTs (NT15 and NT08) were associated with lower

Table 2: Fractionation rate using two fluorescent reagents for tROS/RNS with FCM on BEAS-2B cells exposed to MWCNTs at 1 and 24 h.

(a) Fractionation rate (%) of 10,000 cells at 1 h (mean ± SE, $n = 3$)

Fraction	Control	NT15	NT15+Fe	NT15-30	NT15-26	NT15-22	NT15-13
tROS	3.8 ± 0.4	5.3 ± 0.7	5.9 ± 0.4	5.1 ± 0.6	5.1 ± 0.2	4.5 ± 0.3	10.0 ± 0.2
Superoxide	9.9 ± 0.2	5.7 ± 0.1	5.0 ± 0.6	3.7 ± 0.2	5.5 ± 0.5	5.5 ± 0.7	13.2 ± 2.2
Peroxide	2.0 ± 0.2	5.7 ± 1.2	8.4 ± 1.3	7.6 ± 1.4	5.9 ± 0.7	4.6 ± 0.9	8.6 ± 1.3
Negative	84.3 ± 0.3	83.3 ± 1.8	80.7 ± 1.2	83.6 ± 2.0	83.5 ± 0.3	85.4 ± 0.7	68.2 ± 1.0
Fraction	Pyocyanin	NT08	NT08+Fe	NT08-30	NT08-26	NT08-22	NT08-13
tROS	42.2 ± 2.1	6.6 ± 0.8	7.6 ± 0.6	7.3 ± 0.6	8.1 ± 0.3	7.7 ± 0.8	9.2 ± 0.4
Superoxide	1.8 ± 0.3	3.7 ± 0.5	2.8 ± 0.3	3.9 ± 1.0	4.0 ± 0.7	5.0 ± 0.8	6.3 ± 0.7
Peroxide	26.7 ± 1.5	10.7 ± 0.8	15.1 ± 1.6	12.4 ± 2.5	11.3 ± 1.6	10.5 ± 2.0	11.9 ± 1.4
Negative	29.3 ± 2.6	79.0 ± 1.3	74.5 ± 1.9	76.4 ± 1.9	76.6 ± 1.0	76.8 ± 2.0	72.6 ± 0.9

(b) Statistical significance compared between different types of MWCNTs by the Tukey-Kramer method (mean ± SE, $n = 3$, $^*P < 0.05$, $^{**}P < 0.01$)

Fraction	MWCNT-150	MWCNT-80
tROS	Control versus NT15+Fe*, NT15-13** NT15-13 versus NT15**, NT15+Fe**, NT15-30**, NT15-26**, NT15-22**	Control versus NT08+Fe*, NT08-30*, NT08-26**, NT08-22*, NT08-13**
Superoxide	Conrol versus NT15**, NT15+Fe*, NT15-30**, NT15-26**, NT15-22* NT15-13 versus NT15**, NT15+Fe**, NT15-30**, NT15-26**, NT15-22**	Control versus NT08**, NT08+Fe**, NT08-30*, NT08-26*, NT08-22*, NT08-13*, NT08+Fe versus NT08-13*
Peroxide	Control versus NT15+Fe*, NT15-26*, NT15-13*	Conrol versus NT08**, NT08+Fe*, NT08-26*, NT08-13*
Negative	Control versus NT15-13* NT15-13 versus NT15**, NT15+Fe**, NT15-30**, NT15-26**, NT15-22**	Conrol versus NT08*, NT08+Fe*, NT08-26*, NT08-13**

(c) Fractionation rate (%) of 3,000 or fewer cells at 24 h (mean ± SE, $n = 3$)

Fraction	Control	NT15#	NT15+Fe#	NT15-30#	NT15-26	NT15-22	NT15-13#
tROS	3.4 ± 2.1	6.3 ± 0.6	7.1 ± 0.6	11.1 ± 1.8	7.0 ± 0.4	7.4 ± 0.9	18.9 ± 3.4
Superoxide	5.9 ± 0.3	17.9 ± 2.6	14.5 ± 1.0	19.8 ± 2.0	17.7 ± 3.2	17.6 ± 2.6	20.1 ± 1.7
Peroxide	2.0 ± 1.5	4.7 ± 0.2	7.3 ± 0.6	8.9 ± 0.9	5.8 ± 0.2	5.5 ± 1.0	8.9 ± 1.8
Negative	88.7 ± 3.5	71.1 ± 2.1	71.2 ± 1.6	60.2 ± 4.2	69.5 ± 3.1	69.5 ± 1.9	52.1 ± 3.8
Fraction	Pyocyanin	NT08	NT08+Fe	NT08-30	NT08-26	NT08-22	NT08-13
tROS	50.5 ± 2.3	9.9 ± 1.0	9.9 ± 2.3	9.6 ± 2.2	10.1 ± 1.8	9.9 ± 1.3	10.7 ± 1.5
Superoxide	20.8 ± 0.7	21.5 ± 1.9	17.6 ± 1.4	17.3 ± 1.6	25.3 ± 1.3	28.7 ± 2.5	41.7 ± 3.1
Peroxide	1.3 ± 0.1	4.2 ± 0.8	5.6 ± 1.3	4.3 ± 1.6	3.0 ± 0.6	2.5 ± 0.4	1.4 ± 0.4
Negative	27.4 ± 1.7	64.5 ± 0.3	66.9 ± 2.3	68.8 ± 2.2	61.6 ± 1.4	58.9 ± 0.9	46.2 ± 1.4

= less than 3,000 cells.

cell viability than the MWCNTs treated thermally in our laboratory for each series except the NT15-26. Based on these observations, MWCNT treatment temperature was apparently not directly related to cell viability, indicating that the impurities (i.e., mainly iron) and/or carbon defects were not the principal cause of cytotoxicity. Interestingly, NT15 MWCNTs were associated with higher viability than NT15+Fe and NT15-13, which both contain substantial amounts of iron, but NT08 MWCNTs were associated with lower cell viability than NT08+Fe and NT08-13.

3.2. tROS/RNS Production. Generally, cellular tROS/RNS are produced and eliminated rapidly. However, we assayed tROS/RNS at 1 h and at 24 h after exposing cells to MWCNTs because the cells internalized MWCNTs over time. Only 3,000 or fewer cells were assayed for the 24 h time point because the cells were injured, but we assayed 10,000 cells at the 1 h time point. Figure 2 and Tables 2(a) and 2(b) show each fraction of the population resulting from FCM analysis. At 1 hr, the fraction of tROS-positive cells was significantly higher in NT15+Fe and the MWCNT-80 series without NT-08 than in the control samples. However, the tROS-positive fractions were no higher in the experimental sample than in the pyocyanin sample, which was a positive control. At 1 hr, the superoxide-positive fraction was significantly lower in all experimental samples than in the control sample, except that the superoxide-positive fraction in NT15-13 sample was not significantly different from that in the control sample.

Although the peroxide-positive fraction of cells treated with some grades of MWCNTs was significantly higher than that of the control cells, the values were consistently less than half of the values associated with the pyocyanin samples. The alteration of MWCNT-80 series was larger than that of MWCNT-150 series in the peroxide-positive fractions. NT15-13 MWCNTs were significantly different from the MWCNT-150 series in the tROS, superoxide, and negative fractions, and there was a significant difference between only NT08+Fe and NT08-13 in the MWCNT-80 series for the superoxide fraction. The cell counts from the 24 h timepoint were too low to result in statistically significant differences; nevertheless, we present the results as reference data (Table 2(c)). At 24 hr, the tROS, superoxide, and peroxide fractions were larger in all MWCNT-treated cells than in control cells, and the tROS and superoxide fractions were larger in all 24 h samples than in the 1 h samples.

3.3. Cytokine Secretion. Recently, we reported that BEAS-2B cells exposed to MWCNTs secreted IL-6 and IL-8 [18]. All MWCNT treatments resulted in significant increased IL-6 and IL-8 secretions when compared to the control treatment, and all, except NT15-30, resulted in higher IL-8 secretion than did LPS, which was a positive control (Figure 3). There were statistically significant differences in the MWCNT-150 series though there were no significant differences in the MWCNT-80 series. However, secretion associated with NT15-30 and NT15-13 in the MWCNT-150 series and with NT08-30 and NT08-13 in MWCNT-80 tended to be lower than that with other MWCNTs in the respective series for both cytokines.

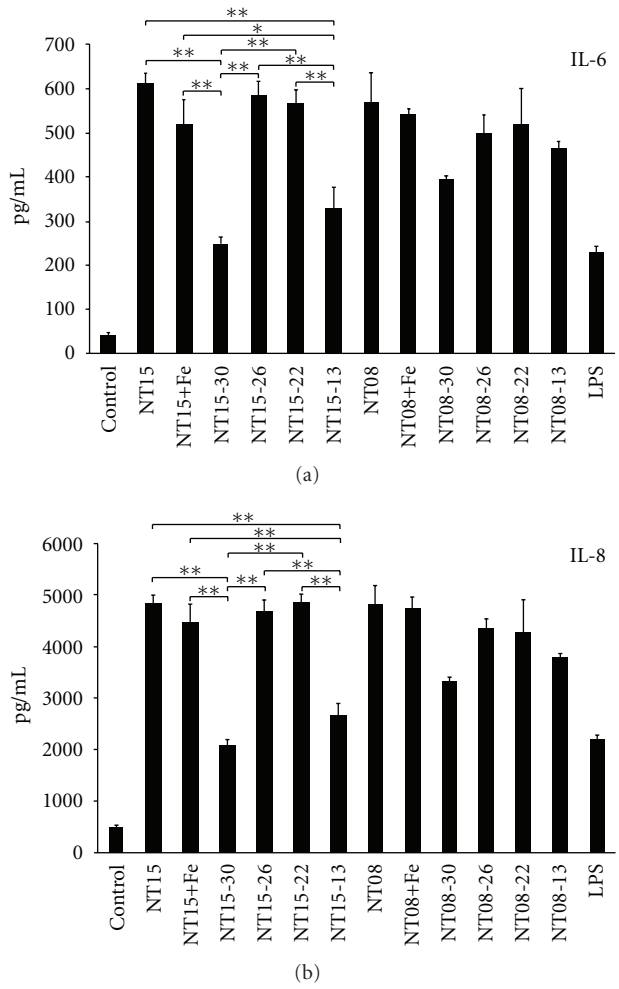

Figure 3: The cytokine secretion from BEAS-2B cells treated with different MWCNTs. The cells were exposed to MWCNTs for 24 h. The upper graph shows IL-6 secretion, and the lower graph shows IL-8 secretion from cells treated with 10 μg/mL of each MWCNT, the MWCNT-150 and MWCNT-80 series (mean ± SE, $n = 3$, $^{*}P < 0.05$, $^{**}P < 0.01$).

4. Discussion

Carbon nanotubes (CNTs) are expected to be useful for a wide variety of industrial applications, and postprocessing procedures will depend on the individual application. In the biomedical field, the research on drug delivery systems and diagnostic imaging that use CNTs is advanced [20, 21]. However, doubts about efficacy and safety of modified CNT remain [22], and the influence of different manufacturing processes for CNTs, as biomaterials, has not been examined thoroughly. In this study, we evaluated the influence of different graphitization temperatures on the MWCNTs of two different diameters.

The graphitization temperature has a crucial influence on the impurities content and crystalline of MWCNTs, and these factors are reportedly critical for the safety of CNTs [23–25]. However, our results did not indicate that carbon defects and impurities directly affected three biological responses, cell viability, tROS production, and cytokine secretion. Each biological response did not show mutual relativity and did not correlate to impurities or the defects, although both the MWCNT-150 and MWCNT-80 series had fewer defects and impurities depending on the treatment temperature. However, the diameter of MWCNTs did affect cell viability and tROS production. MWCNT-80 series gave rise to the seemingly contradictory results that relative cell viability was high while tROS production was also high. Therefore, cellular tROS production may have been critical to cytotoxicity. IL-6 and IL-8 secretion increased with all MWCNT exposure regardless of the MWCNT diameter, and secretion associated with NT15-30 and NT15-13 and NT08-30 and NT08-13, treatments tended to be lower than secretion associated with treatments involving MWCNT of the same diameter. However, the data from NT15-30 or NT08-30 treated with graphitization at 3000°C and NT-13 or NT08-13 without graphitization were not able to clarify commonalities in this research. Additional iron did not affect the biological responses of original MWCNTs except for the cell viability counts associated with the N15 and N15+Fe treatments. These results also indicated that the iron contained in the MWCNTs is not crucial because the cell viability of NT15-13, which included 13,000 ppm iron, was the lowest in the MWCNT-150 series, but NT08-13, which included 21,000 ppm iron, was associated with high

viability. Finally, the MWCNTs processed at the maximum temperature in the lab had the highest biocompatibility overall regardless of diameter.

In this study, we found that the graphitization temperature of MWCNTs in the manufacturing process affected biological response to the MWCNTs, but the biological responses did not have regularity and was affected by the diameter of the MWCNTs. In other words, we should investigate the condition that results in the lowest biological responses for each MWCNT in the manufacturing process before that MWCNT is used for applications in biology and medicine. It is our duty to optimize the biocompatibility of the nanomaterial itself in order to develop application for the nanomaterials.

Acknowledgments

The authors thank the staff of the Division of Instrumental Analysis in the Research Center for Human and Environmental Sciences of the Shinshu University for their help. This research was supported by the Program for Fostering Regional Innovation in Nagano and a Grant-in-Aid (no. 19002007) from the Ministry of Education, Culture, Sports, Science and Technology of Japan.

References

[1] M. Endo, M. S. Strano, and P. M. Ajayan, "Potential applications of carbon nanotubes," *Topics in Applied Physics*, vol. 111, pp. 13–61, 2008.

[2] N. Saito, Y. Usui, K. Aoki et al., "Carbon nanotubes: biomaterial applications," *Chemical Society Reviews*, vol. 38, no. 7, pp. 1897–1903, 2009.

[3] C. A. Poland, R. Duffin, I. Kinloch et al., "Carbon nanotubes introduced into the abdominal cavity of mice show asbestos-like pathogenicity in a pilot study," *Nature Nanotechnology*, vol. 3, no. 7, pp. 423–428, 2008.

[4] A. Takagi, A. Hirose, T. Nishimura et al., "Induction of mesothelioma in p53+/- mouse by intraperitoneal application of multi-wall carbon nanotube," *Journal of Toxicological Sciences*, vol. 33, no. 1, pp. 105–116, 2008.

[5] N. Kobayashi, M. Naya, M. Ema et al., "Biological response and morphological assessment of individually dispersed multi-wall carbon nanotubes in the lung after intratracheal instillation in rats," *Toxicology*, vol. 276, no. 3, pp. 143–153, 2010.

[6] H. Ellinger-Ziegelbauer and J. Pauluhn, "Pulmonary toxicity of multi-walled carbon nanotubes (Baytube(R)) relative to α-quartz following a single 6 h inhalation exposure of rats and a 3 months post-exposure period," *Toxicology*, vol. 266, no. 1–3, pp. 16–29, 2009.

[7] L. Ma-Hock, S. Treumann, V. Strauss et al., "Inhalation toxicity of multiwall carbon nanotubes in rats exposed for 3 months," *Toxicological Sciences*, vol. 112, no. 2, pp. 468–481, 2009.

[8] D. W. Porter, A. F. Hubbs, R. R. Mercer et al., "Mouse pulmonary dose- and time course-responses induced by exposure to multi-walled carbon nanotubes," *Toxicology*, vol. 269, no. 2-3, pp. 136–147, 2010.

[9] J. Muller, M. Delos, N. Panin, V. Rabolli, F. Huaux, and D. Lison, "Absence of carcinogenic response to multiwall carbon nanotubes in a 2-year bioassay in the peritoneal cavity of the rat," *Toxicological Sciences*, vol. 110, no. 2, pp. 442–448, 2009.

[10] S. Hirano, Y. Fujitani, A. Furuyama, and S. Kanno, "Uptake and cytotoxic effects of multi-walled carbon nanotubes in human bronchial epithelial cells," *Toxicology and Applied Pharmacology*, vol. 249, no. 1, pp. 8–15, 2010.

[11] L. Tabet, C. Bussy, N. Amara et al., "Adverse effects of industrial multiwalled carbon nanotubes on human pulmonary cells," *Journal of Toxicology and Environmental Health Part A*, vol. 72, no. 2, pp. 60–73, 2009.

[12] N. A. Monteiro-Riviere, R. J. Nemanich, A. O. Inman, Y. Y. Wang, and J. E. Riviere, "Multi-walled carbon nanotube interactions with human epidermal keratinocytes," *Toxicology Letters*, vol. 155, no. 3, pp. 377–384, 2005.

[13] M. De Nicola, D. M. Gattia, S. Bellucci et al., "Effect of different carbon nanotubes on cell viability and proliferation," *Journal of Physics Condensed Matter*, vol. 19, no. 39, Article ID 395013, pp. 395013–395019, 2007.

[14] K. Pulskamp, S. Diabate, and H. F. Krug, "Carbon nanotubes show no sign of acute toxicity but induce intracellular reactive oxygen species in dependence on contaminants," *Toxicology Letters*, vol. 168, no. 1, pp. 58–74, 2007.

[15] L. Guo, D. G. Morris, X. Liu, C. Vaslet, R. H. Hurt, and A. B. Kane, "Iron bioavailability and redox activity in diverse carbon nanotube samples," *Chemistry of Materials*, vol. 19, no. 14, pp. 3472–3478, 2007.

[16] V. E. Kagan, Y. Y. Tyurina, V. A. Tyurin et al., "Direct and indirect effects of single walled carbon nanotubes on RAW 264.7 macrophages: role of iron," *Toxicology Letters*, vol. 165, no. 1, pp. 88–100, 2006.

[17] H. Haniu, Y. Matsuda, K. Takeuchi, Y. A. Kim, T. Hayashi, and M. Endo, "Proteomics-based safety evaluation of multi-walled carbon nanotubes," *Toxicology and Applied Pharmacology*, vol. 242, no. 3, pp. 256–262, 2010.

[18] T. Tsukahara and H. Haniu, "Cellular cytotoxic response induced by highly purified multi-wall carbon nanotube in human lung cells," *Molecular and Cellular Biochemistry*, vol. 352, pp. 57–63, 2011.

[19] M. Endo, "Grow carbon fibers in the vapor phase," *Chemtech*, vol. 18, no. 9, pp. 568–576, 1988.

[20] V. S. Thakare, M. Das, A. K. Jain, S. Patil, and S. Jain, "Carbon nanotubes in cancer theragnosis," *Nanomedicine*, vol. 5, no. 8, pp. 1277–1301, 2010.

[21] S. R. Ji, C. Liu, B. Zhang et al., "Carbon nanotubes in cancer diagnosis and therapy," *Biochimica et Biophysica Acta*, vol. 1806, no. 1, pp. 29–35, 2010.

[22] G. Pastorin, "Crucial functionalizations of carbon nanotubes for improved drug delivery: a valuable option?" *Pharmaceutical Research*, vol. 26, no. 4, pp. 746–769, 2009.

[23] I. Fenoglio, G. Greco, M. Tomatis et al., "Structural defects play a major role in the acute lung toxicity of multiwall carbon nanotubes: physicochemical aspects," *Chemical Research in Toxicology*, vol. 21, no. 9, pp. 1690–1697, 2008.

[24] J. Muller, F. Huaux, A. Fonseca et al., "Structural defects play a major role in the acute lung toxicity of multiwall carbon nanotubes: toxicological aspects," *Chemical Research in Toxicology*, vol. 21, no. 9, pp. 1698–1705, 2008.

[25] X. Hu, S. Cook, P. Wang, H. M. Hwang, X. Liu, and Q. L. Williams, "In vitro evaluation of cytotoxicity of engineered carbon nanotubes in selected human cell lines," *Science of the Total Environment*, vol. 408, no. 8, pp. 1812–1817, 2010.

Hindawi Publishing Corporation
Journal of Nanotechnology
Volume 2012, Article ID 196189, 7 pages
doi:10.1155/2012/196189

Research Article

Uptake of Single-Walled Carbon Nanotubes Conjugated with DNA by Microvascular Endothelial Cells

Joseph Harvey,[1] Lifeng Dong,[2] Kyoungtae Kim,[3] Jacob Hayden,[3] and Jianjie Wang[1]

[1] *Department of Biomedical Sciences, Missouri State University, Springfield, MO 65897, USA*
[2] *Department of Physics, Astronomy, and Materials Science, Missouri State University, Springfield, MO 65897, USA*
[3] *Department of Biology, Missouri State University, Springfield, MO 65897, USA*

Correspondence should be addressed to Jianjie Wang, jwang@missouristate.edu

Received 26 July 2011; Accepted 13 August 2011

Academic Editor: Dongwoo Khang

Single-walled carbon nanotubes (SWCNTs) have been proposed to have great therapeutic potential. SWCNTs conjugated with drugs or genes travel in the systemic circulation to reach target cells or tissues following extravasation from microvessels although the interaction between SWCNT conjugates and the microvascular endothelial cells (ECs) remains unknown. We hypothesized that SWCNT-DNA conjugates would be taken up by microvascular ECs and that this process would be facilitated by SWCNTs compared to facilitation by DNA alone. ECs were treated with various concentrations of SWCNT-DNA-FITC conjugates, and the uptake and intracellular distribution of these conjugates were determined by a confocal microscope imaging system followed by quantitative analysis of fluorescence intensity. The uptake of SWCNT-DNA-FITC conjugates (2 μg/mL) by microvascular ECs was significantly greater than that of DNA-FITC (2 μg/mL), observed at 6 hrs after treatment. For the intracellular distribution, SWCNT-DNA-FITC conjugates were detected in the nucleus of ECs, while DNA-FITC was restricted to the cytoplasm. The fluorescence intensity and distribution of SWCNTs were concentration and time independent. The findings demonstrate that SWCNTs facilitate DNA delivery into microvascular ECs, thus suggesting that SWCNTs serving as drug and gene vehicles have therapeutic potential.

1. Introduction

Emerging evidence supports the great potential of nanotechnology for medical applications with respect to diagnosis and therapeutic treatment of disease [1, 2]. Most recently, Welsher et al. reported promising findings by using a second near-infrared window imaging system in real time [3]. They found that single-walled carbon nanotubes (SWCNTs), intravenously injected into mice, were distributed throughout the body and reached a steady level approximately 30 sec after injection. Meanwhile, the liver, lungs, muscles, and kidneys all generated constant signal, indicating consistent blood flow in these organs. These findings indicate that SWCNTs are able to traverse the microvascular barrier into surrounding tissues. Furthermore, they reported that no toxic side effects were detected by necropsy, histology, and blood chemistry measures in those mice three months after receiving SWCNT injection [4]. The data support the promising potential of SWCNTs in medical applications, yet the mechanism(s) underlying extravasation of SWCNTs remains unknown.

Understanding how SWCNTs interact with microvascular endothelial cells (ECs) is critical for developing therapeutic treatments using highly efficient gene/drug delivery systems due to the pivotal roles of microvascular ECs in the structure and function of the microvasculature. Vascular ECs are in the vanguard for exposure to blood-born elements because they serve as the lining surface of blood vessels. In addition to being a major component of the microvascular wall, microvascular ECs dynamically mediate a variety of vascular functions, including EC-dependent vasomotion, thrombosis formation, vascular inflammation, and vascular exchange (permeability). Most drugs and genes need to be delivered to their target tissues by the systemic circulation after they are absorbed or injected into the blood stream. Subsequently, these drugs and genes traverse the vascular

barrier and arrive at the surrounding tissues, a situation referred to as solute exchange. Importantly, all solute exchanges between circulating blood and metabolizing tissue as well as angiogenesis occur at the level of microvessels.

SWCNT uptake by microvascular ECs is an initial step in the process of drug and gene delivery into either vascular ECs or parenchymal cells. For all the therapeutic treatments with a strategy of specifically targeting microvascular ECs (e.g., antiangiogenesis to reduce tumor growth), SWCNTs conjugated with molecular cargo need to be transported into microvascular ECs. For the treatments targeting parenchymal cells (e.g., tumor cells), the SWCNT-drug conjugates must interact with microvascular ECs in the process of extravasation. In general, there are two pathways (paracellular and transcellular) responsible for large molecules to pass through the vascular barrier. Because SWCNTs often have lengths from hundreds of nanometers to several micrometers and are considered to be in the same size range as macromolecules, we predict that SWCNT-DNA conjugates will predominantly traverse the microvascular barrier via the transcellular pathway (transcytosis) [5]. Entering the microvascular ECs is an initial step in the process of transcytosis. Therefore, understanding the interaction between SWCNTs and microvascular ECs is critical for developing advanced drug and gene delivery systems using SWCNTs. To date, the effect of carbon nanotubes on microvascular ECs remains unknown.

Only a limited number of studies exist concerning the interactions between SWCNTs and vascular ECs [6, 7]. Moreover, large vascular ECs, including HUVECs (human umbilical vein endothelial cells) or aortic ECs [8], were typically used for these studies. Heterogenic properties between large vascular and microvascular ECs [9, 10], however, should be considered. It is inappropriate to extrapolate the findings from studies using large vascular to microvascular ECs. Appropriately, this is the first study, to our knowledge, designed to determine the interactions between SWCNTs and microvascular ECs. We hypothesized that SWCNT-DNA conjugates would be taken up by microvascular ECs and that this process would be facilitated by SWCNTs compared with DNA alone. We employed a biocompatible SWCNT-DNA conjugate [11, 12] labeled with FITC fluorophore (SWCNT-DNA-FITC) and primary cultured microvascular ECs derived from rat skeletal muscles [13] to study the interactions between them. We report here that SWCNT-DNA-FITC conjugates were detected in the nuclei of microvascular ECs at 6 hrs after the cells were exposed to the conjugates (at a concentration as low as 2 μg/mL), while DNA-FITC alone was restricted to the cytoplasm under identical conditions. Quantitative analysis of confocal images provided evidence to support the hypothesis that SWCNTs facilitated DNA uptake by microvascular ECs.

2. Materials and Methods

2.1. Preparation of SWCNT-DNA-FITC Conjugates. To prepare an aqueous SWCNT solution, 1 mg of SWCNT powder (BuckyUSA Company) was dispersed in 1 mL ssDNA (5′ CCT GAG CCA TGA TCA AAC CTG TGC AGT) or DNA-FITC (5′ FITC CCT GAG CCA TGA TCA AAC CTG TGC AGT, Alpha DNA, 1 mg/mL) solution. The suspension was sonicated on ice for 60 minutes to avoid the degradation of DNA molecules and then centrifuged at 120,000 g for 60 minutes. After centrifugation, the supernatant containing individual SWCNTs was decanted, whereas the precipitates containing catalyst particles, bundled nanotubes, and amorphous carbon debris were discarded [11, 12].

2.2. Rat Microvascular ECs. Microvascular ECs were isolated from abdominal skeletal muscles of rats, cultured with M199 medium containing essential supplements, and characterized as previously described [13]. Briefly, the excised abdominal skeletal muscles were digested with an enzyme solution consisting of dispase (0.12 mg/mL; Worthington, Lakewood, NJ), trypsin (0.12 mg/mL; Invitrogen, Carlsbad, Calif), collagenase type II (0.84 mg/mL), and bovine serum albumin (BSA; 1.62 mg/mL) in M199 medium. Microvascular ECs were isolated by using Dynabeads (Dynal, Brown Deer, Wis) coated with *Griffonia simplicifolia* lectin and then cultured. The culture medium consisted of M199 medium supplemented with 5 mg/mL endothelial growth supplement, 0.1 mg/mL glutamine, 10000 unit/mL antibiotic/antimycotic (Gibco, Carlsbad, Calif), 5 unit/mL heparin sodium (Sigma Aldrich, St. Louis, Mo), and 20% Fetal Bovine Serum (FBS; HyClone Lab, Inc. Logan, Utah) for the first two passages, then 10% FBS afterward.

2.3. Nanoparticle Distribution in Primary Cultured Microvascular ECs. ECs were seeded on gelatin (0.2%)-coated Lab-Tek II Chamber Slides with a cell density of 10^4 cells/cm^2. Grown to approximately 80% confluency in 48 hrs, cells were treated with either SWCNT-DNA-FITC or DNA-FITC solution at various concentrations. After various incubation times, ECs were fixed by using 2% paraformaldehyde for 10 min at 37°C and subsequently stained with 1% DAPI (0.5 μg/mL) for 1 min at room temperature. Dulbecco's phosphate buffered saline (DPBS) containing 0.05% Tween-20 (DPBST-20) was used to wash the cells following fixation and staining procedures.

2.4. Spinning Confocal Microscopy. The microvascular ECs were examined with an Olympus IX81 inverted microscope equipped with a laser light source, motorized stage capable of 1 μm z-axis increments, spinning confocal box (Yokogawa X1M1L), and electron multiplying EM-CCD camera (Hamamatsu, ImagEM). All the images were acquired with a 60X oil immersion objective lens and identical exposure time and appropriate filter setup controlled by Slidebook software (v5.0).

2.5. Quantification of Fluorescence Intensity. Fluorescence intensity of SWCNT-DNA-FITC or DNA-FITC in microvascular ECs was quantitatively analyzed by using Image-Pro Plus 6.0 software. Briefly, a background signal level for each image was set using the average optical density (OD) value from four regions (each region contains >15,000 square pixels), where no cells or any fluorescence were detected.

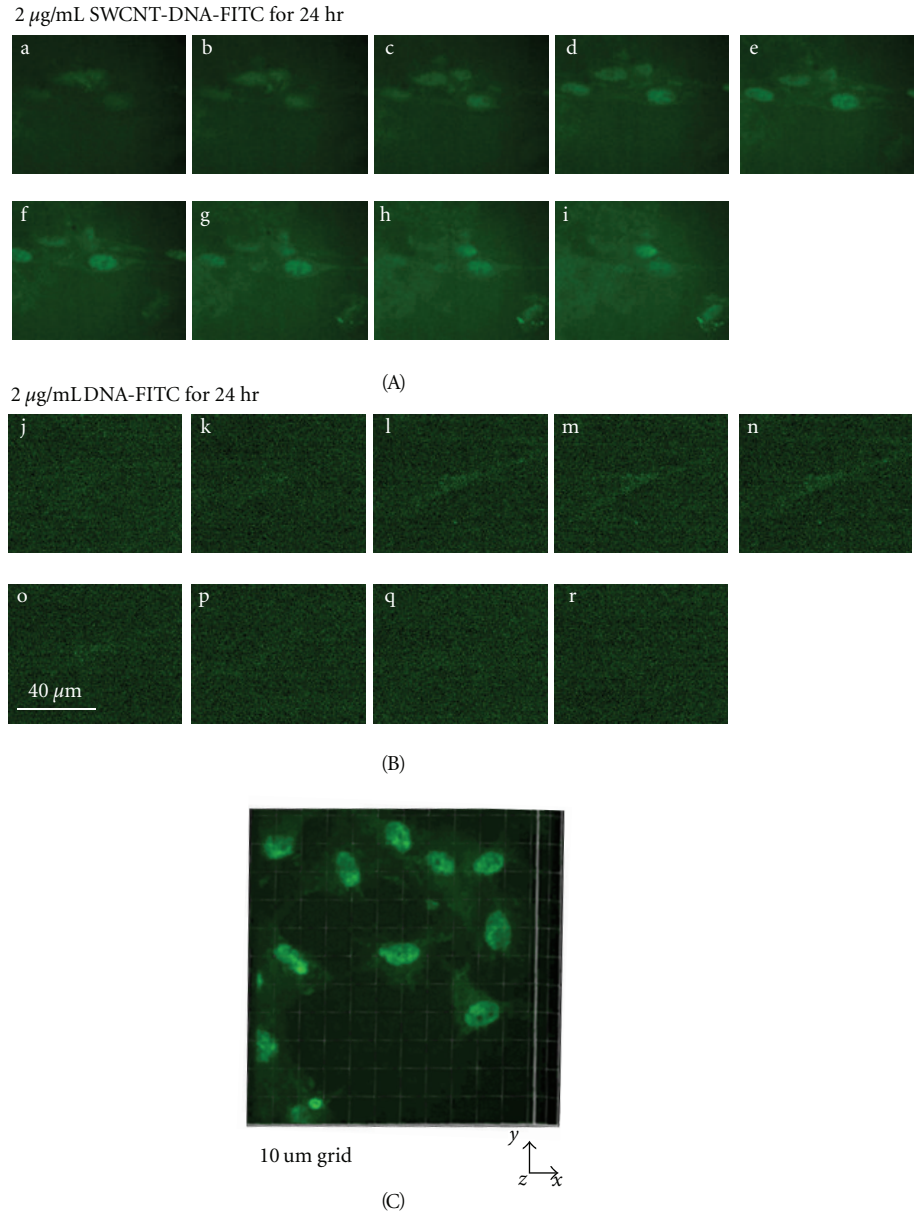

Figure 1: A series of z-stack images demonstrating differential distribution of SWCNT-DNA-FITC (2 μg/mL) versus DNA-FITC (2 μg/mL) conjugates in microvascular ECs: (A) (a to i), representative optical section series of SWCNT-DNA-FITC conjugates in microvascular ECs at 24 hrs post incubation; (B) (j to r), representative optical section series of DNA-FITC present in microvascular ECs at 24 hrs post incubation; (C), sample 3-D image from a video (supplemental materials) acquired from ECs by a spinning confocal imaging system 48 hrs after incubation with SWCNT-DNA-FITC (2 μg/mL). The scale bar in (B) (o) is applicable to all images (a–r).

Consequently, each OD value obtained from this image was subtracted from the background OD. To assess fluorescence intensity of SWCNT-DNA-FITC or DNA-FITC within a cell, 5 areas of interest (AOI) from each cell were selected. The average OD value from 5 identical AOI within a cell represented the fluorescence intensity for this cell. Each image OD value, calculated as the average OD from up to 5 cells per image, represented one experiment ($n = 1$). The criteria for cell and AOI selection were as follows: (1) cells with well-defined cell shape and the strongest signal; (2) each AOI (100~200 pixels^2 in surface area) with the brightest area in the cell body excluding cell processes.

2.6. Statistical Analysis. All values are presented as mean ± SEM. GraphPad Prism 5 software was employed for statistical analysis. Comparisons between two groups, SWCNT-DNA-FITC versus DNA-FITC, at given concentrations and specific time points, were analyzed by unpaired student's t-test. Values of $P < 0.05$ were accepted as being statistically significant.

3. Results and Discussion

3.1. Uptake and Intracellular Distribution of SWCNT-DNA Conjugates in Microvascular ECs. To investigate the interactions between microvascular ECs and SWCNTs, we isolated, cultured, and characterized primary microvascular ECs from rat skeletal muscles. Importantly, the results derived from this *in vitro* study using primary cultured microvascular ECs will guide us to investigate further the efficacy of the drug- or gene-SWCNT delivery system in species- and tissue-matched intact microvessels in living animals [13, 14].

Individual short SWCNTs with 800–900 nm in average length [11, 12] were used in the SWCNT-DNA-FITC conjugates. To identify the effect of SWCNTs on DNA uptake by microvascular ECs, the cells were treated with SWCNT-DNA-FITC (2 μg/mL) and DNA-FITC (2 μg/mL), respectively. The images of microvascular ECs exposed to SWCNT-DNA-FITC conjugates for 24 hrs were acquired by a spinning scanning confocal imaging system and demonstrated in Figure 1. SWCNT-DNA-FITC conjugates appeared to be localized in the EC nuclei, a conclusion determined by the position, shape, and area of FITC fluorescence as shown in a set of z-stack images in Figure 1(A). In contrast, DNA-FITC was dispersed weakly in the cytoplasm of microvascular ECs (Figure 1(B)) and often found on or close to the plasma membrane (Figure 2(a)), but not in the nucleus. The nuclear localization of SWCNTs was also manifested in a 3D projection image (Figure 1(C)) and a supplementary z-scan video (see Supplementary Materials available online at doi: 10.1155/2012.196189). The results support our hypothesis that DNA conjugated to SWCNTs is taken up by microvascular ECs. In view of the finding that SWCNT-DNA-FITC, but not DNA-FITC, accumulates in the nucleus, it is likely that SWCNTs play a facilitating role in delivering the DNA to the nuclei of microvascular ECs. Thus, our results suggest that SWCNTs could be used as vectors for gene delivery to microvascular EC targets.

SWCNTs used in this study did not appear to have adverse effects on cellular morphology and proliferation, observations supported by the previous studies using astrocytoma cells [11, 12]. However, the formation of aggregates was observed in the culture medium following the addition of SWCNT-DNA-FITC solution for the cell treatment groups, but not DNA-FITC solution for the control groups. The aggregates adhered to the surfaces of microvascular ECs even after fixation and washing procedures. The morphology and numbers of microvascular ECs treated with SWCNT-DNA-FITC conjugates at various concentrations within 48 hrs did not differ with control ECs treated with DNA-FITC alone (data not shown), assessed by a transmitted light imaging system. The functional and molecular influence of the aggregations on microvascular ECs remains to be studied.

3.2. Quantitative Evidence for the Facilitation of DNA Uptake by Microvascular ECs through SWCNTs. To quantitatively assess the amount of DNA conjugated to SWCNTs taken up by microvascular ECs, we analyzed the fluorescence intensity of SWCNT-DNA-FITC conjugates by measuring OD values. For this purpose, images of microvascular ECs, treated with

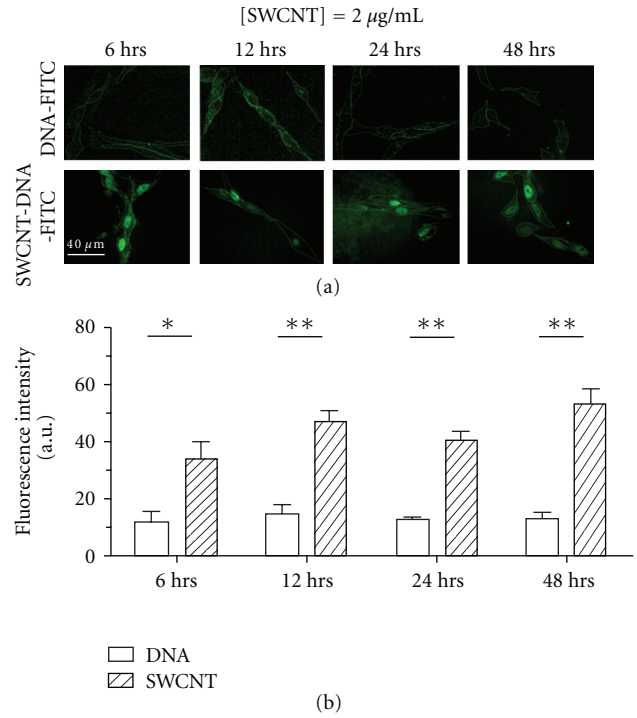

Figure 2: Distribution and fluorescence intensity of SWCNT-DNA-FITC (2 μg/mL) and DNA-FITC (2 μg/mL) at various time intervals within 48 hrs. (a) Representative projection images suggest that SWCNT-DNA-FITC conjugates are distributed in microvascular EC nuclei (lower panel); DNA-FITC appears to be restricted to the cytoplasm (upper panel). (b) SWCNT-facilitated DNA transport into microvascular ECs. Fluorescence intensity was quantitatively assessed by measuring optical density of confocal images as described in Materials and Methods. The P-values less than 0.05 and 0.01 are expressed as * and **, respectively (n = 3–11). The scale bar is applicable to all images.

SWCNT-DNA-FITC conjugates or DNA-FITC at various concentrations (2, 4, and 10 μg/mL) for up to 48 hrs (at 6, 12, 24, and 48 hrs), were acquired. Interestingly, the OD value of SWCNT-DNA-FITC conjugate in microvascular ECs registered approximately a 3~4-fold increase compared to that of DNA-FITC after incubation at a concentration of 2 μg/mL (33.5 ± 6.3 (n = 4) versus 11.3 ± 3.8 (n = 3) at 6 hrs; 47.0 ± 3.4 (n = 6) versus 14.8 ± 3.4 (n = 6) at 12 hrs; 40.4 ± 3.3 (n = 7) versus 12.7 ± 1.0 (n = 6) at 24 hrs; 53.7 ± 5.4 (n = 6) versus 13.2 ± 2.2 (n = 11) at 48 hrs) as shown in Figure 2. As microvascular ECs were treated with SWCNT-DNA-FITC conjugates at a concentration of 10 μg/mL, the uptake of SWCNT-DNA-FITC by microvascular ECs was also found to be greater than that of DNA-FITC (40.3 ± 5.5 (n = 4) versus 12.7 ± 2.2 (n = 3) 6 hrs; 46.7 ± 2.7 (n = 3) versus 2.3 ± 0.9 (n = 3) at 12 hrs; 38.7 ± 7.6 (n = 6) versus 18.3 ± 2.9 (n = 6) at 24 hrs; 37.6 ± 4.5 (n = 12) versus 16.5 ± 1.8 (n = 6) at 48 hrs) (Figure 3). These data demonstrate again that SWCNTs facilitate DNA uptake by microvascular ECs. However, this action was neither concentration dependent within the tested range from 2 μg/mL to10 μg/mL (Figure 4(a)) nor time dependent within the periods from 6 hrs to 48 hrs

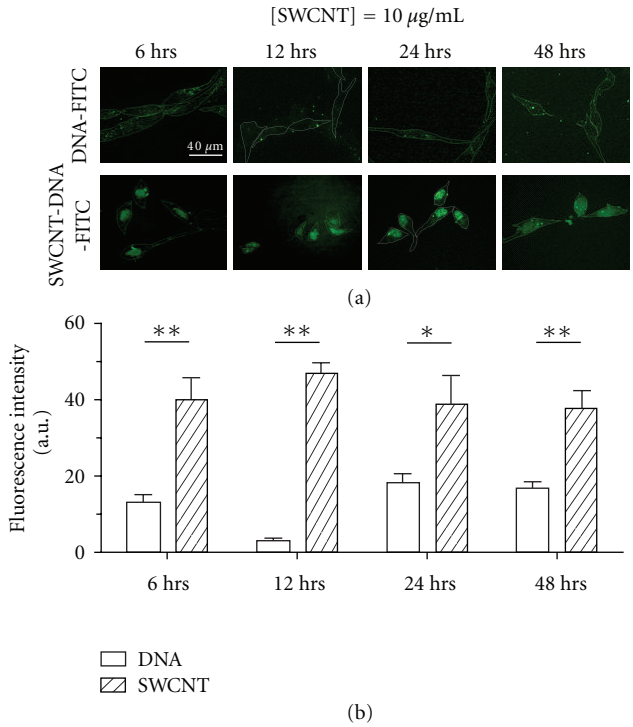

Figure 3: Intracellular compartmentalization and fluorescence intensity of SWCNT-DNA-FITC (10 μg/mL) and DNA-FITC (10 μg/mL) in microvascular ECs and observed at 6, 12, 24, and 48 hrs. (a) Representative projection images acquired by confocal microscopy; (b) Quantitative analysis of fluorescence intensity of SWCNT-DNA-FITC and DNA-FITC conjugates. The P-values less than 0.05 and 0.01 are expressed as * and **, respectively (n = 3–12). The scale bar is applicable to all images.

(Figure 4(b)). Although there were no major differences in the fluorescence intensity of internalized SWCNT-DNA-FITC conjugates over the time course and among treatments with various concentrations of SWCNTs, we observed a trend that 2 μg/mL SWCNTs combined with 12 hrs incubation yields optimal, efficacious delivery (Figure 4). Therefore, for future studies, we recommend that microvascular ECs be treated with 2 μg/mL SWCNT-DNA-FITC for 12 hrs in order to understand mechanisms by which SWCNTs enter microvascular ECs.

The mechanisms underlying SWCNT uptake by microvascular ECs remain unknown at the present time. In general, there are three ways by which extracellular molecules enter a cell: simple diffusion, carrier-mediated transport (e.g., ion channels or transporters), and endocytosis. SWCNTs, macromolecules, are internalized into the intracellular compartment through endocytosis, evidenced by several studies using different types of mammalian cells [6, 15]. Endocytosis can be further categorized as pinocytosis, phagocytosis, and clathrin- and caveolae-mediated endocytosis. Pinocytosis and phagocytosis are main pathways for macrophages, while clathrin- and caveolae-mediated pathways are used by most cells including endothelial cells [16, 17]. Kam found that the uptake of SWCNT-DNA conjugates by two tumor cell lines, HeLa and HL60 tumor cells, was attenuated by disrupting the formation of clathrin-coated vesicles. The evidence supports the internalization of SWCNT-DNA via clathrin-mediated endocytotic mechanism [15]. Compared with Kam's study, the current one used primary skeletal muscle microvascular ECs derived from the exchange microvessels to investigate the uptake of SWCNT-DNA. To our best knowledge, different types of cells have heterogeneous functions, structures, and mechanisms, even within vascular endothelial cells across vascular trees [10]. Lining the inner side of exchange microvessels, microvascular ECs used in the current study engage in transcytosis to allow macromolecules traversing the microvascular barrier. Endothelial cells possess more caveolae than clathrin-coated pits. The number of caveolae is the highest in capillary endothelial cells, compared with arteries, arterioles, venules, and veins, particularly in heart, lung, and skeletal muscle [10]. In the process of transcytosis, caveolae-mediated endocytosis plays an important role as an initial step of the transcellular pathway across endothelial cells [5, 10, 18]. In addition to clathrin- and caveolae-mediated endocytosis, Muro and coworkers demonstrate that nanoparticles, composed of polystyrene latex microspheres, were taken up by HUVECs via the cell-adhesion-molecule- (CAM-) mediated endocytotic process. The CAM-mediated endocytosis was revealed by colocalization of nanoparticles and endocytotic markers, including early endosome antigen [19] and Na+/H+ exchange ion channel (associated with CAM-mediated endocytosis) [20]. It was noted that Muro's study used HUVEC, while we used microvascular EC besides different nanoparticles. In addition, studies using a mathematical model to calculate the energy cost needed for carbon nanotubes piercing through the bilayer of the plasma membrane demonstrate indirectly that the most likely pathway of carbon nanotube delivery into cells is by endocytosis due to a substantial energy requirement [21].

So far, the answer to whether or not microvascular ECs take up SWCNTs by endocytotic processes and what endocytotic mechanisms are employed remain to be determined. Understanding these mechanisms requires characterizing the spatial-temporal relationship between SWCNTs and microvascular ECs.

We found that the fluorescence intensity of the SWCNT-DNA-FITC conjugate in microvascular ECs was concentration and time independent. These results indicate that SWCNTs do not accumulate over time in microvascular ECs and that the level of SWCNTs in cells reached a plateau 6 hrs after incubation. Since SWCNTs are highly stable structures [6], we predict that microvascular ECs are not able to degrade internalized SWCNTs via lysosomes but expel them over time (exocytosis). The process, in which molecules, in this case of SWCNTs, undergo endocytosis and then exocytosis, is referred to as transcytosis. Transcytosis is one of the pathways by which macromolecules, such as drugs and large proteins, pass through microvascular barriers [5, 22]. This concept has significant implications in terms of using SWCNTs as carriers to deliver drugs/genes into parenchymal cells after SWCNTs move from microvessels

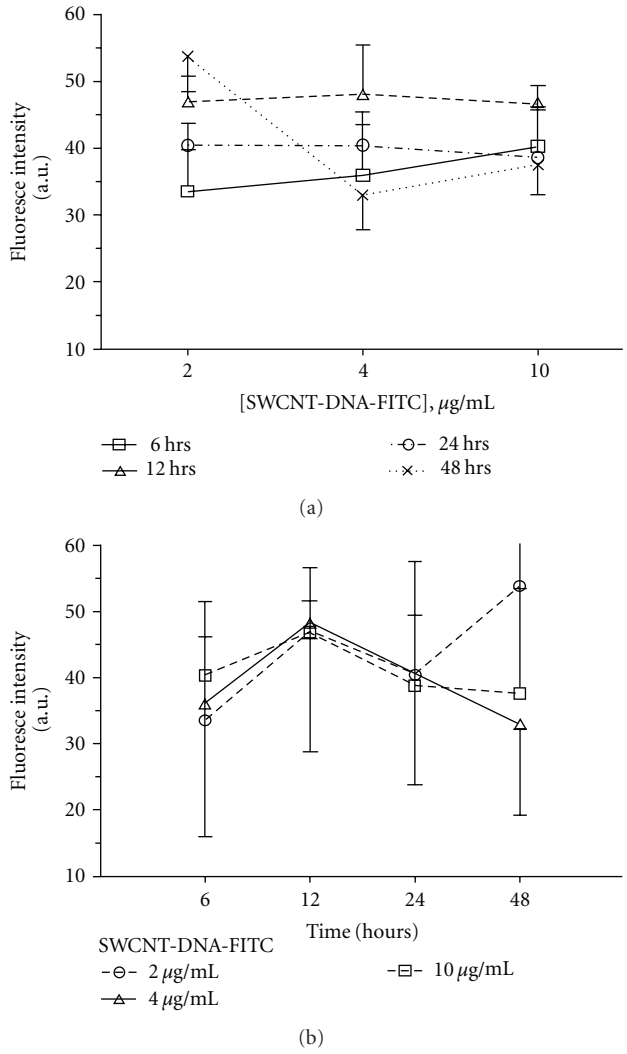

Figure 4: Quantity of SWCNT-DNA-FITC conjugates retained in EC nuclei is concentration- and time-independent. (a) Relationship between quantity of SWCNTDNA-FITC in the nuclei and the concentrations of SWCNT-DNA-FITC conjugates; (b) Time-course of fluorescence intensity of SWCNT-DNA-FITC in the nuclei of microvascular ECs.

into the surrounding interstitium. However, the timing of DNA release from SWCNT-DNA conjugates, critical information for designing a drug delivery system with high efficacy, remains to be studied.

4. Conclusions

This study is the first to demonstrate that SWCNT-DNA conjugates are taken up by microvascular ECs. We observed that intracellular fluorescence intensity of SWCNT-DNA-FITC in microvascular ECs was greater than the fluorescence intensity of DNA-FITC alone, suggesting that the uptake was facilitated by SWCNTs. In addition, SWCNT-DNA conjugates were most likely localized in the nuclei of microvascular ECs, whereas DNA was distributed in the cytoplasm. The SWCNT uptake by microvascular ECs was concentration and time independent. These data suggest that SWCNTs may provide impressive therapeutic potential as vehicles for delivery of drugs or genes to either microvascular ECs or parenchymal cells.

Acknowledgments

The authors thank Missouri State University and the Cottrell College Science Award from the Research Corporation for Science Advancement for supporting this work. The spinning confocal microscope imaging system was supported by the National Science Foundation (Award no. MRI-RUI 0923024). They gratefully thank Dr. Michael Craig for critical suggestions and discussions about the paper.

References

[1] F. Liang and B. Chen, "A review on biomedical applications of single-walled carbon nanotubes," *Current Medicinal Chemistry*, vol. 17, no. 1, pp. 10–24, 2010.

[2] Z. Liu, K. Chen, C. Davis et al., "Drug delivery with carbon nanotubes for in vivo cancer treatment," *Cancer Research*, vol. 68, no. 16, pp. 6652–6660, 2008.

[3] K. Welsher, S. P. Sherlock, and H. Dai, "Deep-tissue anatomical imaging of mice using carbon nanotube fluorophores in the second near-infrared window," *Proceedings of the National Academy of Sciences of the United States of America*, vol. 108, no. 22, pp. 8943–8948, 2011.

[4] Z. Liu, C. Davis, W. Cai, L. He, X. Chen, and H. Dai, "Circulation and long-term fate of functionalized, biocompatible single-walled carbon nanotubes in mice probed by Raman spectroscopy," *Proceedings of the National Academy of Sciences of the United States of America*, vol. 105, no. 5, pp. 1410–1415, 2008.

[5] D. Mehta and A. B. Malik, "Signaling mechanisms regulating endothelial permeability," *Physiological Reviews*, vol. 86, no. 1, pp. 279–367, 2006.

[6] A. Albini, V. Mussi, A. Parodi et al., "Interactions of single-wall carbon nanotubes with endothelial cells," *Nanomedicine*, vol. 6, no. 2, pp. 277–288, 2010.

[7] W. W. Cheng, Z. Q. Lin, B. F. Wei et al., "Single-walled carbon nanotube induction of rat aortic endothelial cell apoptosis: reactive oxygen species are involved in the mitochondrial pathway," *International Journal of Biochemistry and Cell Biology*, vol. 43, no. 4, pp. 564–572, 2011.

[8] L. Zhiqing, X. Zhuge, C. Fuhuan et al., "ICAM-1 and VCAM-1 expression in rat aortic endothelial cells after single-walled carbon nanotube exposure," *Journal of Nanoscience and Nanotechnology*, vol. 10, no. 12, pp. 8562–8574, 2010.

[9] W. C. Aird, "Phenotypic heterogeneity of the endothelium: II. Representative vascular beds," *Circulation Research*, vol. 100, no. 2, pp. 174–190, 2007.

[10] W. C. Aird, "Phenotypic heterogeneity of the endothelium: I. Structure, function, and mechanisms," *Circulation Research*, vol. 100, no. 2, pp. 158–173, 2007.

[11] L. Dong, K. L. Joseph, C. M. Witkowski, and M. M. Craig, "Cytotoxicity of single-walled carbon nanotubes suspended in various surfactants," *Nanotechnology*, vol. 19, no. 25, Article ID 255702, 2008.

[12] L. Dong, C. M. Witkowski, M. M. Craig, M. M. Greenwade, and K. L. Joseph, "Cytotoxicity effects of different surfactant

molecules conjugated to carbon nanotubes on human astrocytoma cells," *Nanoscale Research Letters*, vol. 4, no. 12, pp. 1517–1523, 2009.

[13] J. Wang, S. Bingaman, and V. H. Huxley, "Intrinsic sex-specific differences in microvascular endothelial cell phosphodiesterases," *American Journal of Physiology—Heart and Circulatory Physiology*, vol. 298, no. 4, pp. H1146–H1154, 2010.

[14] J. Wang and V. H. Huxley, "Adenosine A2A receptor modulation of juvenile female rat skeletal muscle microvessel permeability," *American Journal of Physiology—Heart and Circulatory Physiology*, vol. 291, no. 6, pp. H3094–H3105, 2006.

[15] N. W. S. Kam, Z. Liu, and H. Dai, "Carbon nanotubes as intracellular transporters for proteins and DNA: an investigation of the uptake mechanism and pathway," *Angewandte Chemie—International Edition*, vol. 45, no. 4, pp. 577–581, 2006.

[16] R. V. Stan, "Endocytosis pathways in endothelium: how many?" *American Journal of Physiology—Lung Cellular and Molecular Physiology*, vol. 290, no. 5, pp. L806–L808, 2006.

[17] B. S. Ding, T. Dziubla, V. V. Shuvaev, S. Muro, and V. R. Muzykantov, "Advanced drug delivery systems that target the vascular endothelium," *Molecular Interventions*, vol. 6, no. 2, pp. 98–112, 2006.

[18] P. Oh, P. Borgström, H. Witkiewicz et al., "Live dynamic imaging of caveolae pumping targeted antibody rapidly and specifically across endothelium in the lung," *Nature Biotechnology*, vol. 25, no. 3, pp. 327–337, 2007.

[19] S. Muro, X. Cui, C. Gajewski, J. C. Murciano, V. R. Muzykantov, and M. Koval, "Slow intracellular trafficking of catalase nanoparticles targeted to ICAM-1 protects endothelial cells from oxidative stress," *American Journal of Physiology—Cell Physiology*, vol. 285, no. 5, pp. C1339–C1347, 2003.

[20] S. Muro, M. Mateescu, C. Gajewski, M. Robinson, V. R. Muzykantov, and M. Koval, "Control of intracellular trafficking of ICAM-1-targeted nanocarriers by endothelial Na+/H+ exchanger proteins," *American Journal of Physiology—Lung Cellular and Molecular Physiology*, vol. 290, no. 5, pp. L809–L817, 2006.

[21] S. Pogodin and V. A. Baulin, "Can a carbon nanotube pierce through a phospholipid bilayer?" *ACS Nano*, vol. 4, no. 9, pp. 5293–5300, 2010.

[22] C. C. Michel and F. E. Curry, "Microvascular permeability," *Physiological Reviews*, vol. 79, no. 3, pp. 703–761, 1999.

Hindawi Publishing Corporation
Journal of Nanotechnology
Volume 2012, Article ID 928924, 7 pages
doi:10.1155/2012/928924

Research Article

Antimicrobial Activity of Single-Walled Carbon Nanotubes Suspended in Different Surfactants

Lifeng Dong,[1] Alex Henderson,[2] and Christopher Field[3]

[1] *Department of Physics, Astronomy, and Materials Science, Missouri State University, Springfield, MO 65897, USA*
[2] *Department of Biology, Truman State University, Kirksville, MO 63501, USA*
[3] *Department of Biomedical Sciences, Missouri State University, Springfield, MO 65897, USA*

Correspondence should be addressed to Lifeng Dong, lifengdong@missouristate.edu

Received 29 June 2011; Accepted 16 August 2011

Academic Editor: Michael M. Craig

We investigated the antibacterial activity of single-walled carbon nanotubes (SWCNTs) dispersed in surfactant solutions of sodium cholate, sodium dodecylbenzene sulfonate, and sodium dodecyl sulfate. Among the three surfactants, sodium cholate demonstrated the weakest antibacterial activity against *Salmonella enterica*, *Escherichia coli*, and *Enterococcus faecium* and thereby was used to disperse bundled SWCNTs in order to study nanotube antibiotic activity. SWCNTs exhibited antibacterial characteristics for both *S. enterica* and *E. coli*. With the increase of nanotube concentrations from 0.3 mg/mL to 1.5 mg/mL, the growth curves had plateaus at lower absorbance values whereas the absorbance value was not obviously affected by the incubation ranging from 5 min to 2 h. Our findings indicate that carbon nanotubes could become an effective alternative to antibiotics in dealing with drug-resistant and multidrug-resistant bacterial strains because of the physical mode of bactericidal action that SWCNTs display.

1. Introduction

Due to their unique chemical and physical properties, single-walled carbon nanotubes (SWCNTs) have been extensively investigated as the building blocks for nanoscale electronic devices [1–3] and the catalyst supports for direct ethanol/methanol fuel cells [4–6]. For these applications, the bundled nanotubes usually need to be dispersed into individual nanotubes through surfactant stabilization of the hydrophobic nanotube surfaces. Several surfactants, such as sodium dodecyl sulfate (SDS), sodium dodecylbenzene sulfonate (SDBS), and sodium cholate (SC), were reported to efficiently disperse bundled nanotubes into suspensions of individual nanotubes [7, 8]. With the increasing production of SWCNTs and their broad applications, it is critical to evaluate the biomedical implications of nanotubes in terms of antibacterial activities and human health impacts. In our previous study, both SDS and SDBS and their conjugates with SWCNTs demonstrated toxicity to 1321N1 human astrocytoma cells even as low as 0.05 mg/mL for 30 min. On the other hand, the proliferation and viability of the cells were not affected by SWCNTs alone or by conjugates of SWCNTs with various concentrations of SC [9, 10]. In this study, we investigated further the antimicrobial activity of the same SWCNTs and their conjugates with SDS, SDBS, and SC. The utilization of the same solutions of SWCNTs and their surfactant conjugates provides comparative results of the effects of the SWCNTs on bacterial and mammalian cells. As reported in the literature, SWCNTs have given different and sometimes contradictory toxicity results, likely due to the heterogeneous nanotube samples consisting of metal catalysts, catalyst supports, amorphous carbon, and carbon nanoparticles [11, 12].

The antimicrobial activity of SWCNTs has been reported to be related to a number of factors. Yang et al. tested three different lengths of SWCNTs (<1 μm, 1–5 μm, and ~5 μm). At the same weight concentrations, longer nanotubes exhibited stronger antimicrobial activity [13]. Arias and Yang et al. also demonstrated that SWCNTs having surface groups of –OH and –COOH exhibited extremely strong antimicrobial activity to both Gram-positive and Gram-negative bacterial cells, whereas SWCNTs-NH_2 demonstrated little toxicity [14]. Vecitis et al. reported that electronic structure is an important factor regulating SWCNT antimicrobial activity [15]. Kang et al. reported that the size (diameter) of nano-tubes is a key factor governing their antibacterial effects [16]. In this

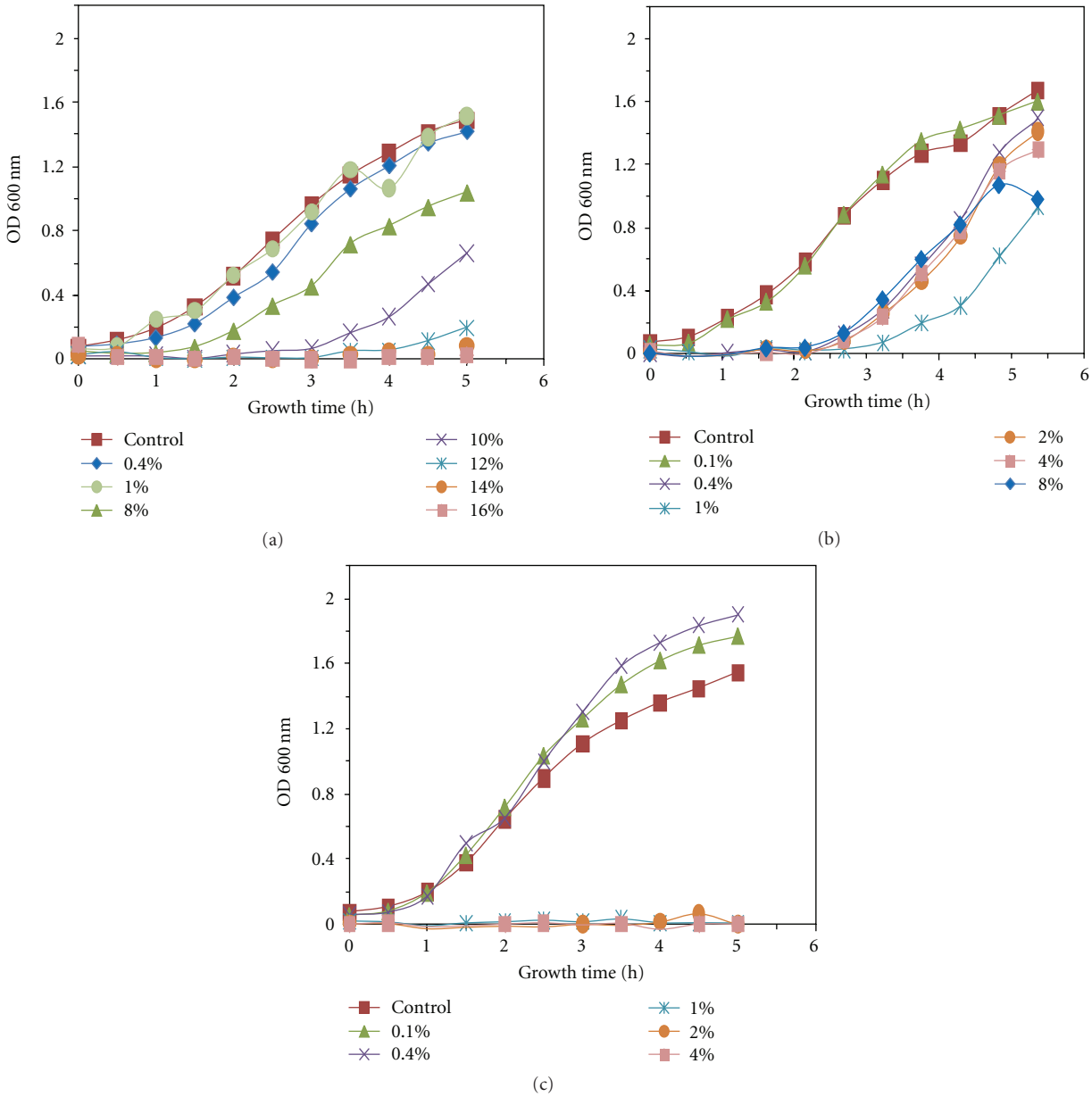

FIGURE 1: OD growth curves of *S. enterica* in BHI broth at 37°C after treatment with surfactant-only solutions and incubation for 1 h: (a) treated with 0.4, 1, 8, 10, 12, 14, and 16% SC; (b) treated with 0.1, 0.4, 1, 2, 4, and 8% SDS, and (c) treated with 0.1, 0.4, 1, 2, and 4% SDBS. Controls were cells without surfactant treatments. A blank was used before each reading. Blanks were samples without cells or surfactant.

study, the antimicrobial activity of SWCNTs suspended in different surfactants was evaluated by the appearance of the exponential bacterial growth phase. The effects of SWCNTs' concentration and treatment time on their antimicrobial activity were also tested.

2. Materials and Methods

2.1. Chemicals. brain heart infusion (BHI) was purchased from Becton, Dickinson, and Company (Sparks, MD). SDS, SC, and SDBS were purchased from Sigma-Aldrich (St. Louis, MO). Solution concentrations were made by diluting a stock surfactant solution to the specified concentration using sterile Milli-Q (mQ) water. Carbon nanotubes were purchased from BuckyUSA (Houston, TX).

2.2. Bacterial Cultures. The cultures were prepared by inoculating BHI broth in a test tube with bacteria transferred from a plate to the test tube using a cotton swab. The cultures grown were *Escherichia coli* (*E. coli*) (ATCC #11303), *Salmonella enterica* (*S. enterica*) (ATCC #19585), and *Enterococcus faecium* (*E. faecium*) (ATCC #19634). The culture to be studied the next day was incubated in a 37°C shaker with constant agitation at 200 rpm overnight. Incubation time

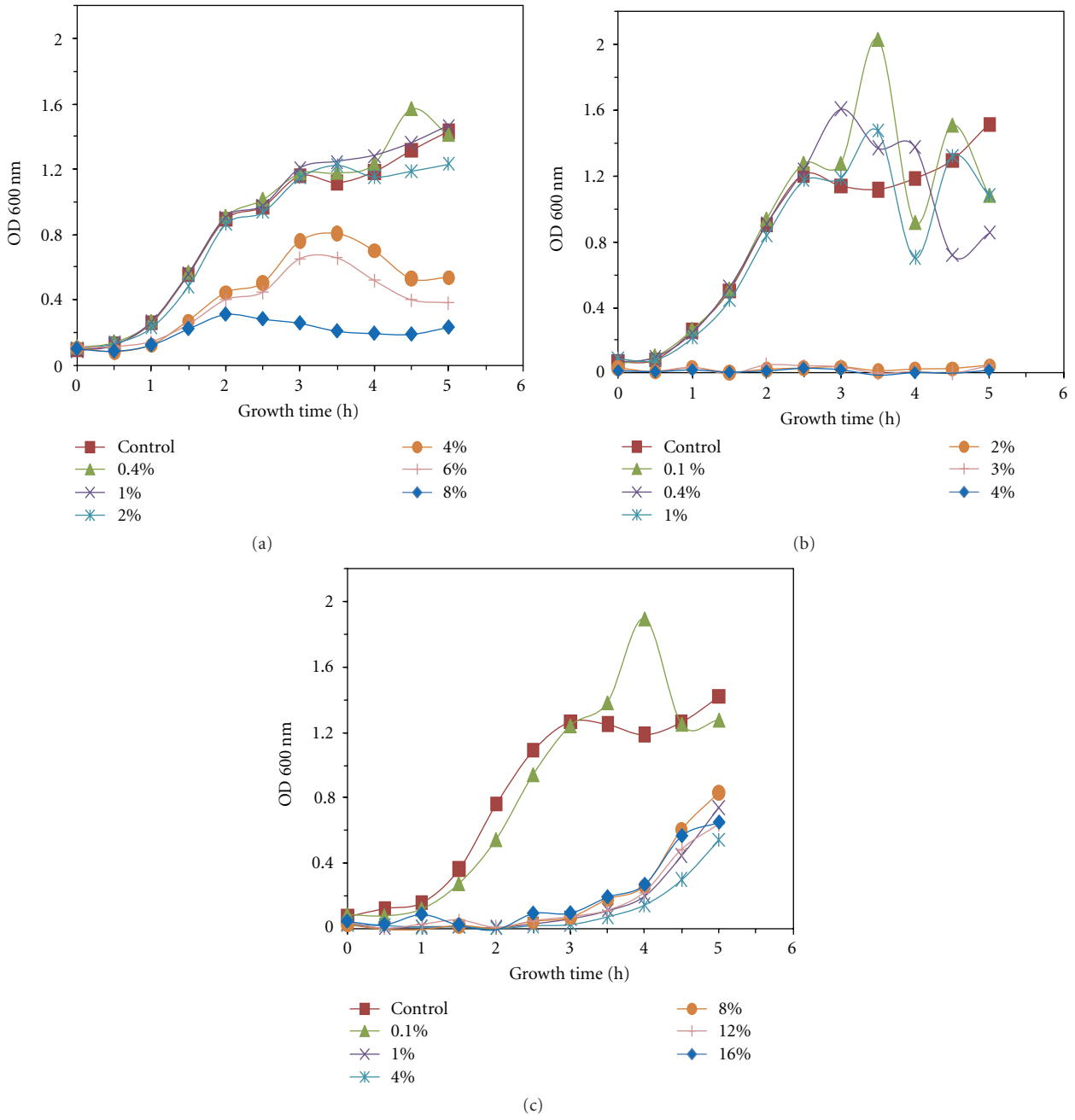

FIGURE 2: OD growth curves of *E. coli* after treatment with surfactant-only solutions and incubation for 1 h: (a) treated with 0.4, 1, 2, 4, 6, and 8% SC; (b) treated with 0.1, 0.4, 1, 2, 3, and 4% SDBS, and (c) treated with 0.1, 1, 4, 8, 12, and 16% SDS. Other conditions are the same as in Figure 1.

was approximately 18–20 h. One milliliter of the incubated culture was centrifuged at 3300 g for 2 min. The supernatant was removed, and the remaining pellet was washed with 1 mL mQ water three times. The bacterial cells were resuspended in 1 mL mQ water.

2.3. Treatment of Bacterial Cells with SWCNTs. Fifty microliters of the cell suspension were diluted in 500 μL of surfactant or SWCNT/surfactant solution and allowed to incubate at 37°C and 200 rpm for 1 h or for a designed treatment time. The blank solution contained 550 μL of mQ water, and the control solution contained 500 μL of mQ water and 50 μL of cell solution. After the incubation, 1.45 mL of BHI broth was added to each solution for a final volume of 2 mL.

2.4. Optical Density (OD) Growth Curve Measurements. After the addition of BHI, 100 μL aliquots were taken from the solutions every 30 min for the next 5 h and tested for optical density. The remaining solutions continued to incubate in the shaker at 37°C and 200 rpm. Cell growth

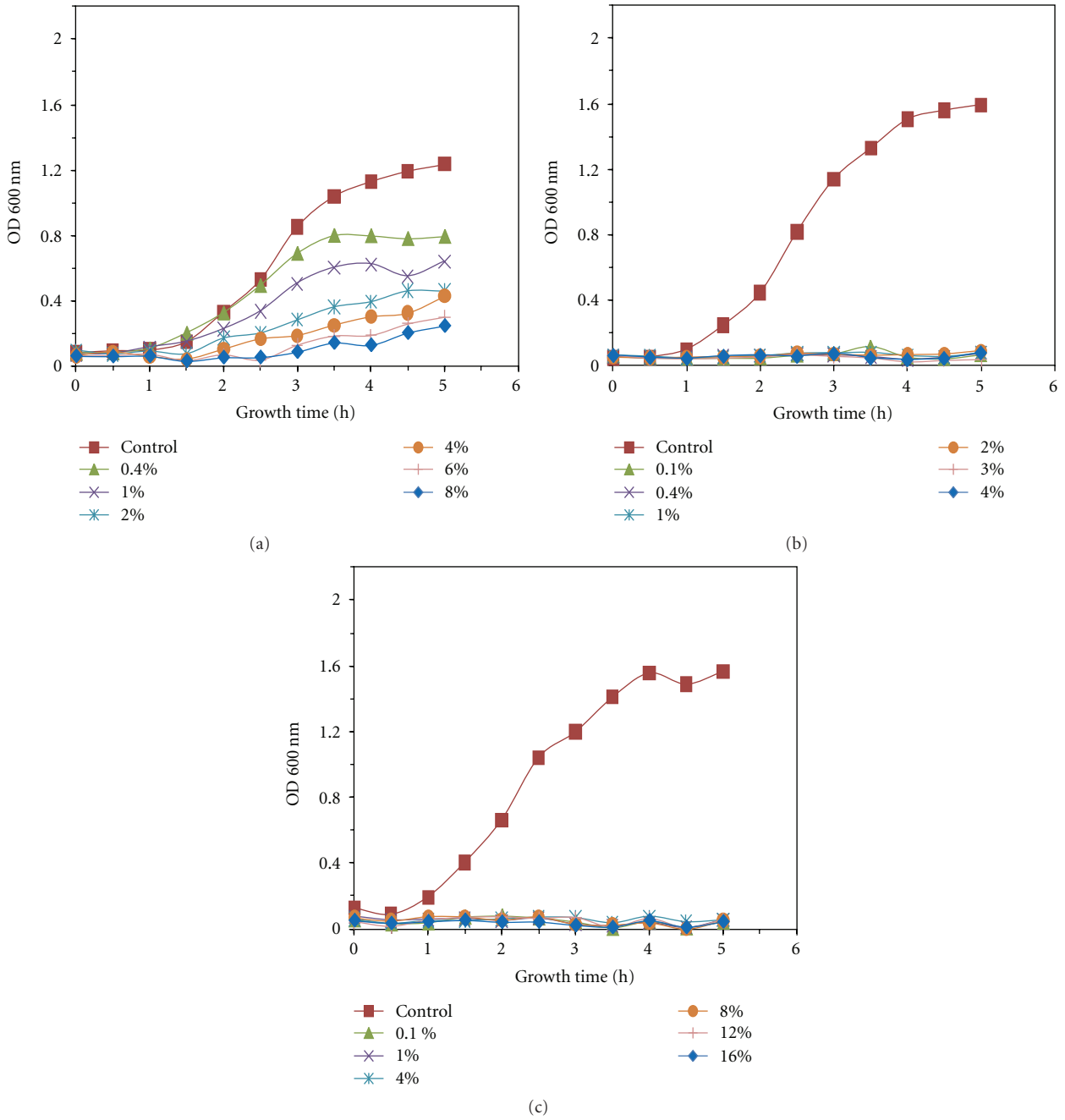

FIGURE 3: OD growth curves of *E. faecium* after treatment with surfactant-only solutions and incubation for 1 h: (a) treated with 0.4, 1, 2, 4, 6, and 8% SC; (b) treated with 0.1, 0.4, 1, 2, 3, and 4% SDBS, and (c) treated with 0.1, 1, 4, 8, 12, and 16% SDS. Other conditions are the same as in Figure 1.

was measured using a Beckman Coulter DU 520 spectrophotometer at 600 nm. Growth curves were created by plotting OD values versus time. The SWCNT-containing graphs were created by subtracting a blank containing the same SWCNT concentration as the experimental sample in order to create values consistent with the control that did not contain SWCNTs. After subtracting the SWCNT blank, absorbance was related to the quantity of cells. The time delay of exponential growth directly results from the initial viable bacterial cell number. Therefore, a delay in growth time indicates a lower initial viable cell number. This result means that a negative deviation from the control growth curve indicates antibacterial activity. All experiments were executed in triplicate.

3. Results and Discussion

3.1. Antibacterial Effects of Various Surfactants. Prior to the investigation on nanotube interactions with bacteria cells, we studied how various surfactants interacted with

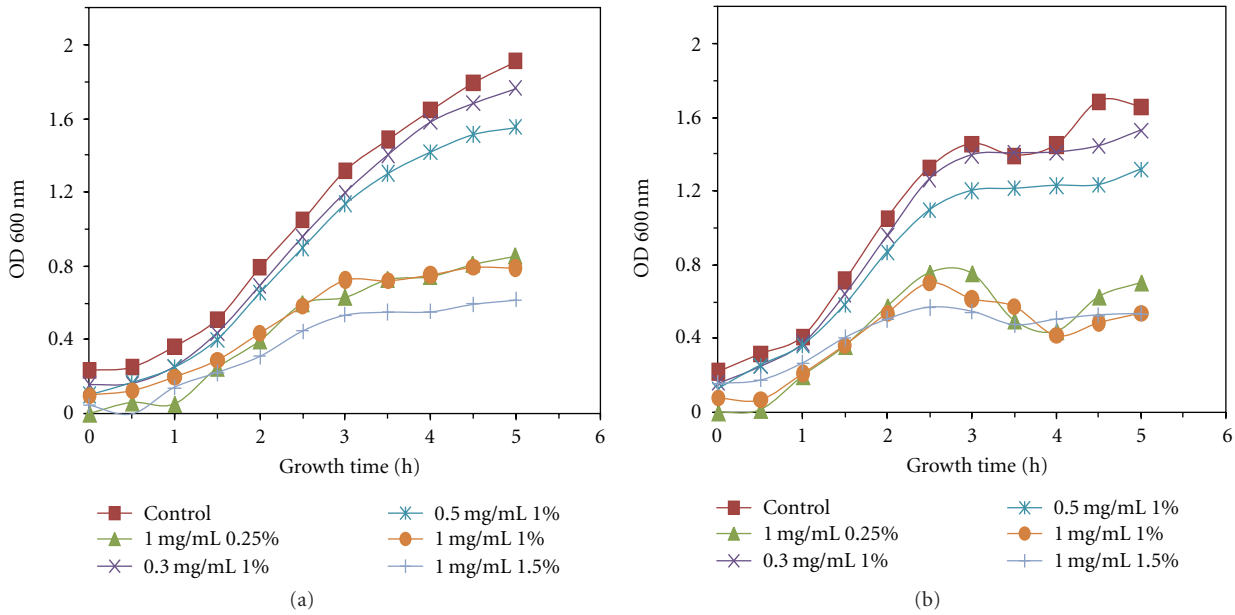

Figure 4: OD growth curves of (a) *S. enterica* and (b) *E. coli* after treatment with SWCNT + surfactant solutions and incubation for 1 h. The legend shows SWCNT concentration in mg/mL and SC surfactant concentration in %. A blank containing the same SWCNT concentration as the experimental sample was subtracted from each of the SWCNT-containing data sets in order to measure absorbance created by cells. Other conditions are the same as in Figure 1.

the *S. enterica, E. coli, and E. faecium* in the absence of SWCNTs. Figure 1(a) shows SC interaction with *S. enterica*. Sodium cholate displayed nearly complete killing of *S. enterica* at treatment concentrations of 12% and greater. Ten percent SC treatment delayed exponential growth for approximately 3 h. Eight percent SC delayed growth for approximately 1.5 h. Sodium cholate did not inhibit growth at 0.4% and 1% treatments. Figure 1(b) displays SDS interaction with *S. enterica*. All concentrations greater than 0.4% showed similar results, delaying growth for approximately 2 h. Interestingly, 1% SDS generated a slightly enhanced antibacterial effect compared to other concentrations. *S. enterica* in SDBS is displayed in Figure 1(c). One percent and greater SDBS treatments demonstrated complete bacterial killing. Levels lower than 1% did not deviate much from the control.

Figure 2(a) shows the SC effect on *E. coli*. Eight percent SC treatments demonstrated the strongest antibacterial activity while concentrations of 2% and smaller showed minimal antibacterial effects. *E. coli* in SDBS is given in Figure 2(b). Treatments with concentrations of 2% and greater provided complete killing, yet concentrations of 1% and lower caused minimal deviation from the control. Sodium dodecyl sulfate had similar effects on *E. coli* (Figure 2(c)) as it did on *S. enterica*. Each concentration, other than 0.1%, demonstrated comparable results, delaying exponential growth for approximately 3 hours.

Cultured *E. faecium* was much more sensitive to the surfactants than either *S. enterica* or *E. coli*. In SC (Figure 3(a)), the growth curves decreased in order of increasing surfactant concentration. Sodium dodecylbenzene sulfonate, shown in Figure 3(b), demonstrated complete effectiveness at all tested concentrations, and SDS also showed complete effectiveness at all tested concentrations (Figure 3(c)). Due to its vulnerability with our tested surfactants, no further experiments were conducted on *E. faecium*.

3.2. Antibacterial Effects of SWCNTs. Based on the results above, SC proved to be the best candidate to investigate antibacterial effects of SWCNTs since it contained the highest surfactant concentration without inhibiting bacterial growth. A treatment concentration of 1% was selected due to its ability to disperse SWCNTs effectively yet not inhibit bacterial cell growth. This indicates that all or almost all of the growth inhibition created by SC + SWCNT solutions is due to carbon nanotube activity. In addition to using 1% SC solutions, we also included a 0.25% SC trial in order to verify how different surfactant concentrations affect SWCNT activity through increased or decreased dispersion. Figure 4(a) displays *S. enterica* tested in SC solutions with varying SWCNT concentrations. The growth curves decreased in order of increasing SWCNT concentration. Interestingly, the solutions of 1 mg/mL SWCNTs + 0.25% SC and 1 mg/mL SWCNTs + 1% SC showed similar curves. These results suggest that concentrations of 0.25% SC were able to disperse 1 mg/mL SWCNTs as well as 1% SC. Figure 4(b) shows *E. coli* tested in SC solutions with varying concentrations of SWCNTs. The growth curves decreased in order of increasing SWCNT concentration and generated a curve similar to that of *S. enterica* in the solutions containing 1 mg/mL SWCNTs + 0.25% SC and 1 mg/mL SWCNTs + 1% SC. A plateau effect is seen in these trials in which higher concentrations of SWCNTs cause the growth curve to plateau at lower absorbance values. This observation suggests that SWCNTs limit cell growth via a concentration-dependent mechanism.

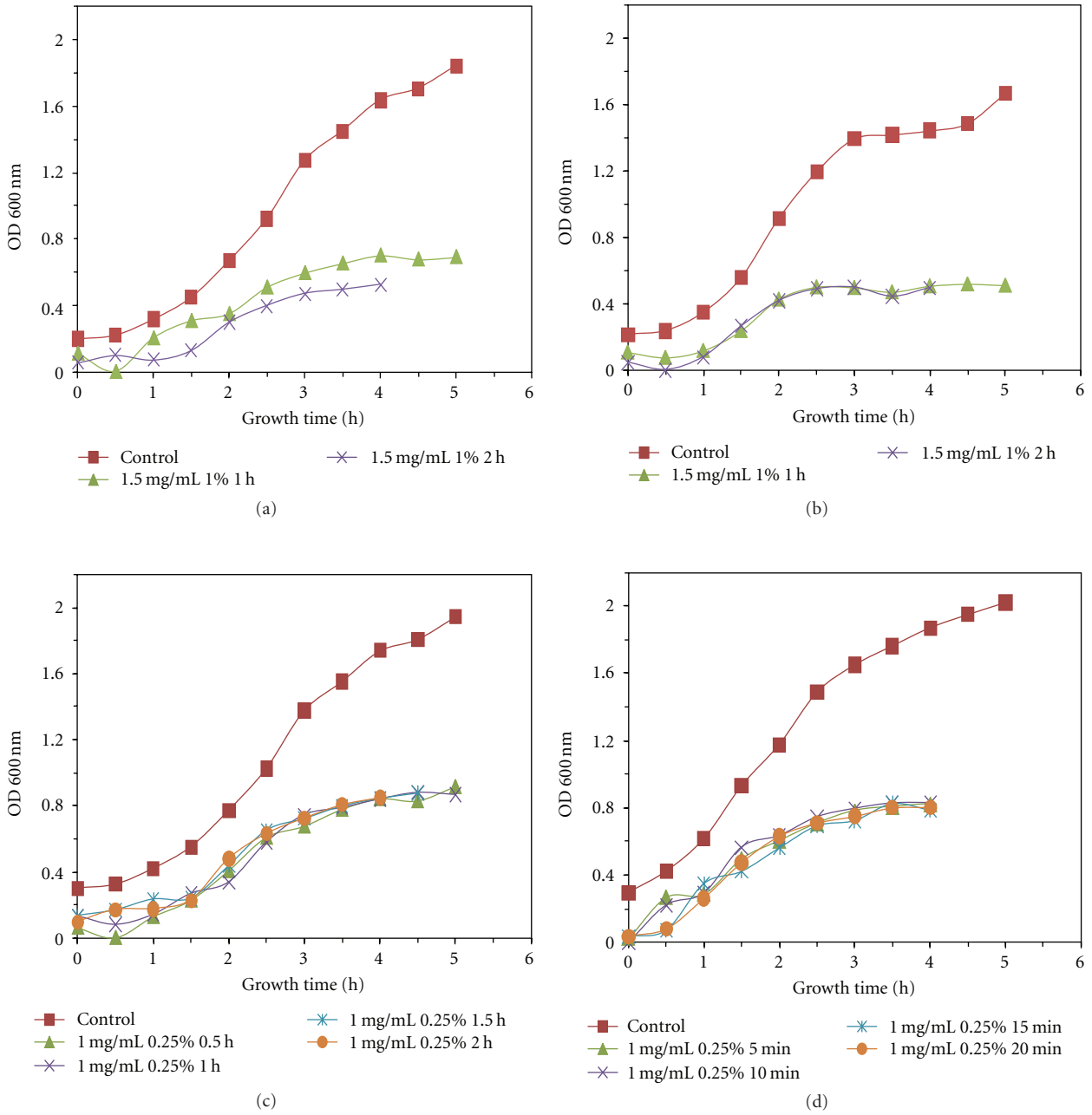

Figure 5: OD growth curves of bacterial cells after treatment with SWCNT + surfactant solutions. The legend shows SWCNT concentration in mg/mL, SC surfactant concentrations in %, and incubation times in h or min: (a) *S. enterica* and (b) *E. coli* treated with 1.5 mg/mL and 1% for 1 h and 2 h, (c) *S. enterica* treated with 1 mg/mL and 0.25% for 0.5 h, 1 h, 1.5 h, and 2 h, and (d) *S. enterica* treated with 1 mg/mL and 0.25% for 5 min, 10 min, 15 min, and 20 min. Nanotube blanks were created as in Figure 4. Other conditions are the same as in Figure 1.

Figures 5(a) and 5(b) show *S. enterica* and *E. coli* in solutions of 1.5 mg/mL SWCNTs + 1% SC with incubation times of 1 h and 2 h, respectively. There was no discernible difference in cell growth between the two incubation times. Figure 5(c) shows *S. enterica* in solutions of 1 mg/mL SWCNTs + 0.25% SC with incubation times of 0.5 h, 1 h, 1.5 h, and 2 h. These differences in incubation time had no effect on cell growth. Because 0.5 h incubation produced no difference in growth rate, a test was executed using identical SWCNT and SC concentrations with incubation times of 5 min, 10 min, and 15 min (Figure 5(d)). These results also show that incubation time is not a factor at the times tested, thus providing indication that SWCNTs produce an antibacterial effect quickly (<5 min). Growth curves in Figures 5(a)–5(d) also exhibit a lowered plateau as seen in Figures 4(a)-4(b), providing additional evidence that SWCNT concentration is the primary factor in producing the antibacterial effect.

4. Conclusions

Sodium cholate proved to be a desired surfactant with which we examine SWCNT antibacterial activity because it displayed the weakest inhibitory activity among broadly used surfactants. Sodium cholate did not provide complete bactericidal effects on *S. enterica* until the bacterium was treated with 12% SC in solution. By contrast, SDS and SDBS demonstrated total or nearly total effectiveness at 1% concentrations. Similar findings with *E. coli* indicated that SC can be used to disperse bundled SWCNTs into individual nanotubes and thereby examine SWCNT antibiotic ability. On the other hand, *E. faecium* is too sensitive to the surfactants to examine SWCNT implications. Results from the SWCNT tests indicate that nanotube concentration is the deciding factor in antibacterial effect. Incubation times ranging from 5 min to 2 h did not produce different results. It is promising to see the strong antibacterial effect of SWCNTs in solution with SC, because this same combination of materials proved to have low toxicity for 1321N1 human astrocytoma cells in our previous studies. Low toxicity to humans and high antibiotic effect make SWCNT-surfactant solutions relevant in biomedical applications and problems surrounding drug-resistant and multidrug-resistant bacterial strains. Further studies are required to test the legitimacy of a SWCNT-SC mixture and understand the mechanisms which could explain both low human toxicity and high antibacterial effect.

Acknowledgments

This work was partially supported by a Summer Faculty Fellowship from Missouri State University, the Cottrell College Science Award from Research Corporation for Science Advancement, and the American Chemical Society Petroleum Research Fund (47532-GB10). The authors thank Dr. Michael M. Craig for helpful discussions and editing.

References

[1] S. J. Tans, A. R. M. Verschueren, and C. Dekker, "Room-temperature transistor based on a single carbon nanotube," *Nature*, vol. 393, no. 6680, pp. 49–52, 1998.

[2] L. Dong, J. Jiao, C. Pan, and D. W. Tuggle, "Effects of catalysts on the internal structures of carbon nanotubes and corresponding electron field-emission properties," *Applied Physics A*, vol. 78, no. 1, pp. 9–14, 2004.

[3] L. Dong, V. Chirayos, J. Bush et al., "Floating-potential dielectrophoresis-controlled fabrication of single-carbon-nanotube transistors and their electrical properties," *Journal of Physical Chemistry B*, vol. 109, no. 27, pp. 13148–13153, 2005.

[4] T. Maiyalagan, B. Viswanathan, and U. V. Varadaraju, "Nitrogen containing carbon nanotubes as supports for Pt - Alternate anodes for fuel cell applications," *Electrochemistry Communications*, vol. 7, no. 9, pp. 905–912, 2005.

[5] A. Halder, S. Sharma, M. S. Hegde, and N. Ravishankar, "Controlled attachment of ultrafine platinum nanoparticles on functionalized carbon nanotubes with high electrocatalytic activity for methanol oxidation," *Journal of Physical Chemistry C*, vol. 113, no. 4, pp. 1466–1473, 2009.

[6] H. Z. Dong and L. F. Dong, "Electrocatalytic activity of carbon nanotube-supported Pt-Cr-Co tri-metallic nanoparticles for methanol and ethanol oxidations," *Journal of Inorganic and Organometallic Polymers and Materials*. In press.

[7] M. S. Arnold, A. A. Green, J. F. Hulvat, S. I. Stupp, and M. C. Hersam, "Sorting carbon nanotubes by electronic structure using density differentiation," *Nature Nanotechnology*, vol. 1, no. 1, pp. 60–65, 2006.

[8] V. C. Moore, M. S. Strano, E. H. Haroz et al., "Individually suspended single-walled carbon nanotubes in various surfactants," *Nano Letters*, vol. 3, no. 10, pp. 1379–1382, 2003.

[9] L. Dong, K. L. Joseph, C. M. Witkowski, and M. M. Craig, "Cytotoxicity of single-walled carbon nanotubes suspended in various surfactants," *Nanotechnology*, vol. 19, no. 25, Article ID 255702, 2008.

[10] L. Dong, C. M. Witkowski, M. M. Craig, M. M. Greenwade, and K. L. Joseph, "Cytotoxicity effects of different surfactant molecules conjugated to carbon nanotubes on human astrocytoma cells," *Nanoscale Research Letters*, vol. 4, no. 12, pp. 1517–1523, 2009.

[11] S. Liu, L. Wei, L. Hao et al., "Sharper and faster "Nano darts" kill more bacteria: a study of antibacterial activity of individually dispersed pristine single-walled carbon nanotube," *ACS Nano*, vol. 3, no. 12, pp. 3891–3902, 2009.

[12] G. Jia, H. Wang, L. Yan et al., "Cytotoxicity of carbon nanomaterials: single-wall nanotube, multi-wall nanotube, and fullerene," *Environmental Science & Technology*, vol. 39, no. 5, pp. 1378–1383, 2005.

[13] C. Yang, J. Mamouni, Y. Tang, and L. Yang, "Antimicrobial activity of single-walled carbon nanotubes: length effect," *Langmuir*, vol. 26, no. 20, pp. 16013–16019, 2010.

[14] L. R. Arias and L. Yang, "Inactivation of bacterial pathogens by carbon nanotubes in suspensions," *Langmuir*, vol. 25, no. 5, pp. 3003–3012, 2009.

[15] C. D. Vecitis, K. R. Zodrow, S. Kang, and M. Elimelech, "Electronic-structure-dependent bacterial cytotoxicity of single-walled carbon nanotubes," *ACS Nano*, vol. 4, no. 9, pp. 5471–5479, 2010.

[16] S. Kang, M. Herzberg, D. F. Rodrigues, and M. Elimelech, "Antibacterial effects of carbon nanotubes: size does matter!," *Langmuir*, vol. 24, no. 13, pp. 6409–6413, 2008.

Hindawi Publishing Corporation
Journal of Nanotechnology
Volume 2012, Article ID 954601, 9 pages
doi:10.1155/2012/954601

Research Article

Biomolecular Triconjugates Formed between Gold, Protamine, and Nucleic Acid: Comparative Characterization on the Nanoscale

Robert K. DeLong,[1] Lisa Cillessen,[2] Chris Reynolds,[3] Adam Wanekaya,[3] Tiffany Severs,[3] Kartik Ghosh,[4] Michael Fisher,[5] Stephanie Barber,[6] John Black,[7] Ashley Schaeffer,[1] and Kristin J. Flores[1]

[1] *Cell and Molecular Biology Program, Department of Biomedical Sciences, Missouri State University, Springfield, MO 65897, USA*
[2] *College of Pharmacy, The Ohio State University, Columbus, OH 43210, USA*
[3] *Department of Chemistry, Missouri State University, Springfield, MO 65897, USA*
[4] *Department of Physics Astronomy and Materials Science, Missouri State University, Springfield, MO 65897, USA*
[5] *School of Medicine, University of North Carolina at Chapel Hill, Chapel Hill, NC 27599, USA*
[6] *George Warren Brown School of Social Work, Washington University in St. Louis, St. Louis, MO 63130, USA*
[7] *School of Medicine, University of Pittsburgh, Pittsburg, PA 15261, USA*

Correspondence should be addressed to Robert K. DeLong, robertdelong@missouristate.edu

Received 15 June 2011; Accepted 11 August 2011

Academic Editor: Dongwoo Khang

DNA and RNA micro- and nanoparticles are increasingly being used for gene and siRNA drug delivery and a variety of other applications in bionanotechnology. On the nanoscale, these entities represent unique challenges from a physicochemical characterization perspective. Here, nucleic acid conjugates with protamine and gold nanoparticles (GNP) were characterized comparatively in the nanorange of concentration by UV/Vis NanoDrop spectroscopy, fluorimetry, and gel electrophoresis. Given the intense interest in splice-site switching oligomers (SSOs), we utilized a human tumor cell culture system (HeLa pLuc-705), in which SSO-directed splicing repair upregulates luciferase expression, in order to investigate bioactivity of the bionanoconjugates. Process parameters important for bioactivity were investigated, and the bimolecular nanoconjugates were confirmed by shifts in the dynamic laser light scatter (DLLS), UV/Vis spectrum, gel electrophoresis, or sedimentation pattern. The data presented herein may be useful in the future development of pharmaceutical and biotechnology formulations, processes, and analyses concerning protein, DNA, or RNA bionanoconjugates.

1. Introduction

Nanoparticles bearing siRNA have been tested recently in clinical trials [1]. RNA oligonucleotides known as splice-shifting oligomers (SSOs) have the ability to correct errors that occur in gene splicing at the RNA level, potentially a novel means of controlling an important molecular pathology underlying cancer [2] and possibly other human diseases [3]. Although protamine has long been known to bind and condense DNA into nanoparticles [4] active for gene delivery [5], condensation of RNA is more controversial [6, 7]. Considering the well-known cell-penetrating and nuclear localization capabilities of protamine [8], we presume it could play a critical role for the delivery of SSOs [9].

To investigate the bioactivity and biocompatibility of the conjugates in this study, we utilize the well-described HeLa pLuc-705 cell culture system, in which luciferase is upregulated by delivery of specific SSOs [10–12]. This luminescence-based assay can be used for quantifying RNA nanoconjugate delivery. We use this system, along with high-throughput screening, to explore the process parameters that are important for the RNA nanoconjugate SSO

bioactivity. To demonstrate the biocompatibility of the triconjugates, we use the MTT (3-(4,5-dimethylthiazol-2-yl)-2,5-diphenyltetrazolium bromide) assay to investigate the metabolic activity of the HeLa pLuc-705 cell line, after incubation with the conjugates. Recently, we reported detection of RNA nanoparticles after protamine complexation to RNA by dynamic laser light scatter spectroscopy (DLLS) [9]. Moreover, gold nanoparticles (GNPs) are taken up by HeLa cells [13], and surface modification of GNPs has been shown to affect their interaction at the plasma membrane and intracellular activity [14]. In this study we characterize conjugates of GNP, with protamine and RNA, in comparative analyses using luminometery, UV/Vis spectroscopy, fluorescence, and gel electrophoresis assays.

2. Experimental

2.1. GNP, Protamine, and Other Reagents. GNPs with a uniform size of ~20–30 nm were synthesized using the standard method of citrate reduction of $HAuCl_4$ salt. Hydrogen tetrachloroaurate (III) trihydrate ($HAuCl_4 \cdot 3H_2O$) was obtained from Fisher Scientific (Fair Lawn, NJ). Sodium citrate was obtained from Spectrum Chemical Corp. (New Brunswick, NJ). To produce the GNPs, an aqueous solution of $HAuCl_4$ (1 mM, 500 mL) was brought to reflux while stirring, and 50 mL of 38.8 mM trisodium citrate solution was rapidly added. After 15 min, the preparation was allowed to cool to room temperature and subsequently filtered through a 0.45 μm filter.

Plasmid DNA encoding Hepatitis B DNA vaccine was obtained as previously described [9]. In some cases, lambda phage DNA (Sigma-Aldrich) was used in the spectral and conjugate studies. The protamine stock was purchased from Sigma-Aldrich as Grade III protamine sulfate salt, derived from herring. Ribonucleic acid (RNA) diethylaminoethanol salt Type IX was also purchased from Sigma-Aldrich and dissolved in RNase-free water just prior to use. A protamine : H_2O standard curve was prepared by dissolving protamine in water at 2 mg/mL, then performing serial dilutions to produce 1 mg/mL, 0.5 mg/mL, 0.25 mg/mL, 0.125 mg/mL, and 0.0625 mg/mL solutions. An RNA : H_2O standard curve was prepared similarly by dissolving RNA in water at 2 mg/mL, then performing serial dilutions to produce 1 mg/mL, 0.5 mg/mL, 0.25 mg/mL, 0.125 mg/mL, and 0.0625 mg/mL solutions.

2.2. High-Throughput Experimental Design to Analyze the Parameters That Affect Bioactivity. Using the HeLa pLuc-705 model, a high-low experimental design was combined with multiparameter screening with a measurable biological activity outcome: relative luminescence (RLU) due to the SSO delivery. The parameters tested included number of cells, time of transfection, mixation rate, and protamine, SSO, magnesium, and ethanol concentration, as illustrated in Figure 2.

2.3. Dynamic Laser Light Scatter Spectroscopy (DLLS). DLLS was conducted on a Malvern Zetasizer Nano-ZS90. Samples were analyzed in 1 mL double-distilled deionized water in UV-transparent Sarstedt cuvettes. Briefly, 1 mg/mL protamine was added to DNA at 0.1 mg/mL while vortexing for 5–10 sec and/or to approximately 50 microlitres of GNPs (3×10^{-8} M). The conjugates were then analyzed directly by DLLS or UV/Vis spectroscopy.

2.4. Fluorimetric and NanoDrop UV/Vis Spectroscopy. Fluorimetric and NanoDrop UV/Vis spectroscopy was conducted as described previously [9] for the Hoechst assay, and the PicoGreen assay was performed in parallel following manufacturer's recommendations. RNA stock solutions were prepared with RNase-free H_2O. Experiments were executed in triplicate, and indicated by Samples A, B, and C for each graph. Serial dilution was performed with 250 μL of solution with 250 μL of RNase free H_2O. Absorbance spectral scans were performed from 190 to 300 nm on a Thermo Fisher NanoDrop 2000c. The UV/Vis absorption spectrum for RNA was also performed in triplicate for 100 ng/μL along with its serial dilution and standard curve for the absorbance values (ordinate) versus concentration (abscissa). For the spectral shift experiments, 90 μL of GNP stock solution was added to 5 μL (10 mg/mL) RNA solution, 5 μL RNase free water, the suspension was vortexed incubated at room temperature for 15 to 20 mins mixed and read on the NanoDrop directly. For GNP-Protamine, 90 μL GNP stock solution and 5 μL (2 mg/mL) stock protamine solution, 5 μL RNase free water was mixed and read as above. For the GNP-protamine : RNA, 90 μL GNP stock solution and 5 μL (10 mg/mL) RNA solution with 5 μL (2 mg/mL) stock protamine solution was mixed and read as above.

2.5. Gel Electrophoresis. Gel electrophoresis was accomplished as described previously [9]. Briefly, the gels contained 2% mass/volume agarose in 1X (v/v) TAE buffer. Each RNA sample contained ethidium bromide (Sigma-Aldrich, St. Louis, MO) at a final concentration of approximately 0.1 mg/mL. Samples contained equal volumes of bromophenol blue loading dye and 5 mg/mL RNA solution. RNA gels were run at 60 V visualized on a Gel Logic imaging station.

2.6. Sedimentation Coupled to UV/Vis NanoDrop. For the sedimentation analysis by UV/Vis NanoDrop, all samples were prepared in triplicate, from the following stock solutions: 200 μL aliquot of the GNP solution, 200 μL of 1.0 mg/mL protamine solution, and 200 μL 5.0 mg/mL RNA solution.

For the GNP only sample, 20 μL of GNP stock solution was added to each microcentrifuge tube. The absorbance from each sample was read, in triplicate, at 525 nm, using the NanoDrop 2000. The samples were centrifuged for 7 minutes at 15,000 rpm, at 10°C. An absorbance reading of the supernatant was taken immediately, at 525 nm.

For the GNP : protamine sample, 20 μL of GNP stock solution was added to each microcentrifuge tube, followed by the addition of 20 μL of protamine stock solution. The samples were vortexed for 8 seconds, and allowed to incubate at room temperature for 5 minutes. The absorbance was

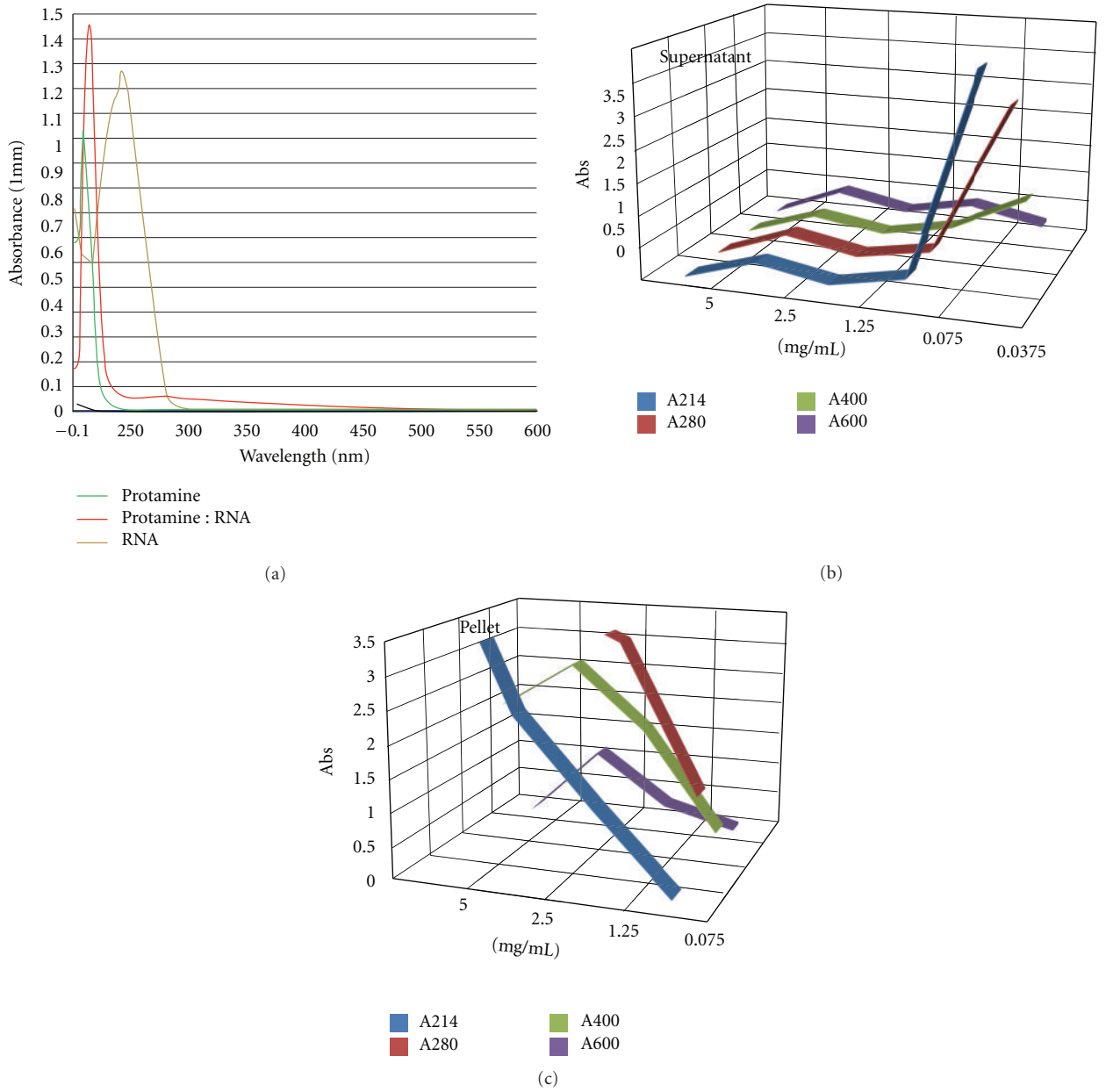

Figure 1: NanoDrop UV/Vis analysis of protamine : RNA and analysis of the sedimentation profiles at 214, 280, 400, and 600 nm.

read; the samples were centrifuged, followed by another absorbance reading of the supernatant, as stated above.

For the GNP : RNA sample, 20 μL of GNP stock solution was added to each microcentrifuge tube, followed by the addition of 20 μL of RNA stock solution. The samples were vortexed for 8 seconds, and allowed to incubate at room temperature for 5 minutes. The absorbance was read at 260 nm. After the samples were centrifuged for 7 minutes at 15,000 rpm, at 10°C, an absorbance reading of the supernatant was taken at 260 nm.

For the sedimentation analysis of the triconjugates, 20 μL of GNP stock solution was added to each microcentrifuge tube, followed by the addition of 20 μL of protamine stock solution, and 20 μL of the RNA stock solution. The samples were vortexed for 8 seconds, and allowed to incubate at room temperature for 5 minutes. The absorbance was read at 260 nm; the samples were centrifuged, followed by another absorbance reading of the supernatant, at 260 nm.

2.7. MTT Assay to Quantify Metabolic Activity after Incubation with Conjugates. Metabolic activity of the HeLa pLuc-705 cells was assessed by the reduction of the yellow tetrazolium salt MTT (3-(4, 5-dimethylthiazol-2-yl)-2,5-diphenyltetrazoliumbromide) to purple, insoluble formazan. All cell culture work was performed under the laminar flow hood, using sterile technique. The HeLa pLuc-705

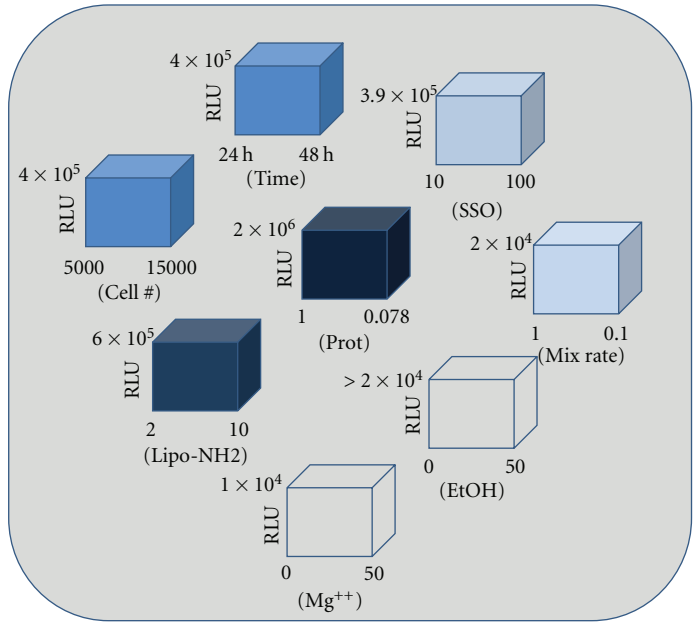

Figure 2: High-throughput screening experimental design analyzing parameters affecting SSO bioactivity in the Hela pLuc-705 system. RLU: relative luminescence, Lipo-NH2: lipofectamine, Prot: protamine concentration, ETOH: ethanol concentration, Mg^{++}: magnesium concentration.

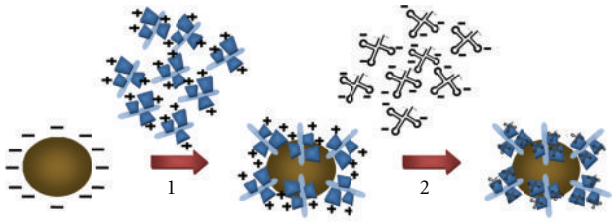

Figure 3: Hypothetical formation of biomolecular triconjugates of GNPs, protamine, and nucleic acid (figure not drawn to scale).

cells, suspended in 1X phenol red-free DMEM/10% FBS/1% penicillin and streptomycin, were seeded in 96-well plates in a volume of 100 μL per well. The cells were incubated at 37°C overnight, to allow them to attach. The DMEM was removed, and the cells were carefully washed with sterile 1X PBS. The GNPs and the conjugates, prepared as previously described, were centrifuged for 7 minutes at 15,000 rpm. The supernatant was removed, and the pellets were resuspended in serum-free, phenol red-free DMEM. From these solutions, 100 μL was added to each well, with 24 wells containing the GNPs and medium only, 24 wells containing the conjugates and medium, and 24 wells containing only the serum-free, phenol red-free medium. The plates were incubated overnight at 37°C. After incubation, the medium was removed and the cells were washed with sterile 1X PBS to remove any GNPs or conjugates, to avoid any interference with the absorbance readings. To each well, 100 μL of fresh serum-free, phenol red-free medium was added, along with 10 μL of a 12 mM MTT stock solution, prepared by adding 1 mL of sterile 1X PBS to 5 mg MTT (Invitrogen). The samples were mixed with the pipettes, and the plates were incubated for 4 hours at 37°C. All but 25 μL of the medium was removed, and 50 μL of DMSO was added to each well to solubilize the formazan. The solutions were mixed with the pipette, and allowed to incubate for 10 minutes at 37°C. The solutions were mixed again with the pipette, and the absorbance was read at 540 nm. This experiment was repeated three times, and the results are graphed in Figure 10.

3. Results and Discussion

3.1. Analysis and Sedimentation of Protamine : RNA. Direct NanoDrop measurement of protamine : RNA and microfuge sedimentation are shown in Figure 1. Macromolecule ($tRNA_{phe}$), rapidly mixed on a dual pump flow head with protamine, was sedimented at 13 k, and the supernatant and pellet or supernatant fractions tested on a NanoDrop UV/Vis instrument at 214, 260, 400, or 600 nm for peptide, RNA, or particle light scatter properties, respectively. The data demonstrate quantitative transferal of the protamine and RNA from the supernatant to the pellet. Light scatter of the particles formed is measured at 400 or 600 nm.

3.2. Measuring SSO Bioactivity in the HeLa pLuc-705 Model. We investigated the parameters that are important for SSO bioactivity in a high-low two-level experimental design. The experimental design and the data are shown in Figure 2. By looking at the relative luminescence (RLU), we conclude that the protamine concentration demonstrated the greatest positive outcome on splice-shifting activity whereas magnesium and ethanol concentration had a negative effect [15]. As shown in Figure 2, formulation-process variables were

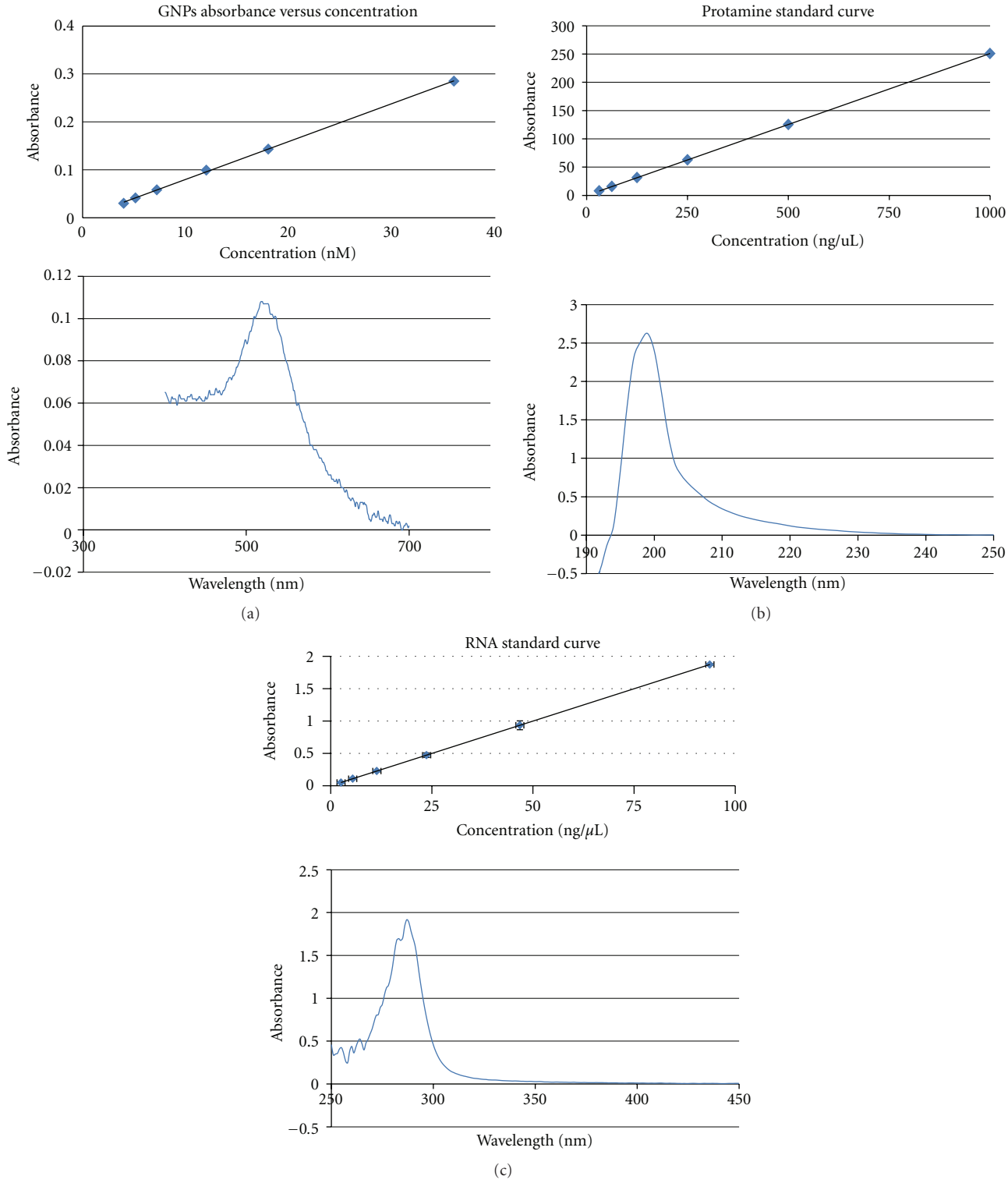

Figure 4: NanoDrop UV/Vis spectra (GNP, protamine, and RNA). Linear range in inset.

shown to affect the cells' luminescence by as much as 10^5–10^6 over background.

3.3. Au-Protamine : RNA Conjugates. GNPs are taken up by HeLa cells [13]. SSO delivery requires membrane penetration and nuclear localization, both of which are known capabilities of protamine [8]. Therefore, our next step was to create conjugates of GNP with protamine as illustrated in Figure 3. As diagrammed in Step 1, positively charged protamine molecules bind to the negatively charged gold nanoparticles

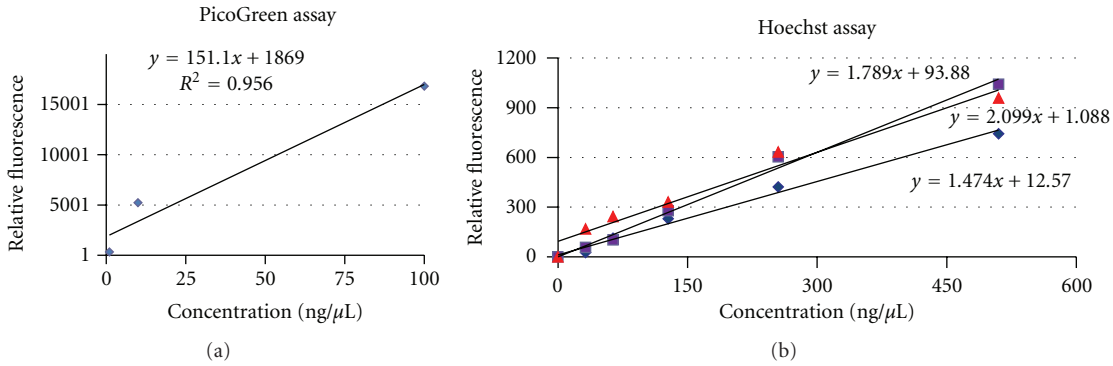

Figure 5: (a) PicoGreen and (b) Hoechst assays for dsDNA, demonstrating the increase in fluorescence as concentration increases in the ng/uL range.

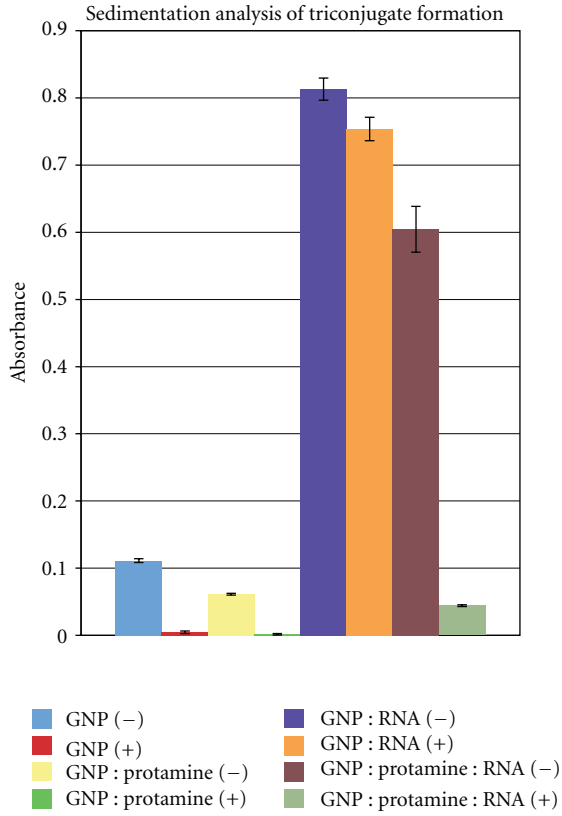

Figure 6: Loss of absorbance from the supernatant sedimentation analysis of GNP, GNP : protamine, GNP : RNA, or GNP : protamine : RNA; ± indicates before microcentrifuge spin (−) or after spin (+).

created by the citrate surface. In Step 2, negatively charged RNA molecules bind to the positively charged protamine molecules bound to a gold nanoparticle, completing the protamine/RNA/gold nanoparticle triconjugate.

3.4. Nano-Drop UV/Vis Analysis of the Nanoconjugate Components. The individual components of the triconjugates (e.g., GNP, protamine, or RNA) can be monitored by

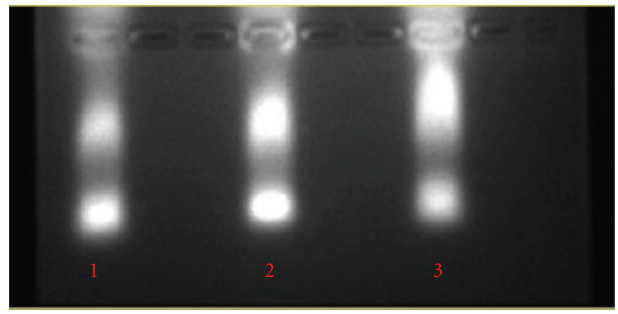

Figure 7: Agarose gel shift of RNA (lane 1), RNA + GNP (lane 2), or RNA + protamine + GNP (lane 3)).

NanoDrop UV/Vis (see Figure 4). Linear range of the standard curve is shown in the inset in units of nanograms per microliter or nanomolar. Maxima were RNA (260 nm), protamine (214–220 nm), and GNP (520–525 nm).

3.5. Fluorescence Analysis of DNA in the Nanorange. Double-stranded DNA (dsDNA) triconjugates with GNP and protamine can also be constructed. Concentration of dsDNA is obtained in the nanogram per microliter range by PicoGreen or Hoechst assays. Standard curves for dsDNA analysis, where fluorescence is a function of the DNA concentration, are shown in Figure 5.

3.6. Analysis of the Conjugates by Sedimentation. GNP, GNP-protamine, or GNP-protamine : RNA samples were analyzed on the UV/Vis NanoDrop before or after sedimentation on a microcentrifuge. The GNP in the supernatant was monitored at 525 nm and the RNA at 260 nm as described previously. These data are shown in Figure 6.

As can be seen in the figure, the greatest loss from the supernatant, based on the absorbance of the starting material, occurred for GNP-protamine : RNA triconjugate, thereby indicating the interaction of all three components.

3.7. Analysis of the Conjugates by Gel Shift. In a parallel experiment to that shown above in Figure 6, the GNP, GNP-RNA, or GNP-protamine : RNA were analyzed by agarose

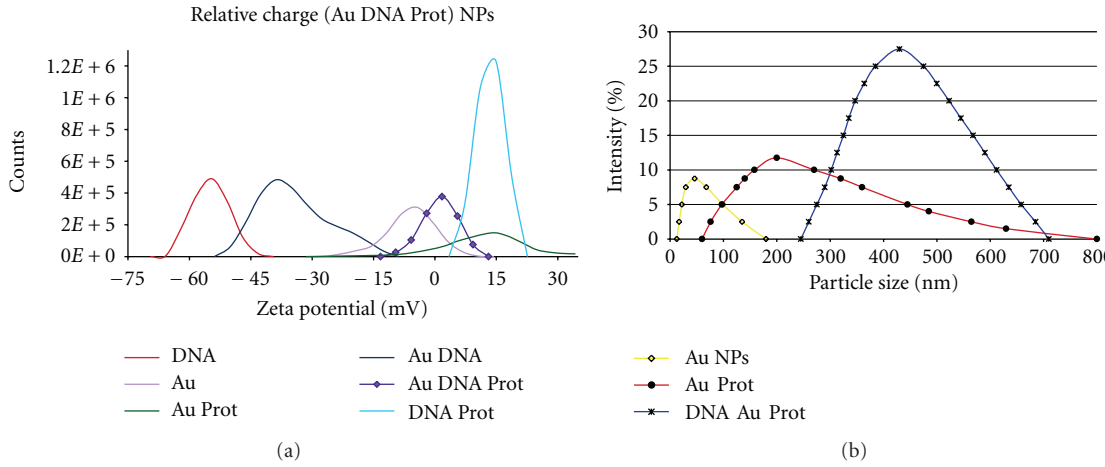

Figure 8: Evidence for bionanoconjugates made between GNPs, protamine, and DNA by DLLS analysis of (a) surface charge and (b) size distribution by intensity.

gel electrophoresis. These data are shown in Figure 7. A slight shift was observed upon interaction of RNA with GNP, and a more obvious shift occurred after the introduction of protamine, again suggesting the presence of the triconjugate species. Increased staining intensity in the well was observed previously for protamine : RNA nanoparticles [9].

3.8. Surface Charge and Size of the Conjugates. Zeta potential of the GNPs in the presence or absence of protamine and/or nucleic acid (DNA in this case) is shown in Figure 8(a). Potential of GNP alone was slightly less than zero. On the other hand, when protamine was added to either the GNPs or DNA, the zeta potential value increased to 12.5 mV and 13.4 mV, respectively, due to the positive charges on protamine. When all three were combined, the zeta potential value decreased to 1.20 mV, indicating a strong interaction.

Figure 8(b) shows the expected effect of conjugation on the particle's size. For the sample containing only the GNPs, the particle size is estimated to be approximately 38 nm. After complexing the GNP with protamine, as previously described, the particle size increases to approximately 200 nm. When the DNA is added, the sizes increases accordingly, to approximately 420 nm. This is further evidence that the conjugates are formed with all three components.

3.9. Spectral Shift upon Conjugate Formation. The GNP spectrum, shown in Figure 9, demonstrates the absorbance peak at approximately 520–530 nm, characteristic of particles in the low nanometer size range used here. The spectrum of the DNA displays the typical nucleic peak at 260 nm, which exhibits a greatly increased absorbance after interaction with protamine or protamine : gold. The mixture of DNA and protamine produced spectra that indicated strong interactions between the two molecules. The protamine : nucleic acid interaction is incompletely understood, and although the zeta potential data above suggest that the interaction is electrostatic in nature, the data also reveal an enhancement of absorbance for the DNA peak at 260 nm, thus implicating

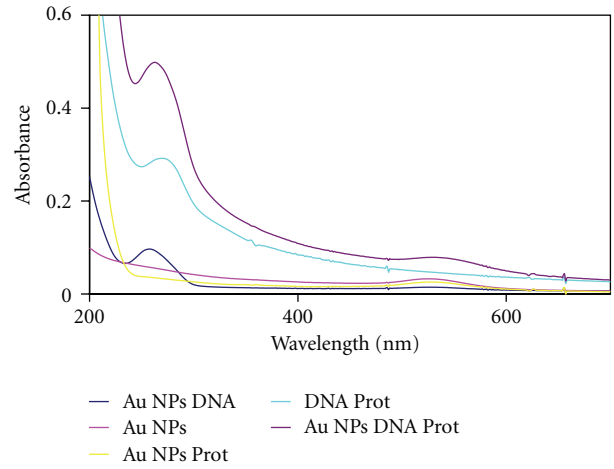

Figure 9: Evidence for bionanoconjugates made between GNPs, protamine, and DNA by UV/Vis.

some structural rearrangement. RNA : protamine and GNP-protamine : RNA were amplified and shifted further (data not shown).

3.10. Biocompatibility of Triconjugates. As previously reported, gold nanoparticles are taken up by HeLa cells [13]. The absorbance readings shown below, in Figure 10, confirm that the HeLa pLuc-705 cells retained their metabolic activity after the 24-hour incubation time with gold nanoparticles only, and with conjugates of gold nanoparticles, protamine, and RNA. This confirms that the conjugates are not cytotoxic, and this is a safe system for SSO delivery.

4. Conclusions

The high-low screening design experiment demonstrated that protamine, ethanol, and magnesium yielded the greatest influence on SSO bioactivity. The data, therefore, suggest

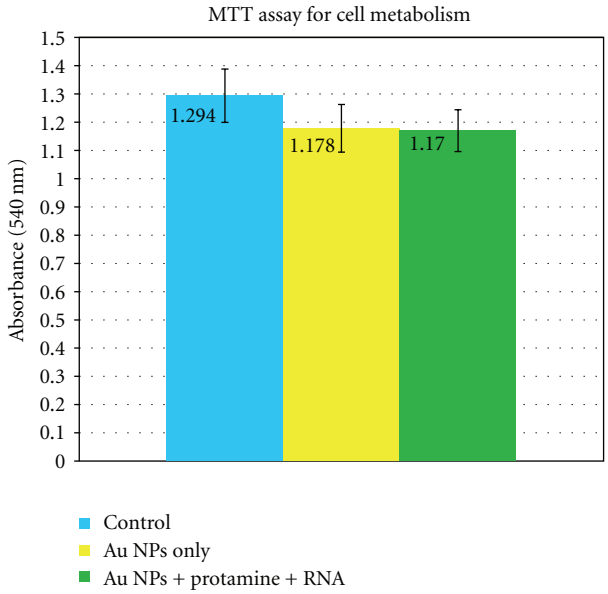

Figure 10: Evidence of continued cellular metabolic activity after incubation with triconjugates.

that creating conjugates in which protamine could affix RNA onto the GNP might be warranted. The data contraindicates condensing and/or precipitating protamine : RNA nanoparticles as a result of varying the ionicity and hydrophobicity [6, 15]. Modeling of protamine, based on dark field microscopy [16] and earlier studies [17, 18], suggests that protamine condenses DNA into nanoparticles, which here we hypothesize (Figure 3) can be extended to entrap RNA onto the protamine-GNP conjugates.

To understand the triconjugate of RNA, GNPs, and protamine by UV/Vis spectroscopy, it is first necessary to determine the spectrum of each component individually. Changes in the wavelength or peak amplitude after addition of a second and third component suggests their interaction whereas unchanged peaks indicate their dispersion. In erefFigurefig4, the individual peaks for nucleic acid, GNPs, and protamine are illustrated, which are compared subsequently to solutions of these components in combination, seen in Figure 9. Again, shifts in the amplitude or absorbance maximum in the RNA or gold UV/Vis spectra suggest triconjugate interaction between the three species: protamine, RNA, and GNP.

NanoDrop UV/Vis has nanorange sensitivity like its fluorescence counterparts, the PicoGreen and Hoechst assays, yet is not dependent on a double-stranded nucleic acid fordye binding. Although UV/Vis data suggests interaction between the triconjugates, at present it is uncertain that these fluorescent dyes can confirm this putative interaction; however, we did note a slight gel shift after staining with the fluorescent dye ethidium and consider this observation to be consistent with interactions between GNP, protamine, and RNA.

The NanoDrop instrument can rapidly quantify nucleic acids, protamine, or gold conjugates in UV or visible mode in the nanomolar or nanogram per microliter range, although its utility in evaluating breakdown products or biomaterial and nanomaterial compatibility with proteins and nucleic acids remains in question. For on-particle analysis, however, DLLS and NanoDrop UV/Vis observations are critical for optimizing preparation and delivery.

There is substantial interest in the formulation and delivery of therapeutic nucleic acids as nanoparticles for delivery in humans [1]. Here, methods amenable for the analysis of macromolecular RNA and DNA, and those present as nanoparticles, have been compared. DLLS, fluorimetric, UV/Vis spectroscopic, and electrophoretic methods are all capable of nanorange detection. Accordingly, these assays are likely to have mainstay applications in the clinical progression of delivering nucleic acids into patients in the form of nanoparticles.

Acknowledgments

The authors would like to thank their collaborators, particularly Drs. Lifeng Dong, Michael Craig, Richard Garrad, and Garry Glaspell for their generous support, encouragement, and helpful discussions. R. K. DeLong, K. Ghosh, and A. Wanekaya are supported by an AREA/R15 Grant from the National Cancer Institute titled, "Anti-Cancer RNA Nanoconjugates" (1 R15 CA139390-01).

References

[1] M. Davis, J. Zuckerman, C. Choi et al., "Evidence of RNAi in humans from systemically administered siRNA via targeted nanoparticles," *Nature*, vol. 464, no. 7291, pp. 1067–1070, 2010.

[2] J. A. Bauman, S. D. Li, A. Yang, L. Huang, and R. Kole, "Anti-tumor activity of splice-switching oligonucleotides," *Nucleic Acids Research*, vol. 38, no. 22, pp. 8348–8356, 2010.

[3] M. A. Garcia-Blanco, "Alternative splicing: therapeutic target and tool," *Progress in Molecular and Subcellular Biology*, vol. 44, pp. 47–64, 2006.

[4] E. Collins, J. C. Birchall, J. L. Williams, and M. Gumbleton, "Nuclear localisation and pDNA condensation in non-viral gene delivery," *Journal of Gene Medicine*, vol. 9, no. 4, pp. 265–274, 2007.

[5] L. Benimetskaya, N. Guzzo-Pernell, S. T. Liu, J. C. Lai, P. Miller, and C. A. Stein, "Protamine-fragment peptides fused to an SV40 nuclear localization signal deliver oligonucleotides that produce antisense effects in prostate and bladder carcinoma cells," *Bioconjugate Chemistry*, vol. 13, no. 2, pp. 177–187, 2002.

[6] B. Scheel, R. Teufel, J. Probst et al., "Toll-like receptor-dependent activation of several human blood cell types by protamine-condensed mRNA," *European Journal of Immunology*, vol. 35, no. 5, pp. 1557–1566, 2005.

[7] L. Li, S. A. Pabit, S. P. Meisburger, and L. Pollack, "Double-stranded RNA resists condensation," *Physical Review Letters*, vol. 106, no. 10, article 108101, 2011.

[8] F. Reynolds, R. Weissleder, and L. Josephson, "Protamine as an efficient membrane-translocating peptide," *Bioconjugate Chemistry*, vol. 16, no. 5, pp. 1240–1245, 2005.

[9] R. K. DeLong, U. Akhtar, M. Sallee et al., "Characterization and performance of nucleic acid nanoparticles combined with protamine and gold," *Biomaterials*, vol. 30, no. 32, pp. 6451–6459, 2009.

[10] O. Nakagawa, X. Ming, L. Huang, and R. L. Juliano, "Targeted intracellular delivery of antisense oligonucleotides via conjugation with small-molecule ligands," *Journal of the American Chemical Society*, vol. 132, no. 26, pp. 8848–8849, 2010.

[11] S. Resina, R. Kole, A. Travo, B. Lebleu, and A. R. Thierry, "Switching on transgene expression by correcting aberrant splicing using multi-targeting steric-blocking oligonucleotides," *Journal of Gene Medicine*, vol. 9, no. 6, pp. 498–510, 2007.

[12] S. H. Kang, M. J. Cho, and R. Kole, "Up-regulation of luciferase gene expression with antisense oligonucleotides: implications and applications in functional assay development," *Biochemistry*, vol. 37, no. 18, pp. 6235–6239, 1998.

[13] B. D. Chithrani, A. A. Ghazani, and W. C. Chan, "Determining the size and shape dependence of gold nanoparticle uptake into mammalian cells," *Nano Letters*, vol. 6, no. 4, pp. 662–668, 2006.

[14] R. R. Arvizo, O. R. Miranda, M. A. Thompson et al., "Effect of nanoparticle surface charge at the plasma membrane and beyond," *Nano Letters*, vol. 10, no. 7, pp. 2543–2548, 2010.

[15] Z. Reich, R. Ghirlando, and A. Minsky, "Secondary conformational polymorphism of nucleic acids as a possible functional link between cellular parameters and DNA packaging processes," *Biochemistry*, vol. 30, no. 31, pp. 7828–7836, 1991.

[16] F. P. Ottensmeyer, R. F. Whiting, and A. P. Korn, "Three dimensional structure of herring sperm protamine Y-I with the aid of dark field electron microscopy," *Proceedings of the National Academy of Sciences of the United States of America*, vol. 72, no. 12, pp. 4953–4955, 1975.

[17] Z. Lin, C. Wang, X. Feng, M. Liu, J. Li, and C. Bai, "The observation of the local ordering characteristics of spermidine-condensed DNA: atomic force microscopy and polarizing microscopy studies," *Nucleic Acids Research*, vol. 26, no. 13, pp. 3228–3234, 1998.

[18] L. R. Brewer, M. Corzett, and R. Balhorn, "Protamine-induced condensation and decondensation of the same DNA molecule," *Science*, vol. 286, no. 5437, pp. 120–123, 1999.

Hindawi Publishing Corporation
Journal of Nanotechnology
Volume 2012, Article ID 748909, 11 pages
doi:10.1155/2012/748909

Review Article

Micro- and Nano-Carrier Mediated Intra-Articular Drug Delivery Systems for the Treatment of Osteoarthritis

Zhiyue Zhang and Guihua Huang

School of Pharmaceutical Sciences, Shandong University, 44 West Wenhua Road, Jinan, Shandong 250012, China

Correspondence should be addressed to Guihua Huang, hgh2003@gmail.com

Received 11 March 2011; Accepted 24 April 2011

Academic Editor: Lifeng Dong

The objective of this paper is to provide readers with current developments of intra-articular drug delivery systems. In recent years, although the search for a clinically successful ideal carrier is ongoing, sustained-release systems, such as polymeric micro- and nanoparticles, liposomes, and hydrogels, are being extensively studied for intra-articular drug delivery purposes. The advantages associated with long-acting preparations include a longer effect of the drug in the action site and a reduced risk of infection due to numerous injections consequently. This paper discusses the recent developments in the field of intra-articular sustained-release delivery systems for the treatment of osteoarthritis.

1. Introduction

Arthritis is a degenerative joint disease common among elderly people that causes progressive joint degeneration leading to chronic pain and reduced quality of life [1–4]. Osteoarthritis (OA) and rheumatoid arthritis (RA), two main kinds of arthritis, are among the most important inflammatory diseases, afflicting 40 million people (15%) in the US alone in 1995 and expected to afflict 59.4 million (18.2%) by the year 2020 [5]. And osteoarthritis (OA) is the most prevalent musculoskeletal condition that causes joint pain. The incidence of OA increases with age, and approximately 100% of men and women at age 75–79 years shows some signs of OA [6]. Current available treatment is of symptoms, directed to relieve the pain and regain function [7], but outcomes are limited. For example, oral administration of NSAID tablets relieves inflammation and pain but causes gastrointestinal adverse effects; other effective treatments are surgeries, but they will cause the second damage to the joint as well as high cost.

Local drug delivery strategies may provide for the development of more successful OA treatment outcomes that have potential to reduce local joint inflammation and joint destruction, offer pain relief, and restore patient activity levels and joint function [8]. Intra-articular drug delivery is very useful for treating local disease flareups, synovitis, and pain in joints. The Food and Drug Administration (FDA) has approved intra-articular hyaluronic acid formulations for osteoarthritis of the knee [9]. The intra-articular (IA) route of administration has potential for targeting drug delivery to affected tissues in treating arthritis, thereby minimizing the attendant side effects of systemically administered drugs [10].

However, current preparations of intra-articular drug delivery often require frequent injections that have a high financial burden, impaction to patient's quality of life, rapid degradation and clearance of injected pharmacologic agents, and also increase the risk of complications [11]. Micro- and nanocarrier-mediated drug delivery systems, including polymeric particles, liposome, and hydrogel, are well-established as methods for sustained release in intra-articular applications. These systems could prolong drug retention time, reduce the clearance of drug into joint cavity, and increase patient compliance as well as therapeutic effect of pharmaceutical agents. This process guaranteed a longer effect of the drug in the action site and consequently, a reduced risk of infection due to numerous injections [12]. Sustained therapeutic drug concentrations can also be achieved with intra-articular slow-release drug delivery

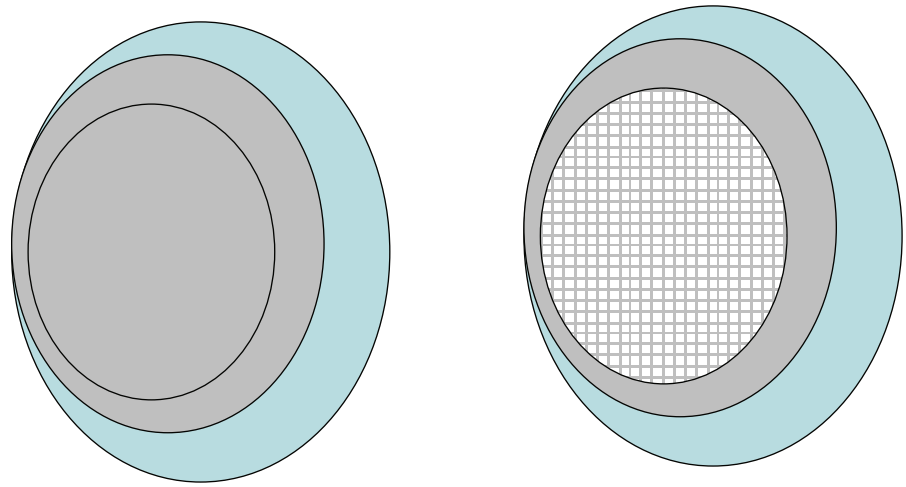

Figure 1: Schematic representation of a microsphere and a microcapsule. In microspheres, the whole particle consists of a continuous polymer network. Microcapsules present a core-shell structure with a liquid core surrounded by a polymer shell.

device, rather than repeated injections. It has been shown that sustained intra-articular drug concentration can be realized through coupling the desired drug to liposomes, microparticles, or hydrogels. The purpose of this paper is to summarize the current state of intra-articular long-acting injection preparations applied to the treatment of osteoarthritis. The main goal in the future is to increase the residence time of the drug in the joint as well as improve its diffusion within the target tissue [13].

2. Micro- and Nano-Carrier Mediated Drug Delivery Systems for IA Formulations

2.1. Polymeric Particles. Biodegradable particles have proven to be very useful drug delivery systems and provide prolonged drug release and lasting delivery because of sustained release of the microencapsulated material. Due to their advantage of being biodegradable and biocompatible, polymeric micro- and nanocarriers in formulations of therapeutic drug delivery systems have gained widespread application. The drug is dispersed or encapsulated in a microparticle matrix, and, depending on the preparation method, microspheres or microcapsules can be obtained (Figure 1). Among the microparticulate systems, microspheres have a special importance since it is possible to target drugs and provide controlled release [14]. Meanwhile, micro- and nanoparticulate drug delivery systems have been studied extensively using various kinds of biodegradable polymers during the past two decades [15].

Commonly used materials and their derivatives for preparing micro- and nanoparticles bifurcate natural materials including chitosan, gelatin, alginate, and other materials and synthetic materials, such as PLA(polylactide), PLGA(poly(lactic-co-glycolic acid)), PCL(polycaprolactone), and other synthetic ones [16]. Prolonged time of drug release and decreased toxicity and stimulation can be achieved via intra-articular controlled release system of polymeric particles [17].

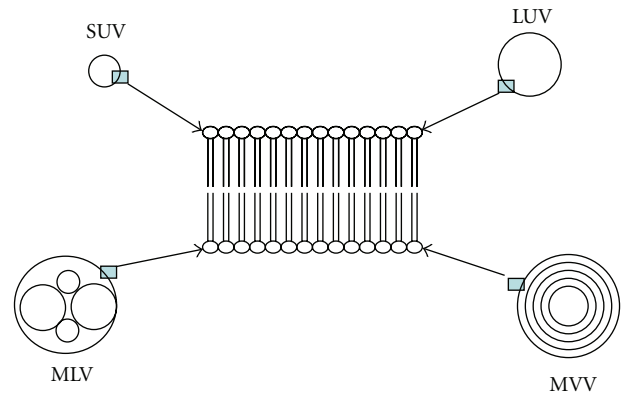

Figure 2: The classification of liposomes. SUV: small unilamellar vesicles; LUV: large unilamellar vesicles; MLV: large multilamellar vesicles; MVV: multivesicular vesicles.

The most commonly used methods of microencapsulation encompass solvent extraction or evaporation, coacervation, and spray drying [18]. The composition and preparation methods of microcapsules were found to be closely related to drug release and microcapsule degradation. Meanwhile, the release profile was monophasic or biphasic depending on the formulation [19].

2.2. Liposomes. Liposomes are spherical vesicles or cavities made up of phospholipids that usually, but not by definition, contain a core of aqueous solution and have been proposed as efficient carriers for controlled drug delivery (Figure 2). They are able to entrap hydrophilic drugs in the large aqueous interior and lipophilic drugs inserted in the lipid bilayer [20]. Moreover, hydrophobic drugs such as dexamethasone are incorporated in the bilayer structure of liposomes, whereas hydrophilic drugs such as diclofenac are encapsulated in the internal aqueous chamber [21]. Derived from naturally occurring, biodegradable and nontoxic lipids, liposomes are

good candidates for local targeting of therapeutic agents to the site of interest, while reducing systemic toxicity. And the residence of encapsulated drugs within the knee joint was greatly prolonged. For example, liposomal iohexol declined biexponentially with a terminal elimination half-life of 134 hours compared with free iohexol which was undetectable 3 hours after injection [20, 22]. Liposomes are good candidates although a liposomal corticosteroid formulation containing dexamethasone-21-palmitate (Lipotalon) available in Germany is the only intra-articular liposomal product used in human patients [20].

Conventional methods of liposome manufacture can be said to involve four basic stages: drying down of lipids from organic solvents, dispersion of the lipids in aqueous media, purification of the resultant liposomes, and analysis of the final product [23] (Figure 3). In order to optimize the liposomal formulation for local use, liposomes with appropriate size, surface properties, and composition should be selected with respect to the site of administration, the disease, and the drug used. In a word, a balance is of importance between the stability of the liposomes and their ability to deliver drugs [24].

2.3. Hydrogels. Since the pioneering work of Wichterle and Lim in 1960 on crosslinked HEMA hydrogels, hydrogels have been of great interest to biomaterial scientists for many years because of their hydrophilic character and potential to be biocompatible [25]. Hydrogels are hydrophilic polymer networks which may absorb from 10–20% (an arbitrary lower limit) up to thousands of times their dry weight in water and may be chemically stable or degrade and eventually disintegrate and dissolve. They are called "reversible" or "physical" gels when the networks are held together by molecular entanglements and/or secondary forces including ionic, H-bonding, or hydrophobic forces [26]. Both natural and synthetic materials have been used to form scaffolds. Naturally derived materials often have desirable biological properties and also possess limited mechanical strength or fast degradation profiles that may not be suitable for clinical applications. Synthetic polymers, although not as bioactive as natural scaffolds, can provide the necessary properties to produce scaffolds with desired controllable physical and chemical characteristics. Many kinds of synthetic hydrogel polymers, such as methyl methacrylate, poly(2-hydroxyethyl)methacrylate (polyHEMA) hydrogel, poly(vinyl alcohol) (PVA) hydrogel, and are developed to repair or replace the damaged articular cartilage [27]. Hydrogels are required to have acceptable biodegradability and biomedical purposes. Figure 4 revealed a great variety of crossing approaches developed to prepare desired hydrogels.

Not only does sustained drug release reduce administration times and undesired side effects, but also it improves the patients' compliance and comfort significantly. When applied in a drug delivery system, the injectable drug/polymer formulation can be free of any organic solvent in the drug-loading process (an organic solvent might denature labile therapeutic agents like proteins), and the rate of drug release is easily adjusted via altering the material

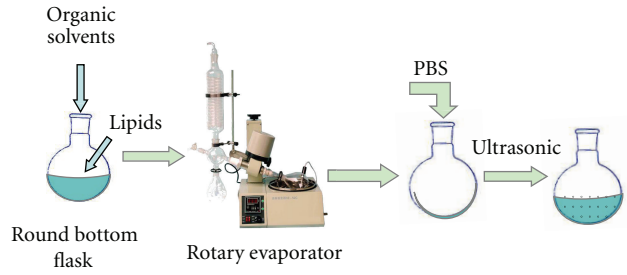

Figure 3: Conventional liposome preparation method: film dispersion method.

properties. These hydrogel formulations are useful for parenteral and topical injection for a site-specific action [28]. Their affinity to absorb water is attributed to the presence of hydrophilic groups such as –OH, –CONH–, $–CONH_2–$, and $–SO_3H$ in polymers forming hydrogel structures [29]. In contrast, the polymeric networks of hydrophobic characteristics (e.g., poly(lactic acid) (PLA) or poly(lactide-co-glycolide) (PLGA)) are limiting water-absorbing capacities (<5–10%), and the polymer is thus hydrated to different degrees (sometimes more than 90% wt.) depending on the nature of the aqueous environment and polymer composition due to the contribution of these groups and domains in the network [30].

3. NSAIDs Delivery Systems

Nonsteroidal anti-inflammatory drugs (NSAIDs) are a series of drugs having anti-inflammatory, analgesic, and antipyretic effects which alleviate pain by counteracting the cyclooxygenase (COX) enzyme which synthesizes prostaglandins, creating inflammation [31]. In whole, the NSAIDs prevent the prostaglandins from ever being synthesized, reducing or eliminating the pain [32].

NSAIDs can reduce short-term pain in osteoarthritis of the knee slightly better than placebo, but the current analysis does not support long-term use of NSAIDs for this condition. As serious adverse effects are associated with oral NSAIDs, only limited use can be recommended [33]. Cyclo-oxygenase-2 (COX 2) inhibitors are selective types of nonsteroidal anti-inflammatory drugs (NSAIDs) developed for the treatment of acute inflammation in joints. Although evidence shows that COX 2 inhibitors are as effective as traditional NSAIDs in relieving pain [34], they decrease arthritis without the gastrointestinal side effects associated with traditional NSAIDs.

Intra-articular administration of NSAIDs could be an alternative to delivery administration which avoids their devastating effects. However, the short synovial half-life of NSAIDs would require frequent injections to maintain therapeutic intra-articular levels. For this reason, sustained drug delivery devices are needed to offer an excellent alternative to multiple intra-articular injections [35]. The working hypothesis was that increased NSAIDs efficacy and alleviation of adverse effects can be achieved by local administration of a new slow-release NSAID-carrier formulation.

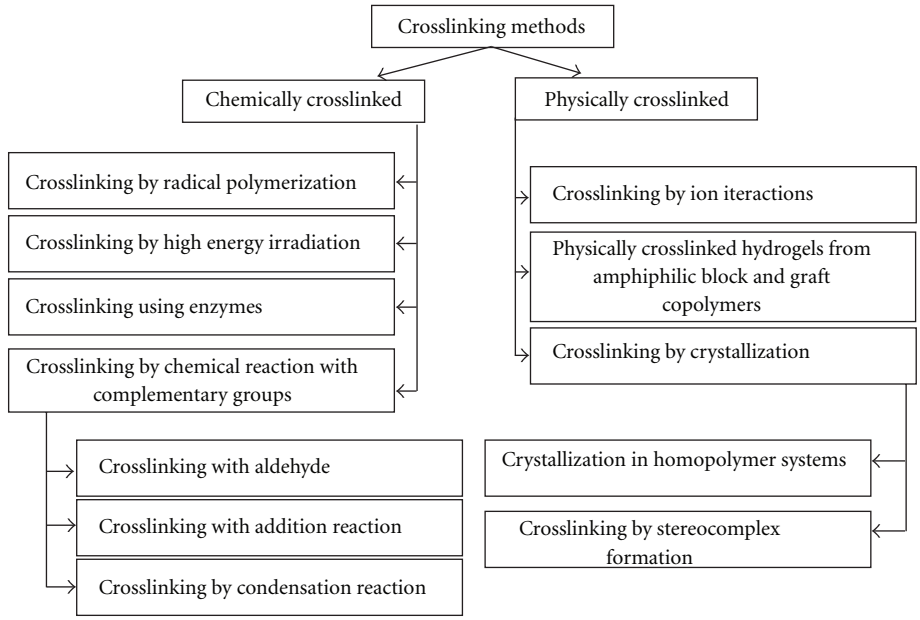

Figure 4: Novel crosslinking methods used in hydrogels [30].

3.1. Polymer Particles. Polymer particles loaded with an NSAID (such as diclofenac), destined for intra-articular administration, have been developed using different polymers such as chitosan, PLA, PLGA, and Poli δ-valerolactona (PV) [36]. In the present study, controlled release parenteral formulations of diclofenac sodium were prepared for intra-articular administration [15].

Diclofenac is a nonsteroidal anti-inflammatory drug (NSAID) advocated for use in painful and inflammatory rheumatic and certain nonrheumatic conditions. It is available in a number of administration forms which can be given orally, rectally, or intramuscularly. Conveniently, dosage adjustments are not required in the elderly or in those patients with renal or hepatic impairment. The drug has a relatively short elimination half-life, which limits the potential for drug accumulation. The efficacy of diclofenac in numerous clinical trials is equivalent to that of the many newer and established NSAIDs with which it has been compared [37]. Available data suggest that, in patients with osteoarthritis, diclofenac sodium is comparable in efficacy and tolerability with naproxen, ibuprofen, sulindac, and diflunisal. As oral diclofenac is generally given in 3 divided daily doses, it may be at a disadvantage relative to less frequent administration with naproxen, diflunisal, and sulindac in osteoarthritis, although there is some evidence of diclofenac's efficacy when administered twice daily or once daily as a slow-release tablet [38].

Saravanan et al. [39] have previously reported on the targeting of diclofenac sodium in joint inflammation using gelatin magnetic microspheres which focuses on the formulation of gelatin microspheres for intra-articular administration to overcome complications in the administration of magnetic microspheres and achieve higher targeting efficiency. Drug-loaded microspheres were prepared by the emulsification/crosslinking method, characterized by size distribution, drug loading, scanning electron microscopy (SEM), Fourier transform infrared (FT-IR) spectroscopy, differential scanning calorimetry (DSC), X-ray diffraction (XRD), gas chromatography, and in vitro release studies along with targeting efficiency of microspheres that was studied in vivo in rabbits. The microspheres showed drug loading of 9.8, 18.3, and 26.7% w/w with an average size range of 37–46 μm depending upon the drug-polymer ratio. They were spherical in nature and free from surface drug as evidenced by the SEM photographs and the absence of drug-polymer interaction, and the amorphous nature of entrapped drug was revealed by FT-IR, DSC, and XRD. Gas chromatography confirms the absence of residual glutaraldehyde. The formulated microspheres could prolong the drug release up to 30 days in vitro. About 81.2 and 43.7% of administered drug in the microspheres were recovered from the target joint after 1 and 7 days of post intra-articular injection, respectively, revealing good targeting efficiency. The microspheres prepared were able to prolong the drug release over 24–30 days, and the application of sonication during in vitro release study has slightly increased the release rate. After intra-articular administration of microspheres, 77.7% of injected dose was recovered at the target site which revealed good targeting efficiency [40].

H. P. Thakkar and R. R. Murthy have compared the characteristics of the microspheres of chitosan prepared using two different crosslinking agents: formaldehyde and glutaraldehyde crosslinking and simple heat treatment. Chitosan microspheres were prepared by emulsification crosslinking method and characterized for entrapment efficiency, particle size, in vitro drug release, and surface morphology studied by scanning electron microscopy (SEM). The entrapment efficiency of the glutaraldehyde

and formaldehyde crosslinked microspheres was significantly higher ($P < .05$) than the heat-crosslinked ones which showed the fastest release in vitro drug release [41]. Meanwhile, in vitro drug release studies indicated that the microspheres crosslinked using glutaraldehyde showed slower release rate than those crosslinked with formaldehyde.

3.2. Liposomes. In the case of arthritic diseases, it has been reported that the intra-articular administration of anti-inflammatory drugs encapsulated in liposomes shows prolonged residence in the joint and reduction of inflammation [42, 43]. For example, liposome-entrapped methotrexate injected intra-articularly was 10-fold more potent than the free drug in suppressing the development of arthritis. Liposomes are used to encapsulate both hydrophilic and hydrophobic small molecules as well as macromolecules such as proteins and genes.

Free lactoferrin disappeared rapidly from the injected joint, with two-thirds lost by 2 h and only 2% remaining at 24 h. However, entrapment in positively charged liposomes markedly enhanced retention time, with close to 50% still present after 6 h and 15% at 24 h. Surprisingly, lactoferrin entrapped in pH-sensitive negatively charged liposomes was lost from the joint even more rapidly than the free protein, being virtually undetectable by 24 h [44].

To increase NSAID efficacy and alleviate the adverse effects, Inbar Elron-Gross prepared a new slow-release NSAID-carrier formulation by local administration. Diclofenac was the test NSAID, and collagomers—novel vesicular-shaped microparticles based on collagen-lipid conjugates—were the carriers. Collagomers were stable in simulated synovial fluid and showed high-efficiency drug encapsulation (85%) and slow drug release (τ 1/2 = 11 days) as well as high affinity to target cells (Kd = 2.6 nM collagen) [45].

4. Glucocorticoids Delivery Systems

Glucocorticoids are potent drugs that have a multitude of pharmacological actions both at genomic and nongenomic levels. It was suggested that intra-articular steroids often ameliorate acute exacerbations of knee osteoarthritis associated with significant effusions, symptomatic involvement of inter joint and other nonweight-bearing articulations, synovial cysts, and lumbar facet arthropathy. Judicious use of intra-articular injections seldom produces significant adverse effects [46].

Many of the diseases in which glucocorticoids are routinely administered are featured by angiogenesis and enhanced capillary permeability, permitting targeted delivery using long-circulating drug delivery systems. By encapsulation of glucocorticoids in long-circulating liposomes, drug levels at the site of the pathology are markedly higher, increasing and prolonging therapeutic efficacy in models of osteoarthritis, multiple sclerosis, and cancer [47].

Glucocorticoids (GCs) provide one of the most effective treatments for osteoarthritis; however, their long-term use is marred by undesired side effects. Increased understanding of the mechanisms of glucocorticoid action enables the development of novel drugs, such as SEGRAs or liposomal glucocorticoids, to improve their benefit/risk ratio [48].

A variety of methods are currently used for intra-articular glucocorticoids (GCs) injection to the osteoarthritis, each with the goal of minimizing the potential for tissue damage. However, clinical tests have shown that intra-articular glucocorticoids are not devoid of side effects despite their net efficacy. For example, because of their crystalline structure, a condition referred to as crystal-induced arthritis was described in 10% of the patients receiving an intra-articular injection. Moreover, due to lymph drainage or macrophage uptake, the residence time of corticosteroid molecules in the joint is very short and frequent intra-articular injections are required in order to obtain a sustained clinical result. The complications of such frequent injections in terms of infections or joint instability remain severe although rare. All these aspects emphasize the need to develop drug delivery systems allowing the sustained release of the active substance in order to reduce the frequency of the intra-articular injections together with the related potential deleterious effects [11].

4.1. Polymer Particles. Glucocorticoids are widely used for the treatment of a number of diseases of nonendocrine origin. Owing to their strong anti-inflammatory actions, they have been used for rheumatism, asthma, inflammatory bowel diseases, as well as for the treatment of dermatitis and allergies [49]. The prime obstacle for conventional administration is the dose-dependent systemic side effects. Selective delivery of drugs to specific target sites would reduce the necessary dose of a given drug while still achieving an effective local concentration. As a result, the therapeutic efficacy would be increased. The use of particulate drug carriers is a possible strategy to achieve site-specific drug delivery and to decrease undesirable interactions at other body sites. In recent years, polymer particles have emerged as one of the most promising controlled release dosage forms, and several micro- and nanoparticle-based products for parenteral use are commercially available (e.g., Enantone, Decapeptyl Depot, and Pravidel) [50].

Horisawa et al. developed DL-lactide/glycolide copolymer (PLGA) nanospheres incorporating a water-soluble corticosteroid (betamethasone sodium phosphate (BSP)) with prolonged anti-inflammatory action. BSP-loaded nanospheres were prepared by an emulsion solvent diffusion method in oil (caprylate and caprate triglyceride). The drug release rate from the nanospheres in PBS was controlled by the molecular weight and the lactic/glycolic acid (LA/GA) ratio of the polymers. Sustained drug release occurred for over three-week in vitro release study demonstrated, and the joint swelling decreased significantly by administering BSP-loaded nanospheres during a 21-day period after intra-articular challenge in the antigen-induced arthritic rabbit. The histologic safety of nanospheres administration to inflamed synovial tissue was confirmed. Meanwhile, prolonged local anti-inflammatory action in joint diseases without biologic damage can be provided by the PLGA particulate system [51].

In Butoescu's study, for the aim of locally treating inflammatory conditions such as arthritis, SPIONs and the corticosteroid dexamethasone acetate (DXM) are coencapsulated into PLGA microparticles. The microparticles in the joint with an external magnet can be maintained due to the magnetic properties conferred by the SPIONs. As superparamagnetic microparticles present the double advantage of internalization by the synoviocytes and a prolonged drug action due to magnetically increased microparticle residence time in the joint, DXM-containing ones seem to be promising drug delivery systems for the local treatment of arthropathies. The encapsulation process did not affect the magnetic properties of SPIONs or their oxidation state. Moreover, DXM and SPIONs were completely embedded into the microparticles, as demonstrated by the zeta potential [52, 53].

4.2. Liposomes. Dexamethasone is a potent anti-inflammatory and immunosuppressive glucocorticoid used for the treatment of inflammatory and autoimmune conditions such as osteoarthritis, edema, and multiple myeloma, as an adjunct with chemotherapy, and for nasal and eye allergies. The encapsulation of dexamethasone in carrier systems such as liposomes and microspheres can diminish the adverse effects and reduce the total amount of drug required. Liposomal and microsphere dexamethasone formulations have been investigated for hypersensitivity pneumonitis [21].

There are a number of literature reports concerning liposome formulations of dexamethasone and other glucocorticoids [54]. However, the physicochemical properties of these liposomes vary considerably. U. Bhardwaj and D. J. Burgess investigated the effects of process including sonication and extrusion, and formulation parameters such as lipid type, incorporation of cholesterol and dexamethasone on the physicochemical properties and thermotropic behavior of dexamethasone-loaded liposomes. The similar mean diameter of all the nonextruded liposomes indicated that particle size appeared to be dependent on the initial film thickness, since the concentration and volume of the lipid solutions were kept constant for all liposome preparations. Sonication- and extrusion-induced interdigitation leads to a decrease in space between the acyl chains and the higher loss of dexamethasone from the extruded DPPC liposomes. Cholesterol incorporation has been reported to increase membrane stability, decrease permeability, and increase encapsulation of hydrophilic drugs. However, both cholesterol and dexamethasone have a similar hydrophobic steroidal molecular structure and compete for the same sites in the liposome membrane. Cholesterol is more lipophilic ($\log p \sim 7.17$) than dexamethasone ($\log p \sim 1.74$) and therefore should be preferentially incorporated/partitioned in the liposome membranes, leading to a decrease in dexamethasone encapsulation. The rank order of dexamethasone release from the nonextruded liposomes was similar to that from the extruded liposomes at both 37°C and 25°C. Release profiles from DMPC and DPPC were similar at 37°C. However, for nonextruded DPPC liposomes, heterogeneous distribution of dexamethasone reduced the main transition onset temperature even lower than that for the extruded liposomes. Nevertheless, dexamethasone release from nonextruded liposomes was slower than that from extruded liposomes at both 37 and 25°C. Therefore, it would appear that the rate-controlling step for release of dexamethasone (to bulk) is diffusion across the multilamellar structure of the nonextruded liposomes [21].

Conventional chronic and acute treatments for osteoarthritis (OA) are by oral NSAIDs (such as diclofenac) and intra-articular injected glucocorticosteroids (such as dexamethasone) [55]. In free form, diclofenac and dexamethasone generate severe adverse effects with risks of toxicity; local injections of liposomal formulations for diclofenac and dexamethasone (each alone and their combination) were investigated to reduce these drawbacks. Employing RIA and immunoblot assay techniques, it was verified that the encapsulated drugs retained their biological activities: inhibitions of cyclooxygenases enzyme activity (diclofenac) and of cyclooxygenases protein expression (dexamethasone). A single intra-articular injection of each liposome-drug(s) formulation sufficed to reduce knee joint inflammation in OA rats over a timespan of 17 days using live-animal MRI.

5. Hyaluronic Acid Delivery Systems

Hyaluronic acid (HA), a polysaccharide consisting of a long chain of disaccharide, is a natural component of cartilage and plays a fundamental role in the maintenance of the tropic status of the cartilage. The various preparations of HA from different sources and molecular weights are widely used for more than 30 years in the treatment of knee OA to provide a further decrease in pain and stiffness and increase physical function [56]. The Western Ontario and McMaster Universities Osteoarthritis Index (WOMAC) has been used as a validated tool to assess the improvements in knee OA. The formulations include high molecular weight HA (HMW-HA) and low molecular weight HA (LMW-HA), but most studies demonstrated an improvement in all three variables from baseline, independent of the molecular weight HA used [57].

Intra-articular hyaluronic acid (HA) has been proposed as an alternative to steroids and nonsteroidal anti-inflammatory drugs (NSAIDs) for the intra-articular treatment of OA. In conclusion, this controlled comparative study suggests that intra-articular hyaluronic acid of MW 500–730 kDa (Hyalgan) exerts beneficial effects. As leading to a reduction of synovial inflammation and a slowing cartilage damage progression, comparative study confirms its validity as an alternative (not only symptomatological but also structural) to intra-articular steroids and NSAIDs in the treatment of OA of the knee [58].

Bannuru et al. compared the efficacy of intra-articular hyaluronic acid with corticosteroids for knee osteoarthritis (OA) and found that intra-articular corticosteroids appear to be relatively more effective for pain than intra-articular hyaluronic acid from baseline to week 4. By week 4, the 2 approaches have equal efficacy. However, hyaluronic acid has greater efficacy beyond week 8. Understanding this trend is useful to clinicians when treating knee OA [59].

As Hyal clearance is extremely rapid and degradation quick in vivo by enzymatic or hydrolytic reactions, localisation of response is likely to be a problem, which takes place in biological environments [60].

5.1. Polymer Particles. Hyaluronic acid (HA) is a physiologic component of the synovial fluid and is reduced in OA joints. Therefore, due to its viscoelastic properties and protective effect on articular cartilage and soft tissue surfaces of joints, intra-articular injection of HA can restore the normal articular homoeostasis. These effects are evident when HA is properly administered into the articular space; therefore, the use of "image-guided" infiltration techniques is mandatory [61].

In the preliminary study, the HA/Col II microspheres have shown to provide favorable ECM characteristics, with appropriate mechanical strength, and exhibited a 3D inclination. By injecting an HA/Col II mixture solution through a pair of HCPDEs under the influence of a high electrostatic field, microspheres were readily prepared with good sphericity and narrow size distribution. The watery microspheres were about 500–600 μm in size and able to retain their nontoxicity upon treatments, such as gelation, crosslinking, and thermal treatment [62].

5.2. Hydrogels. Hydrogels are three-dimensional, hydrophilic, polymeric networks which are composed of homopolymers or copolymers and capable of imbibing large amounts of water or biological fluids. Due to the presence of chemical crosslinks (tie points, junctions) or physical crosslinks, such as entanglements or crystallites, they are insoluble but can swell in water [63].

A 50% crosslinked Hyal hydrogel (Hyal 50%) was synthesized in order to overcome the problem of rapid clearance of the polysaccharide hyaluronic acid (Hyal) in the treatment of osteoarthritis (OA). The 50% refers to the amount of COOH groups of the polysaccharide involved in the crosslinking reaction, that is, 50% of the total amount. We decided to make the polysaccharide water insoluble by crosslinking it in order to obtain a longer effect of Hyal in the action site (joint) and consequently to reduce the risk of infection due to numerous injections. The result of this reaction was the formation of a hydrogel.

Moreover, the local pharmacological treatment with hyaluronic acid has also been claimed to be a useful tool in OA treatment. Now, the Hyal 50% hydrogel treatment seems to improve chondrocytes density and matrix appearance. Without evidence of tissue reaction or inflammation in the rabbit OA model, hydrogel tends to produce a smoother and more regular articular surface for a long period of time (50 days).

6. Chondroitin Sulfate Delivery Systems

Chondroitin sulfate (CS) is a safe and tolerable therapeutic agent for the management of OA whose effects include benefits that are not achieved by current medicines and include chondroprotection and the prevention of joint space narrowing [64–66]. CS is effective for the treatment of OA, at least in part, and its therapeutic benefits occur through three main mechanisms [67]: (1) stimulation of extracellular matrix production by chondrocytes; (2) suppression of inflammatory mediators; (3) inhibition of cartilage degeneration. These in vitro findings motivate the consideration of CS for intra-articular therapeutic injections for the treatment of painful joint degenerative diseases and as a potential prophylactic against the progression of cartilage degeneration.

There has been growing interests in potential chondroprotective agent chondroitin sulfate (CS), a kind of natural element that forms the cartilage extracellular matrix [68]. From the analysis, chondroitin is found to be effective in improving the visual analog scale pain, mobility, and responding status of OA patients [69]. The safety of CS is excellent. However, bioavailability of CS is only in the region of 10–15%. CS was used widely to treat OA via oral administration with mixed results [70, 71]. The biological effects of sulfated glycosaminoglycans have been widely studied for their potential therapeutic benefits.

The anti-inflammatory and antiapoptotic effects of chondroitin sulfate (CS) are increasingly used to treat osteoarthritis [72]. Furthermore, several studies have described the benefits of chondroitin sulfate in applications for cartilage tissue engineering. The therapeutic effects of glucosamine and chondroitin sulfate in OA have been studied for 20 years, and their symptom relieving efficacies were recently analyzed by high-quality meta-analysis [73].

6.1. Liposomes. Chondroitin sulphate is a sulphated GAG composed of a long unbranched polysaccharide chain with a repeating disaccharide structure of N-acetylgalactosamine and glucuronic acid. The in vitro studies demonstrated that CS has both anabolic effects on cartilage metabolism and anticatabolic properties [74]. Several studies have shown clinical benefits of CS administration in patients with OA [75–77]. Moreover, in the case of arthritic diseases, it has been reported that the intra-articular administration of anti-inflammatory drugs encapsulated in liposomes shows prolonged residence in the joint and reduction of inflammation.

Liposomes have been proposed as a means to target intra-articularly injected anti-inflammatory agents to phagocytic cells in inflamed synovial joints [78]. Liposomes prepared from naturally occurring biodegradable and nontoxic lipids are good candidates for local delivery of therapeutic agents. Treatment of arthritis by intra-articular administration of anti-inflammatory drugs encapsulated in liposomes prolongs the residence time of the drug in the joint [79]. In order to use liposome-entrapped chondroitin sulphate in the local treatment of inflammatory disorders, Trif et al. [43] studied ultrastructural characterization of liposomes-entrapped chondroitin sulphate and proved their in vitro biocompatibility in a human dermal fibroblast culture system. Results indicated that appreciable cytotoxic effects were not induced by chondroitin sulphate, empty liposomes, and liposome-chondroitin sulphate systems, and cells maintain normal morphology when compared to control fibroblasts.

6.2. Hydrogels. Hydrogels have been used extensively in the development of the "SMART" drug delivery systems ("SMART" drug delivery system (SDDS) is the multitargeted, pH responsive, stimuli-sensitive delivery systems, which are capable of self-regulation, integrated sensing, monitoring, and remote activation). A hydrogel is a network of hydrophilic polymers that can swell in water and hold a large amount of water while maintaining the structure. A three-dimensional network is formed by crosslinking polymer chains which can be provided by covalent bonds, hydrogen bonding, van der Waals interactions, or physical entanglements [80].

Specifically, neutral poly(ethylene glycol) (PEG) hydrogels were employed where negatively charged chondroitin sulfate (ChS), one of the main extracellular matrix components of cartilage, was systematically incorporated into the PEG network at 0%, 20%, or 40% to control the fixed charge density [81]. J. H. Hui [68] selected five types of hydrogel carriers (a-CD-EG 4400, a-CD-EG 8400, a-CD-EG 13300, a-CD-PEG 20000, and a-CD-PEG 35000). According to the biocompatibility studies, they found that no sign of redness or swelling around the knee was observed on days 3, 7, and 21 after injection before the rabbits were killed with 0.5 mL of the three kinds of hydrogel or normal saline in the knee joints. Combining the results from the in vitro and in vivo studies, a-CD-EG4400 was chosen as the carrier of CS in the treatment of joint defect in rabbits due to its ability to remain viable for the longest period of time while slowly retaining and releasing CS. Intra-articular injection of CS (100 mg/mL) carried by a-CD-EG 4400 hydrogel was effective in postponing osteoarthritis in rabbits by improving both the biomechanical and histological properties of the knee joints.

7. Conclusions

The ability to deliver highly therapeutic agents to diseased sites specifically is crucial for effectively treating all human illnesses. Intra-articular drug delivery can be a good means of targeting drug to the large joints (knees and hips) and has been expected to gain prominence for several reasons, such as only a minimum amount of drug is required to exert the desired pharmacological activity. A key requirement for drug delivery is demonstration of an ability to provide for increased intra-articular drug concentrations and residence time following administration to the joint space, as well as decreased systemic exposure to the drug. Many factors that influence the efficacy of a drug delivery vehicle for promoting sustained intra-articular residence time have been presented by several reviews, including particle size, vehicle safety, hydrophobicity, and charge.

However, successful commercialisation of any drug delivery technique requires careful consideration of a number of parameters particularly in elderly patients, including efficiency, cost, potential for toxicity, retention inside the body, sustainability of drug concentrations, and drug elimination kinetics [82]. The delivery techniques being investigated currently are paid little attention to many of these criteria, and any future endeavours will need to address these deficiencies before these techniques can become clinically exploitable.

References

[1] E. C. Sayre, L. C. Li, J. A. Kopec et al., "The effect of disease site (knee, hip, hand, foot, lower back or neck) on employment reduction due to osteoarthritis," *Plos One*, vol. 5, no. 5, pp. 1–7, 2010.

[2] O. Sangha, "Epidemiology of rheumatic diseases," *Rheumatology*, vol. 39, no. 2, pp. 3–12, 2000.

[3] D. J. Hunter, J. J. McDougall, and F. J. Keefe, "The symptoms of osteoarthritis and the genesis of pain," *Medical Clinics of North America*, vol. 93, no. 1, pp. 83–100, 2009.

[4] M. Fransen, S. McConnell, G. Hernandez-Molina, and S. Reichenbach, "Does land-based exercise reduce pain and disability associated with hip osteoarthritis? A meta-analysis of randomized controlled trials," *Osteoarthritis and Cartilage*, vol. 18, no. 5, pp. 613–620, 2010.

[5] S. S. Bansal, A. Joshi, and A. K. Bansal, "New dosage formulations for targeted delivery of cyclo-oxygenase-2 inhibitors—focus on use in the elderly," *Drugs and Aging*, vol. 24, no. 6, pp. 441–451, 2007.

[6] R. C. Lawrence, C. G. Helmick, F. C. Arnett et al., "Estimates of the prevalence of arthritis and selected musculoskeletal disorders in the United States," *Arthritis and Rheumatism*, vol. 41, no. 5, pp. 778–799, 1998.

[7] I. Elron-Gross, Y. Glucksam, D. Melikhov, and R. Margalit, "Cyclooxygenase inhibition by diclofenac formulated in bioadhesive carriers," *Biochimica et Biophysica Acta—Biomembranes*, vol. 1778, no. 4, pp. 931–936, 2008.

[8] K. D. Allen, S. B. Adams, and L. A. Setton, "Evaluating intra-articular drug delivery for the treatment of osteoarthritis in a rat model," *Tissue Engineering Part B*, vol. 16, no. 1, pp. 81–92, 2010.

[9] G. Kogan, L. Šoltés, R. Stern, and P. Gemeiner, "Hyaluronic acid: a natural biopolymer with a broad range of biomedical and industrial applications," *Biotechnology Letters*, vol. 29, no. 1, pp. 17–25, 2007.

[10] S. H. R. Edwards, M. A. Cake, G. Spoelstra, and R. A. Read, "Biodistribution and clearance of intra-articular liposomes in a large animal model using a radiographic marker," *Journal of Liposome Research*, vol. 17, no. 3-4, pp. 249–261, 2007.

[11] P. M. Mountziaris, P. R. Kramer, and A. G. Mikos, "Emerging intra-articular drug delivery systems for the temporomandibular joint," *Methods*, vol. 47, no. 2, pp. 134–140, 2009.

[12] G. Leone, M. Fini, P. Torricelli, R. Giardino, and R. Barbucci, "An amidated carboxymethylcellulose hydrogel for cartilage regeneration," *Journal of Materials Science: Materials in Medicine*, vol. 19, no. 8, pp. 2873–2880, 2008.

[13] X. Chevalier, "Intraarticular treatments for osteoarthritis: new perspectives," *Current Drug Targets*, vol. 11, no. 5, pp. 546–560, 2010.

[14] M. Tunçay, S. Çaliş, H. S. Kaş, M. T. Ercan, I. Peksoy, and A. A. Hincal, "In vitro and in vivo evaluation of diclofenac sodium loaded album in microspheres," *Journal of Microencapsulation*, vol. 17, no. 2, pp. 145–155, 2000.

[15] M. Tunçay, S. Çaliş, H. S. Kaş, M. T. Ercan, I. Peksoy, and A. A. Hincal, "Diclofenac sodium incorporated PLGA (50:50) microspheres: formulation considerations and in vitro/in vivo evaluation," *International Journal of Pharmaceutics*, vol. 195, no. 1-2, pp. 179–188, 2000.

[16] Y. Shi and G. Huang, "Recent developments of biodegradable and biocompatible materials based micro/nanoparticles for delivering macromolecular therapeutics," *Critical Reviews in Therapeutic Drug Carrier Systems*, vol. 26, no. 1, pp. 29–84, 2009.

[17] N. K. Green, C. W. Herbert, S. J. Hale et al., "Extended plasma circulation time and decreased toxicity of polymer-coated adenovirus," *Gene Therapy*, vol. 11, no. 16, pp. 1256–1263, 2004.

[18] H. Tamber, P. Johansen, H. P. Merkle, and B. Gander, "Formulation aspects of biodegradable polymeric microspheres for antigen delivery," *Advanced Drug Delivery Reviews*, vol. 57, no. 3, pp. 357–376, 2005.

[19] J. W. McGinity and P. B. O'Donnell, "Preparation of microspheres by the solvent evaporation technique," *Advanced Drug Delivery Reviews*, vol. 28, no. 1, pp. 25–42, 1997.

[20] M. Trie, C. Guillen, D. M. Vaughan et al., "Liposomes as possible carriers for lactoferrin in the local treatment of inflammatory diseases," *Experimental Biology and Medicine*, vol. 226, no. 6, pp. 559–564, 2001.

[21] U. Bhardwaj and D. J. Burgess, "Physicochemical properties of extruded and non-extruded liposomes containing the hydrophobic drug dexamethasone," *International Journal of Pharmaceutics*, vol. 388, no. 1-2, pp. 181–189, 2010.

[22] H. M. Burt, A. Tsallas, S. Gilchrist, and L. S. Liang, "Intra-articular drug delivery systems: overcoming the shortcomings of joint disease therapy," *Expert Opinion on Drug Delivery*, vol. 6, no. 1, pp. 17–26, 2009.

[23] M. R. Mozafari, "Liposomes: an overview of manufacturing techniques," *Cellular and Molecular Biology Letters*, vol. 10, no. 4, pp. 711–719, 2005.

[24] M. R. Mozafari, "Liposomes: an overview of manufacturing techniques," *Cellular and Molecular Biology Letters*, vol. 10, no. 4, pp. 711–719, 2005.

[25] O. Wichterle and D. Lím, "Hydrophilic gels in biologic use," *Nature*, vol. 185, no. 4706, pp. 117–118, 1960.

[26] A. S. Hoffman, "Hydrogels for biomedical applications," *Advanced Drug Delivery Reviews*, vol. 54, no. 1, pp. 3–12, 2002.

[27] F. Li, G. Wu, J. Wang, and C. Wang, "Tribological properties of poly(vinyl alcohol) hydrogel in response to ceramic femoral component," *Iranian Polymer Journal*, vol. 18, no. 11, pp. 881–890, 2009.

[28] L. Yu and J. Ding, "Injectable hydrogels as unique biomedical materials," *Chemical Society Reviews*, vol. 37, no. 8, pp. 1473–1481, 2008.

[29] N. A. Peppas and A. R. Khare, "Preparation, structure and diffusional behavior of hydrogels in controlled release," *Advanced Drug Delivery Reviews*, vol. 11, no. 1-2, pp. 1–35, 1993.

[30] M. Hamidi, A. Azadi, and P. Rafiei, "Hydrogel nanoparticles in drug delivery," *Advanced Drug Delivery Reviews*, vol. 60, no. 15, pp. 1638–1649, 2008.

[31] C. P. Duffy, C. J. Elliott, R. A. O'Connor et al., "Enhancement of chemotherapeutic drug toxicity to human tumour cells in vitro by a subset of non-steroidal anti-inflammatory drugs (NSAIDS)," *European Journal of Cancer*, vol. 34, no. 8, pp. 1250–1259, 1998.

[32] H. Heli, A. Jabbari, S. Majdi, M. Mahjoub, A. A. Moosavi-Movahedi, and S. Sheibani, "Electrooxidation and determination of some non-steroidal anti-inflammatory drugs on nanoparticles of Ni-curcumin-complex-modified electrode," *Journal of Solid State Electrochemistry*, vol. 13, no. 12, pp. 1951–1958, 2009.

[33] J. M. Bjordal, A. E. Ljunggren, A. Klovning, and L. Slørdal, "Non-steroidal anti-inflammatory drugs, including cyclo-oxygenase-2 inhibitors, in osteoarthritic knee pain: meta-analysis of randomised placebo controlled trials," *British Medical Journal*, vol. 329, no. 7478, pp. 1317–1320, 2004.

[34] J. Hippisley-Cox and C. Coupland, "Risk of myocardial infarction in patients taking cyclo-oxygenase-2 inhibitors or conventional non-steroidal anti-inflammatory drugs: population based nested case-control analysis," *British Medical Journal*, vol. 330, no. 7504, pp. 1366–1369, 2005.

[35] A. Fernández-Carballido, R. Herrero-Vanrell, I. T. Molina-Martínez, and P. Pastoriza, "Biodegradable ibuprofen-loaded PLGA microspheres for intraarticular administration: effect of Labrafil addition on release in vitro," *International Journal of Pharmaceutics*, vol. 279, no. 1-2, pp. 33–41, 2004.

[36] S. Y. Lin, K. S. Chen, H. H. Teng, and M. J. Li, "In vitro degradation and dissolution behaviours of microspheres prepared by three low molecular weight polyesters," *Journal of Microencapsulation*, vol. 17, no. 5, pp. 577–586, 2000.

[37] P. A. Todd and E. M. Sorkin, "Diclofenac sodium. A reappraisal of its pharmacodynamic and pharmacokinetic properties, and therapeutic efficacy," *Drugs*, vol. 35, no. 3, pp. 244–285, 1988.

[38] R. N. Brogden, R. C. Heel, G. E. Pakes, and G. S. Avery, "Diclofenac sodium: a review of its pharmacological properties and therapeutic use in rheumatic diseases and pain of varying origin," *Drugs*, vol. 20, no. 1, pp. 24–48, 1980.

[39] M. Saravanan, K. Bhaskar, G. Maharajan, and K. S. Pillai, "Development of gelatin microspheres loaded with diclofenac sodium for intra-articular administration," *Journal of Drug Targeting*, vol. 19, no. 2, pp. 96–108, 2010.

[40] M. Saravanan, J. Anbu, G. Maharajan, and K. S. Pillai, "Targeted delivery of diclofenac sodium via gelatin magnetic microspheres formulated for intra-arterial administration," *Journal of Drug Targeting*, vol. 16, no. 5, pp. 366–378, 2008.

[41] H. P. Thakkar and R. R. Murthy, "Effect of cross-linking agent on the characteristics of celecoxib loaded chitosan microspheres," *Asian Journal of Pharmaceutics*, vol. 2, no. 4, pp. 246–251, 2008.

[42] S. Türker, S. Erdoğan, A. Y. Özer et al., "Scintigraphic imaging of radiolabelled drug delivery systems in rabbits with arthritis," *International Journal of Pharmaceutics*, vol. 296, no. 1-2, pp. 34–43, 2005.

[43] M. Trif, L. Moldovan, M. Moisei, O. Craciunescu, and O. Zarnescu, "Liposomes-entrapped chondroitin sulphate: ultrastructural characterization and in vitro biocompatibility," *Micron*, vol. 39, no. 7, pp. 1042–1045, 2008.

[44] G. S. Canto, S. L. Dalmora, and A. G. Oliveira, "Piroxicam encapsulated in liposomes: characterization and in vivo evaluation of topical anti-inflammatory effect," *Drug Development and Industrial Pharmacy*, vol. 25, no. 12, pp. 1235–1239, 1999.

[45] I. Elron-Gross, Y. Glucksam, I. E. Biton, and R. Margalit, "A novel Diclofenac-carrier for local treatment of osteoarthritis applying live-animal MRI," *Journal of Controlled Release*, vol. 135, no. 1, pp. 65–70, 2009.

[46] R. G. Gray and N. L. Gottlieb, "Intra-articular corticosteroids. An updated assessment," *Clinical Orthopaedics and Related Research*, vol. 177, pp. 235–263, 1983.

[47] R. M. Schiffelers, M. Banciu, J. M. Metselaar, and G. Storm, "Therapeutic application of long-circulating liposomal glucocorticoids in auto-immune diseases and cancer," *Journal of Liposome Research*, vol. 16, no. 3, pp. 185–194, 2006.

[48] C. M. Spies, J. W. Bijlsma, G. R. Burmester, and F. Buttgereit, "Pharmacology of glucocorticoids in rheumatoid arthritis," *Current Opinion in Pharmacology*, vol. 10, no. 3, pp. 302–307, 2010.

[49] W. Jubiz and A. W. Meikle, "Alterations of glucocorticoid actions by other drugs and disease states," *Drugs*, vol. 18, no. 2, pp. 113–121, 1979.

[50] A. Berthold, K. Cremer, and J. Kreuter, "Collagen microparticles: carriers for glucocorticosteroids," *European Journal of Pharmaceutics and Biopharmaceutics*, vol. 45, no. 1, pp. 23–29, 1998.

[51] E. Horisawa, T. Hirota, S. Kawazoe et al., "Prolonged anti-inflammatory action of DL-lactide/glycolide copolymer nanospheres containing betamethasone sodium phosphate for an intra-articular delivery system in antigen-induced arthritic rabbit," *Pharmaceutical Research*, vol. 19, no. 4, pp. 403–410, 2002.

[52] N. Butoescu, C. A. Seemayer, M. Foti, O. Jordan, and E. Doelker, "Dexamethasone-containing PLGA superparamagnetic microparticles as carriers for the local treatment of arthritis," *Biomaterials*, vol. 30, no. 9, pp. 1772–1780, 2009.

[53] N. Butoescu, O. Jordan, A. Petri-Fink, H. Hofmann, and E. Doelker, "Co-encapsulation of dexamethasone 21-acetate and SPIONs into biodegradable polymeric microparticles designed for intra-articular delivery," *Journal of Microencapsulation*, vol. 25, no. 5, pp. 339–350, 2008.

[54] V. A. Tsotas, S. Mourtas, and S. G. Antimisiaris, "Dexamethasone incorporating liposomes: effect of lipid composition on drug trapping efficiency and vesicle stability," *Drug Delivery*, vol. 14, no. 7, pp. 441–445, 2007.

[55] I. Elron-Gross, Y. Glucksam, and R. Margalit, "Liposomal dexamethasone-diclofenac combinations for local osteoarthritis treatment," *International Journal of Pharmaceutics*, vol. 376, no. 1-2, pp. 84–91, 2009.

[56] F. Atamaz, Y. Kirazli, and Y. Akkoc, "A comparison of two different intra-articular hyaluronan drugs and physical therapy in the management of knee osteoarthritis," *Rheumatology International*, vol. 26, no. 10, pp. 873–878, 2006.

[57] B. Scott, *The benefits of intra-articular high molecular weight hyaluronic acid injections compared to low molecular weight intra-articular hyaluronic acid in the reduction of pain, disability, and stiffness in adult patients with osteoarthritis of the knee*, M.S. thesis, School of Physician Assistant Studies, 2009.

[58] L. Frizziero and I. Pasquali Ronchetti, "Intra-articular treatment of osteoarthritis of the knee: an arthroscopic and clinical comparison between sodium hyaluronate (500–730 kDa) and methylprednisolone acetate," *Journal of Orthopaedics and Traumatology*, vol. 3, no. 2, pp. 89–96, 2002.

[59] R. R. Bannuru, N. S. Natov, I. E. Obadan, L. L. Price, C. H. Schmid, and T. E. McAlindon, "Therapeutic trajectory of hyaluronic acid versus corticosteroids in the treatment of knee osteoarthritis: a systematic review and meta-analysis," *Arthritis Care and Research*, vol. 61, no. 12, pp. 1704–1711, 2009.

[60] R. Barbucci, S. Lamponi, A. Borzacchiello et al., "Hyaluronic acid hydrogel in the treatment of osteoarthritis," *Biomaterials*, vol. 23, no. 23, pp. 4503–4513, 2002.

[61] M. Abate, D. Pulcini, A. Di Iorio, and C. Schiavone, "Viscosupplementation with intra-articular hyaluronic acid for treatment of osteoarthritis in the elderly," *Current Pharmaceutical Design*, vol. 16, no. 6, pp. 631–640, 2010.

[62] S. J. Chang, S. M. Kuo, I. Manousakas, G. C. Niu, and J. P. Chen, "Preparation and characterization of hyaluronan/collagen II microspheres under an electrostatic field system with disc electrodes," *Acta Biomaterialia*, vol. 5, no. 1, pp. 101–114, 2009.

[63] N. A. Peppas, P. Bures, W. Leobandung, and H. Ichikawa, "Hydrogels in pharmaceutical formulations," *European Journal of Pharmaceutics and Biopharmaceutics*, vol. 50, no. 1, pp. 27–46, 2000.

[64] G. Verbruggen, S. Goemaere, and E. M. Veys, "Chondroitin sulfate: S/DMOAD (structure/disease modifying anti-osteoarthritis drug) in the treatment of finger joint OA," *Osteoarthritis and Cartilage*, vol. 6, supplement A, pp. 37–38, 1998.

[65] M. Kobo, K. Ando, T. Mimura, Y. Matsusue, and K. Mori, "Chondroitin sulfate for the treatment of hip and knee osteoarthritis: current status and future trends," *Life Sciences*, vol. 85, no. 13-14, pp. 477–483, 2009.

[66] M. Cohen, R. Wolfe, T. Mai, and D. Lewis, "A randomized, double blind, placebo controlled trial of a topical cream containing glucosamine sulfate, chondroitin sulfate, and camphor for osteoarthritis of the knee," *Journal of Rheumatology*, vol. 30, no. 3, pp. 523–528, 2003.

[67] P. S. Chan, J. P. Caron, G. J. M. Rosa, and M. W. Orth, "Glucosamine and chondroitin sulfate regulate gene expression and synthesis of nitric oxide and prostaglandin E_2 in articular cartilage explants," *Osteoarthritis and Cartilage*, vol. 13, no. 5, pp. 387–394, 2005.

[68] J. H. Hui, S. W. Chan, J. Li et al., "Intra-articular delivery of chondroitin sulfate for the treatment of joint defects in rabbit model," *Journal of Molecular Histology*, vol. 38, no. 5, pp. 483–489, 2007.

[69] B. F. Leeb, H. Schweitzer, K. Montag, and J. S. Smolen, "A metaanalysis of chondroitin sulfate in the treatment of osteoarthritis," *Journal of Rheumatology*, vol. 27, no. 1, pp. 205–211, 2000.

[70] S. K. Tat, J. P. Pelletier, F. Mineau, N. Duval, and J. Martel-Pelletier, "Variable effects of 3 different chondroitin sulfate compounds on human osteoarthritic cartilage/chondrocytes: relevance of purity and production process," *Journal of Rheumatology*, vol. 37, no. 3, pp. 656–664, 2010.

[71] D. Uebelhart, E. J. M. Thonar, P. D. Delmas, A. Chantraine, and E. Vignon, "Effects of oral chondroitin sulfate on the progression of knee osteoarthritis: a pilot study," *Osteoarthritis and Cartilage*, vol. 6, supplement A, pp. 39–46, 1998.

[72] J. Egea, A. G. García, J. Verges, E. Montell, and M. G. López, "Antioxidant, antiinflammatory and neuroprotective actions of chondroitin sulfate and proteoglycans," *Osteoarthritis and Cartilage*, vol. 18, supplement 1, pp. S24–S27, 2010.

[73] S. C. Vlad, M. P. LaValley, T. E. McAlindon, and D. T. Felson, "Glucosamine for pain in osteoarthritis: why do trial results differ?" *Arthritis and Rheumatism*, vol. 56, no. 7, pp. 2267–2277, 2007.

[74] A. Fioravanti and G. Collodel, "In vitro effects of chondroitin sulfate," *Advances in Pharmacology*, vol. 53, pp. 449–465, 2006.

[75] V. Prabhakar and R. Sasisekharan, "The biosynthesis and catabolism of galactosaminoglycans," *Advances in Pharmacology*, vol. 53, pp. 69–115, 2006.

[76] D. O. Clegg, D. J. Reda, C. L. Harris et al., "Glucosamine, chondroitin sulfate, and the two in combination for painful

knee osteoarthritis," *The New England Journal of Medicine*, vol. 354, no. 8, pp. 795–808, 2006.

[77] D. Uebelhart, M. Malaise, R. Marcolongo et al., "Intermittent treatment of knee osteoarthritis with oral chondroitin sulfate: a one-year, randomized, double-blind, multicenter study versus placebo," *Osteoarthritis and Cartilage*, vol. 12, no. 4, pp. 269–276, 2004.

[78] J. Mönkkönen, J. Liukkonen, M. Taskinen, T. D. Heath, and A. Urtti, "Studies on liposome formulationsfor intra-articular delivery of clodronate," *Journal of Controlled Release*, vol. 35, no. 2-3, pp. 145–154, 1995.

[79] A. S. Williams, J. P. Camilleri, R. M. Goodfellow, and B. D. Williams, "A single intra-articular injection of liposomally conjugated methotrexate suppresses joint inflammation in rat antigen-induced arthritis," *British Journal of Rheumatology*, vol. 35, no. 8, pp. 719–724, 1996.

[80] Y. Qiu and K. Park, "Environment-sensitive hydrogels for drug delivery," *Advanced Drug Delivery Reviews*, vol. 53, no. 3, pp. 321–339, 2001.

[81] I. Villanueva, S. K. Gladem, J. Kessler, and S. J. Bryant, "Dynamic loading stimulates chondrocyte biosynthesis when encapsulated in charged hydrogels prepared from poly(ethylene glycol) and chondroitin sulfate," *Matrix Biology*, vol. 29, no. 1, pp. 51–62, 2010.

[82] S. S. Bansal, A. Joshi, and A. K. Bansal, "New dosage formulations for targeted delivery of cyclo-oxygenase-2 inhibitors: focus on use in the elderly," *Drugs and Aging*, vol. 24, no. 6, pp. 441–451, 2007.